



CATÓLICA

ESCOLA SUPERIOR DE BIOTECNOLOGIA

PORTO

FUNCTIONAL INGREDIENTS FROM VALORIZATION OF MELON (*Cucumis melo* L.) BY-PRODUCTS: PRODUCTION, BIOACTIVITY AND POTENTIAL APPLICATION

Thesis submitted to *Universidade Católica Portuguesa* to attain the degree of PhD in
Biotechnology – with specialization in Food Science and Engineering

By

Ricardo Gómez García

December 2021



CATÓLICA

ESCOLA SUPERIOR DE BIOTECNOLOGIA

PORTO

FUNCTIONAL INGREDIENTS FROM VALORIZATION OF MELON (*Cucumis melo* L.) BY-PRODUCTS: PRODUCTION, BIOACTIVITY AND POTENTIAL APPLICATION

Thesis submitted to *Universidade Católica Portuguesa* to attain the degree of PhD in
Biotechnology – with specialization in Food Science and Engineering

By

Ricardo Gómez García

Supervisor: ***Professor Maria Manuela Estevez Pintado*** (*Universidade Católica Portuguesa*)

Co-supervisor: ***Professor Ana Raquel Madureira*** (*Universidade Católica Portuguesa*) and
Professor Cristóbal Noé Aguilar González (*Universidad Autónoma de Coahuila, México*)

December 2021

To my family and friends:

“If I have seen further than others, it is by standing on the shoulders of Giants”

Issac Newton

The authors thanks the National Council of Science and Technology (CONACyT, Mexico) for PhD fellowship support granted (CVU number **807416**). Also the authors would like to thank to the project MultiBiorefinery.: Estratégias multiuso para a valorização de uma gama alargada de subprodutos agroflorestais e das pescas: Um passo em frente na criação de uma biorrefinaria” financiado pelo Programa Operacional Competitividade e Internacionalização (POCI- 01-0145-FEDER-016403) e pelo Programa Operacional Regional de Lisboa (LISBOA-01-0145-FEDER-016403), na sua componente FEDER e pela Fundação para a Ciência e Tecnologia, I.P. na componente nacional (SAICTPAC/0040/2015).



Resumo

Atualmente, as indústrias de processamento de frutas são responsáveis pela produção e acumulação de grandes quantidades de subprodutos vegetais, os quais são em alguns casos descartados em aterros como resíduos, causando problemas ambientais e económicos. Os subprodutos do melão não são uma exceção e fazem parte deste problema devido à proporção gerada que representa cerca de 30% em resíduo (peso fresco), durante o seu processamento industrial. O desenvolvimento de uma estratégia de valorização integral para os subprodutos do melão através de processos verdes e sustentáveis no contexto de resíduos zero e bioeconomia circular é uma tarefa importante. Isto permitirá a sua valorização total e reincorporação na cadeia de valor industrial como uma fonte rica em ingredientes naturais e bioativos, demonstrando aplicabilidade de elevado valor económico e redução do impacto ambiental. O objetivo principal deste trabalho de doutoramento foi explorar de forma integral e com resíduo zero o valor dos subprodutos de melão e o desenvolvimento de ingredientes funcionais ricos em moléculas bioativas e de alto valor agregado, incluindo diferentes frações ricas em pigmentos, polifenóis, proteínas funcionais (anticongelantes e enzimas coagulantes), pectina, microcelulose e uma farinha rica em fibra. Além disso, permitiu igualmente desenvolver um processo extrativo integrado em cascata utilizando tecnologias limpas e avaliar as propriedades biológicas e tecnológicas dos ingredientes funcionais obtidos para estabelecer o seu valor e potencial aplicação.

Inicialmente, cascas frescas de melão foram fracionadas por processos mecânicos dentro das abordagens de resíduo zero e biorefinaria, gerando três frações, que foram caracterizadas.

I) A fração do precipitado (PF), que representa a menor fração (2,0% do peso fresco total da casca (FW)), é a fração mais rica em proteínas (34,90% w/w), clorofilas (174,84 mg/100 g FW) e carotenoides totais (98,59 mg/100 DM), com o β -caroteno, luteína, β -criptoxantina e violaxantina quantificados como principais. Essa fração também foi valorizada através de processos de rutura combinados com métodos de extração sólido-líquido para separar e isolar todos os constituintes importantes, incluindo proteínas, clorofilas e xantofilas.

II) A fração sólida (SF) representa 21,5% do FW e é a fração mais rica de fibra (44,42% p/p), a qual revelou a composição de celulose, hemicelulose e lenhina (27,67%, 8,2% e 26,5% p/p, respetivamente) apresentando grande potencial como ingrediente rico em fibra antioxidante. Associado ao seu perfil de compostos bioativos, esta fração também foi submetida a condições simuladas do trato gastrointestinal (TGI) e posteriormente avaliada por fermentação fecal *in vitro* com o objetivo de desenvolver um protótipo de farinha funcional para promoção da saúde, principalmente associado ao seu potencial prebiótico. Os resultados da análise do gene 16rRNA mostraram que o SF não impactou negativamente a diversidade da microbiota intestinal e permitiu a produção positiva de ácidos gordos de cadeia curta (acetato > propionato > butirato). Além disso, a fração SF

também mostrou elevado teor em pectina, pelo que em uma segunda abordagem esta também foi extraída testando diferentes ácidos combinados com temperatura, sendo o ácido cítrico aquele que exibiu melhor eficácia, permitindo 34% w/w de rendimento de extração e 60-70% de esterificação metílica, e apresentando boas propriedades emulsificantes e gelificantes. Após a extração da pectina da fração SF, os resíduos lenhocelulósicos do melão foram submetidos a extração da celulose microcristalina (MCC) por dois métodos utilizando NaOH: o tradicional e termoalcalino. Os resultados mostraram maior grau de cristalinidade pelo método termoalcalino do que pelo processo tradicional (51-61% e 54- 55%, respectivamente).

Finalmente, III) a fração líquida (LF), a fração mais representativa em peso fresco com cerca de 70% pelo seu elevado conteúdo em água (>90%). Esta fração mostrou uma elevada atividade antioxidante pelos métodos ABTS, DPPH e ORAC atribuídos ao alto teor de polifenóis (798,43 mg GAE/100 g MS). A fração LF foi submetido às condições do TGI. O conteúdo fenólico total (CFT) foi mantido na boca e fase gástrica (453,69 e 425,89 mg/100 g de MS, respectivamente), enquanto no intestino delgado foi observada uma diminuição drástica (atingindo 313,37 mg/100 g de MS) que corresponde a 54-57% de índice de recuperação (IR), no entanto a atividade antioxidante de ABTS e DPPH ainda foi significativa, que confirmam a capacidade de tais compostos exercerem as suas propriedades bioativas (54-76% índice de acessibilidade (IAC)). Por outro lado, esta fração apresentou efeito prebiótico (2% p/v) sobre os principais grupos benéficos da microbiota intestinal, os *Lactobacillus* sp. e *Bifidobacterium* sp., modulando o seu crescimento e o metabolismo positivamente. Além disso, a cucumisina (CUC), foi extraída através de uma abordagem de química verde usando carragenina como agente precipitante, mostrando ser uma estratégia eficaz para isolá-la com um rendimento de 0,17 g CUC/100 g de sub-produtos, e mostrando melhor grau de purificação e atividade proteolítica do que o processo de precipitação tradicional (17,65 e 1,60 vezes, respectivamente), mantendo as suas propriedades biológicas. As proteínas do melão extraídas por este processo de precipitação verde também exibiram propriedades anticongelantes, possivelmente atribuídas à grande semelhança na estrutura e pesos moleculares (6,2 e 3,5 kDa) com outras proteínas anticongelantes já relatados do tipo III (domínio C-terminal, poucos resíduos de alanina e nenhum resíduo de cisteína) e do tipo I (ricos em alanina), respectivamente.

Resumidamente, os resultados deste trabalho de valorização integral de cascas de melão contribuirão para um desenvolvimento sustentável nas indústrias de processamento de frutas, permitindo obtenção de novos ingredientes/aditivos funcionais por meio de estratégias limpas e com preservação da sua bioatividade e funcionalidade.

Palavras-chave: Subprodutos de melão, Valorização de biorresíduos, Bioeconomia circular, Ingredientes funcionais, proteínas bioativas

Abstract

Currently, fruit processing industries are responsible for the production and accumulation of large amounts of vegetable by-products, which are in some cases disposed of in landfills as waste, causing environmental and economic problems. Melon by-products are no exception and are part of this problem due to the proportion generated, which represents about 30% in residue (fresh weight), during its industrial processing. The development of an integral valorisation strategy for melon by-products through green and sustainable processes in the context of zero waste and circular bioeconomy is an important task. This will allow its full valorisation and reincorporation into the industrial value chain as a rich source of natural and bioactive ingredients, demonstrating the applicability of high economic value and reduced environmental impact. The main objective of this Ph D work was to fully explore and with zero-waste the value of melon by-products and the development of functional ingredients rich in bioactive molecules with high added value, including different fractions rich in pigments, polyphenols, functional proteins (antifreeze and coagulating enzymes), pectin, microcellulose and a flour rich in fiber. In addition, it also allowed the development of an integrated downstream extractive process using clean technologies and the evaluation of the biological and technological properties of the obtained functional ingredients to establish their value and potential application.

Initially, fresh melon peels were fractionated by mechanical processes within the zero-waste and biorefinery approaches, generating three fractions, which were characterized.

I) The pellet fraction (PF), which represents the smallest fraction (2.0% of the total fresh weight of the peels (FW)), is the richest fraction in proteins (34.90% w/w), chlorophylls (174.84 mg/100 g FW) and total carotenoids (98.59 mg/100 dry matter (DM)) with β -carotene, lutein, β -cryptoxanthin and violaxanthin quantified as the main ones. This fraction has also been valorised through disruption processes combined with solid-liquid extraction methods to separate and isolate all important constituents, including proteins, chlorophylls and xanthophylls.

II) The solid fraction (SF) represents 21.5% of the FW and is the richest fraction in fiber (44.42% w/w), which revealed the composition of cellulose, hemicellulose and lignin (27.67%, 8.2% and 26.5% w/w, respectively), showing great potential as an ingredient rich in antioxidant fiber. Associated with its bioactive compound profile, this fraction was also subjected to simulated conditions of the gastrointestinal tract (GIT) and subsequently evaluated by *in vitro* fecal fermentation with the objective to develop a prototype of functional flour for health promotion, mainly associated with its prebiotic potential. The results of the 16rRNA gene analysis showed that SF did not impact negatively the intestinal microbiota diversity and allowed the positive production of short-chain fatty acids (acetate > propionate > butyrate). In addition, the SF fraction also showed high pectin content, so in a second approach, it was also extracted by testing different acids

combined with temperature, being citric acid the one that exhibited the best efficacy, allowing 34% w/w extraction yield and 60-70% methyl esterification, and showing good emulsifying and gelling properties. After extracting pectin from the SF fraction, the lignocellulosic residues from melon were subjected to extraction of microcrystalline cellulose (MCC) by two methods using NaOH: traditional and thermoalkaline. The results showed a higher degree of crystallinity by the thermoalkaline method than by the traditional process (51-61% and 54-55%, respectively).

Finally, III) the liquid fraction (LF), the most representative fraction in fresh weight with about 70% due to its high-water content (>90%). This fraction showed high antioxidant activity by the ABTS, DPPH and ORAC methods attributed to the high polyphenol content (798.43 mg GAE/100 g DM). The LF fraction was subjected to the conditions of the GIT. The total phenolic content (TPC) was maintained in the mouth and gastric phase (453.69 and 425.89 mg/100 g DM, respectively), while in the small intestine a drastic decrease was observed (reaching 313.37 mg/100 g DM), which corresponds to 54-57% of recovery index (RI), however, the antioxidant activity of ABTS and DPPH was still significant, which confirm the capacity of such compounds to exert their bioactive properties (54-76% accessibility index (ACI)). On the other hand, this fraction had a prebiotic effect (2% w/v) on the main beneficial groups of the intestinal microbiota, the *Lactobacillus* sp. and *Bifidobacterium* sp., modulating positively its growth and metabolism. Furthermore, cucumisin (CUC) was extracted through a green chemistry approach using carrageenan as a precipitating agent, proving to be an effective strategy to isolate it with a yield of 0.17 g CUC/100 g of by-products, and with better purification factor of proteolytic activity than the traditional precipitation process (17.65 and 1.60-folds, respectively), maintaining its biological properties. The melon proteins extracted by this green precipitation process also exhibited antifreeze properties, possibly attributed to the great similarity in structure and molecular weights (6.2 and 3.5 kDa) with other proteins previously reported such as type III antifreeze proteins (C-terminal domain, few alanine residues and no cysteine residues) and type I (alanine-rich), respectively.

Briefly, the results of this work on the integral valorization of melon peels will contribute to a sustainable development in the fruit processing industries, allowing the obtention of new functional ingredients/additives through clean strategies and preserving their bioactivity and functionality.

Keywords: Melon by-products, Biowaste valorisation, Circular bioeconomy, Functional ingredients, Bioactive proteins

Acknowledgements

To Escola Superior de Biotecnologia – Universidade Católica Portuguesa, to accept me as an international Ph D student and provide the necessary conditions to carry out this research work.

To the Mexican National Council of Science and Technology (CONACyT, Mexico) for the PhD fellowship support granted, providing me the opportunity to develop this research thesis.

The success is never succeeded by one single person, but by the synergy of different people.

Therefore, I really would like to express my deep gratitude to the following people:

To my supervisor Prof. Manuela Pintado, firstly for accepted me as your student. Many thanks for all your teachings, which allowed me to become a better researcher and person. All the good outcomes were possible thanks to your excellence standards, great knowledge and human-being quality.

To my Co-supervisor Prof. Cristóbal Aguilar for always challenge me to go out of my comfort zone and do things that I never think to be able to do. Many thanks for your support and always believe in me. Thanks for your friendly and professional valuable advice and comments, which allowed me to get more personal and professional competences.

To my Co-supervisor Ph D. Ana Raquel Madureira for always support me and provide me much of your time. Thanks for your knowledge and teachings.

To my dear friend Ph D. Débora Campos for always encourage me to do new things. Many thanks for your help and support in the official and extra-official works. It is a pleasure to meet and coincide with brilliant and challenging persons like you.

To my dear fiend M. Sc. Ana A. Vilas-Boas for provide me your friendship and constant funny moments. Many thanks for your help and support. It is a pleasure to meet smart and kind persons like you.

To the current and previous laboratory colleagues and friends who created a comfort and friendly environment at the CBQF's laboratories since my first day, having fun and scientific moments.

To my close friend M. Sc. Ivanoé García for always help me and your priceless friendship.

To my family, my parents and sisters, for all the messages of encouragement and support, your love and also concerns. Many thanks for the all the things that all of you have done for me and to accept all my decisions and goals that I propose to myself in my life.

Table of Contents

<i>Resumo</i>	<i>IV</i>
<i>Abstract</i>	<i>VI</i>
<i>Acknowledgements</i>	<i>IX</i>
<i>Table of Contents</i>	<i>XI</i>
<i>List of Tables</i>	<i>XVII</i>
<i>List of Figures</i>	<i>XXIa</i>
<i>Scope and outline</i>	<i>XXXI</i>
PART I - Bibliographic Survey	1
<i>CHAPTER 1 - Valorisation of food agro-industrial by-products: from the past to the present and perspectives</i>	<i>3</i>
Abstract	3
1. Introduction	4
1.1. From the past: Traditional and soft chemistry for agro-food by-products exploitation.....	6
1.2.1. To the present: Agro-food by-products as bioresources, not as pollutants	10
1.2.2 Future perspectives: Current innovative advances and behaviours with emphasis on agro-food by-products valorisation	14
1.2.3 Practical applications and future research prospects	24
1.3 Concluding comments.....	26
<i>CHAPTER 2 - Valorization of Melon fruit (Cucumis melo L.) by-products: Phytochemical and biofunctional properties with emphasis on recent trends and advances</i>	<i>27</i>
Abstract	27
2.1. Introduction	28
2.2 Muskmelon Anatomical Description	29
2.3 Phytochemical and nutritional composition of melon fruit	30
2.3.1 Phenolic compounds.....	31
2.3.2 Carotenoids compounds	33
2.3.3 Essential oils and fatty acids.....	37
2.4 Biological activities and human health	40
2.4.1 Antioxidant activity	40
2.4.2. Provitamin A activity	41
2.4.3 Anticancer activity.....	44
2.4.4 Antimicrobial activity.....	45
2.5 Recent Research and Advanced trends for Future Prospects	46
2.5.1 Existing patents regarding melon fruit	47
2.5.2. Melon by-products as functional ingredients	48
2.5.3. In Solid-state fermentation	49
2.5.4. Eco-green technologies for protein extraction	49
2.5.5. Production of micro- and nano-cellulose composites	50
2.6. Conclusions.....	50
<i>Objectives</i>	<i>53</i>

PART II – Production, characterisation and bioactivity 55*CHAPTER 3 – A chemical valorisation of melon peels towards functional food ingredients: bioactivities, profile and antioxidant properties 57*

Abstract	57
3.1. Introduction	58
3.2. Materials and Methods	59
3.2.1. Chemicals	59
3.2.2. Melon peels.....	59
3.2.3. Chemical composition of melon peels.....	60
3.2.4. Preparation of melon peels extracts	64
3.2.5. Total phenolic content (TPC)	64
3.2.6. Total insoluble bound phenolics (IBP)	64
3.2.7. Total carotenoids content (TCC)	65
3.2.8. Identification and quantification of phenolics and carotenoids by HPLC	65
3.2.9. Identification of phenolic compounds by LC-ESI-UHR-QqTOF-MS	66
3.2.10. Total chlorophylls content (TCHC).....	67
3.2.11. Antioxidant activity determination	67
3.2.12. Oxygen radical absorbance capacity assay (ORAC)	68
3.2.13. Statistical Analysis Section.....	69
3.3. Results and discussion.....	69
3.3.1. Proximate chemical composition.....	69
3.3.2 Structural carbohydrates of the insoluble fractions (SF and PF)	71
3.3.3 Extractable pectins in the SF	72
3.3.4 Total phenolics (TPC) and total carotenoids (TCC) content	72
3.3.5. Identification and quantification of phenolic compounds by HPLC/LC-MS.....	74
3.3.6. Identification and quantification of carotenoid compounds by HPLC	75
3.3.7. Total chlorophylls content	78
3.3.8. Antioxidant Activity	78
3.3.9. Melon peels as potential functional ingredients	79
3.4. Conclusions	81

CHAPTER 4 –Valorisation of pigments protein enriched fraction from melon peels (Cucumis melo L. inodorus) to complete integral valorisation as a zero-waste approach 83

Abstract	83
4.1. Introduction	84
4.2. Materials and Methods	86
4.2.1. Chemical	86
4.2.2. Melon peels fractionation	86
4.2.3. Disruption and Solid-liquid extraction of proteins	87
4.2.4. Solid-liquid extraction of pigments	88
4.2.5. Chlorophylls and carotenoids separation.....	88
4.2.6. Total protein content.....	90
4.2.7. Quantification of pigments	90
4.3. Results and discussion.....	90
4.3.1 Protein extraction by bead milling method.....	90
4.3.2. Effect of solid-liquid ratio (SLR) on chlorophylls extraction yield	93
4.3.3. Recovery of carotenoids and chlorophylls	95
4.4. Conclusions	99

CHAPTER 5 – Impact of in vitro simulation digestion on bioactive compounds, bioactivity and cytotoxicity of melon (Cucumis melo L. inodorus) peel juice powder 101

Abstract	101
5.1. Introduction	102
5.2. Materials and Methods	104

5.2.1. Chemicals and reagents	104
5.2.2. Preparation of melon peel extract (MLE)	104
5.2.3. In vitro simulated gastrointestinal digestion.....	104
5.2.4. Accessibility and stability of melon bioactive compounds through in vitro gastrointestinal digestion	105
5.2.5. Total phenolic content (TPC)	106
5.2.6. Antioxidant activity determination by ABTS and DPPH.....	107
5.2.7. Identification and quantification of polyphenols by HPLC	107
5.2.8. Identification and quantification of sugars and organic acids by HPLC	108
5.2.9. Prebiotic potential.....	108
5.2.10. Evaluation of cytotoxicity: Metabolic activity assay	109
5.2.11. Statistical analysis	110
5.3. Results and discussion	110
5.3.1. Stability and accessibility of bioactive compounds of melon peel juice during in vitro GIT digestion	110
5.3.3. Cytotoxicity.....	123
5.4. Conclusions.....	124
<i>CHAPTER 6 – Prebiotic effect, bioactive compounds and antioxidant activity of melon peel (Cucumis melo L. inodorus) flour subjected to in vitro gastrointestinal digestion and human faecal fermentation</i>	125
Abstract	125
6.1. Introduction	126
6.2. Material and methods.....	128
6.2.1. Chemicals and reagents	128
6.2.2. Melon peel material.....	128
6.2.3. Preparation of melon peel flour (MPF)	129
6.2.4. In vitro simulated gastrointestinal digestion.....	129
6.2.5. Stability and accessibility of melon polyphenols along in vitro gastrointestinal digestion .	130
6.2.6. In vitro faecal fermentation assay - Prebiotic effect.....	131
6.2.7. Gut microbiota evaluation	132
6.2.8. Total phenolic content (TPC)	133
6.2.9. Antioxidant activity determination by ABTS and DPPH.....	134
6.2.10. Identification and quantification of polyphenols by HPLC	134
6.2.11. Identification and quantification of sugars and organic acids – short chain fatty acids by HPLC	135
6.2.12. Statistical analysis	135
6.3. Results and discussion	137
6.3.1. Effects of GIT simulation on melon peel flour compounds: Stability and accessibility	137
6.3.2. Human gut microbiota fermentation	144
6.4. Conclusion	154
PART III – Industrial interest value-added ingredients	155
<i>CHAPTER 7 – Valorisation of melon (Cucumis melo L. inodorus cultivar) industrial by-products as rich sources of high-methoxyl pectin: Improvement of hot-acid extraction and performance properties ...</i>	<i>157</i>
Abstract	157
7.1. Introduction	158
7.2. Materials and methods	160
7.2.1. Chemicals	160
7.2.2. Melon peel by-products.....	160
7.2.3. Hot acid extraction of pectin methodology	160
7.2.4. Physicochemical properties evaluation	161
7.2.5. Determination of the degree of methyl esterification (DM).....	164
7.2.6. Chemical groups evaluation by FTIR spectroscopy.....	165
7.2.7. Pectins molecular weight determination by HPLC-SEC.....	165

7.2.8. Emulsifying capacity (EC) assessment.....	165
7.2.9. Gel preparation	166
7.2.10. Rheological measurements	166
7.3. Results and discussion.....	167
7.3.1. Effect of different acids on pectin extraction yield and chemical composition.....	167
7.3.2. Chemical characterization	168
7.3.2. Structural analysis.....	169
7.3.3. Molecular weight (MW) of pectins	170
7.3.4. Emulsifying properties of pectins	173
7.3.5 Rheological properties of pectin-gel samples.....	175
7.4. Conclusions	178
<i>CHAPTER 8 – Production and characterisation of microcrystalline cellulose from industrial melon by-products residues using a biorefinery approach</i>	<i>179</i>
Abstract	179
8.1. Introduction	180
8.2. Materials and methods.....	182
8.2.1. Chemicals	182
8.2.2. Biorefinery approach: Deconstruction of melon peels biomass in different fractions and value-added compounds	182
8.2.3. Chemical composition of melon peels residues.....	183
8.2.4. Extraction of cellulose from melon peel residues.....	185
8.2.5. Microcrystalline cellulose (MCC) from cellulose of melon residues.....	186
8.2.6. X-Ray Diffraction.....	186
8.2.7. FTIR.....	186
8.2.8. Scanning Electron Microscopy (SEM).....	187
8.3. Results and discussion.....	188
8.3.1. Chemical composition and structural changes of lignocellulosic melon by-products (LMB) after pectin extraction	188
8.3.2. Microcrystalline cellulose (MCC) extraction and structural composition	189
8.3.3. X-ray diffraction	192
8.3.4. FTIR	195
8.3.5. SEM	197
8.4. Conclusions	199
PART IV – Green chemistry approach and application	201
<i>CHAPTER 9 – Biological protein precipitation: a green process for the extraction of cucumisin from melon (Cucumis melo L. inodorus) by-products.....</i>	<i>203</i>
Abstract	203
9.1. Introduction	204
9.2. Materials and methods.....	205
9.2.1. Chemicals	205
9.2.2. Raw material - Melon peels.....	205
9.2.3. Melon peels juice (MPJ) preparation.....	205
9.2.4. Protein precipitation with ammonium sulphate	206
9.2.5. SDS-PAGE electrophoresis	206
9.2.6. Analysis by size exclusion chromatography (FPLC)	206
9.2.7. Turbidimetric titration curves vs pH.....	207
9.2.8. Turbidimetric titration curves with CRG.....	207
9.2.9. Protein content determination.....	207
9.2.10. Proteolytic activity determination.....	208
9.2.11. Milk-clotting activity	209
9.3. Results and discussions	209
9.3.1. SDS–PAGE analysis and FPLC profile.....	209
9.3.2. Solubility phase diagram of CRG and MPJ proteins	210
9.3.3. Effect of CRG on MPJ proteins.....	211

9.3.4. Complex formation phase diagrams of CRG and MPJ proteins	213
9.3.5. Enzymatic activities: PA and MCA	215
217	
9.3.6. Effect of CaCl ₂ , temperature and pH on MCA.....	217
9.3.7. Melon by-products as sources of proteolytic enzymes.....	220
9.4. Conclusions.....	221
<i>CHAPTER 10 – Proteins-like antifreeze proteins identified and extracted from melon (Cucumis melo L. inodorus cultivar) peels by green precipitation using carrageenan: recrystallization inhibition and amino acid profile.....</i>	<i>223</i>
Abstract	223
10.1. Introduction	224
10.2. Material and methods.....	226
10.2.1. Chemicals	226
10.2.2. Raw material - Melon peels.....	226
10.2.3. Melon peels juice (MPJ) preparation	226
10.2.4. Extraction of melon peel proteins by precipitation with CRG	226
10.2.5. Analysis by size exclusion chromatography (FPLC)	227
10.2.6. Protein content determination.....	227
10.2.7. Identification and quantification of amino acids by HPLC	227
10.2.8. Production of AuNPs.....	228
10.2.9. Colorimetric assay of AFP activity	228
10.2.10. Zeta potential and size of the AuNPs.....	229
10.2.11. Recrystallization inhibition assay	229
10.3. Results and discussion	229
10.3.1. Protein extraction from melon peels juice (MPJ).....	229
10.3.2. Effect of proteins precipitated with CRG on aggregation of AuNPs	230
10.3.4. Amino acid content of MPJ.....	237
10.3.5. Amino acid profile after protein precipitation	238
10.4. Conclusions.....	240
PART V – Conclusions and Final Remarks	241
<i>CHAPTER 11 - Conclusions.....</i>	<i>243</i>
<i>CHAPTER 12 – Future research and development.....</i>	<i>249</i>
References	251
<i>References.....</i>	<i>253</i>

List of Tables

Table 1.4. Spectrum of research studies through the time regarding utilization and valorisation of different food agro-industrial by-products.....	13
Table 1.5. Highlighting different agro-industrial by-products by their richness in value-added compounds.	15
Table 1.6. Agro-industrial by-products as suitable resources for enzymes production and extraction through traditional and green methodologies	16
Table 1.7. Latest scientific contributions within the framework of food waste valorisation	18
Table 2.1. Major groups of melon fruit	31
Table 2.2. Total phenolic and total flavonoids from different by-products of melon fruit	34
Table 2.3. Identified and quantified phenolic compounds by HPLC from peel extracts of various melon varieties.	36
Table 2.4. Profile of fatty acids and bioactive compounds from oil extracts of different melon seeds.....	39
Table 2.5. General spectrum of some studies regarding antioxidant activity from different varieties of melon by-products.	42
Table 2.6. β -carotene and its corresponding vitamin A activity and lutein content in melon pulp from different geographical location of the origin and cultivation.....	45
Table 3.1. Chemical composition of the three different fractions obtained from inodorus melon peels	71
Table 3.2. Proximal structural composition of melon peels fractions	72
Table 3.3. Total phenolic, carotenoid and chlorophyll content evaluated in the extracts of melon fractions	74
Table 3.4. List of phenolic compounds identified and quantified in melon peel fractions detected by HPLC/LC-ESI-UHR-QqTOF-MS.....	77

Table 3.5. Concentration of carotenoids detected in melon peels fractions by HPLC-DAD.	78
Table 5.1. Recovery index (RI%) and Accessibility index (ACI%) of phenolic compounds and antioxidant activity throughout GIT simulation from melon peel juice (MPJ) powder.	117
Table 5.2. Main polyphenols identified and quantified by HPLC-DAD and antioxidant activity during the <i>in vitro</i> gastrointestinal tract simulation of melon peel juice (MPJ) powder.....	118
Table 5.3. Maximum growth rates (μ_{\max} , h ⁻¹) of the tested probiotic bacteria strains grown in media containing MRS media containing glucose (Glu), fructooligosaccharides (FOS) or melon peels juice (MPJ) powder at 10 and 20 mg/mL (1 and 2% w/v, respectively).	123
Table 6.1. Primer sequence and real-time PCR conditions applied for gut microbiota analysis.....	136
Table 6.2. Main phenolics identified and quantified by HPLC-DAD during the <i>in vitro</i> gastrointestinal tract simulation of melon peel flour (MPF).	143
Table 6.3. Recovery index (RI%) and Accessibility index (ACI%) of phenolic compounds throughout GIT simulation from melon peel flour (MPF).	142
Table 6.4. Faecal microbiota composition of volunteer sample donors.	145
Table 6.5. Phenolic compounds identified and quantified by HPLC throughout <i>in vitro</i> faecal fermentation of melon peel flour (MPF) subjected previously to <i>in vitro</i> GIT digestion.	153
Table 7.1. Composition of pectin polysaccharide extracted from inodorus melon peel by- products with different acid agents and comparison with commercial citrus pectin and different pectin sources	171
Table 8.1. Chemical composition of the melon peel residues after pectin extraction ...	189
Table 8.2. Proximal structural composition of melon peels residues after pectin extraction with different acid agents	189
Table 8.3. Mass yields (%)* obtained after each successive chemical treatment.	191

Table 8.4. Proximal structural composition of microcrystalline cellulose (MCC) from melon residues.	191
Table 9.1. Protein purification from melon peels	217
Table 10.1. Protein content of melon peel juice (MPJ) and proteins extracted by precipitation with ι-carrageenan (CRG).....	230
Table 10.2. Amino acid profile by HPLC of melon peel juice (MPJ) and proteins extracted by precipitation with ι-carrageenan (CRG) (COM 0.003	238

List of Figures

Figure 1. Structure of thesis outline.....	XXX
Figure 2. Schematic flow chart for melon peels valorisation and their respective evaluations throughout this research work.....	XXXIII
Figure 1.1. Chemical reactions of the catalytic pyrolysis of lignocellulosic biomass at high temperatures between 300 to 900 °C. Adapted from Tan et al. (2013) and Kim and Choi, (2018).	7
Figure 1.2. Schematic representation of lignocellulosic biomass degradation by solid-state fermentation as a suitable alternative for food waste management and obtention of value-added compounds.	10
Figure 2.1. Major parts of melon fruit (<i>Cucumis melo</i> L.) A) mature fruit of <i>C. melo inodorus</i> cultivar, B) mesocarp, C) peel and seed by-products.....	29
Figure 2.2. Schem focusing on the principal generalities of <i>C. melo</i> fruit.....	32
Figure 2.3. Structure of phenolic compounds identified in melon peels (Mallek-Ayadi, Bahloul and Kechaou, 2017).....	35
Figure 2.4. Structure of principal carotenoids present in melon with provitamin A activity.....	44
Figure 2.5. Antimicrobial mechanisms of action of essential oils (Rao, Chen and McClements, 2019).....	47
Figure 3.1. Proposed fractionation process for melon peels varorisation under zero-waste approach.....	59
Figure 3.2. Total antioxidant activity of the methanolic extracts of <i>inodorus</i> melon peels fractions.....	79
Figure 4.1. Flow chart for melon peels fractionation process and obtetnion of value-added compounds under zero-waste approach.....	89
Figure 4.2. Process diagram proposed for complete valorisation of melon pellet fraction.....	92

Figure 4.3. Spectra profile proteins in solution extracted from melon pellet fraction (PF) by disruption process.....	94
Figure 4.4. Extraction yield of chlorophylls as function of the solid-liquid ratio (SLR) in the initial melon pellet fraction extract.....	94
Figure 4.5. Process flow chart of the sequence isolation and separation of carotenoids (xanthopylls) and chlorophylls by solid-liquid extraction through AmberLite resin.....	97
Figure 4.6. UV-Vis spectra profile of pellet fraction extract and isolated carotenoids and chlorophylls extracts as despected in Figure 4.2.....	96
Figure 4.7 Recovery percentage of chlorophylls and carotenoids as functional of the solid-liquid ratio (SRL) during extraction process with AmbetLite.....	98
Figure 5.1. Concentrations of a) soluble sugars and b) organic acids obtained after each phase of the <i>in vitro</i> gastrointestinal tract simulation (GIT). DM: dry matter. Results are the means of three independent determinations \pm standard deviation. Values with different letters indicate significant differences between each GIT stage, as determined by one-way ANOVA test and Tukey's test ($p < 0.05$).....	113
Figure 5.2. a) Total phenolic content (TPC) and antioxidant activity behaviours and b) concentrations of the main individual phenolic compounds identified by HPLC after each phase of the <i>in vitro</i> gastrointestinal tract (GIT). DM: dry matter; TPC: total phenolic content; GAE: gallic acid equivalent; AAE: ascorbic acid equivalent; TE: trolox equivalent. Results are the means of three independent determinations \pm standard deviation. Values with different letters indicate significant differences between each GIT stage, determined by one-way ANOVA test and Tukey's test ($p < 0.05$).....	114
Figure 5.3. Growth curves of <i>Bifidobacterium</i> and <i>Lactobacillus</i> probiotic strains in MRS media containing glucose (Glu), fructooligosaccharides (FOS) or melon peels juice (MPJ) powder at 10 and 20 mg/mL (1 and 2% w/v, respectively) during 48 h.	121
Figure 5.4. Maximum optical densities (OD at 660 nm) at the corresponding incubation times in experiments with <i>Bifidobacterium</i> and <i>Lactobacillus</i> probiotic strains grown in media containing glucose (Glu), fructooligosaccharides (FOS) or melon peels juice (MPJ) powder at 10 and 20 mg/mL (1 and 2% w/v, respectively) during 48 h.	122

- Figure 5.5. Metabolism of Caco-2 intestinal cells upon the presence of MPJ powder at concentrations of 10 and 20 mg/mL (1% and 2% (w/v), respectively) and after intestinal digestion..... 124
- Figure 6.1. Concentrations of a) soluble sugars and b) organic acids obtained after each phase of the *in vitro* gastrointestinal tract simulation (GIT). DM: dry matter. Results are the means of three independent determinations \pm standard deviation. Values with different letters indicate significant differences between each GIT stage, as determined by one-way ANOVA test and Tukey's test ($p < 0.05$). 139
- Figure 6.3. Relative differences to negative control throughout *in vitro* fecal fermentation. FOS: positive control (2% w/v); MPF: melon peel flour (2% w/v). Data is presented in percentage during fermentation time. Results are the means of five independent determinations \pm standard deviation. Different letters indicate significant differences ($p < 0.05$). The capital letters indicate the differences among the time (12, 24 and 48 h) for the same sample for each microbial genus and small letters indicate the differences between samples (FOS and MPF) for the same microbial genus in same point of time. 147
- Figure 6.4. *Firmicutes:Bacteroidetes* (F:B) ratio evaluation during fermentation with human faeces. FOS: positive control (2% w/v); MPF: melon peel flour (2% w/v). Data is presented in percentage during fermentation time. Results are the means of five independent determinations \pm standard deviation. Different letters indicate significant differences ($p < 0.05$). The capital letters indicate the differences among the time (12, 24 and 48 h) for the same sample for each microbial genus and, small letters indicate the differences between samples (FOS and MPF) for the same microbial genus in same time point. 148
- Figure 6.6. a) Concentration variation of organic acids and b) pH through the *in vitro* fecal fermentation. C-: negative control; FOS: positive control (2% w/v); MPF: melon peel flour (2% w/v). Results are the means of five determinations \pm standard deviation. Results are the means of five independent determinations \pm standard deviation. Different letters indicate significant differences ($p < 0.05$). The capital letters indicate the differences among the time (0, 12, 24 and 48 h) for the same sample for each microbial genus and, small letters indicate the differences between samples (control, FOS and MPF) for the same microbial genus at the same time point. 150

Figure 7.1. Extraction conditions of pectin from melon peels with different acid agents. HCl – Hydrochloric acid; CA – Citric acid; TA – Tartaric acid.	162
Figure 7.2. Flow diagram of the process to extract pectin from melon peels through hot-acid treatment. HCl – Hydrochloric acid; CA – Citric acid; TA – Tartaric acid.	163
Figure 7.3. Fourier transform infrared (FTIR) spectrums of the high methoxyl pectin extracted, with hydrochloric acid (PHCl), citric acid (PCA) and tartaric acid (PTA) compared with commercial pectin from citrus peel (PCP).	172
Figure 7.4. Chromatographic profiles of pectins extracted from <i>Inodorus</i> melon peels, with hydrochloric acid (PHCl), citric acid (PCA) and tartaric acid (PTA) compared with the commercial pectin from citrus peel (PCP) and the standard of the molecular weight of 200 kDa (P200).	175
Figure 7.5. Emulsifying capacity (%EC) and emulsion stability (%ES) of <i>inodorus</i> melon pectins. Values in the graph are the percentage that %ES represents in regard to %EC. Pectin extracted by hydrochloric acid (PHCl), citric acid (PCA) and tartaric acid (PTA); Pectin from citrus peel (PCP) – commercial	174
Figure 7.6. Effect of sucrose concentration (40 – 65% w/v) in pectin gels (1% (w/v), pH 3.50, CaCl ₂ (10 mM)) storage modulus (G'), loss modulus (G''), and the complex modulus (G*). Pectins extracted with hydrochloric acid (PHCl), citric acid (PCA) and tartaric acid (PTA) compared with commercial from citrus peel (PCP).	177
Figure 8.1. Process flow chart for melon peel by-products valorisation under biorefinery approach.	183
Figure 8.2. Flow diagram of the process to obtain microcrystalline cellulose (MCC) from melon residues through thermo-alkaline double-bleaching process. HCl: hydrochloric acid; CA: citric acid; TA: tartaric acid.	188
Figure 8.3. X-ray diffraction patterns of lignocellulosic melon by-products (LMB), melon residues after hot-acid treatment with A) hydrochloric acid (RHCl), C) citric acid (RCA) and E) tartaric acid (RTA) and their microcrystalline cellulose (MCC) B), D) and F), respectively, obtained through the (a) thermo-alkaline, (b) thermo-alkaline double-bleaching and (c) traditional treatments.	194

Figure 8.4. Spectrums of A) lignocellulosic melon by-products (LMB) and melon residues after hot-acid treatment and microcrystalline cellulose (MCC) from B) RHCl, C) RCA and D) RTA through the (a) thermo-alkaline, (b) thermo-alkaline double-bleaching and (c) traditional treatments.	196
Figure 8.5. Spectrum of microcrystalline cellulose (MCC) obtained by thermo-alkaline double-bleaching process from melon residues compared to commercial microcrystalline cellulose (MCC-C).....	197
Figure 8.6. Micrographs of A) LMB and freeze-dried MCC from B) RHCl (left-row), C) RCA (middle-row) and D) RTA (right-row) through the thermo-alkaline double-bleaching treatment.	199
Figure 9.1. a) Electrophoresis gel by SDS-PAGE from <i>Cucumis melo</i> L. <i>inodorus</i> peels and protein molecular size profile by FPLC of b) melon peel juice (MPJ) and c) proteins precipitated with ammonium sulphate MPJ-(NH ₄). M: molecular weight standards...	210
Figure 9.2. a) Turbidimetric evaluation of CUC-CRG non-soluble complex and b) Titration of CUC from melon peels juice with increasing concentration of CRG at different constant concentration of NaCl (Δ 0, ● 200, □ 400 and ■500 mM). All determinations were carried out in triplicated and mean value ± standard deviation...	212
Figure 9.4. a) Total protein content, b) recovery of proteolytic activity and c) milk-clotting activity measured in the complex (● COM) and in the supernatant (● SUP) at different initial concentration of CRG. Proteolytic activity was measured using azocasein 1% w/v; MCA; milk-clotting activity was measured at constant temperature (37 °C) and pH (6.5). All determinations were carried out in triplicated and mean value ± standard deviation.	216
Figure 9.5. Specific proteolytic activity of melon samples at different range of pH using azocasein (1% w/v) as substrate. MPJ: melon peels juice; MPJ-(NH ₄): melon peels juice precipitated with ammonium sulphate; COM 0.003: complex at 0.003% w/v of CRG. All determinations were carried out in triplicated and mean value ± standard deviation...	217
Figure 9.6. Effect of CaCl ₂ , pH and temperature on milk-cotting activity of the COM 0.003 (●) and MPJ (●). a) and b) Effect of CaCl ₂ concentration, c) and d) pH and e) and f) temperature. Data are average of three independent experiments ± standard deviation of determined clotting activity.	219

- Figure 10.1. Ice recrystallization inhibition. In the absence of ISPs, large ice crystals grow at the expenses of smaller ones (ice recrystallization). ISPs stabilize small ice crystals, inhibiting the recrystallization process. Ice crystal growth inhibition by AFPs formed a hexagonal plate with six prism planes visible. New disc adds on to the hexagonal plate with addition of AFPs, eventually forming an ice-crystal barrel that ultimately develops to a bipyramidal ice crystal. Adapted from and Mangiagalli et al. (2020).226
- Figure 10.2. Profile of melon peel proteins by FPLC before and after precipitation by κ -carrageenan (CRG). a) Melon peels juice (MPJ), b) MPJ subjected to precipitation with carrageenan (CRG), c) proteins precipitated by CRG at 0.003% (w/v) and solubilized in buffer of 0.5 M Tris-HCl – 0.5 M NaCl pH 8.2. COM 0.003: complex; SUP: supernatant.233
- Figure 10.3. Graphic representation of AuNPs-based colorimetric assay of AFP activity. In the presence of AFP, the self-assembly (blue) of AuNPs (red) is strongly inhibited after a freezing/thawing cycle, and the freeze-induced assembly can be quantified by the extinction spectrum. Adapted from Park et al. (2013).232
- Figure 10.4. Extinction spectra of AuNPs before and after freezing/thawing process reacted with proteins precipitated by κ -carrageenan (CRG). a) and b) Solutions of citrate gold nanoparticles (Cit-AuNPs) and c) citrate gold nanoparticles modified with mercaptosuccinic acid (Cit-MSA-AuNPs). Before: before freezing; After: after thawing.234
- Figure 10.5. Inhibition of ice recrystallization by melon proteins after precipitation by κ -carrageenan (CRG) (COM 0.003) after a) 5, b) 15 and c) 30 min of incubation at -20 °C. Proposed method.236
- Figure 11.1. Final proposed integrative process for melon peels valorisation into novel functional ingredients under biorefinery approach towards a circular economy-based value chain to achieve the United Nations Sustainability Development Goals.....244

Abbreviations

- AAPH** – 2,2'-azo-bis-(2- methylpropionamide)-dihydrochloride
- ABTS** – 2,2'-azino-bis(3-ethylbenzothiazoline-6-sulphonic acid
- ACI** – Accessibility index
- AD** – Anaerobic digestion
- AFGPs** – Antifreeze glycoproteins
- AFPs** – Antifreeze proteins
- ATPS** – Aqueous-two phase systems
- AuNPs** – Gold nanoparticles
- BC_{DS-IP}** – Bioactive content in the digested sample at the intestinal phase
- BM** – Bioactive molecules
- BS** – Bloodstream
- BSA** – Bovine serum albumin
- CA** – Citric acid
- Cit-AuNPs** – Citrate gold nanoparticles
- COM** – Complex
- CRG** – Carrageenan
- CUC** – Cucumisin
- D-GalA** – *D*-galacturonic acid
- DAD** – Diode Array Detector
- DM** – Dry matter
- DPPH** – 2,2-diphenyl-1-picrylhydrazyl
- DW** – Dry weight
- EAE** – Enzymatic assisted extraction
- EC** – Emulsifying capacity
- ES** – Emulsion stability
- FOS** – Fructooligosaccharides
- FPLC** – Fast Protein Liquid Chromatography

FW – Fresh weight

GAE – Galic acid equivalents

GIT – Gastrointestinal tract

Glu – Glucose

GUAE – Galacturonic acid equivalents

HPLC – High Performance Liquid Chromatography

IRI – Inhibition of the recrystallization

ISP – Ice structuring proteins

LF – Liquid fraction

LMB – Lignocellulosic melon by-products

MCA – Milk-clotting Activity

MCC – Microcrystalline cellulose

MCU – Milk-clotting units

MPF – Melon peel flour

MPJ – Melon peel juice

MPJ-(NH₄) – Melon peels juice precipitated with ammonium sulphate

MSA – Mercaptosuccinic acid

MW – Molecular weight

OD – Optical density

PA – Proteolytic activity

PCA – Pectin from citric acid

PCP – Pectin from citrus peel

PF – Purification factor

PF- Pellet fraction

PHCl – Pectin from hydrochloric acid

PPP – Protein precipitation by polysaccharides

PTA – Pectin from tartaric acid

RCA – Residues from citric acid

RHCl – Residues from hydrochloric acid

- RI** – Recovery index
- ROS** – Reactive oxygen species
- RTA** – Residues from tartaric acid
- SCFA** – Short chain fatty acids
- SDGs** – Sustainable Development Goals
- SEC** – Size Exclusion Chromatography
- SF** – Solid fraction
- SMCA** – Specific milk-clotting activity
- SPA** – Specific proteolytic activity
- SSF** – Solid-state fermentation
- SUP** – Supernatant
- TA** – Tartaric acid
- TC** – Total carbohydrate content
- TCC** – Total carotenoid content
- TCHC** – Total chlorophyll content
- TE** – Trolox equivalents
- THPs** – Thermal hysteresis proteins
- TPC** – Total phenolic content

Scope and outline

Preliminary note: The core of this research thesis comprises 2 reviews of the state of the art (both published) and 8 research papers: 2 published and 3 submitted and 3 under preparation to submit in Peer-reviewed international scientific journals.

This thesis is organized into four parts divided in thirteen chapters. Each different chapter describes how the research/project was evolved throughout the four years of the Ph D program.

The main objective of this research thesis was to develop and characterize functional ingredients through the valorisation of melon by-products (peels) and the evaluation of their bioactive and functional properties for potential industrial applications. A green chemistry approach within the framework of circular economy and zero-waste context was employed to develop an integrative process that enables the production of value-added fractions, avoiding the use of toxic and hazard chemicals, leading to the development of low cost and clean label ingredients. In this regard, three different fractions rich in bioactive compounds such as pigments, pectin, microcellulose and proteins were developed, which could be applied in diverse food, nutraceutical and pharmaceutical industries. The thesis was divided in different parts and chapters in order to systematize the sequence and content of the studies.

Part I include Chapters 1 and 2. The Chapter 1 provides a general revision of the state of the art on industrial food by-products, including generation and valorisation throughout the years for the obtainment of value-added products through different extractive methodologies. Chapter 2 provides a literature revision particularly focused on the richness of phytochemicals and biofunctional molecules present in melon fruit and its by-products and their importance to be valorised due to their bioactive properties and potential industrial applications.

Part II encompasses Chapters 3 to 6. After all the theoretical exploration of food by-products valorisation and their biofunctional characteristics explained in the previous chapters, this part started with Chapter 3 in which a total fractionation of melon peels, evaluating their chemical composition, bioactive compounds and antioxidant properties towards functional food ingredients for latter application in different studies is described. In Chapter 4, we describe the potentiality to obtain proteins, chlorophylls and xanthophylls from a pigment-rich fraction (pellet fraction) using integral fractionation

strategies. Chapter 5 shows the applications of the liquid fraction (melon peel juice) as a carrier of bioactive compounds and the evaluation of their antioxidant and prebiotic activity affected by the impact of the *in vitro* gastrointestinal tract passage. Chapter 6 explores the potential application of the solid fraction (melon peel flour) as a functional flour with prebiotic effect upon human intestinal microbiota after its exposure to the gastrointestinal tract conditions.

Part III explores an alternative approach for melon solid fraction including the extraction and characterization of value-added ingredients (pectin and cellulose) with prospective industrial interest and encompasses Chapters 7 and 8. Chapter 7 describes the valorisation of melon peels as a rich source of pectin, reporting extraction by different acid agents and evaluation of its physicochemical properties. Chapter 8 depicts a biorefinery approach on microcrystalline cellulose development and its physicochemical characteristics obtained from melon peel residues generated after pectin extraction.

Part IV is divided in Chapter 9 and 10, where a green chemistry approach was applied for the extraction of functional/bioactive proteins from melon liquid fraction, using green precipitation with carrageenan. Chapter 9 is focused on the design of a strategy for the recovery of the enzyme cucumisin by forming a non-soluble complex conducted by the interaction with carrageenan well-known as a safe polysaccharide. Chapter 10 describes the identification and characterization of novel protein-like antifreeze proteins after green precipitation process applied on melon liquid fraction.

Part V incorporates Chapters 11 and 12, concluding with the most relevant outputs and future research developments that this research work could offer in the near future, respectively.

Figure 1 shows the schematic organization (parts and chapters) of this thesis.

Part I: State-of-Art

CHAPTER 1

Valorisation of food agro-industrial by-products: from the past to the present and perspectives

CHAPTER 2

Valorization of melon fruit (*Cucumis melo* L.) by-products: phytochemical and biofunctional properties with emphasis on recent trends and advances

Part II: Production, characterization and bioactivity

CHAPTER 3

A chemical valorisation of melon peels towards functional food ingredients: bioactives profile and antioxidant properties

CHAPTER 4

Valorisation of pigments protein enriched fraction from melon peels (*Cucumis melo* L. *inodorus*) to complete integral valorisation as a zero-waste approach

CHAPTER 5

Impact of *in vitro* simulated digestion on bioactive compounds, bioactivity and cytotoxicity of melon (*Cucumis melo* L. *inodorus*) peel juice

CHAPTER 6

Prebiotic effect of melon peel (*Cucumis melo* L. *inodorus*) flour on human gut microbiota after *in vitro* gastrointestinal digestion: bioactive compounds and antioxidant properties assessments

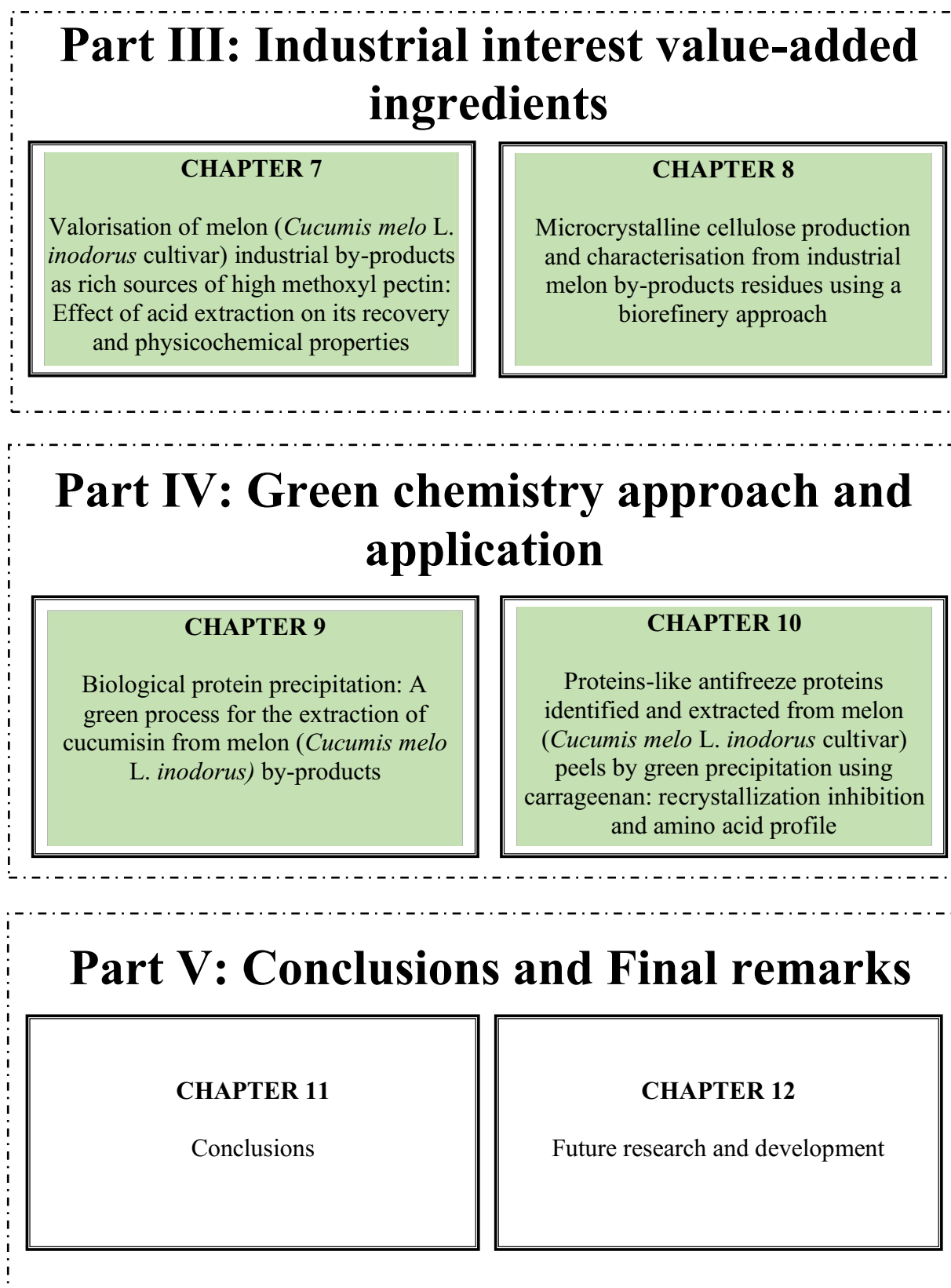


Figure 1. Structure of thesis outline.

Most of the research data presented in chapters that constitute this dissertation have been already submitted and/or published in international peer reviewing scientific journals, according to the following list:

Chapter 1:

Ricardo Gómez-García, Débora A. Campos, Cristobal N. Aguilar, Ana R. Madureira and Manuela Pintado, 2021. Valorisation of food agro-industrial by-products: from the past to the present and perspectives. *Published in the Journal of Environmental Management* **299**, 113571, Elsevier. <https://doi.org/10.1016/j.jenvman.2021.113571>

Chapter 2:

Ricardo Gómez-García, Débora A. Campos, Cristobal N. Aguilar, Ana R. Madureira and Manuela Pintado, 2020. Valorization of melon fruit (*Cucumis melo* L.) by-products: Phytochemical and biofunctional properties with emphasis on recent trends and advances. *Published in the Journal of Trends in Foods Science and Technology* **99**, 507–519, Elsevier. <https://doi.org/10.1016/j.tifs.2020.03.033>

Chapter 3:

Ricardo Gómez-García, Débora A. Campos, Ana Oliveira, Cristóbal N. Aguilar, Ana R. Madureira and Manuela Pintado, 2020. A chemical valorization of melon peels toward functional food ingredients: bioactives profile and antioxidant properties. Published in the *Journal of Food Chemistry*. Vol 335. Elsevier. <https://doi.org/10.1016/j.foodchem.2020.127579>

Chapter 4:

Ricardo Gómez-García, Bárbara M.C. Vaz, Margarida Martins, Manuela Pintado, Sónia P.M. Ventura. Ventura, 2021. Valorisation of pigments protein enriched fraction from melon peels (*Cucumis melo* L. *inodorus*) to complete integral valorisation as a zero-waste approach. *(Under preparation)*

Chapter 5:

Gómez-García, R., Campos, D. A., Aguilar, C. N., Madureira, A. R., and Pintado, M., 2021. Impact of *in vitro* simulated digestion on bioactive compounds, bioactivity and cytotoxicity of melon (*Cucumis melo* L. *inodorus*) peel juice. *Submitted to the Journal of Food and Function*.

Chapter 6:

Ricardo Gómez-García, Mónica Sánchez-Gutiérrez, Célia Freitas-Costa, Ana A. Vilas-Boas, Débora A. Campos, Cristóbal N. Aguilar, Ana R. Madureira and Manuela Pintado. 2021. Prebiotic effect, bioactive compounds and antioxidant activity of melon peel (*Cucumis melo L. inodorus*) flour subjected to in vitro gastrointestinal digestion and human faecal fermentation. ***Submitted to the Journal Food Research International - FOODRES-S-21-06512.***

Chapter 7:

Ricardo Gómez-García, Débora A. Campos, Cristóbal N. Aguilar, Ana R. Madureira and Manuela Pintado. 2021. Valorisation of melon (*Cucumis melo L. inodorus* cultivar) industrial by-products as rich sources of high-methoxyl pectin: Improvement of hot-acid extraction and performance properties. ***Submitted to the journal Carbohydrate Polymers - CARBPOL-S-21-06294.***

Chapter 8:

Ricardo Gómez-García, Débora A. Campos, Cristóbal N. Aguilar, Ana R. Madureira and Manuela Pintado. 2021. Microcrystalline cellulose production and characterisation from industrial melon by-products residues using a biorefinery approach. ***Submitted to the journal Bioresource Technology – BITE-S-21-09875.***

Chapter 9:

Gómez-García, R., Campos, D. A., Aguilar, C. N., Madureira, A. R. and Pintado, M. 2021. Biological protein precipitation: a green process for the extraction of cucumisin from melon (*Cucumis melo L. inodorus*) by-products. ***Published in the Journal of Food Hydrocolloids, 116, 106650. Elsevier. <https://doi.org/10.1016/j.foodhyd.2021.106650>***

Chapter 10:

Ricardo Gómez-García, Débora A. Campos, Cristóbal N. Aguilar, Ana R. Madureira and Manuela Pintado. 2021. Proteins-like antifreeze proteins identified and extracted from melon (*Cucumis melo L. inodorus* cultivar) peels by green precipitation using carrageenan: recrystallization inhibition and amino acid profile. ***Submitted to the Journal of Food Hydrocolloids.***

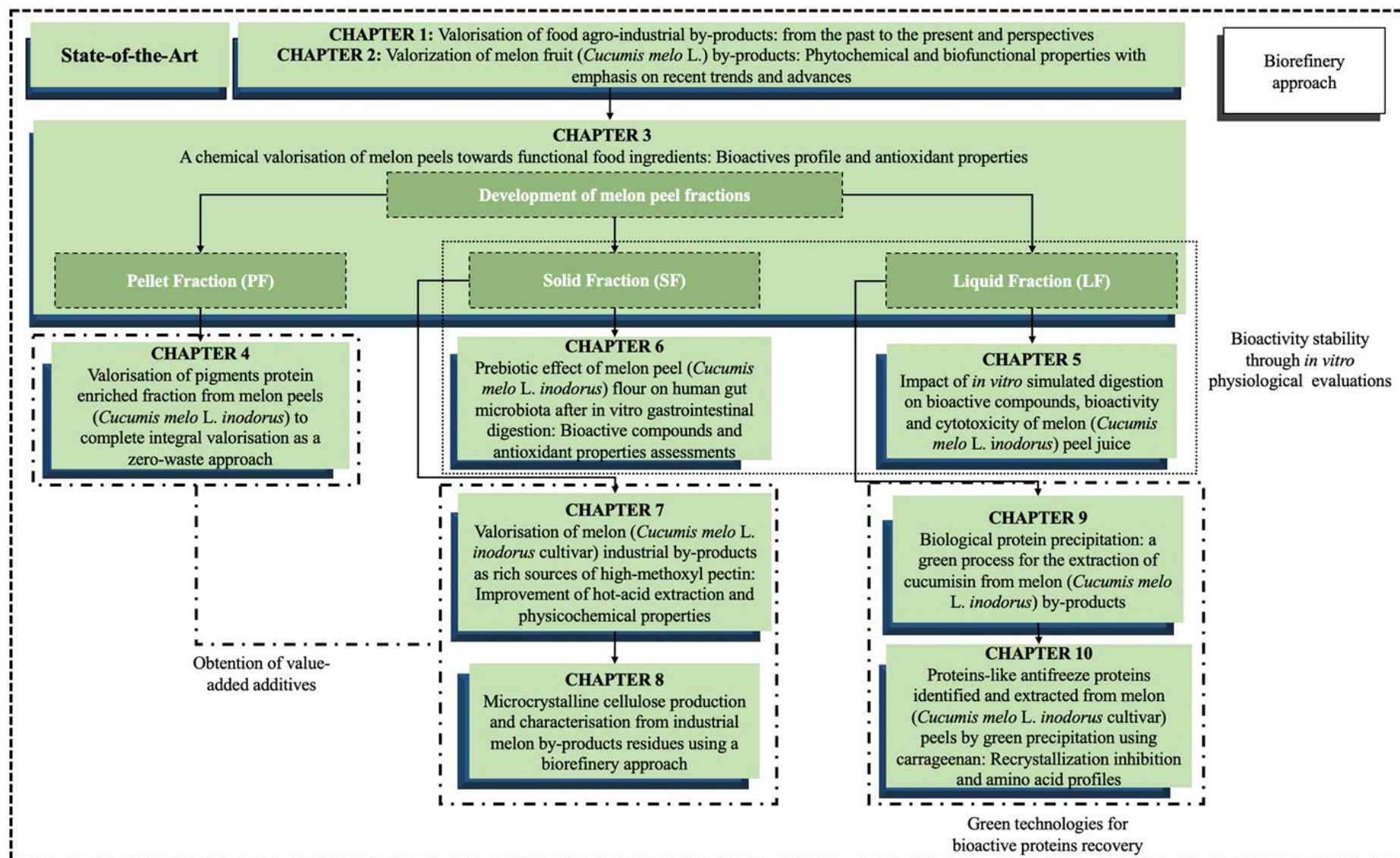


Figure 2. Schematic flow chart for melon peels valorisation and their respective evaluations throughout this research work.

PART I - Bibliographic Survey

CHAPTER 1 - Valorisation of food agro-industrial by-products: from the past to the present and perspectives

Ricardo Gómez-García^{a,b}, Débora A. Campos^a, Cristóbal N. Aguilar^b, Ana R. Madureira^a and Manuela Pintado^{a*}

^a*Universidade Católica Portuguesa, CBQF - Centro de Biotecnologia e Química Fina – Laboratório Associado, Escola Superior de Biotecnologia, Rua Diogo Botelho 1327, 4169-005, Porto, Portugal*

^b*BBG-DIA. Bioprocesses and Bioproducts Group. Food Research Department, School of Chemistry, Autonomous University of Coahuila, Saltillo, Coahuila, Mexico*

Published:

Journal of Environmental Management - Elsevier

Abstract

Food agro-industrial by-products mainly include peels, seeds, stems, bagasse, kernels, and husk, derived during food processing. Due to their overproduction and the lack of sustainable management, such by-products have been conventionally rejected and wasted in landfills, being the principal strategy for their treatment, but nowadays, this strategy has been associated with several environmental, social and economic issues. Hence, we focused on the use of different consolidated biotechnological processes and methodologies as suitable strategies for food by-products management and valorisation, highlighting them as potential bioresources because they still gather high compositional and nutritional value, owing to their richness in functional and bioactive molecules with human health benefits. Food by-products could be utilised for the development of new food ingredients or products for human consumption, promoting their integral valorisation and reincorporation to the food supply chain within the circular bioeconomy concept, creating revenue streams, business and job opportunities. In this review, the main goal was to provide a general overview of the food agro-industrial by-products utilised throughout the years, improving global sustainability and human nutrition, emphasising the importance of biowaste valorisation as well as the methodologies employed for the recovery of value-added molecules.

Keywords: Food by-product, biowaste valorisation, bioactive molecule, green chemistry, circular bioeconomy, resource recovery.

1. Introduction

Currently, it is well-known that food industries generate vast quantities of lignocellulosic by-products from the processing of beer, wine, sugar cane, coffee dregs, vegetables and fruits, among others, which generally are rejected as waste and often have been considered as environmental pollutants (Mallek-Ayadi et al., 2018). These food by-products include a wide range of husk, seeds, stems, roots, pulp remnants, bagasse and peels, which despite their nutritional value, still are dismissed by industries (Da Silva et al., 2014). Globally, the current disposal and poor management of food agro-industrial by-products have demonstrated a negative impact on the environment and the social and economic sectors. In this case, the environment is contaminated by Greenhouse Gas (GHG) emissions because many times, these organic materials are just discarded in landfills, or they are burned to avoid microorganisms, parasites and pests accumulation (Winans et al., 2017). Moreover, these current strategies for food waste management, including disposition in landfills, incineration, and composting and animal feeding, are not considered sustainable or environmentally friendly strategies. Also, these management strategies take part of the social sector due to some respiratory health diseases can be emerged from the toxic pollutants liberated into the air, decreasing human life quality (D'Amato et al., 2010; Blahuskova et al., 2019). On the other hand, from the economic point of view, the circular economy concept has been promoting suitable strategies to manage and valorise these by-products to reduce pollution and promote a sustainable bioeconomy growth between industries, designing and creating new revenue streams (Winans et al., 2017). Thus, such improvements could be achieved through an integral valorisation of this food biowaste since it keeps high content of value-added bioactive molecules (BM), which could be extracted and used as novel industrial raw materials due to they have been shown to possess several bioactive applications (Gómez-García et al., 2021b).

In this regard, the BM work as nutrients and are usually used by plants to protect them against diseases, insects and microorganisms (Ullah et al., 2014). According to their activity in plant metabolism, these molecules are mainly divided into two groups: primary and secondary constituents. Primary constituents contain sugars, amino acids, proteins and chlorophylls, while secondary components comprise alkaloids, flavonoids, saponins, tannins, carotenoid, phenolic compounds and many others (Poiroux-Gonord et al., 2010; Sepúlveda et al., 2012; Rodríguez-Pérez et al., 2013; Shi et al., 2015). Moreover, the BM have shown different applications, especially promoting human health. Indeed, a positive

correlation has been reported for the consumption of these molecules, decreasing the risk of several chronic diseases, including obesity, cardiovascular diseases and certain types of cancer (Ismail et al., 2010). Also, these BM have been shown to have great potential applications in the cosmetic, textile and food industries (Lai et al., 2015; Saini et al., 2015). Thus, by these beneficial characteristics and applications of the BM, different researchers have been intensified their studies to develop biotechnological methodologies to valorise food by-products, such as solid-state fermentation (SSF), enzymatic assisted extraction (EAE), anaerobic digestion (AD), aqueous-two phase systems (ATPS) and protein precipitation by polysaccharides (PPP). In turn, SSF has been defined by different authors as a bioprocess employed within a solid porous matrix with the absence of nearby absence of free water but with enough moisture for microbial growth (Martins et al., 2011). The EAE is based on the cell-wall hydrolysis by cellulolytic enzymes that can break down the cell wall, liberating the intracellular materials linked to the cell polymers (cellulose, hemicellulose and lignin), being exposed for their extraction (Gómez-García et al., 2012). The AD is a process that uses organic waste in the absence of oxygen and transforms it into fuels (Fagbohunge et al., 2017). The ATPS is an ideal separative technique for BM (enzymes and polyphenols) recovery due to its high water content and low interphase tension, which provides favourable conditions for their stability (Sánchez-Trasviña et al., 2015). The PPP is an extractive method that employs electric charged polysaccharides that can interact with proteins, arising soluble or non-soluble complexes by altering pH or ionic strength, conserving their structure and biological activity (Woitovich, Brassesco, and Picó, 2016).

For several years, sustainable chemistry has prompted a significant number of studies highlighting food by-products as rich sources of BM. Such studies have been adopted different strategies to valorise them I) starting with a complete chemical characterisation to identify the target value-added compounds, II) design friendly methods and downstream platforms for their extraction and finally III) the evaluation for their potential application at pilot and industrial scale, guaranteeing food by-products reincorporation to the food value chain as functional food ingredients or additives (Campos et al., 2017; Larios-Cruz et al., 2017; da Silva and Jorge, 2017). The purposes of this review article are to (i) show the potential of food by-products as renewable raw materials to obtain BM and (ii) their applicability in some industries aimed at their employment to reduce environmental, social and economic problems. The following examples have been selected according to available information and their evidence in the recovery of BM by

diverse extractive methodologies.

1.1. From the past: Traditional and soft chemistry for agro-food by-products exploitation

Relevant events have always accompanied human being history. One of them is the "Second Industrial Revolution", where new energy sources, such as electricity and petroleum derivatives (fuels) were developed. For many years both have been increasing the industrial economy positively. Still, unfortunately, the negative environmental impact has been improved as well. Moreover, with the petroleum usage began the "era of plastics", which was the trending topic in Science and Technological studies of research, developing new suitable materials instead of the use of steel and iron ones (Day, 1914), such revolutionary event was ended in the second decade of XIX century (Dombrowski and Wagner, 2014).

On the other hand, while these research works were carried out, different other studies using diverse natural resources were carried out. In turn, some researchers employed unconventional organic materials, which were generated as secondary kinds of stuff (lignocellulosic by-products) during food processing, such as corncobs, cornstalk, husk, grains, bagasse, kernels, peels, etc., to produce different value-added compounds. E.g., Laforge and Mains (1923) utilised corncobs from the corn industry to produce furfural, employing a digester at 180 °C and high-pressure steam, obtained values of recovery between 97 to 98% and also small quantities of acetic acid, acetaldehyde and methanol. A few years later, Albert et al. (1930) published a review highlighting the greatest chemistry services for utilisation of biowaste produced from agricultural industries, where they said that such raw materials were worthless without treatment but could be transformed by chemistry into value-added resources for industrial applications. They also mentioned the employment of corncob to develop commercial products, such as furfural, glue, xylose, lactic acid, acetic acid and oxalic acid, which were obtained by the fusion of the cobs with caustic soda. In the sequence of investigations on the utilisation of this kind of biowaste Levine et al. (1935) carried out a research study for the isolation of organisms capable of hydrolysing lignin from cornstalk under anaerobic conditions. Further, they reported some results about the effect on gas production through this process using different mixture ratios of cornstalk flour/packing sludge and different conditions of time (1 to 50 days), temperature (28–30 °C) and alkali pH (7.0 – 8.0). Particularly, most of these studies on agro-food by-products utilisation were developed under

thermodynamic and pyrolysis process (high temperatures and pressures) to obtain valuable products (**Figure 1.1**). Such is the case of McElhinney et al. (1938), they treated corncobs by destructive distillation process at pyrolysis temperatures between 212 to 537 °C for the obtention of acetic acid, acetone, formic acid, methanol and soluble tar. Baumgarten et al. (1944) also used corn by-products for carotenoids extraction, such as xanthophyll, cryptoxanthol and carotene for animal feed through conventional continuous Soxhlet system and organic solvents. Later, Neubert et al. (1954) employed pear by-products to recover sugars and other soluble solids from juice industries. Their study aimed to obtain sugars to replace conventional refined sugar used in the canning fruit industry. Additionally, they described a little feasible economic research and pilot plant application from the research study, where the use of commercial pectic enzymes allowed to separate soluble from the insoluble fraction in the presence of calcium. Long and Patrick, (1965) investigated the conversion of citrus by-products to 2,3-butylene glycol by *Bacillus polymyxa* through the fermentative process, obtaining yields ranged from 2.3 to 4.4%.

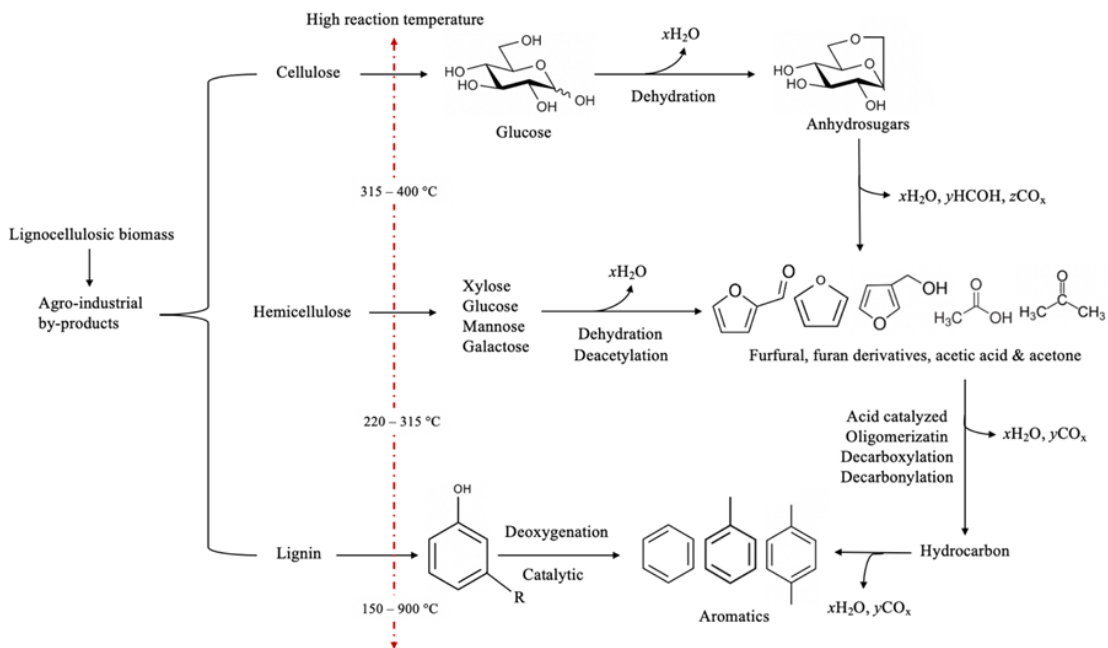


Figure 1.1 - Chemical reactions of the catalytic pyrolysis of lignocellulosic biomass at high temperatures between 300 to 900 °C. Adapted from Tan et al. (2013) and Kim and Choi, (2018).

The utilisation of food processing by-products has been reviewed by Ben-Gera and Kramer, (1969) mentioning a significant number of research studies carried out during the first half of the XX century, covering almost 40 years since 1930-1969. They mainly discussed and showed important information about many studies within food by-products

utilisation and their potential application. Sorting, peeling, trimming, and coring were the main industrial activities that generated many food by-products from the processing of vegetables and fruit. The vegetable and fruit by-products consisted mainly of peels, cores, pits, seeds, culls and overripe and blemished material. **Table 1.1** shows a spectrum of the most generated food by-products in the sixties derived from the processing industries of apple, pear, banana, tomato, beans, potatoes, grape and citrus (fresh basis), highlighting their worthy utilisation for pectin production, protein recovery, oils and flavonoids extraction instead of being only directed for cattle feed (Ben-Gera and Kramer, 1969).

Table 1.1. Spectrum of the most food by-products generated during 60's provided by Ben-Gera and Kramer, (1969).

Vegetable crops: Losses related to the processing^a				
Commodity	Report I	Report II	Report III	Report IV
Asparagus	3.2	41	30	-
Beans, green	5.0	12	-	20
Beans, lima	6.0	85	-	-
Beets	7.0	25	38	40
Carrots	18.0	33	-	52
Corn	20.0	86	72	-
Potatoes	5.0	-	-	-
Tomatoes	5.0	25	-	-
Fruit-processing^a				
Apples	35	47	12	55
Grapefruit	58	-	3.0	-
Lemons	-	-	3.0	-
Orange	-	-	3.0	-
Peaches	40	11	20	-
Pears	42	46	12	-

^aData presented given in % of weight

Data of Reports II, III, IV were based on amount of waste produced from total raw material, whereas the data from Report I were related to loss of edible material only.

Certainly, the plastic era was a consolidated research theme during those years within science and technology development. However, in the early eighties this era finished and the scientists extended their attention and interest to the development of eco-products from food by-products through environmental-friendly processes, promoting a sustainable food production to face the exponential world population increment (Tóth, 1979). Researchers started to recognise food by-products as cheap resources for the obtention of new food ingredients and BM and change the traditional methodologies for a novel eco-friendly and cost-efficient processes for their development and recovery, respectively. Therefore, they began to observe biological processes carried out by nature, which enable to obtain value-added molecules through soft and suitable approaches. The challenges then began to find efficient strategies to implement/simulate these natural

processes to manage agro-food by-products and obtain different valuable products (Bensaude-Vincent and Simon, 2008). Until now, almost all the studies were traditionally performed under extreme and time-consuming conditions, high temperature (higher than 100 °C) and pressure (greater than 1 atm), making costly processes in terms of energy consumption, as well as employing large amounts of toxics, dangerous or corrosive substances, (e.g., hexane, ether, sulfuric or phosphoric acids), delivering contaminant effluent discharges (Wikandari et al., 2015). For these unfavourable reasons using traditional chemistry, arose the biotechnology, which prompted the use of good and safe chemistry, aiming to perform and design eco-friendly processes. Following this, in 1977 Jacques Livage said, "it is possible to carry out chemical reactions at mild temperatures just as in nature, in heterogeneous and aqueous environments" by ending as the principle of "Soft Chemistry" (Douce Chimie). Subsequently, considering these characteristics Lonsane, (1985) described a bioprocess that microorganisms could carry out in solid matrices, where they can grow naturally because of their ability to produce hydrolytic enzymes that can degrade lignocellulosic biomass; this biotechnological approach was called SSF. Later, this method was gained great popularity among some researchers due to it has been attributed with several advantages, regarding high yields/productivities and better product characteristics aimed to its easy reproducibility, and meanly to its great applicability for the production of diverse number of products with industrial interest, including sugars, pigments, phenolic antioxidants and enzymes (**Figure 1.2**) (Viniegra-González et al., 2003). Yang, (1988) employed this method for protein production by amylolytic yeasts utilising sweet potato residues. Garzón and Hours, (1992) used citrus by-products as a substrate for pectinase production by *Aspergillus foetidus* (NRRL 341, ATCC 16878). Thus, SSF methodology converges as a biotechnological process and as a new alternative for the obtention of prized molecules, carried out in a clean environment, free of pollutants and solvents that can be toxic a negative impact on human health.

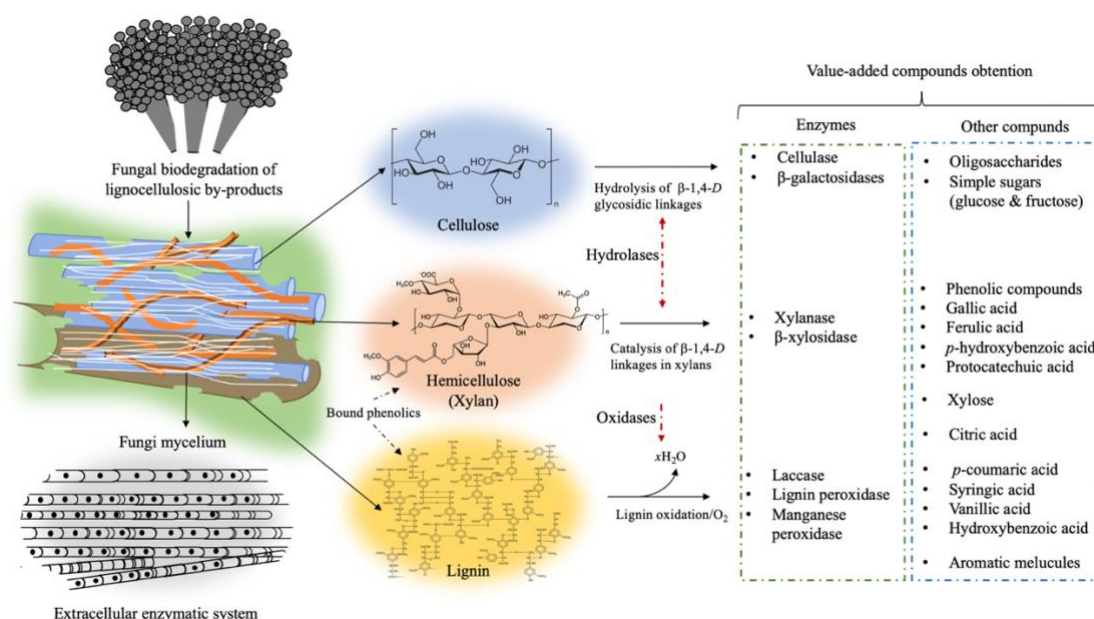


Figure 1.2. Schematic representation of lignocellulosic biomass degradation by solid-state fermentation as a suitable alternative for food waste management and obtention of value-added compounds.

1.2.1. To the present: Agro-food by-products as bioresources, not as pollutants

Indeed, the amount of food by-products available in the past was smaller than the amount currently quantified. Globally is estimated average production of 1.3 billion tons of food by-products, being wasted by the food producers and processing industries with an estimated economic loss of 990 billion dollars. In the United States, 88 million tons of food are wasted every year, equivalent to over 170 million tons of CO_2 with an expected economic loss of 165.6 billion dollars. In 2017, Europe generated 96 million tons of fruits and vegetables, corresponding to 8.5% of the global production and around 30% of that production was discarded as waste (Trigo et al., 2019). According to the FAO (2013), food waste is responsible for 26% of global GHG emissions annually, equivalent to 3.3 Gtons of CO_2 (Martin-Rios et al., 2021). Thus, over the past 50 years, the intensification of agricultural, livestock breeding and food industrial activities have been the principal authors of the overproduction and accumulation of food by-products (Serna et al., 2016; Chojnacka et al., 2021). However, there are no detailed reports on the number of by-products generated from different food processing industries. **Table 1.2** provides an estimation of food by-products generated in 2016 in the form of pomace, bagasse, peels, seeds, cores, husk and stems, being pineapple, melon, apple and tomato the most relevant

crops delivering high amounts of by-products, accounting in total more than 50 million tons after their processing (Ravindran and Jaiswal, 2016; Campos et al., 2020b).

Table 1.2. List of the most representative food agro-industrial by-products according to Ravindran and Jaiswal, (2016) and Rabelo et al. (2011)*.

By-product	Volume available (Ton/year)	Region
Pineapple stem and peels	17,000,000	Worldwide
Melon peels and seeds	12,000,000–3,400,000	
Apple pomace	3,000,000 – 4,200,000	
Olive pomace	2,881,500	
Rice husk	120,000	
Brewer' spent grain	30,000	
Potato peel	70–140	
Tomato pomace	4,000,000	Europe
Cereal waste	40,000–45,000	France
Grape pomace	700	
Vegetable oil	50,000–100,000	
Wheat straw	57,000	USA
Orange peel	700	USA
Sugarcane bagasse*	170,000,000	Brazil

Currently, by-products from food agro-industries are major sources of pollution and can be categorised depending on agricultural activity (**Table 1.3**). In general, these by-products can be arising from different factors, such as during production (non-compliant food), distribution (damaged food) or inadequate storage (rotten food) (Bilal et al., 2017). Generally, these by-products are mainly composed of complex polysaccharides, proteins, carbohydrates, polyphenolic compounds, vitamins, among other relevant compounds (Yusuf, 2017). On the other hand, in serious consideration of global environmental, social and economic issues, researcher scientists have been re-directing their interest in recycling and valorising the food by-products to minimise their negative impact. In the last decade, European waste management has moved forward, for example, in 2005, 63% of food waste was disposed in landfills, while ten years later, this average has been minimised to 24%. Besides, in 2005, only 11% of such waste was recycled, while ten years later, its recycling increased more than two times (above 25%) and is expected to reach higher than 60% by 2030 (Matharu et al., 2016; Imbert, 2017). Nowadays, these sources have been employed by scientists developing new technological tools within the context of soft chemistry to obtain new and diverse bioproducts, performing careful reactions, non-toxic usage of organic solvents, as well as less energy consumption (Bensaude-Vincent and Simon, 2008). Soft chemistry is a type of mild reactive condition that allow obtaining materials or other compounds, which are hard to produce under

classical conditions (e.g., high temperatures). Reactions involved in soft chemistry are included, namely intercalation, deintercalation,

Table 1.3. Types of lignocellulosic waste depending on the agricultural activity (Yusuf, 2017).

Agricultural activity	Characteristics	Disposal
Crop production and harvest	Straw and Stover	Land application, plowing, burning
Fruit and vegetable processing	Biological sludge, trimmings, peels, soils, seeds and pits	Landfilling, animal feed, land application, burning
Sugar processing	Biological sludge, pulp, lime mud	Landfilling, burning, composting, animal feed land application, fertilizer
Dairy product processing	Biological sludge	Landfilling, land spreading
Leather tanning	Fleshings, hair, raw and tanned trimmings, lime and chrome sludge, grease	By-product recovery, landfilling, land spreading
Rice production	Bran, straw, hull	Feeds, mulch/soil conditioner packaging material for glass and ceramics
Coconut production	Stover, cobs, husk, leaves coco meal	Feeds, vinegar, activated carbon, coir production

cation exchange, dehydration, dihydroxylation, redox, and others (Figlarz, 1994). Recently, studies on by-products valorisation from the food supply chain open avenues to the production of different bioproducts, which could help in the improvement of environmental, social and economic sectors, such as biofuels, enzymes, phytochemicals, and functional ingredients, among other molecules (Ravindran and Jaiswal, 2016). **Table 1.4** contain some chronological studies that were carried out throughout time, regarding food by-products exploitation and the obtention of value-added products, emphasising the utilisation of corn cobs and grains for furfural and carotenoids production, respectively (1923), pear pomace for sugars recovery (1954), lime peels for methane production through AD (1983), orange peels for limonene extraction by steam explosion (2011), banana peels for bioethanol production through EAE (2017) and olive pomace for polyphenols extraction and dietary fibre utilisation by faecal fermentation (2021).

Table 1.4. Spectrum of research studies through the time regarding utilization and valorisation of different food agro-industrial by-products.

Agro-food	By-product	Methodology	Product obtained	Reference
Corn	Corncobs	High pressure digester	Furfural	Laforge and Mains, (1923)
Corn	Corncobs	-	Furfural	Albert, (1930)
Corn	Cornstalk	Microbial anaerobic digestion	Fuel gas	Levine et al. (1935)
Corn	Corncobs	Destructive distillation	Methanol; Acetic acid; Acetone	McElhinney et al. (1938)
Corn	Fermented grains	Alcoholic extraction and Soxhlet system	Carotenoids	Baumgarten et al. (1944)
Pineapple	Husk	Ion exchange		Felton, (1949)
Pear	Skin and pomace	EAE	Sugars	Neubert et al. (1954)
Citrus	Citrus molasses	Liquid fermentation by <i>Bacillus polymyxa</i>	Alcohol	Long and Patrick, (1965)
Cassava	Roots	Chemical extraction	Protein	Tóth, (1979)
	Leaves		Starch	
Lime	Peels	AD	Gas methane	Lane, (1983)
Sweet potato	Peels trimming	SSF	Proteins	Yang, (1988)
Orange	Bagasse	SSF	Pectinase	Garzón and Hours, (1992)
Mango	Kernels	EAE	Glucose recovery	Velan et al. (1995)
Pineapple	Peels	SSF	Citric acid	Tran and Mitchell, (1995)
Tomato	Bagasse	Chemical and enzymatic process	Biodegradable films	Poli et al. (2007)
Tomato	Bagasse	Ultrasonic bath and high-performance homogenizer	Polyphenolic Antioxidants	Savatović et al. (2010)
Orange	Peels	Steam explosion	Limonene	Pourbafrani et al. (2010)
Grapes	Skin	SSF	Polyphenolic antioxidants	Martínez-Ávila et al. (2012)
Pomegranate	Peels	SSF	Ellagitannins/Ellagic acid	Ascacio-Valdés et al. (2014)
Gac	Peels	Methanol and Ethanol extraction	Carotenoids	Chuyen et al. (2015)
Lemon	Peels	Traditional Soxhlet extraction	Limonene	Lopresto et al. (2014)
Mango; Passion fruit; Papaya; Melon	Seeds	Cold extraction with chloroform, methanol and water	Fatty acids; Phenolic compounds; Carotenoids	da Silva and Jorge, (2017)
Grapefruit	Bagasse	SSF	Polyphenolic antioxidant	Larios-Cruz et al. (2017)
Orange	Peels	EAE	Pectin and Limonene	John et al., (2017)
Banana	Peels	EAE	Bioethanol	Palacios et al., (2017)
Passion fruit	Peel flour	ATPS	Polygalacturonase enzyme	de Carvalho Silva et al. (2018)
Corn	Corncobs	SSF - ATPS	Xylanase enzyme	Gómez-García et al. (2018)
Orange and Grapefruit	Pulp and Peels	Simultaneous steam distillation and solvent extraction	Volatile flavours	Das et al. (2019)
Tomato	Seed/skin	Ohmic heating extraction	Carotenoids	Coelho et al. (2019)
Coffee	Pulp	SSF	n-demethylases	Peña-Lucio et al. (2020)
Olive	Pomace	Fermentation	Polyphenols – Dietary fibre	Ribeiro et al. (2021)

EAE: enzymatic assisted extraction; SSF: solid state fermentation; anaerobic digestion; ATPS: aqueous two-phase systems.

As the same in the past, BM are continuously the research target, especially by their diverse industrial applications and their great functionality on human health. These BM still are present in significant concentrations in the food by-products, but many cases are not directly available (Dey et al., 2016; Gómez-García et al., 2020). There is an extensive number of research articles about the recovery of polyphenols, carotenoids, chlorophylls, terpenes, flavonoids, oils, organic acid, among other molecules from food by-products describing their extraction and production methodologies through traditional (organic solvents extraction and steam explosion) and novel process (SSF), which have been summarised in **Table 1.5**. Furthermore, production and extraction of proteins with biological activity, also called enzymes, through biotransformation of food by-products have been shown to be strong and important themes of researches from the last ten years (**Table 1.6**) (Panda et al., 2016; Nadar et al., 2017), since enzymes are biocatalysts that shown interesting characteristics for many industries (Stocks, 2013), they have some advantages upon chemical catalysts due to their high specificity, work in mild conditions, reduce time and steps process, minimise toxicity and preserve the environment (Rao et al., 2016). Therefore, having all this evidence in mind and knowing that food by-products are sources of important high value-added compounds, these by-products could be valorised by industries, implementing some of those biotechnological processes within their facilities for the treatment and management of their food by-products to develop novel food products.

In resume, even though the extraction processes of BM in the food industry were achieved through chemical synthesis, using distillation, solvent and supercritical fluids extraction, food by-products were highlighted as valuable renewable raw materials, which should be valorised to generate value-added compounds and avoid pollution caused by their poor management and disposal in landfills. On the other hand, biotechnological methodologies in soft and fine chemistry terms could provide novel, cost-effective and eco-friendly routes with better outputs, which could satisfy the objectives of the circular economy.

1.2.2 Future perspectives: Current innovative advances and behaviours with emphasis on agro-food by-products valorisation

It is an expected fact that higher amounts of food by-products will be generated in the future because of the increasing food demand, such by-products must be suitable managed immediately after their production during food processing through green

Table 1.5. Highlighting different agro-industrial by-products by their richness in value-added compounds.

By-product	Method	Product	Productivity	Reference
Polyphenols				
Watermelon rinds	Organic solvent extraction	4-Hydroxybenzoic acid	958.3 µg/g DW	Al-Sayed and Ahmed, (2013)
		Vanillin	851.8 µg/g DW	
		Chlorogenic acid	196.3 µg/g DW	
Melon peels	Ethanol-water extraction	Flavonoids	204.3 mg/100 g DW	Morais et al. (2015)
Melon peels	Ethanol extraction	3-Hydroxybenzoic acid	33.45 mg/100 g DW	Mallek-Ayadi et al. (2017)
		Apigenin-7-glycoside	29.34 mg/100 g DW	
Olive pomace	Aqueous extraction	Hydroxytyrosol	238.42 mg/100 g DW	Nunes et al. (2018)
		Tyrosol	9.60 mg/100 g DW	
		Pinoresinol	0.63 mg/100 g DW	
Pineapple peels	Extracted by ethanol	Gallic acid	61.13 mg/100 g DW	Lourenço et al. (2021)
		Chlorogenic acid	58.04 mg/100 g DW	
		Ferulic acid	259.2 mg/100 g DW	
Non-complain apples	Ethanol-water extraction	Chlorogenic acid	0.48 mg/g DE	Vilas-Boas et al. (2021)
		(-)-epicatechin	0.30 mg/g DE	
		Phloridzin	0.13 mg/g DE	
Carotenoids, Chlorophylls and Terpenes				
Rice bran	SSF by <i>Rhodotorula glutinis</i>	β-carotene	1.65 mg/kg DW	Roadjanakamolson and Suntornsuk, (2010)
Pineapple bagasse/peels	Organic solvent extraction	β-carotene	156.10 µg/100 g DW	Da Silva et al. (2014)
Papaya bagasse and seeds		β-carotene	490.29 µg/100 g DW	
		Lycopene	85.52 µg/100 g DW	
Orange peels	Extracted by acetone and hexane	10'-apo-β-carotene-10'-ol	nd	Chedea et al. (2010)
Melon peels	Extracted by acetone	Chlorophylls <i>a</i> - Chlorophylls <i>b</i>	45.82 and 32.95 µg/g FW	Fundo et al. (2017)
Orange peels	Steam explosion	Limonene	94.3%	Pourbafrani et al. (2010)
Orange peels	Solid-liquid extraction/ n-hexane	<i>D</i> -limonene	80%	Wikandari et al. (2013)
Organic acids				
Banana peels	SSF by <i>Aspergillus niger</i>	Citric acid	82 g/Kg DW	Kareem and Rahman, (2011)
Bread trimmings	Fermentation by <i>A. succinogenes</i>	Succinic acid	47.3 g/L	Leung et al. (2012)
Green tea leaves	Hot water extraction	Citric acid	2.8 mg/100 g	Das et al. (2019)
		Malic acid	2.2 mg/100 g	
		Succinic acid	0.7 mg/100 g	
		Formic acid	0.5 mg/100 g	

DW: dry weight; FW: fresh weight; nd: non-defining; DE: dry extract; SSF: solid-state fermentation.

Table 1.6. Agro-industrial by-products as suitable resources for enzymes production and extraction through traditional and green methodologies.

By-product	Methodology	Enzyme	Activity	Reference
Production				
Wheat bran and Rice bran	SSF by <i>Trichoderma reesei</i>	Endoglucanase	22.89 IU/g substrate	Dhillon et al. (2011)
		Exoglucanase	13.57 IU/g substrate	
		β -glucosidase	13.58 IU/g substrate	
		Xylanase	3106.34 IU/g substrate	
Pecan nutshell	SSF by <i>Trichoderma</i> strains	Cellulase	41.9 U/L	Medina-Morales et al. (2011)
		Xylanase	32.8 U/L	
Rice straw	Liquid fermentation by <i>Yarrowia lipolytica</i>	Laccase	2140 U/L	Lee et al. (2012)
Sugarcane bagasse	SSF by <i>Aspergillus niger</i> GH1	Ellagitannase	1400 U/L	Buenrostro-Figueroa et al. (2013)
Corncoobs			1200 U/L	
Pomegranate husk	SSF by <i>Aspergillus niger</i>	Ellagitannase	938.8 U/g substrate	De La Cruz et al. (2015)
Corn and olive oil	Liquid fermentation by <i>Leucosporidium scottii</i> L117	Lipase	2.88 U/mL	Duarte et al. (2015)
Corncoobs	SSF by <i>Trichoderma spp.</i>	CMCase	136.2 U/g substrate	Xie et al. (2015)
		FPase	71.3 U/g substrate	
		β -glucosidase	85.2 U/g substrate	
		β -glucosidase	3.2 U/g protein	
Extraction				
Stems of latex plant	Ammonium sulphate precipitation	Religiosin C	29.79 U/mg protein	Sharma et al. (2012)
	Anion-exchange chromatography		40.09 U/mg protein	
	Gel-filtration chromatography		55.01 U/mg protein	
Pineapple stems	ATPS	Bromelain	5900 U/mg protein	Vicente et al. (2016)
Melon juice	Three-phase partitioning	Cucumisin	28.1 U/mL	Gagaoua et al. (2017)
Pineapple stems and peels	PPP	Bromelain	2.7 U/mg protein	Campos et al. (2019)
Melon peels	PPP	Cucumisin	4.24 U/mg protein	Gómez-García et al. (2021a)

SSF: solid-state fermentation; ATPS: aqueous-two phases systems; PPP: protein precipitation by polysaccharides.

technologies, which allow efficient resources recovery, while food wastage and negative environmental impact are avoided. Currently, the circular economy has been recognised food waste management as an important approach to recover BM from food by-products for environmental impact prevention (Ghisellini et al., 2016; Campos et al., 2020c) since the current strategies for its treatment will not be further accepted due to different drawbacks, e.g., a) deposition in landfills requires large landfill spaces, and the transportation costs limit the range of available land, b) incineration of waste converted into gases, ashes and heat, generating significant amounts of thermal energy, but generating large amounts of polluting gasses and toxic fumes, c) composting process converts organic waste into organic matter using microorganisms. This method recycles nutrient, but with significant carbon emissions and is prone to pathogen growth and contamination d) anaerobic digestion uses organic waste in the absence of oxygen and transforms it into fuels, but its high maintenance costs and lower subsidies have made this solution unprofitable. Therefore, these strategies may change in the future, as European Directives 2008/98/EC (article 11) and 1999/31/EC (article 5) represent the EU commitment to reduce landfills usage to 10%, while increasing recycling routes to 65% by 2030 (Esparza et al., 2020; Carmona-Cabello et al., 2020; Gao et al., 2021). Some current research contributions concerning food waste management within the circular bioeconomy are depicted in **Table 1.7**, remarking their research trend subjects and key findings. Nevertheless, the main challenges related to the industrial applications of BM are the reduction of costs associated with their production and purification and the minimisation of hazardous solvents and reagents. In this regard, based on the enormous mass of food by-products highly produced, their I) transportation embodies huge economic expenses and guarantee their II) safety and quality to avoid rotting and contamination by microorganisms. Both represent a big percentage of the total management costs for industries; thus, cost-effective and well-thinking logic strategies should be implemented to achieve a suitable BM obtention For example, gallic acid (polyphenol) is a BM present in several plants, vegetables, and fruits attributed to biological properties, such as antimicrobial activity against some bacteria and fungi strains (Cláudio et al., 2012; Govea-Salas et al., 2016). Presently, this molecule has gained important demand by food industries as a preservative agent, promoting the shelf-life of foods. However, in many cases, it has been chemically synthesized, producing pollution and requiring an excess of energy that means expensive production process (Khatkar et al., 2015)..

Table 1.7. Latest scientific contributions within the framework of food waste valorisation.

Identified bioresource	Trend subjects addressed and discussed								Findings/Highlights	Reference
	Type	Circular Bioeconomy	SDGs	Pollution prevention	Food waste management	Job creation	Resource recovery	Management strategy		
Food supply chain wastes	Review	✓	✓	✓	✓	✓	✓	Recycling and recovery	Potato and orange peel waste cases of study were described as interesting rich feedstocks of proteins, which both could satisfy the global demand for food and vegetable proteins.	Matharu et al. (2016)
Wasted food and food residue	Research	✓		✓	✓		✓	Composting Anaerobic digestion Incineration	Investigates the environmental impact of food waste in terms of Global Warming, Acidification and Eutrophication potentials, highlighting an economic perspective, for minimisation to be beneficial, 0.15 kg of wasted food would need to be reduced per Euro spent.	Oldfield et al. (2016)
Fruit and vegetable discards	Research			✓	✓		✓	Chemical treatment	Investigates the utilization of a safe and food grade chemical to preserve food waste, due to preservation of these materials represent the main challenge for their valorisation because of	Ahmadi et al. (2018)

									their high water and simple sugar content.	
Food waste	Review	✓	✓	✓	✓	✓	✓	Recycling and recovery	Explains and discusses two different tools to successful implement a circular economy within the food value chain, including 45 Strategies Database 100 Implementation Database.	Kalmykova et al. (2018)
Food and kitchen waste	Review	✓		✓		✓		EAE and chemical conversion	Describes an overview of chemical, enzymatic and biotechnological processes to produce chemicals (fuels), materials (biopolymers), bioactive compounds (antioxidants and enzymes) by using food waste as raw material.	Sindhu et al. (2019)
Fruit and vegetable waste	Review	✓		✓		✓		Conventional Landfilling Incineration Composting Emerging EAE SSF	Compares and addresses emerging against conventional strategies to manage food waste for their future integral valorisation, remarking two stages: direct processing into value-added products, followed by processing of the residual by-products and leftover matter by means of conventional waste management technologies.	Esparza et al. (2020)

Organic waste	Review	✓	✓	✓	✓	✓	✓	Anaerobic digestion	Traditional management of food waste was described and correlated in relationship between circular bioeconomy and sustainability, stating that Circularity should be considered as one of the ways to achieve the broadest objective of sustainability.	Mancini and Raggi (2021)
Fruit and vegetable waste	Research			✓		✓		SSF	Describes the utilization of a microorganism to valorise food waste by creating valuable ingredients with higher protein (20.2%), amino acids (45.7%) and fatty acids content than the original biomass.	Ibarruri et al. (2021)
Citrus peel waste	Review	✓		✓		✓		Eco-efficient extraction techniques	Discusses the use of different strategies to recover value-added compounds, emphasizing on solvent-free extraction of essential oils as the most effective method, which provides a high yield in a short extraction time.	Teigiserova et al. (2021)

Organic waste	Research	✓		✓		✓		✓	Anaerobic digestion	This research provides a more technically and economically feasible approach to co-treating and co-utilizing organic waste and landfill leachate.	Gao et al. (2021)
-	Review	✓	✓	✓	✓			✓	Microorganisms usage	Reviewed the use of biotechnology to reduce/eliminate carbon dioxide to mitigate GHG emission and subsequently climate change by using microorganisms.	Zahed et al. (2021)
Agriculture waste	Review	✓		✓		✓		✓	Crop-livestock integration	Applying protein sources to feed animals reduces GHG emissions associated with transportation and compares the potential for their implementation in sustainable agriculture as well as the need to reduce the negative environmental impact.	Chojnacka et al. (2021)
Biodegradable waste	Research	✓		✓		✓	✓	✓	Anaerobic digestion	Reports a case of study for organic waste management by the creation of facility to recover energy and organic fertilizer with capacity >3 Ton to produce >160 thousand m ³ of biogas.	Vlachokostas et al. (2021)

SDGs: Sustainable Development Goals; EAE: Enzymatic Assisted Extraction; SSF: Solid State Fermentation.

For all these unfavourable details, some studies have been carried out under the green chemistry context to recover BM from food by-products. In this scenario, Rojas et al. (2018) showed that polyphenols extracted from mango peels had good antifungal activity against *Colletotrichum gloeosporioides*, *Sclerotinia sclerotiorum* and *Mucor* sp. On the other hand, regarding global social problems, the human being population have been increasing exponentially year by year, according to the United Nations Department of Economic and Social Affairs (2017) the current world population is nearly 7.6 billion people and is projected to increase until nine billion by 2050, which could bring a big future concern regarding food demand to satisfy such population. In this context, the food requirement worldwide is increasing, and there is a need to develop novel foods or improve some already on the market (Torres-Leon et al., 2018). In turn, food by-products could provide an alternative to develop new foods (e.g., cookies or cereal bars) or ingredients supplemented with natural BM, which enhance human health. These new food products have been used on a dry basis as powders or flours and used like food fortifiers, for example, Al-Sayed and Ahmed, (2013) employed watermelon and melon peels powders as a natural fibre-rich in phenolic compounds for cake preparation to improve nutritional characteristics and antioxidant properties. This evidence showed the great potential of food by-products as rich sources of BM with future applications and their reincorporation into the industrial chains, allowing a circular economy implementation by creating new revenue streams. Besides, the future products or ingredients generated from food by-products and the novel technologies implemented should be safe and allow to improve the principal worldwide sectors (environmental, social and economic) to keep the sustainability between human life and environment.

1.2.2.1 Agro-industrial by-products as functional ingredients

Currently, functional foods are described as food ingredients, which exhibit various benefits upon human health, helping in the prevention or risk reduction of certain illnesses as cancers, cardiovascular and inflammatory disorders and diabetes (Silva et al., 2018). Diabetes and its consequences are a serious global concern, which is progressively developed by oxidative stress, this progression is produced by the imbalance between the overproduction of reactive oxygen species (ROS) and the poor consumption of natural antioxidants, such as polyphenols and carotenoids both are well-known by their capability to decrease the negative effect of ROS, avoiding the problems associated with the oxidative stress (Lo et al., 2017). Furthermore, future perspectives for the valorisation of

food by-products could be as functional ingredients due to these raw materials still hold high content of relevant nutrients, namely fibre and different BM, which are linked to the prevention of health diseases (Campos et al., 2020c). For example, these organic materials can be directly used as a source of dietary fibre, and this natural polymer has been contributed to the enhancement of the gut microbiota, such as *Bifidobacterium*, such bacteria has been associated with colon, stomach, breast and prostate cancer prevention (Veiga et al., 2018). Therefore, nowadays scientific data have proven that a rich diet of fibres may promote gut microbiota modulation and increase the concentration of short-chain fatty acids (SCFA) generated by microbiota, providing gastrointestinal health benefits. An increase in SCFA (acetate, propionate, butyrate) production within gut microbiota reduces luminal pH, which helps to prevent colonisation and infections from pathogenic bacteria (Holscher, 2020). On the other hand, polyphenols exhibit a good inhibition effect of digestive enzymes, such as lipase, amylase and glucosidase, minimising hyperglycaemia, which also is strongly associated with diabetes and obesity disorders (Sulaiman and Ooi, 2014). Also, polyphenols can alter the composition of microbial bacteria in the gut due to their ability to inhibit the growth of specific bacteria, especially pathogenic, such as *E. coli*, *S. aureus* and *C. albicans* (Pereira et al., 2007). Moreover, polyphenols are also suggested to present their protective effect as prebiotics because of their inhibitory effect against pathogens, while beneficial bacteria are stimulated and are not affected by them. For example, epicatechin and catechin inhibited foodborne pathogens and increased the count of probiotics, such as *Lactobacillus* and *Bifidobacterium* spp. (Kawabata et al., 2019). Ribeiro et al. (2021) employed olive pomace rich in polyphenols and insoluble fibre as an antioxidant, antimicrobial and prebiotic ingredient for potential beneficial effects on the gut microbiota, they found from an *in vitro* faecal fermentation a positive effect in *Prevotella* spp./*Bacteroides* spp. bacteria and the production of SCFA, mainly acetate > butyrate > propionate. By these functional benefits and based on their richness in BM, food by-products could be employed as sources to develop functional ingredients, such as flours, fibres bars or cereals.

1.2.2.2 Green precipitation process for protein recovery

The valorisation of food by-products encompasses a research field in which protein extraction is performed after processing. However, proteins are currently extracted by traditional methods, employing toxic solvents, saturated salts, gel and ion-exchange

chromatography. These methodologies have diverse limitations associated with low industrial scale, high costs and low purification yields and in many cases, bioactivity loss (Lombardi et al., 2013; Gagaoua et al., 2017). These unfavourable restrictions demand the development of novel green methodologies, such as proteins precipitation by polysaccharides (PPP). Such separative technique has emerged as an alternative method for extraction and purification of proteins due to its advantages against traditional processes related to a simple scale-up process, volume reduction, rapid separation and null use of toxic chemicals (Duarte et al., 2015; Campos et al., 2019). As an example, Campos et al. (2019) employed PPP using carrageenan for the first time to isolate and extract Bromelain (EC 3.4.22.32), which is an enzyme reported with beneficial properties attributed to its anti-inflammatory activity (Vicente et al., 2016), from pineapple industrial stems and peels, highlighting low concentrations of polysaccharide (0.2–0.3% w/v), high recovery yields of bromelain activity (80–90%) and protein (0.3 g/100 g of pineapple by-products). From this innovative investigation, the authors were granted with an European patent (EP 3 252 156 A1) in 2020 (Estevez Pintado, 2017). Gómez-García et al. (2021a) reported the extraction of Cucumisin [EC 3.4.21.25] from melon peels by using carrageenan at very low concentration (0.003 – 0.006% w/v) with a recovery yield of 0.17 g/100 g of by-products, keeping its proteolytic properties (4.24 U/mg protein). Particularly, this enzyme has proteolytic and milk-clotting activities, which could be exploited for the development of plant-based rennet for cheese making industries, representing an alternative against animal rennet, since several issues have been emerged associated with its production, fewer consumers acceptance and high costs (Ben Amira et al., 2017). Therefore, based on the good outcomes given by the PPP, it can be concluded that this technique represents an eco-friendly process for the valorisation of food waste as rich sources of bioactive proteins with high industrial interest. Moreover, it can be inferred that these advances will offer great opportunities for new inventions, development and knowledge for future research, and technology transfer to pilot or industrial environments aimed at developing novel value-added supplements and products.

1.2.3 Practical applications and future research prospects

Although most of the recent techniques mentioned above have high potential applications for the valorisation and exploitation of food agro-industrial by-products, they have not been implemented on a big scale nor in a real waste management case for the obtention

of BM, which could lead to the generation of new business, revenues streams and jobs. In this regard, there are practical strategies that could be adopted to implement circular bioeconomy through the application of green chemistry and biotechnological techniques as future research scope, such as the transference of the technology derived from scientific knowledge into an industrial environment, adopting the three main fields of intervention of the circular economy outlined as the micro, meso and macro levels that could responds to the fact that scientific knowledge most of the times is just disclosed as research articles without any applications at industrial scale and also could help to the researchers increase their competences in the business development field (Elia et al., 2017). For example, the micro-level refers to single enterprises or clients, in this respect universities or research institutes "who have the knowledge" can reach the industries "who have the waste problem" and create/sign a non-disclosure agreement (NDA) to develop a minimum viable product (MVP; pilot scale) to produce value-added products to be tested in the market and find their market fit for future commercialisation. After the evaluation and viability analysis at the micro-level, the next step consists of reaching the meso level, which implies creating eco-industrial parks in which industries will work in symbiotic agreement, exchanging resources, services, products, economic profits and environmental benefits. In the end, the macro-level could be achieved by replicating the industrial parks in different zones of a city and continuing with their expansion to several countries, targeting the developing countries who need and demands faster economic solutions, concerning high-quality jobs and novel business. Scientists must increase their capabilities and acquire new competencies on business development to transfer their knowledge to the industries, taking advantage that many food enterprises (not all) are becoming more receptive and conscious about the food waste issues and the new directives launched by the European Commission, including the Sustainable Development Goals (SDGs) that they should comply in the next few years, as well as the economic impact that enterprises suffered by the COVID-19 pandemic situation. In general, there is a growing awareness to hear innovative ideas to solve their waste problems, while help with their economic stability and meeting the new directives (Forbes et al., 2021; Ducoli et al., 2021). Therefore, researchers must hurry to show their knowledge to the enterprises and reach a mutual agreement in which together could contribute to sustainable development.

1.3 Concluding comments

Undoubtedly, as in the past, even now and future, sustainable solutions for the recycling and valorisation of food by-products for their reincorporation in the industrial chains are the principal challenges in the scientific field. Therefore, all the efforts have been directed to consolidate the total management of these materials to avoid the negative environmental impact and economic losses. Moreover, with all the evidence already reported, highlighting their characteristics and richness in BM, food by-products could be employed to develop novel functional food products or ingredients, representing the principal advantage for their transformation into valuable products within circular bioeconomy framework to the industries. Thus, overall, as at the beginning of the XX century, we are in a transition stage toward something different, more diversified, focused on green technologies and circular bioeconomy promotion to exploit these natural resources for human wellbeing and contribute to sustainable development.

CHAPTER 2 - Valorization of Melon fruit (*Cucumis melo* L.) by-products: Phytochemical and biofunctional properties with emphasis on recent trends and advances

Ricardo Gómez-García^{a,b}, Débora A. Campos^a, Cristóbal N. Aguilar^b, Ana R. Madureira^a and Manuela Pintado^{a*}

^aUniversidade Católica Portuguesa, CBQF - Centro de Biotecnologia e Química Fina – Laboratório Associado, Escola Superior de Biotecnologia, Rua Diogo Botelho 1327, 4169-005, Porto, Portugal

^bBBG-DIA. Bioprocesses and Bioproducts Group. Food Research Department, School of Chemistry, Autonomous University of Coahuila, Saltillo, Coahuila, Mexico

Published:

Journal of Trends in Foods Science and Technology - Elsevier

Abstract

For modern food industry, sustainability of food processing is a major concern coupled to the reduction of waste generation. Fruit and vegetable processing require of modernization to valorize the waste and by-products highly generated, particularly because they are rich in natural beneficial components which are demanded to human health. Melon (*Cucumis melo* L.) processing generate a high amount of peels and seeds, which are recognized with higher content of bioactive compounds than pulp, including polyphenols, carotenoids and oils. In this review, we summarize information about of the bioactive compounds present in the melon fruit, together with the nutritional properties that it presents as a functional food, with a focus on its by-products (pulp, seed and peel). The melon fruit contains important bioactive compounds, mainly the peel has a high content of antioxidants which are of interest in the food, cosmetic and pharmaceutical industries. These findings pretend to support new research concerning the formulation of novel functional foods based on melon by-products. Extracts of melon fruit, mainly from the peel, have been shown to possess phytochemical compounds that exhibit antioxidant, antimicrobial, antidiabetic, antiviral, anti-inflammatory, anti-hypoglycemia and anti-proliferative effects in various *in vitro* and *in vivo* test. However, it is necessary for further analyze the nutritional and functional potential of these by-products, the therapeutic and clinic mechanisms involved and to develop its industrial process as functional or nutraceutical food products.

Key words: *Cucumis melo*; industrial by-products; polyphenols; carotenoids; functional bioactivities

2.1. Introduction

Consumption of some fruits is strongly associated with several health benefits due to their high nutritional value and properties in risks reduction of certain illness such as cancers, cardiovascular diseases and cataracts fully justified and attributed to the presence of bioactive compounds (BCs) in the plant matrices (Shofian et al., 2011; Saini, Nile and Park, 2015). Melon (*Cucumis melo* L.) belongs to the *Cucurbitaceae* family (**Figure 2.1**), which is originated from Iran and Pakistan. It is one of the most popular fruit cultivated in tropical countries considered a valuable cash crop grown worldwide (Rashid et al., 2011). Melon fruit is a tasty and juicy fruit well-known for its nutritive and medicinal properties. Fatty acids, polyphenols and carotenoids are BCs, present in melon with several beneficial activities, which can improve human health. In the past, melon consumption has been categorized as a natural curative agent that plays a therapeutic and preventive role against a number of chronic diseases such as aging, inflammation and certain cancers (Shofian et al., 2011; Rodríguez-Pérez, Quirantes-Piné, Fernández-Gutiérrez, and Segura-Carretero, 2013). In addition, *C. melo* is recommended for the treatment of cardiovascular disorders, diuretic, stomachic and vermifuge (Parle and Singh, 2011). Generally, BCs from melon are ingested through the fresh fruit mesocarp which is the most studied part of the fruit compared with peels and seeds. In this regard, in recent years, *C. melo* and its by-products have been the target fruit of a number of studies intended to use these organic matrices for the recovery and extraction of BCs. On the other hand, based on data published by the FAO, the annual production of melon fruit in the world was more than 40 million tonnes, whereas in Portugal and Mexico it was approximately 57 and 594 thousand tons, respectively (FAOSTAT 2018). Its industrial processing produces a wide range of natural consumer products such as juices, jams, dehydrated pulp and salads or snacks. However, these industrial activities also generate a large number of fruit by-products throughout processing. Most of the industrially produced fruit by-products have been commonly used as animal feed, organic material to prevent soil erosion, and nowadays as biofuel precursors (Lucas-Torres, Lorente, Cabañas and Moreno, 2016). These by-products are increasingly being studied in contrast to other fractions due to their richness in compounds with biological activity (Yan, Teng, and Jhi, 2006). Currently, some researchers have reported higher levels of phenolic compounds and ascorbic acid in peels than in fruit pulp (Goulas and Manganaris, 2012). In contrast to a number of reports on the extraction of BCs from the pulp, studies for the valorization of melon by-products have recently been conducted with renewed and

growing interest. Excellent reviews have been published by researcher (Rolim, Seabra and de Macedo, 2019; Vella, Cautela and Laratta, 2019; Silva et al., 2018), which were aimed at the macromolecular, functional and bioactive explorations, particularly for production of pectin (Adiba et al., 2016; Güzel and Akpınar, 2019), novel oils (Ok and Yilmaz, 2019; Rezig et al., 2019; Alexandra Silva et al., 2019), and even hydrogen-type fuels (Turhal, Turanbaev and Argun, 2018). However, a great effort is needed to develop new efficient methods and feasible strategies for the re-use of melon by-products for the recovery of natural BCs or high nutritional value supplements (Mallek-Ayadi, Bahloul, and Kechaou, 2017). These raw materials could also have potential applications focused on human nutrition, developing new food supplies with functional benefits due to their abundance BCs, in particular vitamins, minerals, fiber, oils, carotenoids and polyphenols (Torres-Leon et al., 2018). Recently, Silva et al. (2018) described the potential of melon by-products as ingredients for novel functional foods.

In this paper, a detailed analysis of the melon by-products has been extensively reviewed, focusing on the richness of BCs with biological properties. The aim of this paper is also to generate research interest in the valorization of melon fruit and its by-products. To this order, firstly, to better understand the phytochemical composition and bioactivity of melon fruit that promotes human health and, secondly, to encourage further novelty in the design and development of innovative products that can solve problems related to food loss, waste and pollution.

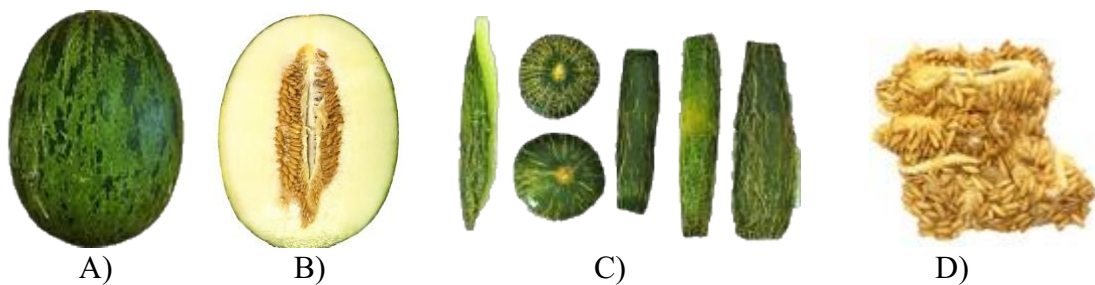


Figure 2.1. Major parts of melon fruits (*Cucumis melo* L.). A) mature fruit of *C. melo inodorus* cultivar, B) mesocarp, C) peel, and seed by-products.

2.2 Muskmelon Anatomical Description

The *Cucurbitaceae* family contains approximately 825 species, such as squash, pumpkins, cucumbers and melons (M. A. Silva et al., 2018). The fleshy fruit is produced from most of the tendril-bearing vine plants, derived from the inferior ovary, the pepo. Each melon fruit varies in size, shape and rind characteristics and the color of the flesh

that depends on the varieties of melon. The outer skin (peel) may be smooth, netted, ribbed, furrowed, yellow-brown, green flesh yellow. Ripe melon is almost found, yellowish-green, and rough-textured. Seeds are cream-colored and over 10 mm long (Saltveit, 2011; Parle and Singh, 2011). The *C. melo* species is further divided into a number of botanical varieties or types. **Table 2.1** shows the three most important varieties of melon fruit; cantalupensis, inodorus and reticulates. The edible part is the most valuable component of the melon fruit due to its high content of BCs and represents at least 65% of the total weight, while the peels and seeds represent 25% and 7%, respectively (Fundo et al., 2017). Although the peels, seeds and bagasse are usually rejected in fruit processing, these by-products have stood out by maintaining a high concentration of BCs and representing a significant percentage of total weight. In the current scenario, approximately 1.81, 6.53, 15.0 and 32.0 million tons of fruit and vegetable by-products are produced by fruit and vegetable processing, packing, distribution and consumption in the industrial sector in India, the Philippines, the USA and China, respectively (Wadhwa and Bakshi, 2013). On the other hand, melon seeds represent a high quantity of these by-products, with almost 984 thousand tons produced per year (FAOSTAT 2018), which promotes hazardous environmental issues related to their accumulation in landfills. For this reason, their management and re-utilization in the context of valorization, namely cost reduction and less use of toxic methodologies, are the main challenge in the field of biotechnology to solve pollution problems and to meet the growing demand for food supplies (Kolayli et al., 2010; Concurso et al., 2012; Atef et al., 2013).

2.3 Phytochemical and nutritional composition of melon fruit

Cucurbitaceae fruit is not a significant sources of calories, and it can be vital sources of dietary fiber, minerals, polyphenols, provitamin A (β -carotene) and vitamin C. Melons are naturally low in fat and sodium, have no cholesterol and provide many essential nutrients such as potassium (Atef et al., 2013). The general aspects and characteristics of melon mesocarp commonly and traditionally used in human consumption as a salad or dessert are shown in **Figure 2.2**. Mesocarp is the most studied part of the melon with respect to nutritional composition determination (Amaro et al., 2010; Falah, Nadine and Suryandono, 2015). For example, see the study of Rodríguez-Pérez, Quirantes-Piné, Fernández-Gutiérrez and Segura-Carretero, (2013) who identified different BCs,

including amino acids and their derivatives, organic acids, phenolic acids and their derivatives, esters, flavonoids, lignans and other polar compounds from the melon pulp of 3 different varieties. These facts support the richness of functional bioactive compounds (especially phenolics, carotenoids and essential oils) in melon fruit.

Table 2.1. Major groups of melon fruit

Groups Name	Characteristics
<i>Cantalupensis</i>	Skin rough and warty, not netted. e.g., European cantaloupe and Algerian melon.
<i>Inodorus</i>	Large, bright-yellow elongated melon with a pale green. e.g., Canary melon, Casaba, Kolkhozintsa melon, Hami melon, honeydew, Navajo Yellow, Piel de Sapo/Santa Claus, sugar melon. Tigger melon and Japanese melons.
<i>Reticulatus</i>	True muskmelons, with netted skin. e.g., Bailan melon, North American cantaloupe, Galia, Ogem, Persian, Sharlyn melons. Modern crossbred varieties, e.g., Crenshaw (Casaba X Persian), Crane (Japanese X N.A cantaloupe).

Source: Saltveit (2011)

2.3.1 Phenolic compounds

Phenolic compounds or polyphenols are widely distributed throughout the plant kingdom. Chemical compounds of this class are the most commonly found in fruits, plant-derived beverages, peels, husks and seeds that are widely known for their biological activity (Martínez-Ávila et al., 2012). Polyphenols are classified into different groups on the basis of their chemical structure, such as tannins, lignans, flavonoids, phenolic acids and others (Martins et al., 2011). The most common polyphenols of melon fruit are flavonoids and phenolic acids. Flavonoids are further divided into several categories such as flavones, flavonols, flavanones and flavanols (Tadmor et al., 2010). While, phenolic acids are simple molecules comprising a different category of hydroxybenzoic and hydroxycinnamic acids (Dey et al., 2016). Such chemical compounds are abundant in plants performing various functions such as pigmentation and plant defence against attacks by microorganisms and insects. Furthermore, they are also recognized as beneficial compounds that could prevent certain neurodegenerative diseases such as Alzheimer's and Parkinson's (Poiroux-Gonord et al., 2010). As a result, these types of BCs have been completely characterized in a number of fruit extracts due to their potential health benefits.

2.3.1.1 Phenolic compounds content in melon fruit

Melon fruit contains a very high concentration of polyphenols (Ullah, Zahoor, Ali and Khan, 2014). These compounds provide potential health benefits, in particular by supporting the cardiovascular system (Rodríguez-Pérez, Quirantes-Piné, Fernández-Gutiérrez and Segura-Carretero, 2013). Total phenolic content (TPC) of sun melon pulp determined by Shofian et al. (2011) found a concentration of 16.71 mg acid equivalents (GAE)/100 g fresh weight (FW). Ismail, Chan, Mariod and Ismail (2010) analysed the TPC of cantaloupe melon pulp, peels, and seeds and found concentrations of 168, 470, 285 mg of GAE/100 g extract, respectively. The total flavonoid content (TFC) was also, reported with 203, 513, 162 µg of rutin equivalents (RE)/100 g extract, respectively. In relation to the quantification of phenolic compounds in melon by-products, **Table 2.2** shows the range of values found in different melon varieties. Recently, Fundo et al. (2017)

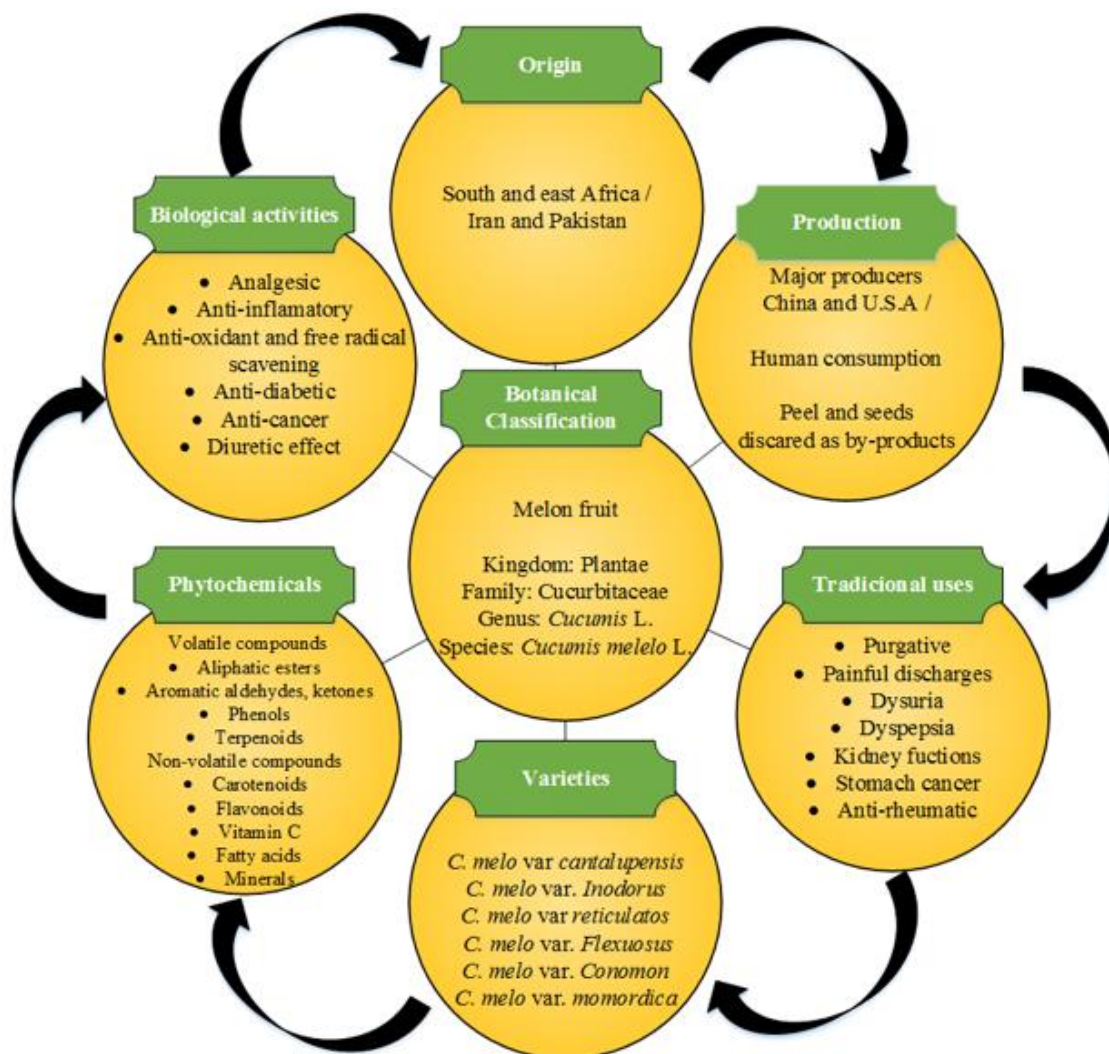


Figure 2.2. Scheme focusing on the principal generalities of *C. melo* fruit.

reported the highest concentration of TPC in methanolic extracts from reticulatus melon seeds (22.91 mg/100 g extract) followed by peel extracts (14.1 mg/100 g extract) and a lower concentration in pulp (9.54 mg/100 g extract). In addition, Mallek-Ayadi, Bahloul, and Kechaou, (2017) quantified and identified eighteen individual phenolic compounds by HPLC (**Table 2.3** and **Figure 2.3**) and reported values of TPC (332 mg GAE/100 g extract) and TFC (95.46 mg QE/100 g extract) in peels of maazoun melon cultivar. Moreover, Al-Sayed and Ahmed (2013) found in melon peels that 4-hydroxybenzoic acid was the most representative phenolic acid (32.53 mg/100 g dry weight = DW) followed by vanillin (19.92 mg/100 g DW), coumaric acid (8.08 mg/100 g DW) and chlorogenic acid (6.62 mg/100 g DW) in Sharlyn melon peels. During their work, these researchers also used the richness of melon by-products to develop natural and functional food rich not only in antioxidants but also in dietary fibers and as a substitute for functional wheat flour in cake making. All of these reports on the diversity and content of phenolic compounds of melon fruit by-products, namely pulp, peels and seeds, show an important and high nutritional value that could be used for the development of novel and cheaper foods or nutrient-enhancing ingredients. This will help overcome the problems of hunger and malnutrition in developing countries.

2.3.2 Carotenoids compounds

Carotenoids are one class of phytochemicals responsible for the natural pigments that are commonly metabolized by algae, photosynthetic bacteria and plants, such as yellow one (lutein), orange (β -carotene) and red (lycopene) in various fruits (Poiroux-Gonord et al., 2010; Arscott, 2013). These compounds are C₄₀ tetraterpenoid pigments, biosynthesized by the linkage of two C₂₀ geranylgeranyl diphosphate molecules (Namitha and Negi, 2010). It can also be classified into two groups on the basis of a functional group. These may be xanthophylls containing oxygen as a functional group including lutein and zeaxanthin, and carotenes or only a parent hydrocarbons chains without any functional group, such as α -, β -carotene and lycopene (Saini, Nile and Park, 2015). Melons are a good source of carotenoids like many other fruits: mainly β -carotene and lutein (Amaro, Oliveira and Almeida, 2015). Nevertheless, other carotenoids have also been detected such as α -carotene, β -carotene, β -cryptoxanthin, phytoene, violaxanthin, neoxanthin and zeaxanthin (Yano et al., 2005; Laur and Tian, 2011; Conduurso et al., 2012). These BCs present in melon play an important role in the photoprotection of the eye (provitamin A), improving immune function and preventing chronic diseases (Arscott, 2013). For these

reasons, carotenoids and their extraction from natural sources are of primary interest to researchers, nutritionists, food processors and consumers in developing new functional products to promote health.

Table 2.2. Total phenolic and total flavonoids from different by-products of melon fruit.

Substrate Type	Sample Type	mg GAE/g extract	mg QE/g extract	Reference
Leaf Pulp	<i>C. melo</i> L.	111.77	59.48	Hashemi, Ebrahimzadeh and Khalili, (2019) Morais et al. (2015)
		80.98	78.88	
		313.45*	72.62**	
Peel	Ambrosia	1.45	–	Ganji, Singh and Friedman, (2019)
	Canary	2.40	–	
	Cantaloupe	0.90	-	
	Cantaloupe	25.48	15.19***	Vella, Cautela and Laratta, (2019)
	Charentias	1.19	–	Ganji, Singh and Friedman, (2019)
	Galia	2.96	–	
	Goddess	1.36	–	
	Hami	2.08	–	
	Hami gold	21.6	–	
	Honeydew	0.96	–	
	Santa claus	1.63	–	
	Tuscan	0.69	–	
	Vine	1.42	–	
Raw peel	<i>C. melo</i> L.	357.80*	204.28**	Morais et al. (2015)
Lyophilized peel		227.07*	199.98**	
Oven dried peel		149.83*	106.18**	
Seed		99.69*	3.61**	Vella, Cautela and Laratta, (2019)
		1.50	0.74***	
	Golden	29.39	20.67	Olubunmi, Olajumoke, Bamidele, and Omolara, (2019)
	Maazoun	3.04	0.87	Mallek-Ayadi, Bahloul, and Kechaou, (2018)

Abbreviations: GAE: gallic acid equivalents; QE: quercetin equivalents

*GAE/100 g dry matter.

**QE/100 g dry matter.

***mg catechin equivalents per g of extract

– not reported

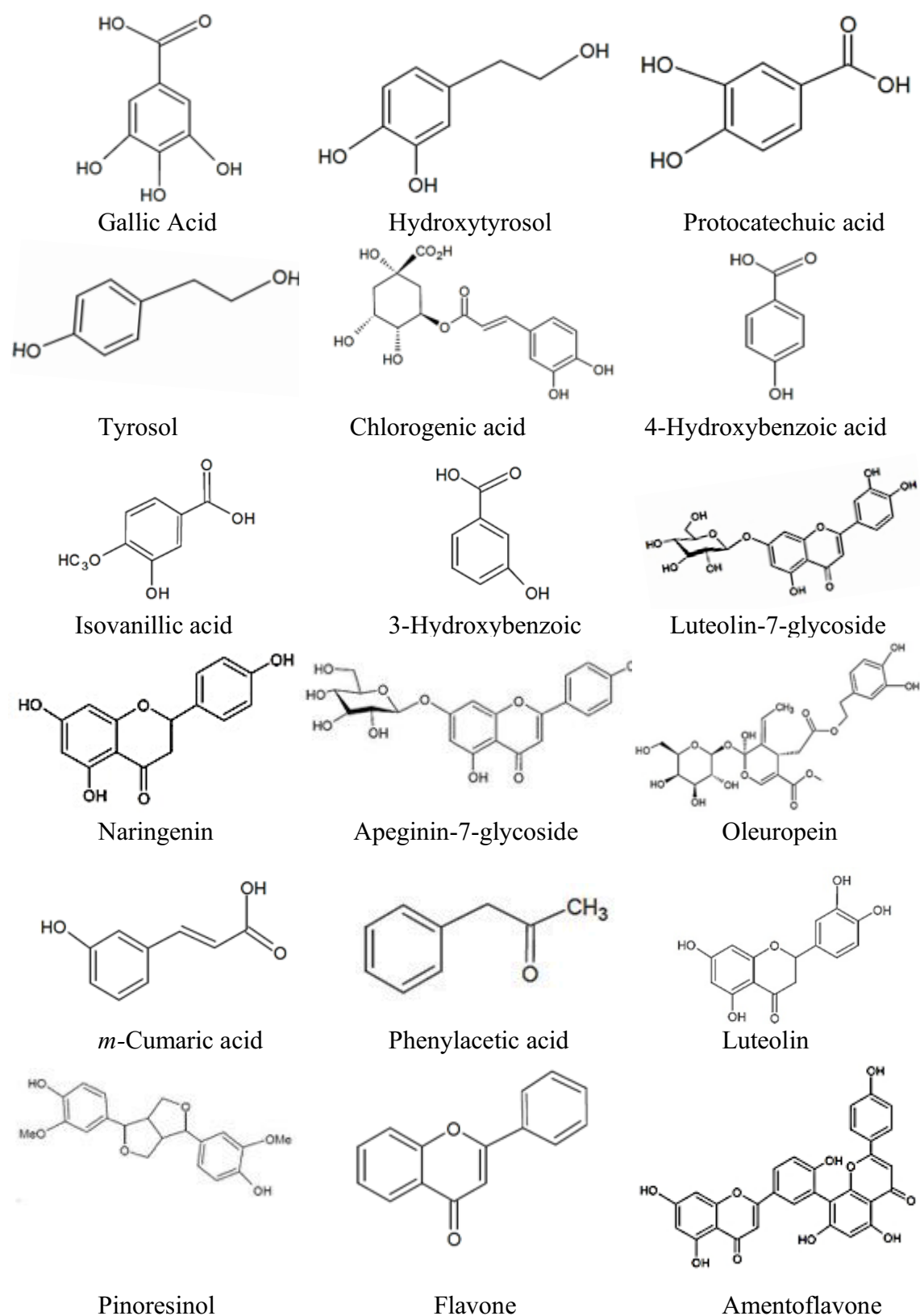


Figure 2.3. Structure of phenolic compounds identified in melon peels (Mallek-Ayadi, Bahloul and Kechaou, 2017).

Table 2.3. Identified and quantified phenolic compounds by HPLC from peel extracts of various melon varieties.

Compounds Name	Class	Melon Variety			
		*Galia M (mg/100 mL)	*Galia H (mg100 mL)	**Cantaloupe (mg/100 g DM)	***Maazoun (mg/100 g DM)
Isovanillic acid	Hydroxybenzoic acids	30	33	–	23.70
3-Hydroxybenzoic acid	Hydroxybenzoic acids	48	53	–	33.45
Chlorogenic acid	Hydroxycinnamic acids	45	16	8	8.25
Neochlorogenic acid	Hydroxycinnamic acids	33	31	–	–
Luteolin-7-o-glucoside	Flavones	55	60	–	16.51
Apeginin-7-o-glucoside	Flavones	18	20	–	29.34
Quercetin-3-galactoside	Flavonol	2	5	–	–
Gallic acid	Hydroxybenzoic acid	–	–	245	12.07
Rutin	Flavonoid	–	–	6	–
Ferulic acid	Hydroxybenzoic acid	–	–	9	–
Ellagic acid	Hydrolyzable tannin	–	–	57	–
Quercetin	Flavonol	–	–	2	–
Kaempferol	Flavonol	–	–	32	–
Hydroxytyrosol	Phenylethanoid	–	–	–	9.11
Protocatechuic acid	Hydroxybenzoic acids	–	–	–	3.46
Tyrosol	Phenolic alcohol	–	–	–	11.35
4-Hydroxybenzoic acid	Hydroxybenzoic acids	–	–	–	8.62
Naringenin	Flavanone glycosides	–	–	–	11.58
Oleuropein	Secoiridoids	–	–	–	18.88
<i>m</i> -Coumaric acid	Hydroxycinnamic acids	–	–	–	19.91
Phenylacetic acid	Benzeneacetic acid	–	–	–	3.27
Luteolin	Flavones	–	–	–	6.73
Pinoresinol	Lignan	–	–	–	1.92
Flavone	Flavones	–	–	–	13.51
Amentoflavone	Flavones	–	–	–	2.69

Sources: *Ganji, Singh, and Friedman, (2019); **Vella, Cautela, and Laratta, (2019); and *** Mallek-Ayadi, Bahloul, and Kechaou, (2017)

Abbreviations: Galia M: Galia melon from Mexico; Galia H: Galia melon from Honduras; DM: dry matter:

– not reported

2.3.2.1 Carotenoids content and diversity in melon fruit

Carotenoid molecules present in melon fruit, contribute to their beneficial bioactivity in the prevention of anti-inflammatory, anti-cancer, neuroprotective and cardiovascular diseases (Saini, Nile, and Park, 2015). In melon, it is possible to find α -carotene, β -carotene, lutein, β -cryptoxanthin, phytoene, violaxanthin, neoxanthin and zeaxanthin (Yano et al., 2005). Atef et al. (2013) recorded 0.56 mg/100 g DW of total carotenoid content (TCC) in the melon pulp while β -carotene and lutein were between 0.06-3.85 and 0.007-0.032 mg/100 g FW respectively, reported by Laur and Tian (2011) in different melon varieties of different geographical origins. Later, levels of β -carotene (1.44 mg/100 g FW) and ζ -carotene (1.08 mg/100 g FW) were also reported by Concurso et al. (2012). The TCC in pulp, peels and seeds were compared by Fundo et al, (2017) in *reticulatus* melon, they found 68.92, 23.46 and 30.51 mg TCC /g FW, respectively. The differences in carotenoid levels in melon may be due to varietal differences, maturity time and growing conditions (Sarungallo et al., 2015). These observations reinforce the value of melon and its by-products as a good source of carotenoids and together with the very scarce reports involving the extraction of melon carotenoids, this subject could generate research interest on the developing eco-friendly methodologies for major recovery yields.

2.3.3 Essential oils and fatty acids

Edible oil is a biological mixture of esters derived from glycerol and a chain of fatty acids (Da Silva and Jorge, 2014). Physical and chemical characteristics of oil are influenced by the type and proportion of the fatty acids on the triacylglycerol. Fatty acids may be classified as short-chain (2-8 C), medium (8-12 C) and long-chain (13-24 C) or saturated (SFA), monounsaturated (MUFA) and polyunsaturated fatty acids (PUFA) depending on the presence or absence of double bonds (Kostik, Memeti, and Bauer, 2013). Long-chain fatty acids (LCFA) are mainly composed of oleic acid (C18:1), linoleic acid (C18:2) and palmitoleic acid (C16:0) (Zhang, Su, Baeyens, and Tan, 2014). They play an important role in the human diet due to the control of the metabolism of cholesterol associated with cardiovascular disease (Dorni, Sharma, Saikia, and Longvah, 2018). Melon peels and seeds by-products have been recognized as a good source of fatty acids whereas seeds are the richest in LCFA in the whole melon (Ismail, 2010). Moreover, oils extracted from seed are rich sources of BCs such as tocopherols, essential fatty acids, phytosterol, carotenoids and squalene. These BCs have been shown to have various potential applications in various industries such as biodiesel, cosmetics and pharmaceuticals

(Górnaś and Rudzińska, 2016). Tocopherols and tocotrienols are lipid-soluble compounds commonly referred to as vitamin E. They are natural antioxidants that play a vital role in the human diet and health. They protect unsaturated fatty acids from oxidation and ensure the stability of lipid membranes through their function. Their derivatives could be used as a natural anticancer and chronic disease agent. (Górnaś, Pugajeva, and Segliņa, 2014a). In addition, biological properties as antioxidants and antimicrobial activity have been reported in oil fractions and have been attributed to the presence of these BCs (Desbois and Smith, 2010).

2.3.3.1 Essential oils and fatty acids content in melon fruit

In the last decade, melon seed valorization is taking place since it has been reported as a rich source of essential oil. Rashid et al. (2011) optimized biodiesel production using melon seeds oil and obtained yields of 75.55-86.00% extracted by Soxhlet method with *n*-hexane and transesterification of melon seeds oil showed that linoleic (4.6%), oleic (21.12%), palmitic (17.68%) and stearic (10.84%) were the major fatty acids in melon seeds. The content of fatty acids and BCs present in various types of melon seeds are shown in **Table 2.4**. Da Silva and Jorge (2014) reported yields of oil fraction from melon seeds of 30.6% DM, integrated by linoleic (59%), oleic (26.4%) and palmitic (8.7%) acid as well as α -tocopherol and γ -tocopherol (20.5 and 249.6 mg/kg, respectively). Górnaś and Rudzińska, (2016) quantified linoleic (59.04%), oleic (24.71%), palmitic (9.57%) and stearic (5.74%) acids from Honeydew melon seeds whereas in previous reports they found α -tocopherol and γ -tocopherol in canary melon seeds ranging from 2.23 to 6.88 and 17.73 to 63.08 mg/100 g of oil, respectively (Górnaś, Pugajeva, and Segliņa, 2014a, b). In a recent study on the composition of fatty acids, oil was extracted from a powdered sample of *maazoun* melon seeds using fatty acid methyl esters (FAMES) and then analyzed by gas chromatography. Linoleic acid (68.98%), oleic acid (15.84%) and palmitic acid (8.71%) were found primarily in the composition of fatty acids, while steric, myrical and erucic acids were found in low concentration (Mallek-Ayadi, Bahloul, and Kechaou, 2018). The broad spectrum of reports on melon seeds and their richness in essential oils highlights the importance of valorizing these by-products for the development of functional foods or ingredients due to the high levels of linoleic, oleic acids and BCs (α -tocopherol and γ -tocopherol) that could potentially contribute to human

health in the prevention of coronary heart disease, chronic disease and LDL-cholesterol (Chuyen et al., 2105).

Table 2.4. Profile of fatty acids and bioactive compounds from oil extracts of different melon seeds.

Composition	Yellow ^a	Maazoun ^b	Honeydew ^c	Canary ^d	<i>Inodorus Naudin</i> ^e
Fatty Acids Profile (%)					
Saturated Fatty Acids					
Myristic (C14:0)	nd	0.04	0.05	–	nd
Pentadecanoic (C15:0)	nd	0.03	0.03	–	nd
Palmitic (C16:0)	17.1	8.71	9.57	–	8.7
Margaric (C17:0)	nd	0.07	nd	–	0.10
Margaroleic (C17:1)	nd	0.03	0.02	–	nd
Stearic (C18:0)	2.8	5.54	5.74	–	*
Arachidic (C20:0)	nd	0.16	0.18	–	nd
Lignoceric (C24:0)	nd	0.06	nd	–	nd
Unsaturated Fatty Acids					
Palmitoleic (C16:1 ω-7)	nd	0.08	0.19	–	nd
Oleic (C18:1)	4.1	15.84	24.71	–	26.4
Linoleic (C18:2)	26.5	68.98	59.04	–	59.0
Linolenic (C18:3)	21.4	0.2	0.18	–	nd
Gadoleic (C20:1 ω-9)	nd	0.12	nd	–	nd
Eicosanoid (C20:1)	nd	0.13	0.12	–	nd
Erucic (C22:0)	nd	nd	0.07	–	nd
Erucic (C22:1 ω-9)	nd	0.02	nd	–	nd
Bioactive Compounds Profile					
Totals Phenolic compounds	–	–	–	–	13.07 mg GAE/100 g DW
Total carotenoids	–	–	–	–	0.63 mg β-carotene/100 g DW
Phytosterols					
Avenasterol	–	–	0.05 (mg/g of oil)	–	–
Δ7–Avenasterol	–	–	0.03 (mg/g of oil)	–	–
β-sitosterol	–	–	0.58 (mg/g of oil)	–	210.2 (mg/100 g DM)
Campestanol	–	–	0.05 (mg/g of oil)	–	–
Campesterol	–	–	0.39 (mg/g of oil)	–	–
Cycloatenol	–	–	0.05 (mg/g of oil)	–	–
Stigmastanol	–	–	–	–	117.1 (mg/100 g DM)
Stigmasterol	–	–	0.19 (mg/g of oil)	–	–
Δ7–Stigmasterol	–	–	0.57 (mg/g of oil)	–	–
Tocols					
Tocopherols					

α -tocopherol	–	–	–	6.88 mg/100 g oil and 2.23 mg/100 g DM	20.5 mg/kg
β -tocopherol	–	–	–	nd	nd
γ -tocopherol	–	–	–	63.08 mg/100 g oil and 17.73 mg/100 g DM	249.6 mg/kg
δ -tocopherol	–	–	–	0.77 mg/100 g oil and 0.20 mg/100 g DM	nd
Tocotrienols					
α -tocotrienol	–	–	–	0.47 mg/100 g oil and 0.10 mg/100 g DM	–
β -tocotrienol	–	–	–	nd	–
γ -tocotrienol	–	–	–	0.90 mg/100 g oil and 0.21 mg/100 g DM	–

Sources: ^aBonesi et al. (2019); ^bMallek-Ayadi, Bahloul, and Kechaou, (2018); ^cGórnaś and Rudzińska (2016); ^dGórnaś, Pugajeva, and Segliņa, (2014a, b); ^eDa Silva and Jorge (2014)

Abbreviations: nd: not detected; – not reported; DM: dry matter

*percentage lower than 0.1%.

2.4 Biological activities and human health

Traditionally, fresh or aqueous extracts of the edible part of melon fruit had been used in the treatment of common diseases such as analgesic, purgative, painful discharges, dysuria and anti-inflammatory (Parle and Singh, 2011). Currently, a few studies of melon pulp, peels and seeds have shown that melon fruit has many useful biological properties, such as antioxidant, provitamin A, anticancer and antimicrobial activity. The following section discusses the various biological activities of phytochemical found in melon fruit by-products.

2.4.1 Antioxidant activity

The high levels of polyphenols and carotenoids are mainly responsible for the antioxidant activity of melon fruit. Carotenoids, particularly β -carotene have been recognized due to

their antioxidant activity against free radicals, which indicate protective roles for reducing the risk of certain types of cancers and cardiovascular diseases (Henan et al., 2016; Vishwakarma, Gupta, and Upadhyay, 2017). The antioxidant activity found in various parts of fruit is shown in **Table 2.5**. For example, Henan et al. (2016) investigated the anti-radical activity by oxidation of 2,2-azinobis-3ethyl-benzothiazoline-6-sulfinic acid (ABTS) of lipophilic extracts from different varieties of melon. The highest antioxidant activity found in *maazoun* melon extracts was 100 g FW equivalent to 160 μ M Trolox (TE) whereas the lowest activity of the *galaouia* variety was 22 μ M TE/ 100 g FW. A previous studies carried out by Shofian et al. (2011) in order to determinate the free radical scavenging activity by reduction of 2,2-diphenyl-1-picrylhydrazyl (DPPH) and ferric-reducing antioxidant activity (FRAP) of methanolic extracts from different fresh and freeze-dry fruit pulp including musk melon (**Table 2.5**). Morais et al. (2015) conducted an experimental study to determine and compare antioxidant activity from the extracts of different tropical fruits parts and their processed peels (including melon fruit by-products). The free radical inhibition of FRAP and DPPH in the extracts of processed peels was found to be greater than the extracts of tropical fruit parts. These evidences demonstrate that melon fruit by-products are a good source of natural antioxidant molecules, and with high potential to be studied towards new applications.

2.4.2. Provitamin A activity

Provitamin A activity is the ability of carotenoids to make vitamin A (retinol and retinal) by the action of carotene dioxygenase (Saini, Nile, and Park, 2015). In addition, provitamin A activity plays a role in lipid oxidation and anticarcinogenic properties, which are very important biological functions (Kuhad, Gupta, and Singh, 2011). The human body cannot synthesize carotenoids compounds, so the only source is the intake of provitamin A compounds from foods. Fruits may therefore be highly regarded as such foods, as they are a rich source of carotenoids (like lycopene, β -carotene, α -carotene, lutein, zeaxanthin, β -cryptoxanthin and others) (Sarungallo et al. 2015). There are only three carotenoids (**Figure 2.4**), such as β -carotene, α -carotene and β -cryptoxanthin, which can be converted to retinol (vitamin A) in the body that we call provitamin A carotenoids (Laur and Tian, 2011). *C. melo* has been regarded as one of the principal sources of β -carotene present in pulp, peels and seeds. Nevertheless, there are limited

studies on its bio-accessibility/bioavailability and provitamin A activity (Fleshman et al., 2011).

Table 2.5. General spectrum of some studies regarding antioxidant activity from different varieties of melon by-products.

Samples	Substrates	Type of Extract	Employed Assay	Remarks	Reference
Ambrosia	Peel powder	Methanolic extract	ABTS (AAE/mL extract)	0.19	Ganji, Singh, and Friedman, (2019)
<i>C. melo</i>	Leaf	Methanolic extract	DPPH IC ₅₀ (µg/mL)	780.1	Hashemi, Ebrahimzadeh, and Khalili, (2019)
	Lyophilized peel	Methanol extract	DPPH IC ₅₀ (µg/mL) FRAP (µmol FeSO ₄ /100 g DM)	189.02 67.75	
	Oven dried peel	Methanol extract	DPPH IC ₅₀ (µg/mL)	370.93	Morais et al. (2015)
			FRAP (µmol FeSO ₄ /100 g DM)	29.36	
	Pulp	<i>n</i> -hexane extract	ABTS IC ₅₀ (mg/mL)	4.9%	Bonesi et al. (2019)
			DPPH IC ₅₀ (mg/mL)	33.5%	
			FRAP µM (Fe (II)/g DM)	6.4	
			β-carotene bleaching test IC ₅₀ (mg/mL)	0.2	
			DPPH IC ₅₀ (µg/mL)	582.7	
			DPPH IC ₅₀ (µg/mL) FRAP (µmol FeSO ₄ /100 g DM)	814.24 28.57	
Raw peel	Methanol extract	DPPH IC ₅₀ (µg/mL)	458.60	Hashemi, Ebrahimzadeh, and Khalili, (2019)	
		FRAP (µmol FeSO ₄ /100 g DM)	49.49		
Canary	Peel powder	Methanolic extracts	ABTS (AAE/mL extract)	0.21	Ganji, Singh, and Friedman, (2019)
Cantaloupe	Peel	Ethanol extracts	DPPH (mg AAE/ g DM)	12.27	Vella, Cautela, and Laratta, (2019)
			FRAP EC ₅₀ (mg/mL)	5.65	
	Pulp	Methanol extracts	DPPH IC ₅₀ (mg/mL)	9.58	Ismail, Chan, Mariod, and Ismail, (2010)
			Hydroxyl radical (g DMSOE/ g)	39.11	
			DPPH IC ₅₀ (mg/mL)	11.9	

			Hydroxyl radical (g DMSOE/ g)	67.19	Ismail, Chan, Mariod, and Ismail, (2010)
	Seeds	Ethanol extracts	DPPH (mg AAE/ g DM)	0.31	Vella, Cautela, and Laratta, (2019)
			FRAP EC ₅₀ (mg/mL)	55.03	
		Methanol extracts	DPPH IC ₅₀ (mg/mL)	25.44	Ismail, Chan, Mariod, and Ismail, (2010)
			Hydroxyl radical (g DMSOE/ g)	37.37	
Cantaloupe	Peel powder	Methanolic extracts	ABTS (AAE/mL extract)	0.14 0.17	Ganji, Singh, and Friedman, (2019)
Galaoui	Pulp	Cetone extracts	ABTS (µM Trolox/100 g FM)	160.92	Henan et al. (2016)
Galia Goddess	Peel powder	Methanolic extracts	ABTS (AAE/mL extract)	0.26 0.20	Ganji, Singh, and Friedman, (2019)
Golden	Seeds	Methanolic extract	DPPH Lipid peroxidation Nitric oxide	75.20% 83.24% 80.50%	Olubunmi, Olajumoke, Bamidele, and Omolara, (2019)
Hami gold Hami melon	Peel powder	Methanolic extracts	ABTS (AAE/mL extract)	0.20 0.14	Ganji, Singh, and Friedman, (2019)
	Peel Pulp Seed	Aqueous extract	FRAP (mmol FeSO ₄ /100 g FM)	0.52 0.24 0.31	Guo et al. (2003)
Honeydew	Peel powder	Methanolic extracts	ABTS (AAE/mL extract)	0.17	Ganji, Singh, and Friedman, (2019)
Maazoun	Pulp	Acetone extracts	ABTS (µM Trolox/100 g FM)	22.00	Henan et al. (2016)
Santa claus	Peel powder	Methanolic extracts	ABTS (AAE/mL extract)	0.20	Ganji, Singh, and Friedman, (2019)
Sharlyn melon	Peel powder	–	DPPH	12.53%	Al-Sayed and Ahmed (2013)
Stambouli	Pulp	Acetone extracts	ABTS (µM Trolox/100 g FM)	127.34	Henan et al. (2016)
Sun melon	Freeze-dry pulp	Methanolic extracts	DPPH FRAP (µmol Trolox/100 g FM)	30% 550	Shofian et al. (2011)
	Fresh pulp	Methanolic extracts	DPPH FRAP (µmol Trolox/100 g FM)	25% 500	
Trabelsi	Pulp	Acetone extracts	ABTS (µM Trolox/100 g FM)	140.01	Henan et al. (2016)
Tuscan Vine	Peel powder	Methanolic extracts	ABTS (AAE/mL extract)	0.13 0.17	Ganji, Singh, and Friedman, (2019)

Abbreviations: AAE: ascorbic acid equivalents; ABTS: 2,2'-azino-bis-3-ethylbenzthiazoline-6-sulphonic acid; DM: dry matter; DMSOE: Dimethyl sulphoxide equivalents; DPPH: ,1-diphenyl-2-picrylhydrazyl; FeSO₄: Ferrous sulfate; FM: fresh matter; FRAP: Ferric reducing antioxidant power

A study previously mentioned of Laur and Tian (2011) employed different varieties of melon fruit and quantified and identified some carotenoids from the pulp and their provitamin A activity. They reported using conversion factors of 0.6 mg β -carotene = 1 IU vitamin A and 12 mg dietary β -carotene = 1 RAE (**Table 2.6**). Since there are few reports about provitamin A activity from melon and its by-products, this will open up a new field of research for the extraction and recovery of valuable molecules from this natural source and the development of functional products with potential health benefits.

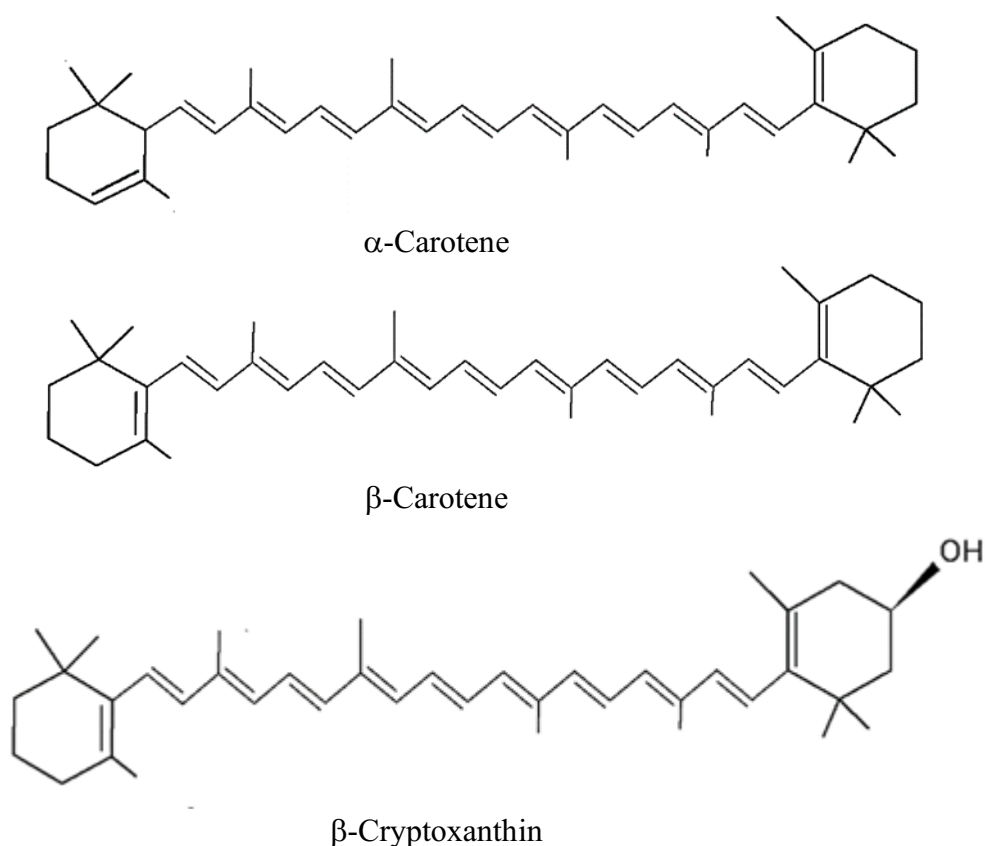


Figure 2.4. Structure of the principal carotenoids present in melon with provitamin A activity.

2.4.3 Anticancer activity

Other biomolecules present in *Cucurbitaceae* family are cucurbitacin, a natural anticancer agent. Cucurbitacins are highly oxygenated tetracyclic-triterpenes with strong taste and toxic effects. However, information about these molecules and their biological activity is limited but some reports indicate the potential of cucurbitacins to treat pathologies such as cancer (Amaro, Oliveira, and Almeida, 2015). Chan et al. (2010) reported that cucurbitacin B inhibits five different leukemia cells. This suggests that cucurbitacin is a potential therapeutic candidate in the treatment of human cancer diseases. Ibrahim et al.

(2016) identified a new triterpenoid (cucumol A) in methanol extracts of the melon *reticulatus* seeds. This new compound showed cytotoxic activity towards L5178Y and Hela cancer cells with ED₅₀ values of 1.30 and 5.40 µg/ml respectively compared to paclitaxel. Moreover, polyphenols and carotenoids provitamin A have also been reported for its biological activities in the treatment of some cancer (Miao and Wang, 2013; Govea Salas et al., 2013). However, reports on the application of polyphenols and carotenoids from melon fruit against human cancer diseases have not been found. Thus, it can be concluded that pharmacological studies have a broad scope for future research in this area.

Table 2.6. β-carotene and its corresponding vitamin A activity and lutein content in melon pulp from different geographical location of the origin and cultivation

Varieties of Melon	GLOandC	β-carotene (µg/100 g FW)	Vitamin A (IU/100 g FW)	Vitamin A (µg RAE/100 g FW)	Lutein (µg/100 g FW)
Cantaloupe	Guatemala	3861	6435	321.8	13.5
UkVar	Honduras	3633	6055	302.7	7.2
Caribbean Gold	CA, USA	2448	4080	204.0	17.3
Durango	CA, USA	3138	5230	261.5	12.7
Oro Rico					
Emerald	CA, USA	124.1	206.8	10.3	28.9
Honeydew	Mexico	172.9	288.1	14.4	32.6
UkVar	CA, USA	109.1	181.8	9.1	25.5
Santa Fe	CA, USA	118.7	197.9	9.9	27.7
Saturno	Honduras	99.0	165.0	8.2	13.7
Summer Dew	CA, USA	63.1	105.1	5.3	10.6
Vanessa					

Source: Laur and Tian (2011)

Abbreviations: RAE: Retinol activity equivalent; GLOandC: Geographical Location of the Origin and Cultivation; CA, USA: California, United States of America; UkVar: Unknown variety; FW: Fresh weight.

2.4.4 Antimicrobial activity

Traditionally, *C. melo* has been used as an anti-parasitic agent (anthelmintic or vermifuge activity) (Vishwakarma, Gupta, and Upadhyay, 2017). However, there is very little information regarding antimicrobial activity from melon fruit and its by-products. A study of methanolic and ethanolic extracts from melon seeds and leaves showed antibacterial inhibition against *Staphylococcus aureus* and Gram-positive in this case (Ibrahim and Mohamed, 2015; Ibrahim et al. 2016). In addition, polyphenol compounds have been well-recognized with antimicrobial activity by inhibiting enzymatic reactions that promote the growth of microorganisms (Martins et al., 2011; Govea Salas et al. 2013). In this context, many publications are very acceptable for the inhibition capacity of plant-based polyphenol-rich extracts due to the antimicrobial activity against several bacteria

and fungi. Pereira et al. (2007) used water olive leaf extracts attributed to the high content of phenolic compounds (oleuropein, luteolin-7-*O*-glucoside, apigenin-7-*O*-glucoside and caffeic acid) and reported the microbial inhibition against bacteria such as *Bacillus cereus*, *B. subtilis* and *S. aureus* [Gram positive], *Pseudomonas aeruginosa*, *Escherichia coli* and *Klebsiella pneumoniae* [Gram negative]) as well as fungi (such as *Candida albicans* and *Cryptococcus neoformans*). Mhamdi, Abbassi, and Abdelly (2015) also identified different phenolic compounds (such as quercetin, flavone, apigenin, luteolin and others) in *Ononis natrix* methanolic extracts and tested for their antimicrobial activity against bacterial strains (*viz.* *Enterococcus faecalis* and *S. aureus*) and fungal strains (*viz.* *C. albicans*) resulting in high growth inhibition. Presently, polyphenols extracted from mango peels showed strong antimicrobial effect against *Colletotrichum gloeosporioides*, *Sclerotinia sclerotiorum*, *Mucor* spp. and *Fusarium oxysporum* strains (Rojas et al., 2018). In addition, essential oils have also been reported as antimicrobial agents presenting different mechanisms of action against Gram-positive and negative bacteria, yeasts and molds have been shown to cause cell membrane damage. These mechanisms are related to alternating the composition of the cell membrane fatty acids, damaging the cytoplasmic membrane and reducing the proton motive force, altering the energy generation of bacteria as well as leakage from metabolites and ions (**Figure 2.5**). These mechanisms have been attributed to the ability to penetrate inside of the cell through the bacterial cell's outer membranes and cytoplasmic membranes. This actions lead to the disintegration of the cell structure, making it more permeable to the surrounding essential oils (Desbois and Smith, 2010; Rao et al., 2019). Thus, all the previously described reports show that melon and its by-products represent an attractive source of valuable BCs (such as oleuropein, luteolin-7-glucoside, apigenin-7-glucoside, and flavone). They have been well proven to have an effective antimicrobial activity. In addition, gallic acid, caffeic acid, hydroxytyrosol, and tyrosol are other polyphenols identified in melon fruit that have also been recognized as antimicrobial molecules (Govea-Salas et al., 2016; Antónia Nunes et al., 2018). Nonetheless, information about antimicrobial properties concerning melon fruit polyphenols is still limited, which will open up a new broad spectrum of naturally occurring antimicrobial studies for food applications to improve the product shelf-life.

2.5 Recent Research and Advanced trends for Future Prospects

2.5.1 Existing patents regarding melon fruit

In various countries, there are few intellectual properties as patents on melon fruit. However, a number of these patents relate to genetic identity and modification, such as the invention of Alexandros Aggelis and coworkers which provides the isolated DNA sequence for fruit ripening from *C. melo* (Aggelis et al., 2000). The procedure for the production of transgenic seedlings from genetically modified buds belonging to the species of *C. melo* containing a single gene introduced by the intermediary of *Agrobacterium tumefaciens* was patented by Michiel De Both et al. (1995).

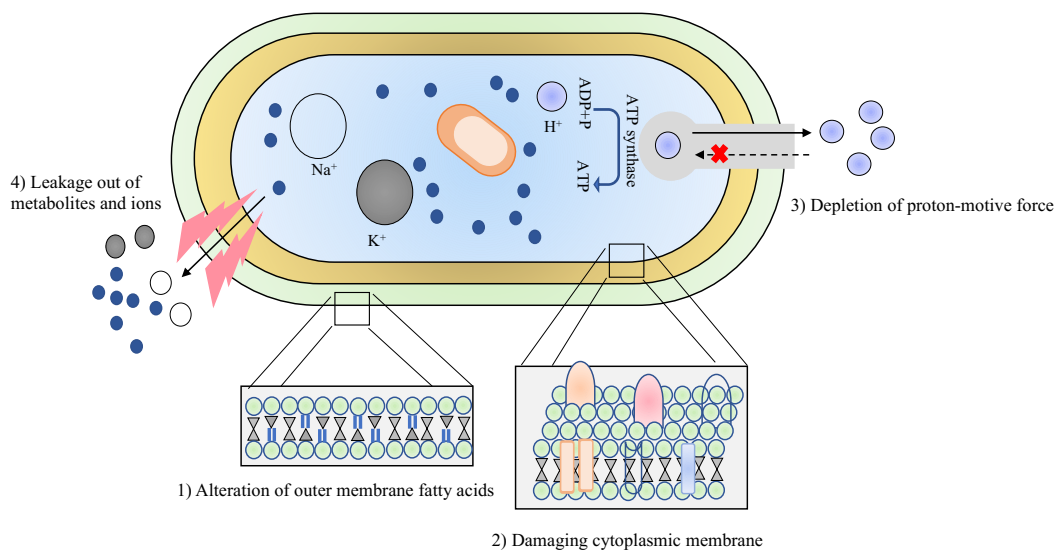


Figure 2.5. Antimicrobial mechanisms of action of essential oils (Rao, Chen, and McClements, 2019).

In addition, Kassies and coworkers patented a method for producing *C. melo* plants that resistant to the Cucumber Vein Yellowing Virus (CVYV) (Kassies et al. (2015). This invention was specifically related to plants which had a genetic element in its genome to combat the viral problem. In a patent disclosure, Garcia-Andres et al. (2016) also showed tolerance to Cucurbit Yellow Stunt Disorder Virus (CYSDV) and lack of negative traits associated with CYSDV tolerance, such as increased fruit size and reduced fruit set. Jeffrey M. Mills also published an innovation relating to melon hybrid SV3394MF plants, seeds and tissue cultures and their parent lines (Mills, 2017). This innovation seted out the methods for the production of a melon plant produced by the crossing of such plants on its own or with any other melon plant. Diergaard et al. (2014) submitted a patent on powdery mildew resistance to the genes of the *Cucumis* family, wherein the amino acid sequence encoded by said resistance-conferring gene. On the other hand, fewer inventions have been published for products or derivatives of melon fruit; for example; Dreyer et al.

(2006) disclosed a composition consisting of an active plant extract containing superoxide dismutase, coated or microencapsulated in a fat-soluble agent based on a fatty substance. “MELON CUTTING BOARDS” was the patent title published by Geier (2014) which describes the artefact for the removal of fruit peels, produced from a variety of materials (including metals, resins and plastics, ceramics or composites). Furthermore, there are also few patents concerned with the development of technologies for the production of new fractions and ingredients from melon fruit and its by-products. In the last ten years, there have been very few patents for the use of melon fruit. Therefore, it can be inferred that this will offer great opportunities for new inventions, development and knowledge for further research in the future, which will set out the methodologies for linking science and technology to the development of new or novel products. Likewise, new patents based on melon products should be a presumed innovation with well-defined industrial uses and close to commercial availability.

2.5.2. Melon by-products as functional ingredients

Nowadays, functional foods are described as food or food ingredients that have diverse health benefits, helping to prevent or reduce the risk of certain diseases such as cancers, cardiovascular and inflammatory disorders and diabetes (Silva et al., 2018). Diabetes and its complications are a serious problem of global concern that is gradually caused by oxidative stress (OS). This progression is due to the imbalance between the over-production of reactive oxygen species (ROS) and the low intake of natural antioxidants (such as polyphenols and carotenoids). It is well known that such BCs are capable of counteracting the negative impact of ROS on OS-related issues (Lo et al., 2017). Beyond those future perspectives for the valorization of melon by-products could be as functional ingredients due to these raw materials still retain a high content of relevant nutrients namely fiber and proteins as well as various BCs (carotenoids and polyphenols), which are linked to the prevention of health diseases. For example, these organic materials can be used directly as a source of dietary fiber (flour). This natural polymer has been used for the modulation of intestinal microbiota, such as *Bifidobacterium*. These bacteria have been associated with colon, stomach, breast and prostate cancer prevention (Veiga et al., 2018). On the other hand, polyphenols exhibit good inhibition of digestive enzymes (such as lipase, amylase and glucosidase) that minimize hyperglycemia which is also strongly associated with diabetes and obesity disorders (Sulaiman and Ooi, 2014). By virtue of these functional properties, and on the basis of their richness in nutrients and bioactive

components, melon by-products could be used as functional ingredients to develop new food products such as cookies, fiber bars or cereals.

2.5.3. *In Solid-state fermentation*

Traditionally, BCs have been recovered from plant matrices through conventional liquid/solid extraction processes using water or a mixture of organic solvents. Emerging technologies such as microwaves, ultrasound or the use of supercritical fluids have also been used (Giacometti et al., 2018). But these processes reflect only the initial pretreatment of total hydrolysis products, which are expensive processes for the successful extraction of BCs (Huynh, Van Camp, Smagghe and Raes, 2014). Industrially, acidic or alkaline pretreatment is used during the hydrolysis process but the products derived may have some toxicity and cause environmental pollution (Wang et al., 2010; Huynh, Van Camp, Smagghe, and Raes, 2014). For example, β -carotene is used in the food, feed, cosmetics and pharmaceutical industries. However, the pigment used in these industries is mostly chemically synthesized with less stability and activity (Roadjanakamolson and Suntornsuk, 2010). These unfavorable methodologies create an obligation to explore new ways of using these lignocellulosic materials. As a result, alternative technologies have been sought that mimic the processes taking place in nature, thus following the soft principle, such as biocatalysis chemistry. Nowadays, solid-state fermentation has been well documented in the use of fruit by-products on a dry weight basis for the production of BCs by microorganisms, such as the production of enzymes and the extraction of polyphenols and carotenoids (Larios et al., 2017; Soccol et al., 2017). In this context, solid-state fermentation coupled with melon by-products could emerge as an important strategy for the recovery of these high-value molecules for their potential applications in the food and pharmacological industries.

2.5.4. *Eco-green technologies for protein extraction*

The valorization of fruit by-products involves a field of study in which protein extraction from fruit by-products is performed after processing. *Cucumisin* [EC 3.4.21.25] is a serine protease which is mainly isolated from the melon mesocarp (Arima et al., 2013). However, this enzyme was however extracted by traditional methods, such as organic solvents, saturated salt solution, gel and ion-exchange chromatography. These methodologies have various limitations, including low industries scale, high costs and low purification rates, and in certain cases stability loss (Gagaoua et al., 2017). These

unfavorable facts force the use and development of eco-green methodologies such as protein extraction by natural polyelectrolytes and aqueous two-stage systems. Such techniques have recently emerged as alternative separation methods for isolation and purification of protein because their advantages relate to a simple scale-up process, a reduction in volume and rapid separation (Campos et al., 2019; Duarte et al., 2015). On the other hand, proteins with proteolytic activity have been addressed as natural catalysts with a strong industrial application intended to avoid toxic and costly reactions. Protein extraction with biological activity is thus an emerging subject in the field of biotechnology for its advantages against chemical catalysts based on fruit by-products including bagasse, peels, seeds, leaf and stem (fresh weight basis).

2.5.5. Production of micro- and nano-cellulose composites

Another potential area in which melon by-products are used is the isolation and production of micro- and nano-cellulose. Some interesting studies have shown that these polymers are obtained from lignocellulosic waste on a dry basis (Zhao et al., 2018). In the last ten years, composites and nanocellulose materials have been attracting the attention of the scientific and industrial communities because they represent renewable and biodegradable materials and claim to replace traditional petroleum products that prevent environmental pollution. (Kargarzadeh et al., 2017). By-products are mainly constituted by lignocellulosic biomass. In this regard, the use of organic matter under the context of valorization has shown a growing interest in which by-products are considered as a matter of treatment, minimization and the development of new reuse strategies to obtain new and value-added products. In this way, melon by-products are very interesting matrices that provide a good source of different molecules for research on new products that are able to solve major issues worldwide, such as human nutrition, pollution and food.

2.6. Conclusions

Melon fruit demonstrated to have very high levels of beneficial BCs in its parts (pulp, peels and seeds), including carotenoids (α -, β -carotene and β -cryptoxanthin), polyphenols (flavonoids and phenolic acids) and fatty acids (oleic, linoleic and palmitoleic acid). Due to the content of BCs still present in melon by-products, they could emerge as a potential resource for the food and pharmaceutical industries. However, there are still many constraints which can be identified as i) inconsistent and conflicting data in the content of total BCs present in the melon fruit, ii) several existing methodologies for the

extraction and quantification of these compounds which can generate different range of values and iii) the BCs concentration in melon is influenced by many factors such a variety, processing, agro-climate and post-harvest storage conditions and may be difficult to standardize final ingredients. These issues make difficult the analysis and standardization of all the existing data to infer consolidate conclusions. On the other hand, the valorization of melon by-products is a critical step in food waste management to solve environmental problems. To achieve this, more research is needed, focusing on the optimization of extractive methodologies as well as the implementation of strategies for the scale-up industrial applicability and guarantee a broad exploitation of melon by-products towards value added molecules and products.

Objectives

The main objective of this thesis was the development of an integral valorisation strategy for the extraction and characterization of value-added bioactive compounds from industrial melon by-products – peels, allowing bioresource recovery and zero-waste approach.

Melon peels are rich resources of several valuable compounds with high industrial interest, including pigments, phenolic antioxidants, dietary fibre (among pectin and cellulose) and proteins. Despite their richness, they have been scarcely explored and studies on valorisation of these melon biomass have not been extensively reported yet. Therefore, to further increase the overall value of this biomass, an exploration of melon peels as resources for obtention of these kinds of natural compounds can be an excellent opportunity to the development of novel functional ingredients, while fruit waste accumulation, environmental and economic issues are avoided. These new ingredients possess bioactive and functional properties that could respond the market needs and consumer demand for natural and clean label products, which subsequently, could be applied in food, nutraceutical and pharmacological industries.

The present research work was carried out at ESB-UCP.

The melon peels were evaluated as resources of bioactive compounds to develop new functional ingredient encompassing the following specific objectives:

- i) Integral fractionation process for the development of functional melon peel ingredients and their chemical characterization for value-added compound identification.
- ii) Separation and isolation of proteins and pigments (chlorophylls and carotenoids) through sustainable strategies.
- iii) *In vitro* evaluations of melon peels flour and powder (bioactives stability, antioxidant and prebiotic properties) through gastrointestinal tract (GIT) digestion and prebiotic effect on human gut microbiota.
- iv) Pectin extraction and characterisation by hot-acid treatment and its potential emulsifying and gelling properties.
- v) Microcrystalline cellulose obtention and characterisation from melon peel residues after pectin extraction.

- vi) Application of a green precipitation technique for the recovery of cucumisin enzyme and evaluation of their potential application as vegetable rennet.
- vii) Identification and extraction of proteins-like antifreeze proteins after green precipitation process and evaluation of their antifreeze activity.

PART II – Production, characterisation and bioactivity

CHAPTER 3 – A chemical valorisation of melon peels towards functional food ingredients: Bioactives profile and antioxidant properties

Ricardo Gómez-García^{a,b}, Débora A. Campos^a, Ana Oliveira^a, Cristóbal N. Aguilar^b,
Ana R. Madureira^a and Manuela Pintado^{a*}

^a*Universidade Católica Portuguesa, CBQF - Centro de Biotecnologia e Química Fina – Laboratório Associado, Escola Superior de Biotecnologia, Rua Diogo Botelho 1327, 4169-005, Porto, Portugal*

^b*BBG-DIA. Bioprocesses and Bioproducts Group. Food Research Department, School of Chemistry, Autonomous University of Coahuila, Saltillo, Coahuila, Mexico*

Published:

Journal of Food Chemistry - ELSEVIER

Abstract

The goal of this work was to characterize the profile of bioactive compounds and the antioxidant activity of *inodorus* melon peels. Melon peels were divided into three fractions: a solid fraction with a higher content of carbohydrates (84.81%); a liquid fraction with a higher ash content (11.5%); and a pellet fraction with a higher protein content (34.90%). The structural carbohydrates study revealed a composition of cellulose (27.68%), hemicellulose (8.2%) and lignin (26.46%) in the solid fraction. The liquid fraction had the highest antioxidant activity based on results from DPPH, ABTS and ORAC assays. Flavones, hydroxybenzoic and hydroxycinnamic acids were the main phenolic classes found in all fractions. In addition, β -carotene, lutein, β -cryptoxanthin and violaxanthin had also been quantified. Melon fractions were rich in nutrients and bioactive substances and could be useful in the development of novel functional products, considering the growing market demand for safe and healthy food products.

Keywords: *Inodorus* melon, by-products valorisation, phenolic compounds, carotenoids antioxidants, dietary fibre, cellulose, pectin, functional ingredients.

3.1. Introduction

Cucumis melo L., commonly referred to as melon, belongs to the Cucurbitaceae family, and is one of the most common fruit cultivated in the tropical countries in the world and its consumption is associated with nutritional benefits as well as bioactive properties (Vishwakarma, Gupta, and Upadhyay, 2017). According to FAOSTAT 2018, the worldwide's melon production is estimated to be 40 million tonnes *per year*, with China as largest producer (12.7 million tonnes *per year*). Commercial melon processing sources are responsible for the massive accumulation of non-edible parts (peels and seeds) of between 8 to 20 million tonnes of waste *per year* worldwide (Rolim et al., 2019). This organic material may potentially provide a cheap source for creating new food products or ingredients or goods that minimize waste and the effects on the environment. At present, melon seeds and peels are by-products mostly produced by the fruit processing industry, with a negative contribution to the overproduction of food waste. Such melon by-products could be valued for their richness in bioactive compounds, in particular polyphenols (flavonoids and phenolic acids), carotenoids (α -, β -carotene and β -cryptoxanthin) and fatty acids (oleic, linoleic and palmitoleic acids), among other compounds (Mallek-Ayadi et al., 2018; Gómez-García et al., 2020). Such bioactive compounds found in melon fruit have shown possible health benefits (Lester, 2008), e.g., melon mesocarp has been used as an analgesic or anti-inflammatory agent as well as for the treatment of certain signs of pain or discomfort such as diarrhea, dysuria and dyspepsia (Parle and Singh, 2011). Several research on melon and its by-products have shown that melon fruit has various biological properties such as anti-cancer, anti-diabetes, anti-microbial and antioxidant activity (Ronny et al., 2010). In the food industry, the interest in extracting bioactive compounds with beneficial properties could meet the increased worldwide demand for nutritious foods and functional foods for various applications, such as food enrichments, fortifiers, food preservatives, colorants, natural antioxidants, etc (Trigo et al., 2020). On the other hand, it has also recognized the valorisation of fruit by-products as an important activity to minimize the harmful impact of food waste on the ecosystem as well as to recover added value compounds and build new streams of income (Campos et al., 2020b). In this case, numerous experiments were carried out during the last ten years and within the background of recovery, concentrating on the techniques for improving bioactive compounds, water replacement of organic solvents and the use of mechanical processes to prevent harmful and costly chemical

substances. Up to now, melon by-products are only explored in certain fractions of the studies, but final waste products are always produced that must be studied.

Therefore, the present work aimed to evaluate the potential of *C. melo* peels (*Inodorus* cultivar) produced by the fruit processing industry as a source of bioactive compounds using an integrated zero-waste recovery process. These fractions are examined for their nutritional properties and content of bioactive compounds and their antioxidant activity and potential for use in the food and pharmacological industries.

3.2. Materials and Methods

3.2.1. Chemicals

ABTS diammonium salt (2,2'-azino-bis(3-ethylbenzothiazoline-6-sulphonic acid)), D-glucose, 2,2-diphenyl-1-picrylhydrazyl, sodium carbonate, 2,2'-azo-bis-(2-methylpropionamide)-dihydrochloride, (97%) (AAPH), fluorescein (F-6377), 6-hydroxy-2,5,7,8-tetramethylbroman-2-carboxylic acid (97%) (Trolox, EC 258-422-8) and Folin-Ciocalteu from Merck (Algés, Portugal). Standards of galacturonic acid, gallic acid, caffeic acid, β -carotene (HPLC $\geq 95\%$, synth., cryst.), ferulic acid, 4-hydroxybenzoic, protocatechuic acid, vanillic acid, violaxanthin (HPLC $\geq 99\%$) and ammonium acetate, D-(+)-glucose, D-(+)-xylose, L-(+)-arabinose, ethyl acetate, ethylenediaminetetraacetic acid (EDTA), hydrochloric acid (HCl), potassium dihydrogen phosphate (KH₂PO₄), sodium hydroxide (NaOH), sulphuric acid (H₂SO₄) as well as the solvents have been used for HPLC analysis (acetonitrile, dichloromethane, formic acid, hexane and methanol) which were purchased from Sigma-Aldrich (Sintra, Portugal) while apigenin, β -cryptoxanthin (HPLC (UV) $\geq 97\%$), hydroxytyrosol, lutein (HPLC (UV) $\geq 95\%$), luteolin, luteolin-7-glycoside, luteolin-6-glycoside, naringenin-7-glycoside, naringenin, tyrosol, and zeaxanthin (HPLC (UV) $\geq 98\%$) from Extrasynthese (Lyon, France).

3.2.2. Melon peels

Melon fruits (*Cucumis melo* var. *inodorus*) were harvested at ripening stage (uncontrolled condition) from the Alentejo region in Portugal during the summer season of 2017, and after that processed by Nuvi Fruits S. A. Company Torres Vedras (Portugal). Fresh melon peels were produced as by-products and then transported to our facilities (CBQF) at -20 °C. The peels were kept at -20 °C until they were processed and pre-treated.

3.2.2.1 Processing of melon peels

Melon peels were processed in order to obtain 3 different fractions identified as solid fraction (SF), liquid fraction (LF), fresh pellet fraction (PF_(f)). The peels were unfrozen at room temperature for 6 h and were weighed. Subsequently, the peels were crushed by a kitchen juice machine, which operates under centrifugation, producing two fractions: the fresh solid fraction (FSF) and the juice fraction (JF). The JF consisted of a rich liquid with a solid remnant of pulp. The FSF was pressed manually to remove the excess of liquid and then placed in an oven dried for 48 h at 60 °C to obtain the SF. The recovered liquid from FSF was combined to the JF and then centrifugated (11469 g for 15 min, 4 °C). The clarified supernatant was identified as the LF and the precipitated solids as the PF. The PF was subsequently divided in two (a half of total weight), one part was kept at -20 °C (PF_(f)) and the other was freeze-dried (PF_{F-D}). There was no waste stream at the end. Till the experiment, all three fractions were stored. All the experiments were carried out in triplicate. The flow chart of proposed fractionation process for melon peels valorisation under zero-waste approach is illustrated in **Figure 3.1**.

3.2.3. Chemical composition of melon peels

Dry matter (DM), moisture, ash, protein, dietary fiber, and melon peel carbohydrate fractions were determined in triplicate according to standard procedures as follows.

3.2.3.1. Dry matter and moisture content

For each fraction, the dry matter was determined using the AOAC (1990) methodology. The moisture content was calculated by drying melon fractions (2 g) in the oven at 105 °C for 24 h until constant weight (AOAC, 1997). The results were expressed as a percentage of DM.

3.2.3.2. Ash

Ash was determined by carbon removal using an initial 2 g of dry samples to be incinerated in a muffle furnace at approximately 550 °C for 24 h (AOAC, 1980). Total ash was expressed as a percentage of DM.

3.2.3.3. Protein content

The total protein of the fractions was determined using the Kjeldahl method (AOAC, 1997). Protein was calculated using the conversion factor (6.25) (Mallek-Ayadi et al., 2017). The data was expressed as a percentage of DM.

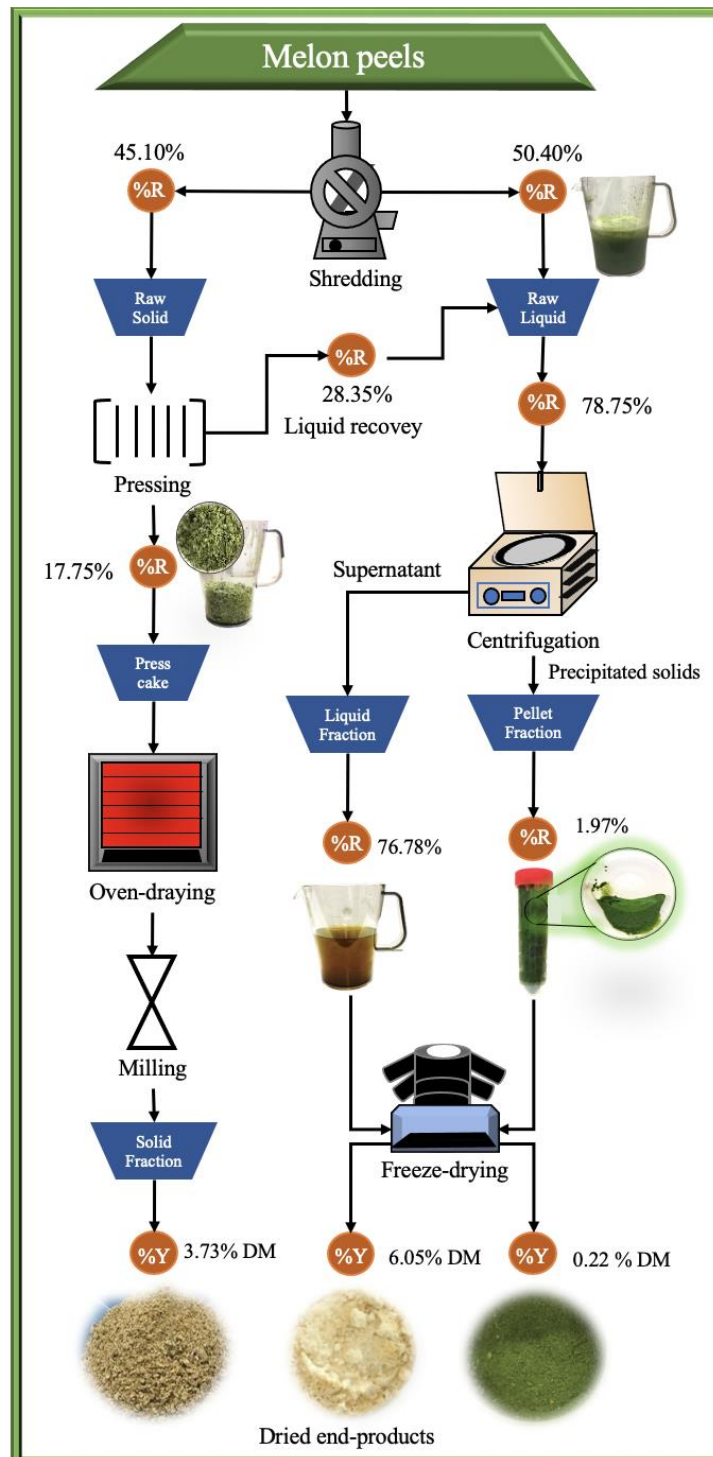


Figure 3.1. Proposed fractionation process for melon peels valorisation under zero-waste approach. %R: recovery percentage; %Y: yield percentage; DM: dry matter.

3.2.3.4. Total fibre content

The quantification of total dietary fiber in each fraction was carried out using the gravimetric technique described by Lee et al. (1992) with slight modifications. 1 g of the sample was hydrolysed with heat-stable α -amylase (E-BLAAM, 100 °C; 30 min; pH 8.2), then digested with protease (E-BSPRT, 60 °C; 30 min; pH 7) and finally with amyl glucosidase (E-AMGDF, 60 °C; 30 min; pH 4.5) (Megazyme analysis kit). The hydrolysed mixture was vacuum filtered using a crucible flask (Pyrex® 50 mL M, Corning, Inc., USA) and washed twice with hot distilled water (80-90 °C), ethanol (95 %) and acetone. After drying, the residual crucible was weighted at 105 °C for 24 h to determine the insoluble fiber. The filtrate was combined with 95 % ethanol (1:4; 60 °C; 60 min) and the precipitates were collected and treated as described above to determine soluble fiber. Total dietary fiber was calculated by adding together the total amount of insoluble and soluble dietary fiber. Extractives and structural carbohydrates (cellulose and hemicellulose) and lignin of SF and PFF-D were quantified according to Sluiter et al. (2008). The dry fraction (0.3 g) was hydrolyzed by the addition of 3 mL of sulphuric acid (72 %) and subsequent incubation at 30 °C for 1 h. The mixture was then diluted to 4 % sulphuric acid by the addition of distilled water, followed by a suspension incubation at 121 °C for 1 h. The hydrolyzed mixture was vacuum filtered (Pyrex® 50 mL M crucible, Corning, Inc., USA) and the solid residues were used for gravimetric analysis of acid-insoluble lignin and the filtrate was used for acid-soluble lignin and sugar quantification. Sugar analysis was performed using the Beckman and Coulter 168 series HPLC (PDA 190-600 nm) (Beckman and Coulter; Fullerton, CA, USA). The separation was carried out using the Aminex HPX-87H column (BioRad, Hercules, CA, USA), with sulphuric acid as a mobile phase at 5 mM, with a flow of 0.6 mL/min, 60 °C. Data acquisition and analysis were carried out using Karat32 software. The detection was performed with an infrared detector (Knauer, Berlin, Germany), the peaks were analyzed and quantified using the calibration curves of each sugar standard. The peaks obtained were analyzed by comparing the retention time with the standard of simple sugars (glucose, arabinose, and xylose). Three independent analyzes were performed for each experiment.

3.2.3.5. Total carbohydrates

Total carbohydrate content of *C. melo inodorus* peel fraction was calculated by the difference of mean values [100 - (% moisture + % ash + % protein + % lipid)] (Lima et al., 2014).

3.2.3.6. Fat content

The total fat content of the melon peel fractions was calculated using the Soxtec method (Soxtec 8000, Foss, Denmark) using 1 g of the sample packed in a cellulose thimble and extracted with 60 mL of hexane at 90 °C for 3 h. The analysis was conducted by triplicate and the results were expressed as a percentage of DM.

3.2.3.7. Total extractable pectin quantification (TEP)

Extractable pectin was only quantified in an SF by measuring three forms of naturally occurring pectins such as water-soluble pectins (WSP), chelator soluble pectin (CSP) and hydroxide soluble pectin (HPS), as previously stated by Deng et al. (2011) with slight modifications. 1 g of SF was homogenized with 40 mL of distilled water (IKA Ultra-turrax T18, Wilmington, USA) at 8000 rpm for 10 minutes. The homogenate was then centrifuged (17920 g for 15 min), filtered through Whatman No. 1 filter paper, and the solid and liquid were collected in separate tubes. WSP was obtained after overnight precipitation with ethanol (95 % v/v) at a ratio of 1:5 (v/v) to -4 °C. CPS was obtained from the solid residue after 10 min of boiling with ethanol (95 % v/v) and then three continuous extractions from the slurry with Na₂-EDTA (50 mM, pH 8.0). In each extraction, the resulting suspension was filtered (Whatman No. 1 filter paper) and the 3 filtered solutions were mixed. The solid fraction obtained from the Na₂-EDTA extractions was then added with 50 mL of NaOH (50 mM) in a roller agitator (15 min) at room temperature. This suspension was filtered (Whatman No. 1 filter paper) and the filtrate was collected for HSP measurement. Galacturonic acid equivalents (GUAE) were used for the quantification of WSP, CSP and HPS using a galacturonic acid analytical standard calibration curve (0.005 – 0.15 mg/mL). Briefly, 250 µL of boric acid-sodium chloride solution plus 250 µL of standard (or sample) and 4 mL of H₂SO₄ (96 %) incubated at 70 °C for 40 min for reaction. Later, the reacted mixture was submerged in cool water at a constant temperature of 1 h, added with 200 µL of dimethylphenol reagent (100 mg of 3,5-dimethylphenol in 100 mL of glacial acetic acid). Finally, all samples were measured at 400 nm and 450 nm in the UV mini 1240 spectrophotometer (Shimadzu Tokyo, Japan) and the results were expressed as g of GUAE/100 g DM with the following equation 3.1:

$$GUAE = \frac{A(t) * V(t) * D * C * 0.91 * 100}{A(s) * W(t)} \quad (3.1)$$

where: $A(t)$ is the difference in absorbance of the sample solution; $V(t)$ is the total volume of sample solution; D is the dilution factor of the sample; C is the concentration of the standard (0.5 mg/mL); $A(s)$ is the difference in absorbance of the 0.1 mg/mL standard; $W(t)$ is the weight of the sample (mg) and 0.91 is the factor for converting experimentally determined values for monosaccharides to polysaccharides.

3.2.4. Preparation of melon peels extracts

Methanol extracts were prepared with 25 mL of solution (methanol/water) (80 % v/v) and 2.5 g of each fraction (SF and PF_(f)) homogenized with the Ultra-Turrax apparatus (T18, Wilmington, USA) at 24 000 rpm for 1 min. The mixture was left under continuous stirring (300 rpm) at room temperature for 30 min. Each resulting sample was centrifuged (4480 g for 15 min, 4 °C) and the supernatants were collected and filtered by 0.45 µm (Orange Scientific, Braine-l'Alleud, Belgium). Only 15 mL aliquot of the extracts were evaporated to dryness (30 °C) in the RCV 2-18 speed-vacuum evaporator (Chris. Osterode am Harz, Germany) and stored at -20 °C until their analysis. During processing, only LF samples were used directly from fresh peels for each corresponding analysis without any treatment.

3.2.5. Total phenolic content (TPC)

The total phenolic content was spectrophotometrically determined for each corresponding extract (SF, LF and PF_(f)) according to the Folin-Ciocalteu reagent method (Singleton and Rossi, 1965). An aliquot of 0.05 mL of extract and 0.05 mL of Folin-Ciocalteu reagent were mixed. After that, 1 mL of sodium carbonate (75 g/L) plus 1.4 mL of distillate water was added to the tube and vortexed, the reaction was incubated for 1 h in the dark at room temperature. Finally, the absorbance was finally measured at 750 nm. Gallic acid was used as a calibration curve standard (0.05-0.50 mg/mL) and the results were expressed as milligrams of gallic acid equivalent per 100 grams of dry matter (mg GAE/g DM).

3.2.6. Total insoluble bound phenolics (IBP)

Insoluble bound phenolics were determined using the method described by Xie et al. (2015) with some modifications. Briefly, 100 g (DM) of SF washed once with distilled water to remove soluble and free phenolic compounds under stirring at room temperature for 30 min. This extract was centrifuged at 4480 g for 10 min, the supernatant was

removed, and the solid matter was oven-dry at 60 °C for 24 h. This solid matter was named SF-IBP. SF-IBP was then released by hydrolyzing 1 g with 20 mL of 4 M NaOH in distilled water at room temperature in an orbital shaker at 250 rpm for 3 h (WIGGENHAUSER SI-100C, Berlin, Germany). The mixture was acidified to pH 1.5-2.0 by continuous addition of 6 M HCl. The mixture of acid was washed four times with ethyl acetate (25 mL). The fraction of ethyl acetate was collected and dried up to a total dryness using a rotary vacuum evaporator at 30 °C. The extract obtained was stored at -20 °C until the analysis was carried out. Limited phenols were measured using the Folin-Ciocalteu method and expressed as mg GAE/100 g DM.

3.2.7. Total carotenoids content (TCC)

Carotenoids were extracted as described by Oliveira et al. (2015) with some modifications. Briefly, 0.75 g of melon peel fraction (SF and PF_(f)) in a polypropylene tube were mixed with 3 mL of cold ethanol and homogenized at 24,000 rpm for 3 min using Ultra-Turrax (IKA T18, Wilmington, NC, USA). Later, 3 mL of hexane was added to the mixture and then centrifuged (4480 g at 4 °C for 15 min). The hexane layer was transferred to the new tube and the residue was re-extracted with 0.75 mL of saturated sodium chloride and 3.6 mL of hexane. The mixture was again centrifuged, and the second hexane layer recovered and combined with the first hexane layer for saponification. Saponification was performed using the resulting hexane extracts (4.5 mL) which were mixed with 4.5 mL of 10 % KOH methanol in a sealed tube wrapped in aluminum foil to exclude light. The reaction remained under agitation for 16 h at 300 rpm and room temperature. After the reaction time, the hexane-rich top phase was collected and washed once with 20 mL of 10 % NaCl solution and three times with deionized water until neutral pH. Carotenoids were finally quantified after saponification by 454 nm absorbance measurement with a UV mini 1240 spectrophotometer (Shimadzu, Tokyo, Japan). A pure β -carotene calibration curve (0.005 – 0.030 mg/mL) standard was used to quantify the total carotenoid content by measuring the absorbance at 454 nm and expressed as mg/100 g DM. All of the extracts were performed in triplicate.

3.2.8. Identification and quantification of phenolics and carotenoids by HPLC

Phenolic compounds and carotenoids were investigated in HPLC-DAD melon peel fractions. Polyphenolic analysis was performed according to the method of Campos et al. (2020c) with some modification using the Waters Series e2695 Separation Module

System (Mildford MA, USA) interfaced with the UV/Vis photodiode array detector (PDA 190-600 nm). Separation was performed in the reverse-phase column (COSMOSIL 5C18-AR-II Packed Column – 4.6 mm I.D. × 250 mm; Dartford, UK). Two different mobile phases were applied, the mobile phase A – water/methanol/formic acid (92.5:5:2.5, v/v/v) – and the mobile phase B – methanol/water/formic acid (92.5:5:2.5, v/v/v) – under the following conditions: injection volume of 50 L, continuous flow of 0.5 mL/min, gradient elution starting at 100 % mobile phase A for 50 min, then gradient reset at 45 % A and 55 % B between 50 to 55 min. Finally, the mobile phase A returns to 100 % and remains at this percentage for 4 min (until 59 min). Data acquisition and analysis were carried out using Software Empower 3. Detection was performed at wavelengths of 280 and 320 nm and identification and quantification were performed using pure standard calibration curves (HPLC grade) by comparing their retention time and wavelength. Carotenoids were investigated by Oliveira, Pintado, and Almeida (2012) in HPLC equipment (Waters Series 600, Mildford MA, USA) using acetonitrile, methanol, dichloromethane, hexane and ammonium acetate (55:22:11.5:11.5:0.02 v/v/v/v/w) under isocratic conditions at 1 mL/min flow rate during 20 min at 30 °C. Injection volume was 50 µL and detection was performed by a 454 nm diode array detector (Waters, Massachusetts, EUA). β-Carotene, lutein, β-cryptoxanthin and violaxanthin were quantified using a pure standard calibration curve expressed as mg/100 g DM of melon peels. For each analysis, three independent analyzes were carried out.

3.2.9. Identification of phenolic compounds by LC-ESI-UHR-QqTOF-MS

Phenolic compounds were also identified by LC-ESI-UHR-QqTOF-MS in the melon peel fractions SF, PF, SF-IBP (methanolic extracts) and LF (direct measurement) by Monforte et al. (2018). The LC-ESI-UHR-QqTOF-MS test was carried out using the UltiMate 300 Dionex UHPLC (Thermo Scientific) coupled to the Ultra-High Resolution Qq-Time-Of - Flight (UHR-QqTOF) mass spectrometer with 50, 000 Full-Sensitivity Resolution (FSR) (Impact II, Bruker Daltonics, Bremen, Germany). Bioactive identification was performed using the Acclaim RSLC 120 C18 column (100 mm x 2.1 mm, 2.2 µm) (Dionex). The volume of injection was 1 µL. Two mobile phases were used, solvent A consisting of formic acid / water (0.1 % v/v) and solvent B of acetonitrile with formic acid (0.1 % v/v). The gradient started at 5 to 95 % in 7 min, which remained constant for 2 min and returned to 5 % B in 1 min and remained at 5 % B for an additional 5 min at a flow rate of 0.25 mL/min. The parameters for MS analysis were set using positive

ionization mode with spectra acquired over a range of m/z from 20 to 1000. The parameters were as follows: capillary voltage (4.5 kV), drying gas temperature (200 °C), drying gas flow (8.0 L / min), nebulizing gas pressure (2 bar), collision RF (300 Vpp), transfer time (120 μ s) and prepulse storage (4 μ s). Post-acquisition internal mass calibration used sodium format clusters with a sodium format delivered by a syringe pump at the start of each chromatographic analysis. High-resolution mass spectrometry was used to identify phenolic compounds present in fractions. The elemental composition of the compounds was confirmed on the basis of accurate mass and isotope-ratio calculations referred to as mSigma (Bruker Daltonics). The exact mass measured was within 5 mDa of the assigned elemental composition and the mSigma values < 20 were confirmed. Identification was carried out using pure standards (1 ppm) of methanol (LC-MS grade). All phenolic compounds were identified on their accurate mass $[M-H]^-$.

3.2.10. Total chlorophylls content (TCHC)

The extraction of chlorophyll was carried out according to Fundo et al. (2017) with some modifications, homogenizing 2.5 g of the corresponding sample (SF and PF_(f)) in 25 mL of methanol (99.9 %) with an ultra-turrax device (5000 g, 5 min). Samples were kept in a dark cold room at 4 °C for 24 h, then the mixtures were centrifuged (4480 g, 10 min, 4 °C) and the supernatants were collected. All the experiments were done in a triplicate. Quantitative chlorophyll determinations of supernatants were performed by reading the absorbance at 665.2 and 652.4 nm (UV mini 1240 spectrophotometer, Shimadzu, Tokyo, Japan) for chlorophyll (*a* and *b*) pigments. Chlorophylls were calculated using the following equations 3.2 to 3.4 for methanol as suggested by Lichtenthaler (1987):

$$\text{Chlorophyll } a \quad C_a = 16.72A_{665.2} - 9.16A_{652.4} \quad (3.2)$$

$$\text{Chlorophyll } b \quad C_b = 34.09A_{652.4} - 15.28A_{665.2} \quad (3.3)$$

$$\text{Total Chlorophyll} \quad C_{a+b} = 1.44A_{665.2} + 24.93A_{652.4} \quad (3.4)$$

3.2.11. Antioxidant activity determination

The DPPH^{•+} assay was performed using the Brand-Williams et al. (1995) method with some modification. The stock solution (600 μ M) was prepared by dissolving 24 mg of DPPH in 100 mL of pure methanol and then stored at -20 °C in the dark. After the preparation of a working solution (60 μ M) by mixing 10 mL of the stock solution with

methanol (90 mL), the working solution was later adjusted to a final absorbance of 0.600 ± 0.100 at 515 nm. In brief, 1.75 mL of DPPH (working solution) was added to 0,250 mL of each corresponding extract (SF, PF_(f) and LF). The reaction mixture was vortexed and kept at room temperature for 30 minutes in the dark. The absorbance was then measured at 515 nm with a UV spectrophotometer. Trolox was used as a standard for the preparation of a calibration curve (0.005-0.08 mg/mL). The results were triplicated and expressed in μM of trolox equivalents (TE)/100 g DM. ABTS^{•+} radical method was performed according to the methodology described by Arnao et al. (2001) with slight modifications. The stock solution was prepared by mixing ABTS^{•+} (7 mM) with potassium persulfate (2.5 mM) in ultra-pure water and kept in stirring at room temperature for 16 h. The solution ABTS^{•+} was diluted with water at an absorbance of 0.700 ± 0.020 at 734 nm. After that, 10 μL of the sample extract was allowed to react with 1 mL of ABTS^{•+} solution for 6 min in the dark and the absorbance was immediately recorded at 734 nm using a spectrophotometer (UV mini 1240 Spectrophotometer, Shimadzu, Tokyo, Japan). The standard curve was made with L-ascorbic acid (AA) (0.05-0.5 mg/mL). All samples were triplicated and expressed in mg ascorbic acid (EAA)/100 g DM equivalents.

The antioxidant activity was calculated using the following equation 3.5:

$$\text{AOA (\%)} = \frac{(\text{ABS of blank} - \text{ABS of sample})}{\text{ABS of blank}} \times 100\% \quad (3.5)$$

3.2.12. Oxygen radical absorbance capacity assay (ORAC)

The ORAC assay was carried out in accordance with the method established by Dávalos et al. (2004). The reaction was performed in a phosphate buffer (75 mM, pH 7.4) using 20 μL of the sample (corresponding dilutions) plus 120 μL of fluorescein (116.66 nM) in a black microplate (Nunc, Denmark) and the combination was pre-incubated at 37 °C for 15 min. Later, 60 μL of 2,2'-azobis-(2-methylpropionamidine)-dihydrochloride (AAPH) (46,6 mM) was added and then incubated at 40 °C for 137 min. A total of 104 measurements were read on the FlouSTAR OPTIMA fluorimeter (BMG Labtech, Offenburg, Germany) at 458 nm and 520 nm. The software used was the Fluostar Control 1.32 R2 version. The calibration curve was made using Trolox (0.0002 to 0.0016 $\mu\text{mol TE/mL}$) as an antioxidant standard and the results were expressed in $\mu\text{mol TE/mL}$ of

extract. It was made blank by using a phosphate buffer instead of a sample. All analyzes were done in triplicate form. Antioxidant curves were normalized to the blank curve corresponding to the same assay by multiplying the original data by $\text{fluorescence}_{\text{blank},t=0}/\text{fluorescence}_{\text{sample},t=0}$. Using the normalized curves, the area under the fluorescence decay curve (AUC) was calculated using equation 3.6:

$$\text{AUC} = 1 + \sum_{i=1}^{i=104} fi/f0 \quad (3.6)$$

Where $f0$ is the initial fluorescence average at 0 min and fi is the fluorescence media at time i . The AUC of each sample read was calculated by the following equation 3.7:

$$\text{AUC} = \text{AUC antioxidant} - \text{AUC control} \quad (3.7)$$

3.2.13. Statistical Analysis Section

Statistical analysis was performed using Windows version 24 of IBM-SPSS Statistics. The results were presented as a mean \pm standard deviation of three independent replicates ($n=3$). The normality of the data distribution was tested by the Kolmogorov-Smirnov test, the homogeneity of the variances by the Levene's test and the significance of the differences between the repetitions were tested by a one-way variance analysis (ANOVA). The null assumption that all means are equal was rejected when the difference between means was $P < 0.05$. After ANOVA, several test comparisons were conducted using Tukey's post-hoc test (homogeneity of the variance was assumed) $P < 0.05$ significance level in those statistically significant variables, and t -student test for chemistry composition, total phenols and individual antiphenolics content and structural carbohydrates, total carotenoids and total chlorophylls activity (DPPH and ABTS). The statistical analyzes performed were considered to be significant at $P < 0.05$.

3.3. Results and discussion

3.3.1. Proximate chemical composition

Table 3.1 shows the average composition of the three fractions obtained by the integral fractionation of the *C. melo* peel fractions. The moisture content of SF is lower (8.03 g/100 g DM) than reported by Mallek-Ayadi et al. (2017) in dehydrated *mazua* cultivar

melon peels (16.95 g/100 g DM) which is beneficial for the microbiological stability of the dried product. Also, the total protein content (0.82 g/100 g DM) in this fraction is lower than that obtained for Sharlyn melon peels (9.07 g/100 g DM) (Al-Sayed and Ahmed, 2013), perhaps because the proteins migrated to LF and PF fractions during processing. These two fractions had a high protein content (21.9 and 34.9 g/100 g DM, respectively). PF was the highest lipid content (5.07 g/100 g DM) and was found to be higher than that reported for Sharlyn melon peels (1.58 g/100 g DM) (Al-Sayed and Ahmed, 2013). In addition, the LF had the highest ash content (11.5 g/100 g DM) compared to the other fractions obtained due to the high concentration of soluble components, mainly carbohydrates and minerals which were solubilized in this fraction. Other authors also found some variability of these parameters in different melon varieties, such as *mazoun* melon peels (3.67 g/100 DM) (Mallek-Ayadi et al., 2017), equal to melon Sharlyn peels (11.09 g/100 g DM) but lower than melon peels (13.09 g/100 g DM) (Al-Sayed and Ahmed, 2013). On the other hand, the amount of total carbohydrate in SF (84.81 g/100 g DM) of *inodorus* peels was higher than that found for *mazuoun* peels (69.77 g/100 g DM) (Mallek-Ayadi et al., 2017). Recently, there has been a great deal of interest in polysaccharides isolated from natural sources, which are often used as food additives for dietary purposes due to their diverse health benefits, such as homeostasis in blood glucose, lipid metabolism and diabetes prevention (Masci et al., 2018). As an example, the SF had the highest total fiber content (44.42 g/100 g DM) comprised mainly by the insoluble and soluble dietary fiber with 40.39 and 4.03 g/100 g of DM, respectively. This value on *inodorus* melon peels was similar to the value of *maazoun* melon peels (41.69 g/ 100 g DM) as reported by Mallek-Ayadi et al. (2017). This higher content could be attributed to the thick skin of the *inodorus* variety, which has been shown to be more difficult than most other melon varieties due to the different conditions of agro-climate growth. Dietary fiber can be classified into two groups, water-soluble fiber (pectin) with beneficial functions and water-insoluble fiber (cellulose and lignin), which is the part of the plant that is resistant to intestinal digestion in the human large intestine. The benefits associated with fiber content are well known, especially for the prevention of diseases such as diabetes, treatment of gastrointestinal disorders, obesity and cardiovascular disease (Atef et al., 2013). Therefore, following the richness of the chemical composition of *inodorus* peel fractions, they could be used to develop new functional food products, increasing the protein and fiber nutritional content. With this approach, the current demand for healthy supplies can be met, which could help to reduce

hunger and malnutrition problems. On the other hand, these melon by-products could be considered as value-added sources of bioactive compounds that can be commercialized between industrial chains in order to reduce economic costs and increase industrial profits.

Table 3.1. Chemical composition of the three different fractions obtained from inodorus melon peels.

Component (%)*	SF	LF	PF
Total protein	0.82 ± 0.07 ^c	21.90 ± 3.53 ^b	34.90 ± 0.84 ^a
Fat	1.48 ± 0.31 ^b	0.25 ± 0.07 ^c	5.07 ± 0.01 ^a
Ash	4.86 ± 0.08 ^c	11.50 ± 0.02 ^b	7.77 ± 0.21 ^a
Total carbohydrates**	84.81 ± 0.14 ^a	66.40 ± 1.20 ^b	52.26 ± 1.67 ^c
Total fiber	44.42 ± 0.39 ^a	29.27 ± 1.02 ^b	26.63 ± 0.67 ^b
Insoluble dietary fiber	40.39 ± 0.16 ^a	8.72 ± 0.33 ^c	16.93 ± 1.48 ^b
Soluble dietary fiber	4.03 ± 0.56 ^c	20.55 ± 2.27 ^a	9.70 ± 1.02 ^b

All determinations were carried out in triplicated and mean value (± standard deviation). Different letters within the same row indicate significant differences between means ($P < 0.05$).

*Results are expressed in % of dry matter basis (g/100 g DM).

**Total carbohydrates content obtained by difference; SF: Solid Fraction; LF: Liquid Fraction; PF: Pellet Fraction.

3.3.2 Structural carbohydrates of the insoluble fractions (SF and PF)

Table 3.2 shows the structural components of SF and PFF-D, where glucose was the major monomer present in each sample (27.68 and 17.01g/100 g DM, respectively), followed by the total lignin polymer (26.46 g/100 g DM) in which insoluble acid (% AIL) and soluble acid (% ASL) lignins were mostly 23.37 and 3.09 g/100 g DM, respectively for SF, compared to PFF-D (22.26 g/100 g DM) for 18.35 and 3.91 g/10 g DM for SF. Xylose and arabinose monomers were also present in fractions of melon peels. Glucose was released from the chain of cellulose, while xylose was released from the chain of hemicellulose. As far as arabinose is concerned, this sugar is derived from hemicelluloses and is usually present in certain plant types and species. Hemicellulose with arabinose is also present in citrus by-products and has been used as a feedstock for the production of bioethanol (John, Muthukumar, Arunagiri, and John, 2017). On the other hand, it was also interesting that insoluble lignin was present in PF at a lower quantity than SF. This can be due to the fact that PF consists mainly of pulp cells and not of peel cells. These values are interesting because there are no studies available on the assessment of the specific structural composition of melon peel fiber by-products. Thus, on the basis of the structural composition of *C. melo* peel fractions, it is possible to

envisage the integral valorisation of this by-product towards valuable materials rich in diverse nutrients and bioactive molecules that can be used in industrial applications, in particular food, nutraceuticals, and cosmetics.

Table 3.2. Proximal structural composition of melon peels fractions.

Component	SF	PF (F-D)
Acid Insoluble Lignin (%AIL)	23.37 ± 3.67 ^a	18.35 ± 1.54 ^a
Acid Soluble Lignin (%ASL)	3.09 ± 0.12 ^a	3.91 ± 0.05 ^b
Glucose (g/100 g DM)	27.68 ± 1.68 ^a	17.01 ± 0.39 ^b
Xilose (g/100 g DM)	6.84 ± 0.37 ^a	4.37 ± 0.19 ^b
Arabinose (g/100 g DM)	1.38 ± 0.39 ^a	0.60 ± 0.16 ^b

SL: solid fraction; PF_(F-D): freeze dried pellet fraction; DM: dry matter; Different letters within the same row indicate significant differences between means (P < 0.05).

3.3.3 Extractable pectins in the SF

Pectin is made up of polygalacturonic methoxylate and is used in a variety of applications, such as biofuels (bioethanol production) and food (thickening agent, gelling agent, and stabilizer) industries. In addition, this polymer has beneficial uses in human health where it helps to restore intestinal function, lower serum cholesterol levels, remove heavy metal ions from the body, and stabilize blood pressure (Raji, Khodaiyan, Rezaei, Kiani, and Hosseini, 2017). The SF had a total concentration of 44.80 g GUAЕ/100 g DM distributed by chelator soluble pectins (CSP) with 30.30 g GUAЕ/100 g DM, followed by water soluble pectins (WSP, 13.35 g GUAЕ/100 g DM) and hydroxide soluble pectins (HPS) at the lowest level of 1.15 g GUAЕ/100 g DM. These contents are lower than those reported by Raji et al. (2017) in Iranian melon peels (48 % DM) during the pectin extraction process. The pectin matrix is also an essential structural component along with cellulose and hemicellulose in the plant cell wall (Deng, Penner, and Zhao, 2011). The higher concentration of CSP present in the SF indicates that pectins are constituents of the melon peel cell wall. With these significant values of pectin, a new study on the valorisation of this polysaccharide could be launched due to their high potential applications in a number of fields such as the food, medicine, and biofuels industries.

3.3.4 Total phenolics (TPC) and total carotenoids (TCC) content

Phenolic compounds or polyphenols are widely distributed in the plant kingdom, such as fruits, plant-derived beverages, husk seeds and peels that are widely known for their biological activity. These compounds offer potential health benefits, in particular by supporting the cardiovascular system (Rodríguez-Pérez, Quirantes-Piné, and Fernández-

Gutiérrez, 2013). **Table 3.3** shows the TPC of the melon peel SF, PF and LF. The LF had the highest polyphenol content of 798.43 mg GAE/100 g DM = 46.80 mg GAE/100 g Fresh Matter (FM), followed by PF (580.77 mg GAE/100 g DM = 66.07 mg GAE/100 g FM) and SF (296.03 mg GAE/100 g DM = 62.19 mg/100 g FM). This higher PF value could be attributed to the presence of more lipophilic compounds, such as flavonoids still associated with insoluble fiber, which were separated during the centrifugation process. All these values seem to be higher than those reported for melon pulp (16.71 mg GAE/100 g FM) (Shofian et al., 2011) and for other melon parts, such as pulp, seeds, and raw peels, with values of 313.45, 99.69, 357.80 mg GAE/100 g DM in the pulp, seed, and raw peels, respectively (Morais et al., 2015). Distinctively, these studies have shown that melon peels are relatively rich in phenolic compounds in relation to melon pulp and seeds. On the other hand, the insoluble bound phenolic compounds were also determined in this work. These are covalently bound to the structural components of the cell wall, such as hemicellulose and lignin (Xie et al., 2015) and were found to be present at a total concentration of 45.43 mg GAE/100 g DM for SF-IBP. To the best of our knowledge, no previous evaluation of the total IBP was performed on melon peels. Carotenoids, on the other hand, are a class of phytochemicals responsible for the natural pigments of different plants, such as lutein (yellow), β -carotene (orange) and lycopene (red), which occur in different fruits. Carotenoids are present in melon fruit and are attributed to their beneficial bioactivity, such as anti-inflammatory, anticancer, neuroprotective and cardiovascular disorders (Fleshman et al., 2011). In this study (**Table 3.3**), the maximum value of TCC was 98.59 mg β -carotene equivalents/100 g DM = 11.21 mg β -carotene equivalents/100 g FM in PF followed by 10.13 mg β -carotene equivalents/100 g DM = 2.12 mg β -carotene equivalents/100 g FM in SF. In the LF, the concentration of carotenoids was below the detection limit as they were lipophilic molecules and were separated and concentrated in the PF during the centrifugation process. In addition, melon peels are moderately rich in carotenoids compared to melon pulp reported by Fleshman et al. (2011), which showed concentrations of 24.23, 21.39 and 17.63 mg β -carotene equivalents/100 g DM in orange dew, honeydew and cantaloupe melons, respectively. Thus, these high values show the importance of melon by-products as a non-conventional rich source of such bioactive compounds for the development of new food ingredients. The identification and quantification of individual phenolic and carotenoid compounds in melon fractions was carried out using HPLC/LC-MS.

Table 3.3. Total phenolic, carotenoid and chlorophyll content evaluated in the extracts of melon fractions.

	TPC (mg GAE/100 g DM)	TCC (β -carotene equivalents/100 g DM)	TCHC (mg/100 g FM)		
			<i>a</i>	<i>b</i>	total
SF	296.03 \pm 7.75 ^c	10.13 \pm 0.21 ^b	8.21 \pm 0.34 ^b	3.53 \pm 0.08 ^b	11.74 \pm 0.29 ^b
LF	798.43 \pm 25.76 ^a	nd	nd	nd	nd
PF	580.77 \pm 5.08 ^b	98.59 \pm 8.53 ^a	109.82 \pm 7.42 ^a	66.02 \pm 4.82 ^a	174.84 \pm 11.76 ^a
SF-IBP	45.43 \pm 9.27 ^d	nm	nd	nd	nd

TPC: Total phenolic content; GAE: gallic acid equivalents; TCC: Total carotenoid content; TCHC: Total chlorophylls content; SL: solid fraction; LF: liquid fraction; PF: pellet fraction; SF-IBP: insoluble bound phenolics from solid fraction; DM: dry matter; FM: fresh matter; nd = not-detected; nm = no measured. Different letters within the same row indicate significant differences between means (P < 0.05).

3.3.5. Identification and quantification of phenolic compounds by HPLC/LC-MS

There are different classifications of polyphenols based on their chemical structure, such as tannins, lignans, flavonoids and phenolic acids, among others. Phenolic acids and flavonoids are the most representative polyphenols found in melon fruits (Horax et al., 2010). These bioactive compounds are widely distributed in plants with different functions, such as pigment colors and plant protection against microorganisms and insects. According to the LC-MS method, four chemical classes of phenolic compounds were identified in melon peel extracts, primarily phenolic acids and flavones, as well as phenyl ethanoids and phenolic alcohols. Fifteen individual phenolic compounds have been identified (**Table 3.4**) and at least nine of them have been quantified by HPLC showing their richness in flavonoids. The previous study showed the identification and quantification of the 10 phenolic compounds of Bitter melon, the two most representative of which were catechin and gallic acid, respectively 154.5 and 49.9 mg/100 g DM (Horax et al., 2010). In a recent study, 18 different phenolic compounds were identified in *maazoun* cultivar melon peel extracts (Mallek-Ayadi et al., 2017), where 3-hydroxybenzoic acid was the major phenolic acid (33.45 mg/100 g extract). In this study, the most relevant phenolic compound for all fractions was luteolin-7-glycoside (318.66 mg/100 g DM) which is a flavonoid with antioxidant properties and the second most representative compound was 4-hydroxybenzoic acid (123.60 mg/100 g DM). In this study, two different phenolic compounds were also identified as luteolin-6-C-glycoside in SF, LF and PF (27.39, 44.08 and 134.73, mg/100 g DM, respectively) and ferulic acid in LF and SF-IBP (16.27 and 6.33 mg/100 g DM, respectively), which have cross-linking

functions in the hemicellulose-lignin complex and possess antioxidant properties. It is important to note that one compound in the SF-IBP has not yet been identified which, based on the monoisotopic mass detected and the ChemSpider database available, has been suggested to be a luteolin-glycoside derivative with a mass of 593. In addition, the highest concentration of gallic acid (90.03 mg/100 g DM) was found for SF. Moreover, protocatechuic acid (0.77 mg/100 g DM), caffeic acid (16.65 mg/100 g DM), p-coumaric acid (36.92 mg/100 g DM) and vanilla acid (5.46 mg/100 g DM) were also found in these fractions. Other identified phenolics were hydroxytyrosol and tyrosol in both SF, LF and SF-IBP. All these phenolics have biological functions, such as antimicrobial, anti-inflammatory, anti-diabetic and antioxidant activity, which are well-attributed to their high free radical-scavenging capacity (Nunes et al., 2018). The sum of all phenolic compounds quantified by the HPLC-DAD analysis was different and lower than that quantified by the spectrophotometer using the Folin-Ciocalteu assay (Table 3.5). These differences could be attributed to the detection limit for quantification of certain phenolic compounds and also to the fact that Folin-Ciocalteu's reagent can react with other molecules (sugars and proteins) present in the extracts causing interference with the measurement, resulting in an overestimation of the total phenolic content. The high diversity of phenolic compounds in the melon peel fraction reveals the importance of the incorporation and valorisation of these compounds in the industrial chains because, among others, some of them have antimicrobial properties against phytopathogens that show potential applications as new food preservatives.

3.3.6. Identification and quantification of carotenoid compounds by HPLC

The HPLC-DAD analysis allowed the identification and quantification of four individual carotenoids in the SF, such as β -carotene (6.67 mg/100 g DM = 1.40 mg/100 g FM), Lutein (0.06 mg/100 g DM = 0.013 mg/100 g FM), β -cryptoxanthin (0.27 mg/100 g DM = 0.06 mg/100 g FM) and violaxanthin (1.67 mg/100 g DM = 0.35 mg/100 g FM). The PF had the highest concentration values (Table 3.5) corresponding to β -carotene (91.52 mg/100 g DM = 10.41 mg/100 g FW), Lutein (0.70 mg/100 g DM = 0.07 mg/100 g FM), β -cryptoxanthin (4.92 mg/100 g DM = 0.56 mg/100 g FM), while violaxanthin was not detected in this fraction. Carotenoids were not detected in LF extracts. For all our best knowledge, no previous studies of carotenoids identification and characterization by HPLC from peels have not been reported. Lower values were reported in different

varieties of melon pulp, especially of and lutein ranging between 0.06-3.85 and 0.007-0.032 mg/100 g FM, respectively (Laur and Tian, 2011). Carotenoids were not detected in LF extracts. In our best knowledge, no previous studies of HPLC identification and characterization of carotenoids from *inodorus* peels have been reported. Lower values have been reported in different varieties of melon pulp, in particular those of β -carotene and lutein between 0.06-3.85 and 0.007-0.032 mg/100 g FM, respectively (Laur and Tian, 2011). Concurso et al. (2012) also reported lower concentrations of β -carotene (1.44 mg/100 g FM) and ζ -carotene (1.08 mg/100 g FM) than those found in this study. These higher values could be explained by the milling process in which melon cell lipid membranes have been disrupted to improve the bioaccessibility of carotenoids. In addition, these bioactive compounds present in melon play an important role in the photoprotection of the human eye (provitamin A) by enhancing immune function and preventing chronic diseases. In fact, provitamin A activity plays an important role in lipid oxidation and anti-carcinogenic properties. Only three carotenoids (such as β -carotene, β -cryptoxanthin and α -carotene) can be converted into vitamin A in the body, and that two of them were presented in the *inodorus* peels (Laur and Tian, 2011). On the other hand, the human body cannot synthesize carotenoid compounds, so the only source is the intake of provitamin A compounds from food. According to Medeiros et al. (2019), the concentration of more than 2 mg TCC/100 g FM in food is considered to be beneficial to health. In this case, melon peel carotenoids show their importance and high nutritional value that could be used to develop functional and cheaper foods or ingredients with higher nutritional properties. Compared to other studies, all differences in results may be linked to different varieties of melon and different factors such as maturity, agro-climate, ripening, and post-harvest storage conditions (Amaro et al., 2018). Dehydration during storage is one of the major post-harvest problems of melon fruit resulting in loss of fruit quality, e.g., water loss, causing negative physical color changes, firmness of texture, and bioactive value (Fundo et al., 2015). These damages have been attributed to high metabolic activity, in particular the respiration rate, which has increased due to the high harvesting temperature, which leads to the rapid consumption of the reserves of carbohydrates, becoming vulnerable and perishable (Zainal et al., 2019).

Table 3.4. List of phenolic compounds identified and quantified in melon peel fractions detected by HPLC/LC-ESI-UHR-QqTOF-MS

No.	Compound	Chemical class	RT	[M-H] ⁻	MS/MS Fragments	Formula	Sample (mg/100 g DM)			
							SF	LF	PF	SF-IBP
1	Gallic acid	Hydroxybenzoic acid	4.7	169.0143	169.0143 (52) 125.0246 (100)	C7H6O5	90.03 ± 0.07 ^a	16.61 ± 0.01 ^b	nd	5.94 ± 0.69 ^c
2	Hydroxytyrosol	Phenylethanoid	5.6	154.16	153.0554 (100) 123.0450 (32)	C8H10O3	ud	ud	nd	ud
3	Vanillic acid	Hydroxybenzoic acid	6.2	167.0352	167.0352 (100)	C8H8O4	5.46 ± 0.02	ud	nd	ud
4	Protocatechuic acid	Hydroxybenzoic acid	6.6	153.0105	109.0237 (100)	C7H8O4	0.77 ± 0.01 ^a	0.38 ± 0.01 ^a	-	0.32 ± 0.09 ^a
5	4-hydroxybenzoic acid	Hydroxybenzoic acid	8.4	137.0240	137.0245 (18) 93.0350 (100) 60.1043 (9)	C7H6O3	30.53 ± 0.09 ^b	123.60 ± 0.13 ^a	nd	7.24 ± 0.01 ^c
6	Tyrosol	Phenolic alcohol	8.5	137.0139	137.0138 (100) 108.0128 (6)	C8H10O2	ud	ud	nd	nd
7	Caffeic acid	Hydroxycinnamic acid	9.3	179.0353	179.0353 (25) 135.0452 (100)	C9H8O4	4.64 ± 0.03 ^a	6.12 ± 0.36 ^c	16.65 ± 1.35 ^b	2.16 ± 0.11 ^d
8	Luteolin-6-glycoside	Flavones	10.2	447.0657	447.0656 (14) 357.0395 (82) 327.0306 (100) 297.0219 (30)	C21H20O11	27.39 ± 2.39 ^c	44.08 ± 3.90 ^b	134.73 ± 1.46 ^a	nd
9	<i>p</i> -Coumaric acid	Hydroxybenzoic acid	11.1	163.0397	163.0397 (16) 119.0499 (100)	C9H8O3	14.24 ± 0.01 ^b	36.92 ± 0.07 ^a	nd	11.46 ± 1.23 ^c
10	Ferulic acid	Hydroxycinnamic acid	11.9	193.0512	193.0512 (27) 178.0272 (72) 134.0375 (100)	C10H10O4	nd	16.27 ± 0.28 ^a	nd	6.33 ± 0.31 ^b
11	Luteolin-7-glycoside	Flavones	12.3	44.0660	447.0658 (22) 285.0225 (100)	C21H20O11	110.53 ± 0.16 ^b	316.37 ± 1.58 ^a	318.66 ± 26.40 ^a	7.62 ± 0.90 ^c
12	Naringenin-7-glycoside	Flavones	13.2	433.0876	271.0445 (100) 150.9948 (52) 119.0436 (15)	C21H22O10	ud	ud	ud	nd
13	Apigenin	Flavones	17.5	269.0456	269.0019 (100) 151.0035 (52)	C15H12O5	ud	ud	ud	nd
14	Naringenin	Flavones	18	271.0614	271.0613 (83) 177.0192 (13) 151.0033 (100) 119.0498 (31)	C15H10O5	ud	ud	ud	nd
15	Luteolin	Flavones	20.4	286.24	285.04 (100) 151.0037 (25)	C15H10O6	ud	ud	ud	nd
Total by HPLC							283.58 ± 2.40	560.34 ± 1.75	470.03 ± 2.09	41.06 ± 1.96
TPC (mg GAE/ 100g DM)							296.03 ± 7.75	798.43 ± 25.76	580.77 ± 5.08	45.43 ± 9.27

RT: retention time; SL: solid fraction; LF: liquid fraction; PF: pellet fraction; SF-IBP: insoluble bound phenolics from solid fraction; TPC: total phenolic content; GAE: gallic acid equivalents; DM: dry matter ; nd: not-detected; ud; under detection limit. Different letters within the same row indicate significant differences between means ($P < 0.05$).

Table 3.5. Concentration of carotenoids detected in melon peels fractions by HPLC-DAD.

Compound	mg/100 g DM	
	SF	PF
β-Carotene	6.67 ± 0.34 ^b	91.52 ± 12.71 ^a
β-Cryptoxanthin	0.27 ± 0.12 ^b	4.92 ± 0.52 ^a
Lutein	0.06 ± 0.02 ^b	0.70 ± 0.16 ^a
Violaxathin	1.67 ± 0.26	nd
Total by HPLC	8.67 ± 0.76	97.16 ± 1.21
TCC (mg β-carotene equivalents/ 100 g DM)	10.13 ± 0.21	98.59 ± 8.53

SL: solid fraction; LF: PF: pellet fraction; DM: dry matter; nd: not detected Different letters within the same row indicate significant differences between means (P < 0.05).

3.3.7. Total chlorophylls content

In addition to carotenoids, chlorophylls are also natural pigments present in melon fruit that are strongly related to the green color characteristics attributed to antioxidant and antimutagenic properties. Cancer, osteoporosis, cataracts, and neurodegenerative diseases are illnesses that could be treated by the use of this molecule (Fundo et al., 2017). Total chlorophyll content was quantified in the three melon fractions; LF did not present chlorophylls as these compounds are typically located in the cell walls linked to the fiber and were more concentrated in the PF during centrifugation. Lichtenthaler (1987) indicated that total chlorophylls consist of chlorophyll *a* as the major pigment and chlorophyll *b* as a secondary pigment. Both chlorophylls are genuine components of photosynthetic membranes and occur at a ratio (a/b) of approximately 3 to 1. In this study, the ratio is almost 2 to 1. Fundo et al. (2017) also determined that total chlorophylls in melon peels obtained values of 7.89 mg/100 g FM spread by chlorophyll *a* (4.59 mg/100 g FM) and chlorophyll *b* (3.30 mg/100 g FM) were very lower than those reported in this study (175.84 mg/100 g FM) divided by chlorophyll *a* (109.82 mg/100 g FM) and chlorophyll *b* (66.02 mg/100 g FM) (**Table 3.3**). These different values can mainly be attributed to differences in the genus, species, and cultivar. Chlorophylls are the most abundant bioactive compounds present in *inodorous* melon peels due to their high concentration on a dry weight basis. As a result, due to their biological properties and potential uses as natural pigments, melon peel chlorophylls could potentially be used in the food, cosmetic, textile and pharmacology industries.

3.3.8. Antioxidant Activity

The antioxidant activity of free radical scavenging peel fraction tests is described in **Figure 3.2**. The LF had the highest antioxidant capacity compared to the other fractions

and had good scavenging effects on DPPH radicals with inhibitions above 80 and 50 % on ABTS radicals representing 924.77 M TE/100 g DM = 54.20 M TE/100 g FM and 344.46 mg AAE/100 g DM = 20.19 mg AAE/100 g FM, respectively. There were few studies on the antioxidant activity of melon peels, such as Al-Sayed and Ahmed (2013), which reported 12.53 % inhibition of DPPH radicals, which is lower than the results of this study. As expected, these are lower than those reported by Henan et al. (2016) in different varieties of melon pulp through the ABTS assay, e.g., Galaoui (160 μ M TE/100 g FM), Trabelsi (140.01 μ M TE/100 g FM) and Stambouli (127.34 μ M TE/100 g FM) but higher than Maazoun (22 μ M TE/100 g FM). Fundo et al. (2017) also reported inhibition of *Cantalupe* melon peel and pulp ABTS radicals equal to 33.68 and 22.04 mg AAE/100 g FM respectively, slightly higher than the results obtained in this study. Morais et al. (2015) analyzed and compared antioxidant extracts from different fruit parts (pulp, seeds and peels) and found that free radical inhibition by ferric reduction of antioxidant activity (FRAP) and DPPH was higher in peels than in other fruit parts. For example, melon raw peels had 49.49 μ mol FeSO₄/100 g DM higher than pulp (28.57 μ mol FeSO₄/100 g DM) and seed (6.50 μ mol FeSO₄/100 g DM). On the other hand, some researchers reported ORAC assay as a more relevant antioxidant technique because it has been used as a biological radical source (Thaipong et al., 2006). For the results of this technique, only LF had significant activity with 52.49 μ M TE/mL of extract. To the best of our knowledge, no previous reports have been published to ORAC assay for melon peels. These antioxidant activity results could be partly attributed to the high content of polyphenols in the *inodorus* melon peels present in each fraction. These bioactive molecules are well documented to be effective in reducing compounds and scavenging free radicals and have also been shown to be more effective than vitamins and carotenoids in plants. However, there is little data on the individual phenolic compounds of *inodorus* melon and their correlation between their antioxidant activity. In addition, this evidence shows the importance of studying melon by-products as a low cost and rich source of natural antioxidant extracts.

3.3.9. Melon peels as potential functional ingredients

Functional foods are currently described as food or food ingredients that are beneficial to health, helping to prevent or reduce the risk of various diseases such as cancer, cardiovascular and inflammatory disorders and diabetes (Silva et al., 2018). Diabetes and

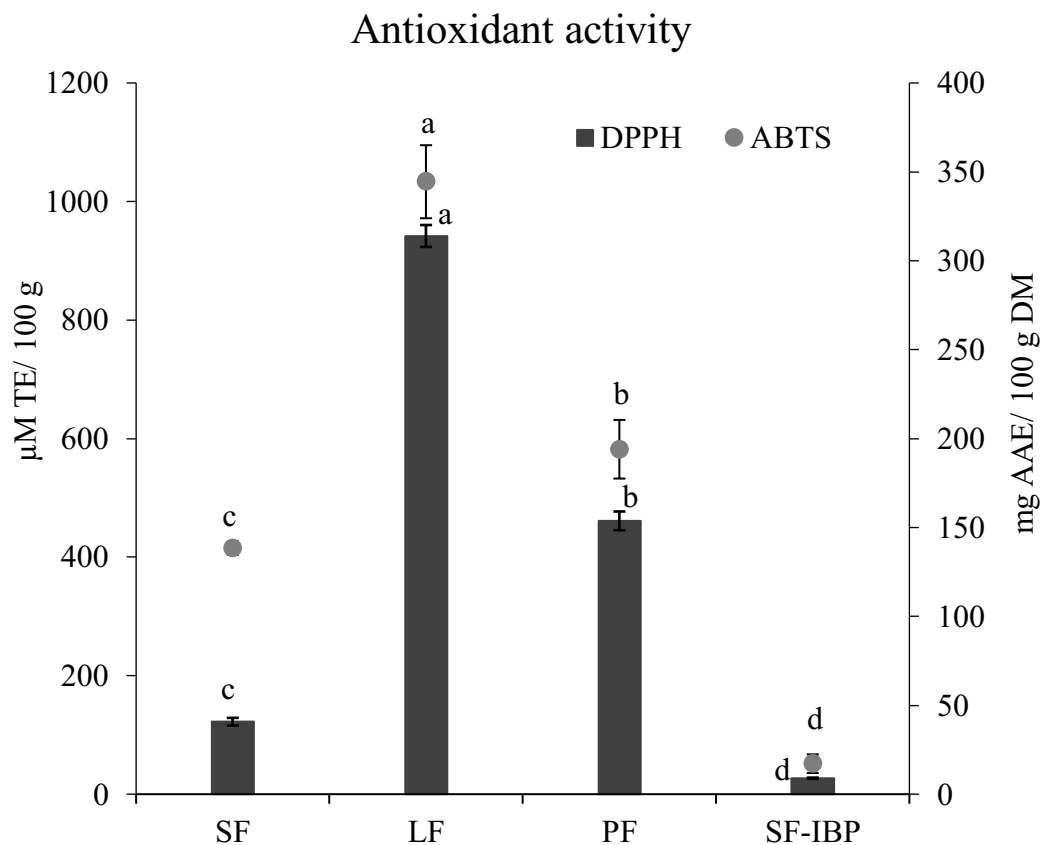


Figure 3.2. Total antioxidant activity (\pm standard deviation) of the methanolic extracts of *inodorus* melon peels fractions. TE: Trolox equivalents; AAE; Ascorbic Acid Equivalents; DM: dry matter; SF: solid fraction; LF: liquid fraction; PF: pellet fraction; SF-IBP: Solid Fraction-Insoluble Bound Phenolics. Different letters within the same row indicate significant differences between means ($P < 0.05$).

its complications are a serious global problem that is gradually developing due to oxidative stress. This rapid progression is caused by the imbalance between the overproduction of reactive oxygen species (ROS) and the low intake of natural antioxidants. Nowadays, it is well documented that natural antioxidants from different fruit sources, such as polyphenols, are capable of counteracting the negative effects of ROS, while also reducing problems associated with oxidative stress (Lo et al., 2017). Beyond that, the results of this study offer new perspectives for the valorisation of *inodorus* melon peels, since these three fractions have proven to be prototypes of functional ingredients due to the high content of the relevant nutrients, namely fiber, pectin and protein, as well as the various bioactive compounds (chlorophylls, carotenoids and polyphenols) which are linked to the prevention of disease. As described above, melon peels were separated using simple mechanical and separation methods such as

centrifugation, decantation, weight and milling. These fractions led to the separation of various biomolecules either by natural phenomena (polarity, solubility, density, stability, pH or selectivity and affinity) without the use of any solvent, e.g., ensuring a low cost and green approach. At the end of the day, new fractions with diverse functional bioactive compounds could be obtained, which would allow different applications and better use of total melon by-products. With this approach, it was possible to obtain SF, which represents almost 21.5 % of fresh weight and is the richest fraction of fiber (cellulose, hemicellulose and lignin). This fraction can be directly used as a source of dietary fiber (flour) that has contributed to the modulation of intestinal microbiota, such as *Bifidobacterium*, which has been associated with the prevention of colon, stomach, breast and prostate cancer (Veiga et al., 2018). LF represents at least 70.0 % of fresh weight and is a fraction with a major antioxidant activity due to its high content of polyphenols, but also contains soluble fiber and proteins. This fraction can be used as an additional ingredient (juice powder) for human health promotion as polyphenols exhibit good inhibition of digestive enzymes (lipase, amylase and glucosidase), minimizing hyperglycemia, which is also strongly associated with diabetes and obesity disorders (Shaïda et al., 2014). Finally, there is the pellet fraction, which represents 2.0 % of fresh weight. It is the richest fraction of chlorophylls, carotenoids and proteins. This fraction can be used as coloring and food additives (powder). In addition, these new and promising results for melon by-products should be demonstrated against different analyzes, such as antioxidant methods, gastrointestinal effects and cytotoxic tests. These assessments will be further used in future research studies to improve the use of melon by-products as potential functional ingredients.

3.4. Conclusions

Melon peels were separated using simple mechanical and separation methods. This processing process led to the extraction of a number of bioactive compounds either by natural phenomena (polarity, solubility, density, pH or selectivity and affinity) without using any solvent, e.g., ensuring a low cost and green approach. Overall, the melon by-products showed significant levels of value-added compounds, fifteen polyphenols (primarily hydroxybenzoic and hydroxycinnamic acids and flavonous acids) and four carotenoids (especially β -carotene and β -cryptoxanthin) which, in turn, are responsible for diverse biological activities (antimicrobial, provitamin A, antioxidant activity, among others) with health promotion. In addition, the re-incorporation of melon by-products into

the food chain as additives, supplements or ingredients rich in nutrients and bioactive substances is the main advantage of the recovery of these materials. This will further address environmental and economic issues linked to their accumulation and/or poor management.

CHAPTER 4 –Valorisation of pigments protein enriched fraction from melon peels (*Cucumis melo* L. *inodorus*) to complete integral valorisation as a zero-waste approach

Ricardo Gómez-García^b, Bárbara M.C. Vaz^a, Margarida Martins^a, Manuela Pintado^b,
Sónia P.M. Ventura^{a*}

^a*CICECO – Aveiro Institute of Materials, Department of Chemistry, University of Aveiro*

Department of Chemistry, CICECO – Aveiro Institute of Materials, University of Aveiro Campus Universitário de Santiago, 3810-193 Aveiro, Portugal

^b*Universidade Católica Portuguesa, CBQF – Centro de Biotecnologia e Química Fina – Laboratório Associado, Escola Superior de Biotecnologia, Rua Diogo Botelho 1327, 4169-005 Porto, Portugal*

Under preparation

Abstract

Nowadays, there is an increasing mutual interest between the importance to decrease environmental pollution and promote circular economy in which scientific and technological processes in the field of food waste valorisation has an important role. Food waste should not be considered only a pollutant because if it is effectively employed it also has big economic relevance due to its high content of value-added compounds with several industrial interest such as proteins, carotenoids and chlorophylls. The aim of this study was to combine several techniques to the obtention of these natural derived pigments from industrial melon by-products. The process included protein extraction generating 8.34 g/100 g sample DW, followed by solid-phase adsorption for carotenoids purification which yielded 2.6-4.6% (w/w), and chlorophylls recovery of ca. 58.35%. Melon peel by-products showed to be good sources of natural derived pigments.

Keywords: *Inodorus* melon, bioresource recovery, melon peels, valorisation, proteins, chlorophylls, carotenoids,

4.1. Introduction

Currently, food processing by-products have long been considered as an organic matter of management, minimization and prevention due to the environmental and economic negative impact prompted by their transportation and disposal (Campos et al., 2020b; Esparza et al., 2020). Specifically, melon fruit by-products are residues of high organic load, which are typically derived during raw materials processing to consumer products (e.g., juices, jams, salads and dehydrated fruit, among others) and result in liquid (wastewater) or solid (bagasse, seeds and peels, among others) waste streams (Gómez-García et al., 2021c; Rolim et al., 2020). Nowadays, fruit by-products have been recognised as source of valuable value-added bioactive compounds and deal with the prospects of feeding fast growing population, consumers demand and industrial market needs (Gómez and Martínez, 2018; Cheng et al., 2018; Campos et al., 2020c). Based on these facts, melon by-products could be considered vital substrates for the recovery of biofunctional compounds, including proteins, chlorophylls, carotenoids and dietary fibre (among others) and the development of novel ingredients with a market and industrial value, allowing their valorisation and total reintegration into the industrial value chain (Gómez-García et al., 2021b). For example, proteins from by-products could be applied as natural fortifier ingredient to counter the protein deficiency of unbalanced diets (Torres-León et al., 2018). Chlorophylls and carotenoids are natural pigments present in fruits that are strongly related to the colour characteristics and attributed with antioxidant, pro-vitamin A and antimutagenic properties, which could be exploited as natural colouring agents for food, textile and pharmaceutical industries (Díaz-Gómez et al., 2017).

On the other hand, one of still common strategies for food by-products management and treatment is their deposition in landfills, which currently has not been considered a sustainable or environmentally friendly strategy since such by-products are excluded and wasted, losing all their richness in value-added compounds and high nutritional value (Gómez-García et al., 2021b; Sindhu et al., 2019). Therefore, suitable strategies for valorisation and exploitation of food related materials that are discharged worldwide are lacking, arising an opportunity to the creation and development of novel eco-friendly technologies/strategies within the framework of circular bioeconomy and zero-waste approach, which nowadays have been prompted the recovery, recycling and sustainability of high-added value ingredients inside food supply chain (Dahiya et al., 2018). Circular bioeconomy concept has been applied for its several benefits, regarding the possibility

to the creation of revenue streams, business and job opportunities, while zero-waste approach allowed bioresource recovery, effective waste management and pollution prevention, contributing to a sustainable development between industries (Imbert, 2017; Panchal et al., 2021). Sustainable extraction, fractionation and isolation of high added-value compounds from food by-products most follow the principles of green chemistry, adapting modifications of the applied methodology in order to comply with the standards of high-quality for their feasible obtention and commercialization, such as i) yield maximization of the target compounds, ii) suiting the demands of industrial processing, iii) high purity of the added-value ingredients (free of impurities and toxic compounds), iv) avoiding deterioration and loss of functionality during processing and v) ensuring the safe grade and clean label ingredient of the final product (Trigo et al., 2019; Rao et al., 2019). Emerging technologies based on non-thermal concepts are today better alternatives for their application in various processes within food industry and they could be easily adapted in the recovery downstream of valuable compounds from food waste (Martins et al., 2021b). Aqueous solutions of surface-active ionic liquids (ILs) and common surfactants have been proposed as solvents to extract chlorophylls and carotenoids from various vegetable matrices and showed superior environmental and economic benefits to extract these kinds of value-added compounds without compromise their stability when compared to the conventional techniques such as chromatography processes or saponification reactions, which not only represent energy or time consuming but also require costly equipment and several steps to achieve an acceptable end-product (Vaz et al., 2022). Surface-active ILs can be a very efficient extractive processes due to their ability to create small pores in the cell membrane, allowing the release of intracellular compounds (cell disruption step) and increasing the solubility of hydrophobic compounds (chlorophylls and carotenoids) in water through the formation of micellar structures, which are formed above the critical micellar concentration (Martins et al., 2020). A simpler and reliable separation process for this purpose is the solid-phase extraction. This is based on the adsorption of chlorophylls on a resin due to intermolecular and interionic interactions (e.g., dipole–dipole, ion–dipole, hydrogen bonding, ion-ion) between chlorophyll derivatives and the tetramethylammonium functional group of AmberLite™ HPR900 OH (previously known as Ambersep 900 OH). AmberLite™ HPR900 OH is a strong basic anionic resin that allows an effective and fast adsorption of chlorophyll, while the carotenoids remain in solution. Its efficiency was already demonstrated for various extracts from green vegetables such as beans, broccoli, spinach,

lettuce, and peas, among others. However, no previous work has successfully eluted the chlorophyll from the resin, allowing the recovery of the chlorophyll as a secondary product, and enhancing the resin's lifetime through more cycles of reuse.

Hence, based on the high content of value-added compounds and their potential industrial applications, melon by-products (peels) could be used as raw materials for the obtention of novel functional compounds, which could allow their reincorporation into the industrial value chain. Therefore, the specific aim of this research work was to evaluate a consolidated simple multistep process to separate proteins, chlorophylls and carotenoids from melon peels using the resin AmberLite™ HPR900 OH and aqueous solutions of surface-active ILs to recover chlorophylls.

4.2. Materials and Methods

4.2.1. Chemical

Di-sodium hydrogen phosphate anhydrous (Na_2HPO_4 , 99 wt%, CAS 7558-79-4), and sodium phosphate monobasic (NaH_2PO_4 , 99-100.5%, CAS 7558-80-7) were used to prepare sodium phosphate buffer, were purchased from Panreac. Ethanol absolute (analytical reagent grade, CAS 64-17-5) used in solid-liquid extraction of pigments was supplied from Fisher Scientific. The strong basic anionic resin, AmberLite™ HPR900 OH (CAS 9017-79-2), composed of 45–65% water and 35–55% quaternary amine styrene–divinylbenzene copolymer of the OH form (Larsen and Christensen, 2005), was acquired at Sigma-Aldrich. The ionic liquid (IL) used in the elution of chlorophylls, dodecyltrimethylammonium bromide ($[\text{N}_{1,1,1,12}]\text{Br}$, 99 wt% of purity, CAS 1119-94-4), was provided from Alfa Aesar. Glycerol (99.88 wt%, CAS 56-81-5), bromophenol blue sodium salt (pure, CAS 34725-61-6), dithiothreitol (DTT, 98 wt%, CAS 3483-12-3), and Tris-HCl 0.5M (pH 6.8) (CAS 1185-53-1), used to prepare the loading buffer for SDS-PAGE analysis were supplied by Fisher Chemical, Merk, NZYtech. RunBlue SDS gel 4-12% 10cmx10cm and RunBlue Teo 20x Teo Tricine SDS, were purchased from Expedeon. Full Range Rainbow Gisp, and BlueSafe used to performe protein staining, were provided by Cytiva and NZYtech, respectively.

4.2.2. Melon peels fractionation

Fresh melon peels used in this work were kindly provided by Nuvi Fruits S. A. Company (Torres Vedras, Portugal) and were transported under freezing temperatures (-20 °C) to CBQF facilities (Centre of Biotechnology and Fine Chemistry in the Faculty of Biotechnology of the Catholic University of Portugal). The melon peels were fractionated as described elsewhere (Gómez-García et al., 2021b), employing a commercial juice machine (HR1869/8, 900 W, Philips) in order to obtain two fresh fractions; solid fraction (SF) and liquid fraction (LF). The SF was employed for pectin and microcrystalline cellulose obtention (data not shown). To remove the green-pigmented solid particles present in the LF a centrifugation was performed (11469 g, 15 min, 4 °C). The clarified supernatant was used for cucumisin enzyme extraction as reported in in chapte 9 (Gómez-García et al., 2021b) and the precipitated solids were collected and labelled as the pellet fraction (PF). The PF was stored in plastic tubes of 50 mL at -20 °C and then transported at low temperature (0 °C), avoiding sun light, to the CICECO facilities (Aveiro Institute of Materials in the Department of Chemistry of the University of Aveiro) and kept at -20 °C until its evaluation. The flow chart for the PF fractionation obtention process is shown in **Figure 4.1**.

4.2.3. Disruption and solid-liquid extraction of proteins

Four different approaches to recover proteins from the pellet fraction were performed. All the assays were performed in triplicate, at room temperature (20 – 25 °C) and protected from light exposure. First, both disruption and extraction were carried out in a shaker IKA TRAYSTER digital under a constant vertical rotation of 80 rpm, for 30 min. A solid-liquid ratio (SLR) of 0.05 g/mL was used, e.g., 0.1 g of biomass and 2 mL of a 20 mM sodium phosphate buffer (pH 7.4). Next, the disruption was performed in a FRITSCH Mini-Mill PULVERISETTE 23 using a stainless-steel grinding bowl (10 mL capacity) and one 10 mm ball, for 5 min at 40 rps. 0.1 g of biomass were weighted to the grinding bowl and the bead milling disruption was carried out. For the extraction step, 2 mL of the same sodium phosphate buffer were added to the biomass and the extraction was performed as before, in a digital shaker (IKA TRAYSTER) under a constant vertical rotation (80 rpm, for 30 min). The other two approaches were based on the use of bead milling method for both steps, namely disruption and extraction. First, the disruption and the extraction steps were carried out separately, e.g., the disruption was performed within 5 min at 40 rps, and then, 2 mL of the sodium phosphate buffer were added and another

5 min of extraction step at 40 rps was performed. Then, both disruption and extraction steps were performed at the same time, e.g., the biomass and the solvent were put in contact for the same conditions, during 5 min at 40 rps. At the end of all approaches, all samples were centrifuged (Thermo Scientific Heraeus Megafuge 16R) at 4700 g, for 45 min at 4°C. The supernatant (protein extract) and the biomass debris were separated and collected.

4.2.4. Solid-liquid extraction of pigments

The solid-liquid extraction of carotenoids and chlorophylls followed the method described by Vaz et al. (2022), using ethanol as solvent, and testing several SLRs at a range of concentrations (0.0067-0.050 g/mL). The biomass was maintained constant and while varying the volume of ethanol. The conditions of extraction were performed at constant vertical rotation (80 rpm, 30 min), protected from light exposure and at room temperature (20-25 °C). After, a centrifugation step was performed (4700 g, 45 min, 4 °C) to separate the cell debris from the supernatant (initial extract), being both stored for further usage. All the assays were done in triplicate.

4.2.5. Chlorophylls and carotenoids separation

The carotenoids and chlorophylls separation was carried out using a commercial resin AmberLite™ HPR900 OH following the process developed by Vaz et al. (2022). First, the resin was washed with distilled water and dried in an oven for 15 min at 50 °C. Then, 5 mL of the optimized initial extract was put in contact with 0.5 g of resin under magnet stirring, for 30 min at room temperature (20–25 °C), protected from light exposure. The carotenoids (present in the organic solution) were recovered due to chlorophylls adsorption to the resin. Next, an optimization of the elution of the chlorophylls, with an aqueous solution of [N_{1,1,1,12}]Br at 370 mM, was performed. Several masses of resin were tested, maintaining the volume of eluent constant at 15 mL, ranging a SLR's (in this case SLR means the ratio between the mass of resin and the volume of eluent from 0.030 to 0.11 g/mL). The conditions of elution were mostly the same of chlorophylls adsorption, only with an increase of time of contact (48.5 min). Finally, chlorophylls were recovered from the IL as by Vaz et al. (2022).

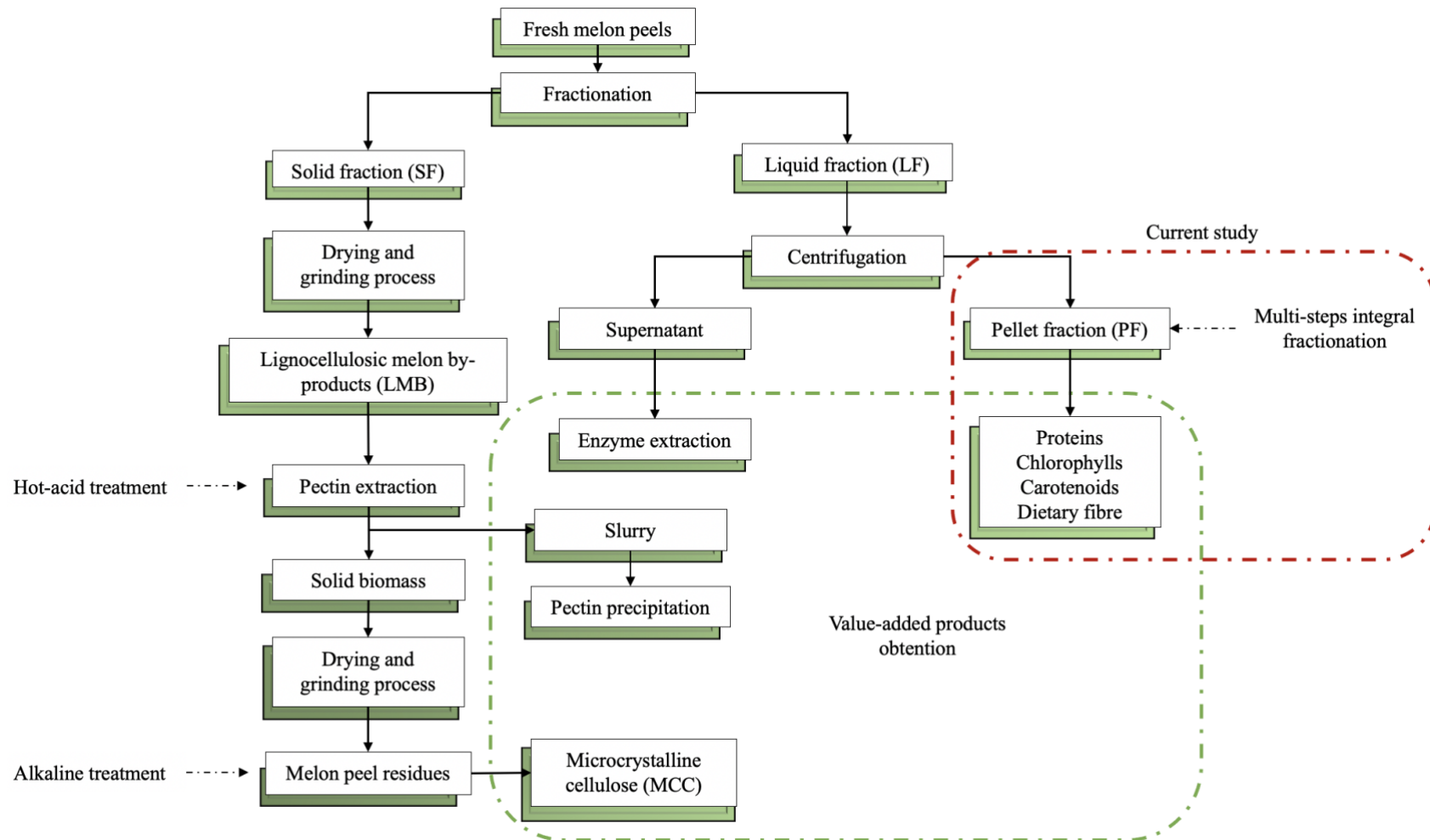


Figure 4.1. Process flow chart for melon peels fractionation process and obtention of value-added compounds under zero-waste approach.

4.2.6. Total protein content

The total protein concentration of the protein extract was determined following the Bicinchoninic Acid (BCA) method using the Novagen® BCA Protein Assay Kit (Merck, Darmstadt, Germany) (Scientific, 2007). The quantification was performed by UV-Vis microplate reader (Synergy HT microplate reader – BioTek) at 562 nm using a previously obtained calibration curve ($R^2 = 0.9909$).

4.2.7. Quantification of pigments

The carotenoid and chlorophyll extracts were quantified using a UV–Vis microplate reader (Synergy HT microplate reader – BioTek), recording the UV–visible spectra between 200 and 700 nm. The carotenoids concentration was achieved through fucoxanthin quantification at 450 nm accordingly to a calibration curve previously obtained in ethanol ($R^2 = 0.998$). The mass percentage of chlorophylls present in each extract (chlorophyll and carotenoid extracts) was calculated relating the chlorophyll mass present in the initial extract and the chlorophyll mass of each collected extract using equation 4.1. The quantification was done using two calibration curves previously determined at 667 nm ($R^2 = 0.9389$ and $R^2 = 0.9805$ for aqueous and organic extracts, respectively).

$$\text{Chlorophyll recovery (\%)} = \frac{\text{Chlorophyll in the collected extract (mg)}}{\text{Chlorophyll in the initial extract (mg)}} \times 100 \quad (4.1)$$

4.3. Results and discussion

4.3.1 Protein extraction by bead milling method

Following the integrated process for the extraction of different value-added products a rich protein extract was obtained as first product stream (**Figure 4.2**). The UV absorption profile of melon PF proteins extract after disruption process are depicted in **Figure 4.3**. As can be observed the protein extracts obtained by each disruption process showed similar behaviours regarding light scattering in the region of 220-260 nm, which could be associated to the well-established UV absorption of proteins within the range of 180 to 230 nm attributed to their peptide bonds. Absorption in the range of 230-300 nm is characteristic of aromatic sidechains of tryptophan (Trp), tyrosine (Tyr), and

phenylalanine (Phe) residues. Also, disulfide bonds that form between two cysteine residues also absorb near 260 nm (Antosiewicz and Shugar, 2016). Moreover, processes number 3 and 4 presented very similar UV absorption profiles and higher absorbance values than the processes 1 and 2. These differences could be due to disruption process by bead milling, which is more efficient braking process than the conventional method for extraction of value-added molecules with the feature to extract them from a limited quantity of raw material. Such molecules are typically intracellular, either in the cytoplasm, in internal organelles or linked to cell membranes, requiring cells disintegration before extraction and liberated/solubilized in the extraction solvent (Ho et al., 2015). Bead milling processes are commonly applied in the chemical industry for the manufacture of paints/lacquers and grinding of minerals and have been successfully applied for the disintegration of yeast cyanobacteria and microalgae for the release of intracellular products, under low energy inputs and mild conditions (Postma et al., 2017). Moreover, based on the results obtained by the BCA colourimetric method, process number 3 exhibited the highest protein content with respect to the other three process (data not shown), obtaining values of 542.3 µg/mL of protein equal to 8.34 g of protein per 100 g sample on a dry weight (DW) basis. These contents go encounter to the growing increasing demand for natural ingredients rich in protein (0.8 g of protein per Kg of body weight) and the social awareness linked to the

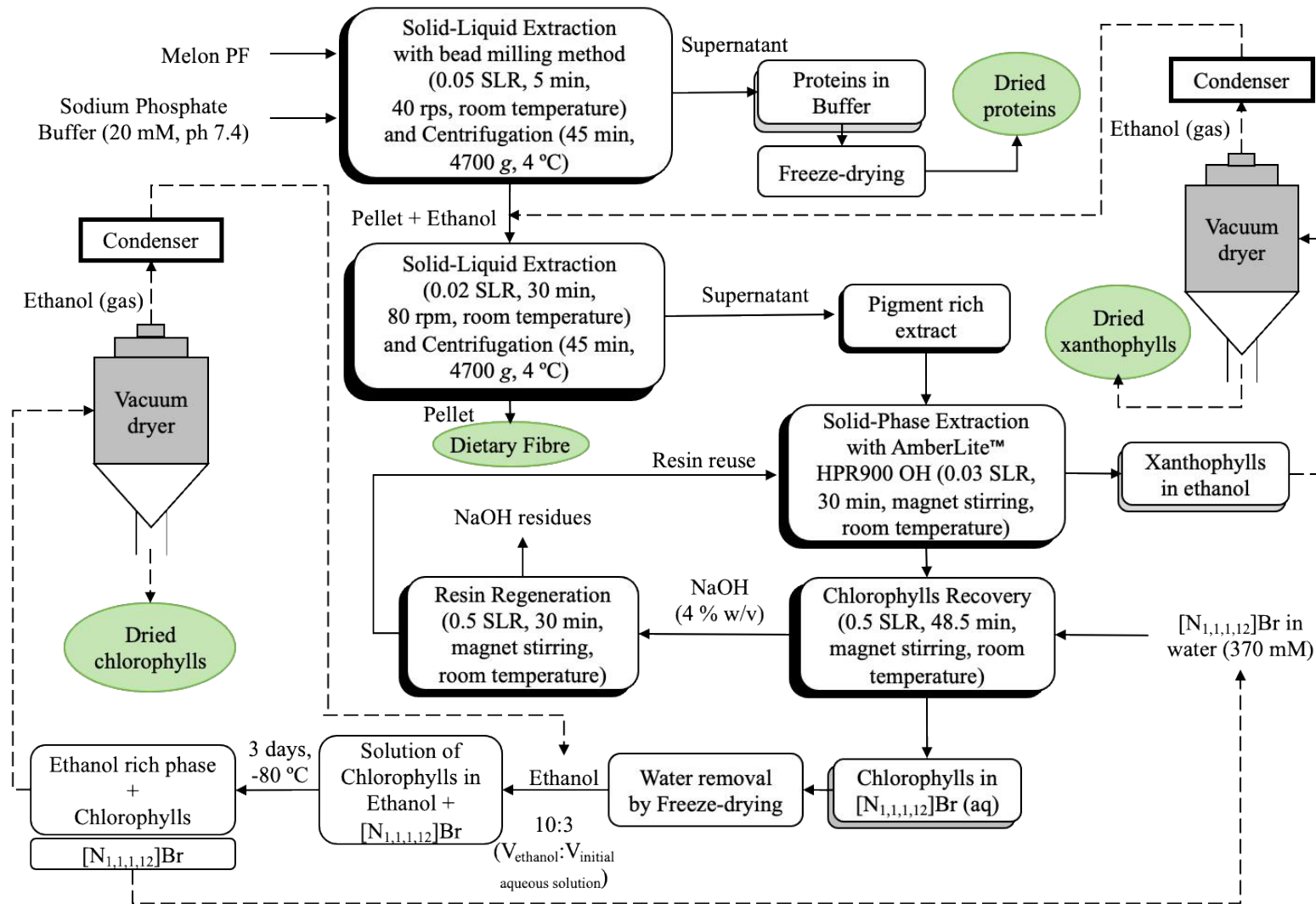


Figure 4.2. Process diagram proposed for the complete valorisation of melon pellet fraction (PF). Dashed lines are only a suggestion of what could be done, not being experimented in this work. Green circles represent the expected value-added end-products. Adapted from Vaz et al. (2022).

Food waste valorisation, opening new opportunities to the development of high value food ingredients, which can be employed as nutraceuticals as well as fortifiers and enrichments for the food industry (Tinline-Goodfellow et al., 2020).

4.3.2. Effect of solid-liquid ratio (SLR) on chlorophylls extraction yield

A second solid-liquid extraction was carried out by mixing the resulting pellet from protein extraction, rich in pigments with ethanol in a different SLRs in order to guarantee an effective extraction yield. Solid-liquid ratio influenced the yield of chlorophylls, when concentrations were varied from 0.0067 to 0.050 (g/mL); this effect over the response is showed in **Figure 4.4**. It can be observed that the highest chlorophylls yield was obtained using a SLR of 0.010 with titles of 1.34 mg/g of sample on a fresh weight (FW) basis (134 mg/100 g FW), at least two times higher when compared with the other SLRs employed. This can be attributed to the increase in solvent volume available for the solute chlorophyll (the principle of extraction being partitioning based on its solubility) resulting in higher yield. The amount of chlorophyll extracted remained the same when higher SRL was used, e.g., SRL 0.020 had the lowest yield (0.58 mg/g FW) followed by SRL 0.050 and 0.033 (0.6 and 0.61 mg/g FW, respectively). An increase in the extraction yield can be attributed to the polarity, which decreases with an increase in ethanol volume. Chlorophyll is relatively less polar and so solubilizes better in less polar solvents (say 100% ethanol in the present case). These findings are similar to the results reported on Chapter 3 (Gómez-García et al., 2021b) using methanol, accounting for 174.84 mg/100 g FW. However, taking into account the environmental and health impact of toxic solvents, ethanol is the most sustainable solvent, since is considered as a GRAS (Generally Recognized as Safe) ingredient. Ethanol is preferable for recovery of bioactive compounds from fruit and vegetables in contrast with acetone, hexane and methanol (Vilas-Boas et al., 2021; López-Salas et al., 2021).

4.3.2.1. Separation of pigments by resin absorption

After identifying the most suitable SLR (0.010) for maximum extraction of chlorophylls, the separation of the carotenoids from chlorophylls was carried out as described in **Figure 4.5**. After centrifugation, the supernatant was collected, and consisted of a rich green-pigment extract (**Figure 5a**). Such extract was eluted in a continuous mode through the

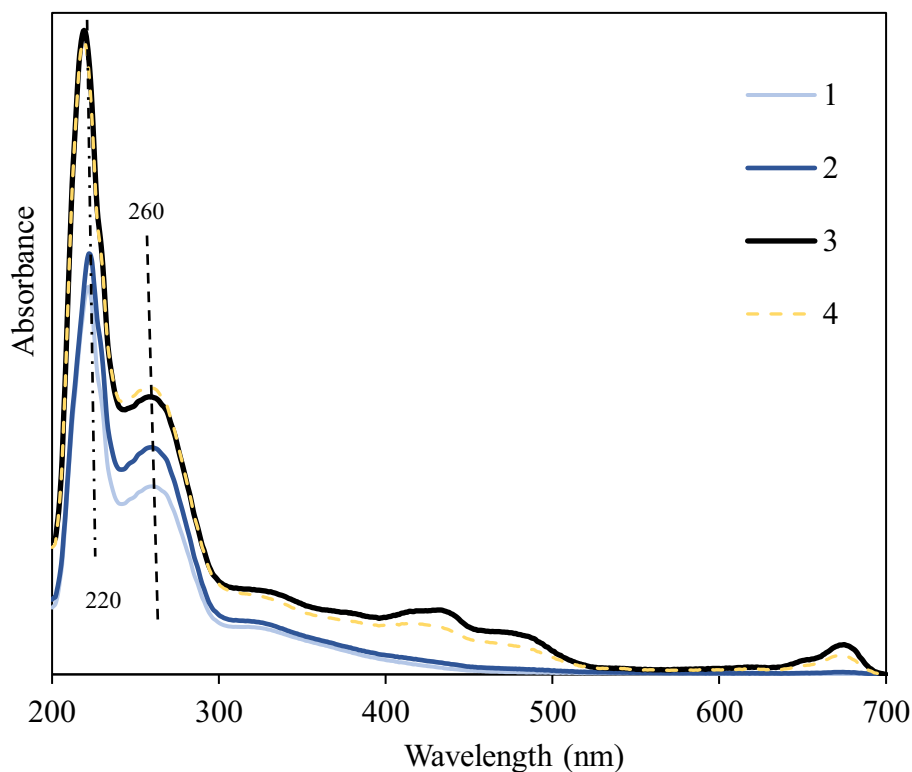


Figure 4.3. UV spectra profile of protein extracts from melon pellet fraction (PF) by disruption process.

1. Disruption and normal extraction (30 min shaker)
2. Disruption with bead milling (5min) followed by normal extraction (30 min)
3. Disruption and extraction with bead milling at the same time (5min)
4. Disruption and extraction with bead milling in 2 different cycles (5min+5min)

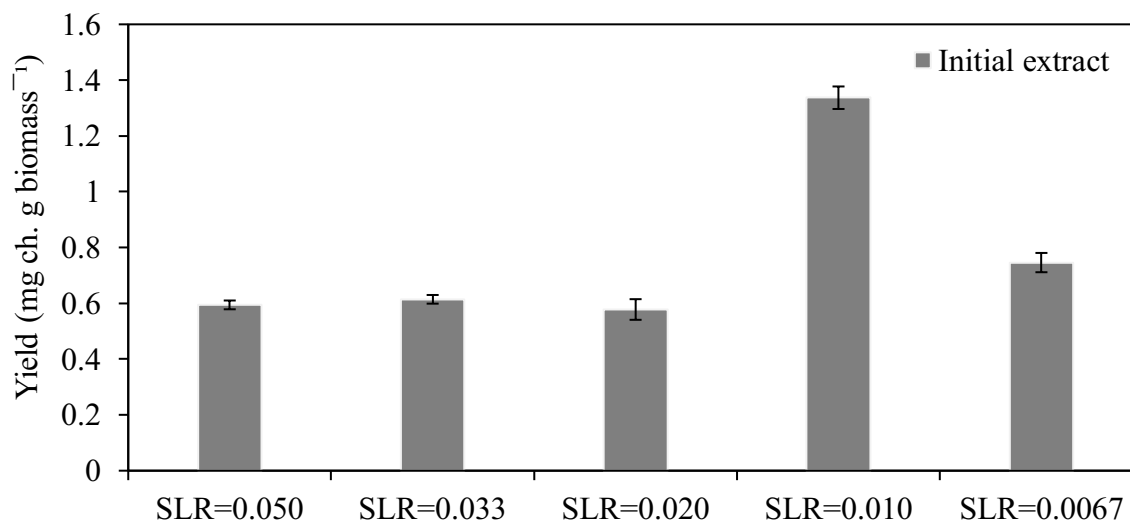


Figure 4.4. Extraction yield of chlorophylls as function of the solid-liquid ratio (SLR) in the initial melon pellet fraction (PF) extract.

commercial resin AmberLite™ HPR900 OH until it reaches saturation indicated by the colour change from a bright pink (**Figure 4.5A**) to a green-dark (**Figure 4.5B**). In this way, carotenoids specially xanthophylls were recovered from the initial extract, showing a characteristic bright yellow color (**Figure 4.5b**), while chlorophylls were adsorbed in the resin. The melon pigments (chlorophylls and carotenoids) extraction was confirmed by measuring their absorbance profiles. Results presented in **Figure 4.6** show that the initial extract gives rise to a broad and less narrowed peaks between the region of 400-600 nm for chlorophylls and 420 to 470 for carotenoids. But despite these irregularities, peaks are very close to the absorbance exhibited by isolated/pure chlorophylls (*a* and *b*) with narrow bands (maxima) in the blue (428 and 453 nm) and red (661 and 642 nm) spectral region (Lichtenthaler, 1987; Urbanovich et al., 2021). In the case of Fisolated yellow carotenoids, a broad absorption with three maxima or shoulders in the blue spectral range between 400 and 500 nm (Biehler et al., 2010; Fleshman et al., 2011). These differences could be explained due to the fact that the maximum absorbance of pigments strongly depend on the type of solvent e.g., with increasing polarity of the solvent, the red maximum absorption of Chl *a* shift from 660 to 665 nm, and the blue maximum absorbance from 428 to 432 nm. This also concerns Chl *b*, which shifts from 642 to 652 nm and 452 to 469 nm (red and blue, respectively). In many cases during chlorophylls and carotenoids extraction, very toxic and corrosive organic solvents are typically used for their obtention, including diethyl ether, acetone, hexane, chloroform (among others). Also, time consuming steps (saponification, clarification, desalination) and reagents (KOH, dichloromethane, citric acid, vitamin C) are used to reach higher recovery and purity yields (Chedea et al., 2010; Cervantes-Paz et al., 2014), making unprofitable and unsuitable processes. Therefore, these practices are not sustainable or environmentally friendly to be implemented on a higher industrial scale.

4.3.3. Recovery of carotenoids and chlorophylls

As described in section 3.1 AmberLite™ HPR900 OH resin was used to separate carotenoids from the chlorophylls. This was achieved due to the adsorption mechanism, which is mediated by ion-ion interactions after the saponification of the chlorophyll and release of phytol. Then occurs mainly through hydrogen-bonds and dipole–dipole interactions between resin and chlorophylls polar units, leaving the carotenoid

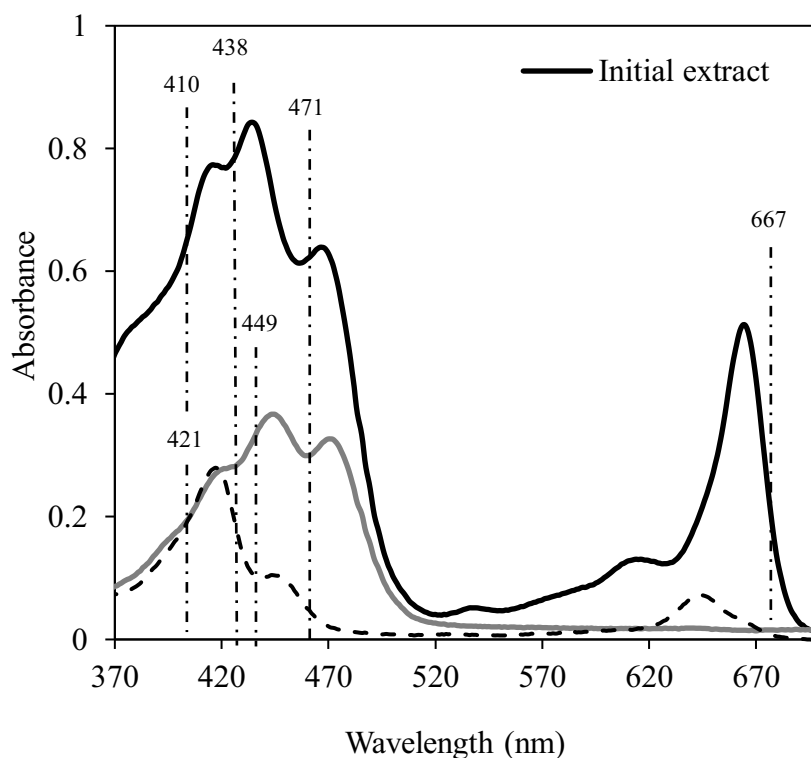


Figure 4.6. Spectra of UV-Vis absorption profile of the pellet fraction extract and isolated carotenoids and chlorophylls extracts as depicted in **Figure 4.2**.

compounds in solution, in this case ethanol. In this sense, carotenoids were recovered in a range of 2.6-4.6% of recovery by varying the SRL from as depicted in **Figure 4.7**. On the other hand, a well-documented IL known as $[N_{1,1,1,12}]Br$ was used to recover chlorophylls from AmberLite resin (**Figure 4.5B**). The $[N_{1,1,1,12}]Br$ seemed to be effective to extract chlorophylls from the resin as can be visualized by the pale green colour presented in the extract obtained (**Figure 4.5c**). This IL and others such as $[N_{1,1,1,14}]Br$ and $[P_{4,4,4,14}]Cl$ were previously used as efficient solvents to extract chlorophylls from algae (*Ulva rigida*) due to their ability to form micelles above a certain concentration, providing the perfect environment to hydrophobic molecules (Martins et al., 2021a). Furthermore, in order to evaluate the effective extraction effect of the IL on the recovery of chlorophylls and carotenoids diverse SLRs were evaluated. As can be seen in **Figure 4.7**, a slight decrease on the recovery yields of chlorophylls occurred by the increase of the SRL from 0.03 to 0.011, and the highest recovery was obtained at 0.03 of SRL (58.35%). This positive dragging effect of the chlorophylls by the IL may be derived by its chemical structure, presenting the same positively charged with respect to present in the functional groups of the resin. In this regard, the kind of interaction between the chlorophyll derivatives and the functional groups of the resin can be replaced by similar interactions but now comprising the cationic IL.

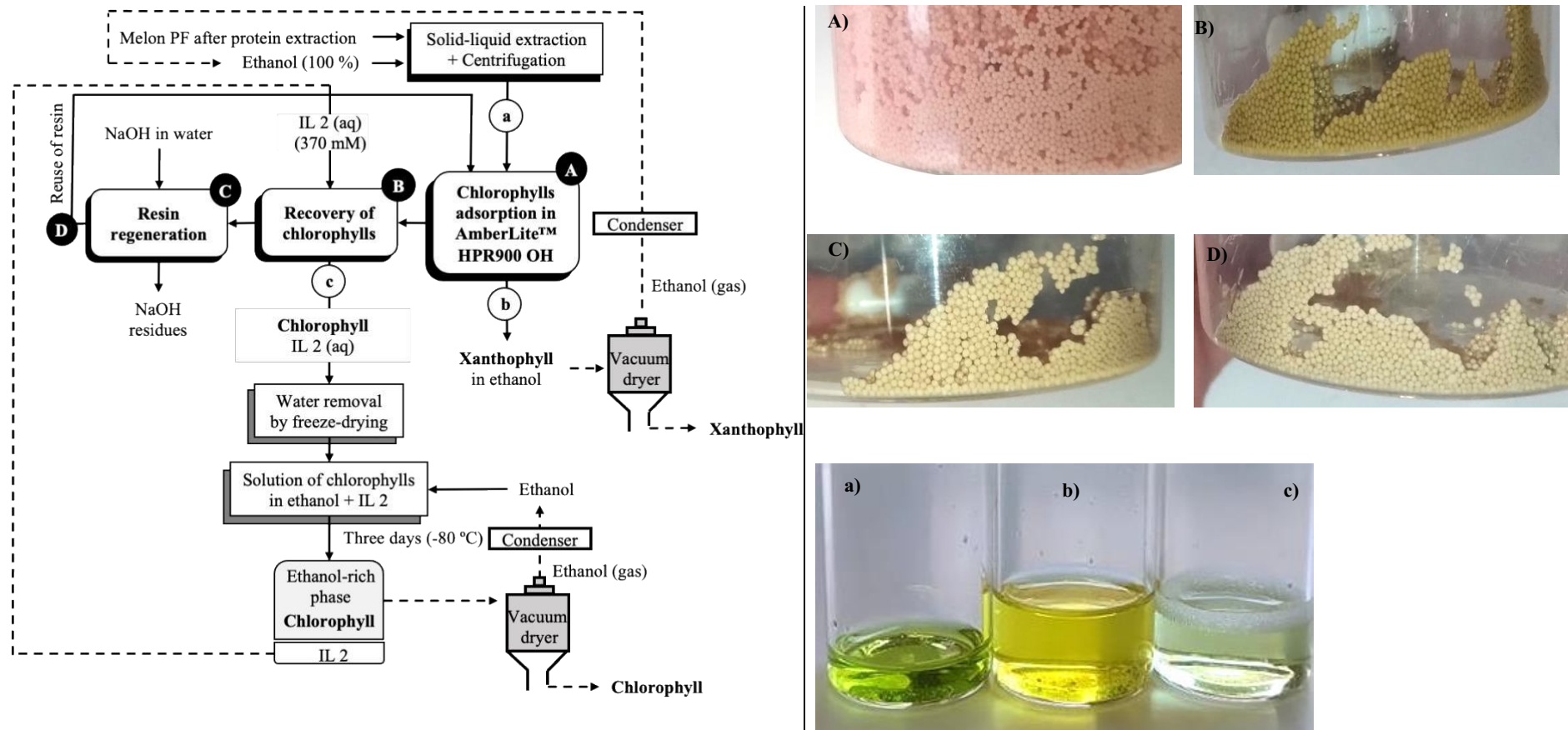


Figure 4.5. Process flow chart of the sequential fractionation of carotenoids (xanthophyll) and chlorophylls through AmberLite resin (ethanol 100%) (left). Photographs of the successive extraction by AmberLite resin A) before usage, B) with adsorbed chlorophylls, C) after desorption of chlorophylls and D) to reuse and the extracts obtained: a) initial extract, b) carotenoid extract and c) chlorophyll extract (right). Adapted from Vaz et al. (2022).

Even that the yields of this study are lower than the reported for optimized chlorophylls extracted from microalgae (*Isochrysis galbana*) using $[N_{1,1,1,12}]Br$ at fixed SLR of 0.070 (g/mL), which obtained obtaining 93.3% of recovery (Vaz et al. 2022) and more than 40% of the chlorophylls still embedded into the resin. These finding are the first ones focused on industrial melon by-products, leaving interesting insights to follow their complete valorisation through the extraction of value-added compounds with industrial interest and certainly recovered by suitable methodologies in order to be closer for their reincorporation into the industrial value chain as bioresources. Additionally, a future procedure to enhance chlorophylls and carotenoids extraction and subsequently to complement the entire process to achieve a complete valorisation of the melon biomass, as well as to reuse organic solvents could be carried out as follow: the recovery of chlorophylls can be performed with IL by freeze-drying the solution, adding ethanol (10:3 ($V_{ethanol}:V_{initial\ aqueous\ solution}$)), and then stocking the solution at $-80\text{ }^{\circ}C$, allowing, in addition to the recovery of chlorophylls, the reuse of the IL. Xanthophylls and chlorophylls can be dried using a vacuum drier at low pressure and temperature to not degrade the pigments, enabling the reuse of ethanol.

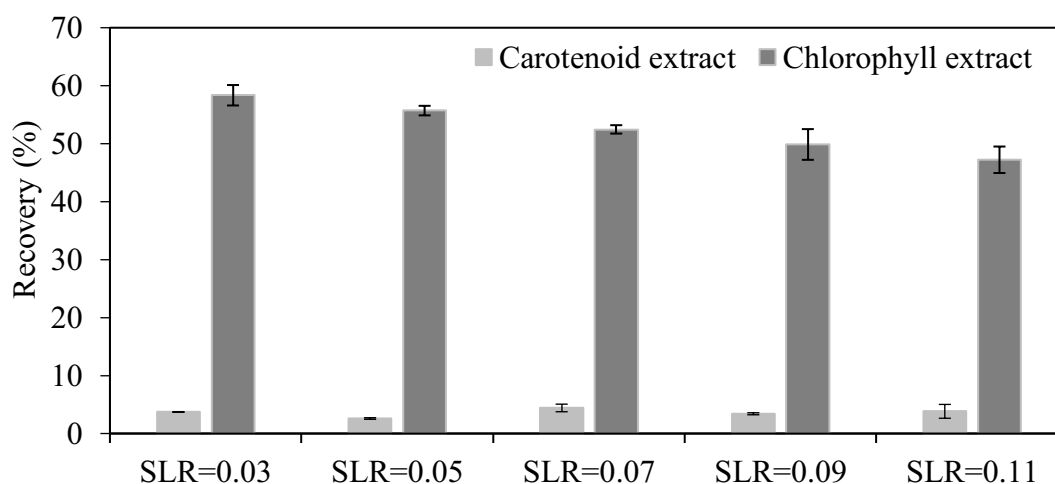


Figure 4.7. Recovery of chlorophylls and carotenoids (% m/v) as function of the solid-liquid ratio (SLR) during extraction process with AmberLite resins.

4.4. Conclusions

The extraction of proteins, chlorophylls and carotenoids from melon peel fraction was achieved by employing sustainable multi-step fractionation process. As a first product stream, proteins were recovered with titles of 8.34 g of protein/100 g sample DW. After the protein extraction, the use of HamberLite resin allowed to obtain and isolate carotenoid rich extract by the chemical adsorption of chlorophylls. Afterward, extraction with an aqueous solution of surface-active IL - [N1,1,1,12]Br, proved to be a effective solvent in the elution of chlorophylls from the HamberLite resin. The operational conditions of this step reached 47-58% of the initial chlorophyll loaded in the resin when [N1,1,1,12]Br was applied as a solvent at low concentration (370 mM). Overall, the design of suitable processes to exploit fruit by-products that allow the extraction at the same time several value-added compounds with better recovery yields, less time-consuming and low usage of toxic solvents are under research to design pilot or industrial downstream platforms, representing better alternatives to achieve an economy wroth between industries and sustainable development.

CHAPTER 5 – Impact of digestion on bioactive compounds, bioactivity and cytotoxicity of melon (*Cucumis melo* L. *inodorus*) peel juice powder

Ricardo Gómez-García^{a,b}, Manuela Machado^a, Ana. A. Vilas-Boas^a, Débora A. Campos^a,
Cristóbal N. Aguilar^b, Ana R. Madureira^a and Manuela Pintado^{a*}

^a*Universidade Católica Portuguesa, CBQF - Centro de Biotecnologia e Química Fina – Laboratório Associado, Escola Superior de Biotecnologia, Rua Diogo Botelho 1327, 4169-005, Porto, Portugal*

^b*BBG-DIA. Bioprocesses and Bioproducts Group. Food Research Department, School of Chemistry, Autonomous University of Coahuila, Saltillo, Coahuila, Mexico*

Submitted

Journal of Food and Function

Abstract

The objectives of this research work were to evaluate the effect of *in vitro* gastrointestinal digestion (GIT) on melon peel juice (MPJ) powder from fruit processing industry by-products, considering (i) the recovery and accessibility indexes, (ii) the changes on antioxidant activity, and (iii) the prebiotic effect. Throughout exposition to GIT conditions a decrease on the total phenolic content (TPC = 65.31%) and antioxidant activity by ABTS = 39.77% and DPPH = 45.91% were observed. However, these both parameters exhibited stable accessibility, accounting with 81.89%, 76.55%, and 54.07% for TPC, ABTS and DPPH, respectively. After gastrointestinal digestion, the non-absorbed fraction exhibited a positive impact on the growth of *Bifidobacterium* and *Lactobacillus* strains, possibly associated with the high content of simple sugar (glucose and fructose). This fraction also showed to be safe on Caco-2 intestinal cells. These findings suggest that MPJ might be used as a potential food functional ingredient.

Keywords: Melon by-products, functional ingredients, phenolic antioxidants, simulated digestion, prebiotic effect.

5.1. Introduction

Functional food ingredients/additives have been stated as food stuffs, which can exert diverse benefits on human health, helping in the prevention or reduction of certain diseases as cancers, cardiovascular and inflammatory disorders and diabetes (Silva et al., 2018). Currently, consumers demand for natural clean label food ingredients are increasing (Rao et al., 2019). In this regard, food waste and by-products are recognized to be excellent sources of high content of value-added bioactive compounds (BCs), including fibres, vitamins, sugars, organic acids, carotenoids and phenolics (among others) with health promoting properties including antimicrobial, antioxidant and prebiotic activities. Thus, bearing these facts in mind, these by-products may be used as natural food ingredients or additives for the preparation of innovative functional food products, which in turn responds to the current trends in clean label and safe food products and increase of food supply products (Torres-León et al., 2018).

In this context, fruit processing industries are confronted with the lack of efficient and proper management of foods before and after food processing, generating great amount of fruit waste and by-products, having environmental and economic negative impacts due to their null applications being discarded in landfills (Campos et al., 2020b). EU commission launched new directives that industries must accept and implement by 2030 within their processing facilities and encourage them to shift from a linear to a circular economy, which in turn improve profitability and valorisation of their food by-products, while environmental pollution is avoided (Imbert, 2017). Currently, the circular economy encompasses outstanding strategies for food waste management and valorisation as a sustainable approach to use these organic biomasses as novel resources for human purposes, since the current strategies for its treatment will not be further accepted due to different disadvantages (large landfill spaces and high transportation costs) (Ghisellini et al., 2016; Gómez-García et al., 2021c). On the other hand, in order to feed the estimated 9 billion people in 2050, FAO forecasts a 20% increase in food production, so in a near future, it is expected an increasing industrial processing and generation of food waste and by-products (Trigo et al., 2019).

Nevertheless, it should be considering that the beneficial effects and effectiveness of food ingredients depend not only on their intake and BCs composition, but also on the changes (negative or positive) produced during each phase of the gastrointestinal digestion. To understand the health promoting effect of functional ingredients a static *in vitro* gastrointestinal digestion system appears to provide a useful alternative to animal and human models for screening of food ingredients; additionally *in vitro* techniques are ethically superior, faster and less expensive than *in vivo* techniques (Madureira et al., 2011; Campos et al., 2020a). Thus, *in*

in vitro gastrointestinal digestion followed by the determination of bioactive compound concentrations and bioactivities as well as the stability and accessibility are the most common and accepted methodologies to create key markers, which help to identify and describe better patterns when compared to the real or *in vivo* models (Gullon et al., 2015; Lucas-gonzalez et al., 2016).

In this scenario, the industrialization and commercialization of melon (*Cucumis melo* L.) fruit is taking part of the great amount of food waste and by-products generation currently released (ca. 1.3 billion tonnes/year). The high industrial melon processing activities have been carried out since it is one of the most important fruits in the world, thanks to its consumer acceptance for its sweet flavour, attractive fragrance, colour and nutritional and medicinal properties. Traditionally, melon fruit was used in the treatment of some common illness well-justified by its high content of BCs (Gómez-García et al., 2020; Rolim et al., 2020). One of the principal by-products generated during melon processing are the peels, which are constituted principally by around 70-75% of water and still keep BCs such as, organic acids, proteins and polyphenols and sugars, which have been shown some interesting beneficial effects on human health. Moreover, great attention has been raised for valorisation of melon by-products with the purpose to avoid or decrease the negative impact related to the environmental contamination and economic losses in order to develop suitable strategies to exploit these materials toward their potential application as functional ingredients/additives with beneficial properties. (Dahiya et al., 2018; Esparza et al., 2020). Presently, the food industries are interested in modernization toward innovations and developments aimed to mitigate their economic losses, while zero-waste approach is achieved, meeting with the future European directives, where the food by-products generated within their facilities is used as raw material for new food supplies and applications. Melon peels utilisation and valorisation could lead to an effective way to not only for the promotion of human health and well-being, but also for their commercial viability by the incorporation into the food value chain (Chiappetta Jabbour et al., 2020).

However, the development of functional food ingredients from melon by-products has not been extensively studied nor the bioaccessibility of biomolecules during the GIT. Therefore, owing to the richness in BCs, the specific aims of this research work were to evaluate the stability of sugar, organic acids and phenolics as well as antioxidant activity throughout the GIT, and the potential prebiotic activity and safety in Caco cells.

5.2. Materials and Methods

5.2.1. Chemicals and reagents

ABTS diammonium salt (2,2-azino-bis (3-ethylbenzothiazoline-6-sulphonic acid)), anhydrous sodium carbonate (Na_2CO_3), Folin-Ciocalteu's reagent, hydrochloric acid (HCl) and sodium hydroxide (NaOH) were purchased from Merck (Algés, Portugal). α -amylase, bile salts pancreatin, calcium chloride dihydrate ($\text{CaCl}_2 \cdot 2\text{H}_2\text{O}$), magnesium chloride hexahydrate ($\text{MgCl}_2 \cdot 6\text{H}_2\text{O}$), pepsin and sodium hydrogen carbonate (NaHCO_3) and standards of gallic acid, caffeic acid, β -carotene (HPLC $\geq 95\%$, synth., cryst.), ferulic acid, 4-hydroxybenzoic, protocatechuic acid, vanillic acid and ammonium acetate, *D*-(+)-glucose, potassium dihydrogen phosphate (KH_2PO_4), sodium hydroxide (NaOH), sulphuric acid (H_2SO_4), as well as the solvents have been used for HPLC analysis (formic acid, hexane and methanol), which were purchased from Sigma-Aldrich (Sintra, Portugal), while hydroxytyrosol, luteolin, luteolin-7-glycoside, luteolin-6-glycoside, naringenin-7-glycoside, naringenin, tyrosol, from Extrasynthese (Lyon, France).

5.2.2. Preparation of melon peel juice (MPJ)

Melon peels were processed as described previously in Chapter 3 Gómez-García et al. (2021b) and split in two fractions, fresh solid fraction (SF) and liquid fraction (LF), employing a commercial juice machine (HR1869/8, 900 W, Philips). The SF fraction was manually pressed to recover the liquid excess, which was mixed with the initial LF and then centrifuged (11469 g, 15 min, 4 °C). The clarified supernatant was called melon peels juice (MPJ). The MPJ was collected and stored at -80 °C and further dried by lyophilisation, obtaining a fine powder.

5.2.3. *In vitro* simulated gastrointestinal digestion

To study the impact of gastrointestinal tract (GIT) upon the stability of bioactive compounds of MPJ, an *in vitro* GIT was performed according to the method previously described by Madureira et al. (2011), with some modifications. Samples were prepared in triplicate by mixing 1 g of lyophilised MPJ in 20 mL of ultra-pure water. Digestion stage was performed with the simulation of gastric fluid, and the intestinal absorption process was simulated by dialysis. All enzyme and reagents solutions were prepared immediately before usage and kept in an ice bath during gastrointestinal digestion. A water bath with mechanical agitation was used to simulate the temperature of the human body at 37 °C and the peristaltic movements. At the end of each GIT phase (oral, stomach and small intestine), aliquots of the digestion samples

were taken and stored at frozen temperatures until their analysis. The TPC as well as antioxidant activity (ABTS and DPPH) was measured before and after exposure to the simulated digestion conditions using the methodologies described above.

5.2.3.1. Mouth simulated digestion

The initial pH of the samples was adjusted between 5.6 and 6.9 using NaOH 0.1 M. The oral digestion was performed with 0.6 mL of α -amylase solution (100 U/mL) and the incubation took place for 1 min at 37 °C and 180 rpm.

5.2.3.2. Stomach simulated digestion

For gastric digestion, the pH of the samples was adjusted to 2.0 using HCl 1M. Pepsin at 25 mg/mL was added at a rate of 0.05 mL/mL of sample to simulate the gastric juice. The mixture was incubated during 1 h in a shaking bath at 37 °C and 130 rpm.

5.2.3.3. Gut simulated digestion

Small intestinal digestion was performed by adjusting pH to 6.0 with NaHCO₃ 1 M. The intestinal juice was simulated by dissolving and mixing 2 g/L of pancreatin and 12 g/L of bile salts; the mixture was added at a concentration of 0.25 mL/mL of sample. The solution was then incubated for 2 h, at 37 °C and 45 rpm, to mimic a long intestine digestion.

5.2.3.4. Small intestine absorption – Dialysis

A cellulose acetate dialysis tube with a molecular weight cut-off of 3 kDa (Spectra/Pro, Spectrum Lab, Breda, Netherlands) was used to reproduce the natural absorption step in the small intestine. The resulting solution from intestinal digestion, was transferred to the membranes which were immersed in a water container at room temperature during 24 h and stirred at 1000 rpm to maintain homogeneity. The water was regularly renewed every 12 h. At the end of the process, the solution that diffused the dialysis membrane represents the bioavailable sample (blood-available), and the solution that was left inside represents the non-absorbable sample (colon-available).

*5.2.4. Accessibility and stability of melon bioactive compounds through *in vitro* gastrointestinal digestion*

5.2.4.1. Recovery and Accessibility index

To analyse the MPJ powder sugar, organic acid and phenolic contents along the *in vitro* digestion stages, two different percentage indexes were studied: recovery (RI%), accessibility indexes (ACI%). The %RI concerns the amounts of phenolic compounds present in the digested food material after mouth, gastric and intestinal digestion, calculated accordingly to the equation 5.1:

$$\text{Recovery index (RI\%)} = \frac{BC_{DS}}{BC_{BD}} * 100 \quad (5.1)$$

where BC_{DS} is the bioactive content (mg/100 g DM) in the digested sample (DS) and BC_{BD} is the bioactive content (mg/100 g DM) quantified in the sample before digestion (BD) (undigested). Bioactive compounds, to exert their effects must be accessible and released from the food matrix and maintain their bioactive form, despite the reactions that might take place in the GIT. Accessibility is defined as the percentage of the bioactive compound solubilized after intestinal dialysis step; this index is the fraction of the bioactive compound that could become available for absorption into the blood system calculated accordingly to the equation 5.2:

$$\text{Accessibility index (ACI\%)} = \frac{BC_{BS}}{BC_{DS-IP}} * 100 \quad (5.2)$$

where BC_{BS} is the bioactive content (mg/100 g DM) at the intestinal absorption phase (bloodstream (BS)) and BC_{DS-IP} is the bioactive content (mg/100 g DM) in the digested sample at the intestinal phase (DS-IP).

5.2.5. Total phenolic content (TPC)

The total phenolic content of samples were determined by the Folin-Ciocalteu method with some modifications (Singleton and Rossi, 1965). In a 96-well plate, aliquots of 20 μ L of samples were mixed with 80 μ L of Folin–Ciocalteu reagent previously diluted 1:10 (v/v) in water and 100 μ L of 7.5% (w/v) sodium carbonate. After 1 h of incubation at room temperature in darkness the absorbance was measured at 750 nm using a microplate reader (Synergy H1, Vermont, USA). Gallic acid was used as standard and results were expressed as mg gallic acid equivalents (GAE)/100 g of dry matter (DM). All measurements were performed in triplicate for each experiment.

5.2.6. Antioxidant activity determination by ABTS and DPPH

The ABTS scavenging activity of samples were determined as described by Arnao, M., Cano, A., and Acosta (2001). Briefly, the ABTS^{•+} radical stock solution was prepared by mixing ABTS^{•+} (7 mM) with potassium persulfate (2.5 mM) in ultra-pure water and kept in stirring at room temperature for 16 h. The solution ABTS^{•+} was diluted with water until reach an absorbance of 0.700 ± 0.020 at 734 nm (Synergy H1 microplate reader, Vermont, USA). After, in a 96-well plate 15 μ L of the sample extract were allowed to react with 200 μ L of ABTS^{•+} solution for 6 min in the dark and the absorbance was immediately recorded at 734 nm. The standard curve was made with L-ascorbic acid (AA) (0.05-0.5 mg/mL). All experiments were in triplicate and expressed in mg ascorbic acid equivalents (AAE)/100 g DE. The DPPH^{•+} assay was performed according to the method of Brand-Williams, W., Cuvelier, M.E., Berset, C. (1995) with some modification. A stock solution (600 μ M) was prepared by dissolving 24 mg of DPPH in 100 mL of pure methanol. The DPPH solution was diluted until a concentration of 60 μ M and adjusted to a final absorbance of 0.600 ± 0.100 at 515 nm (Synergy H1 microplate reader, Vermont, USA). After, in a 96-well plate 25 μ L of sample were mixed with 175 μ L of DPPH solution. The reaction mixture was kept at room temperature for 30 minutes in the dark and the absorbance was then measured at 515 nm. Trolox was used as a standard for the preparation of a calibration curve (0.005-0.08 mg/mL). The results were triplicated and expressed in μ M of trolox equivalents (TE)/100 g DE.

5.2.7. Identification and quantification of polyphenols by HPLC

Polyphenolic profile of melon peel samples was acquired by High Performance Liquid Chromatography coupled to diode-array detector (HPLC-DAD), accordingly to the method described by Campos et al. (2020c) with some modifications. Samples were injected into Waters Series e2695 Separation Module System (Mildford MA, USA) interfaced with the UV/Vis photodiode array detector (PDA 190-600 nm). Separation was performed in reverse-phase column (COSMOSIL 5C1 8-AR-II Packed Column – 4.6 mm I.D. \times 250 mm: Dartford, UK). Chromatographic separation of phenolic compounds was carried out with mobile phase A – water/methanol/formic acid (92.5:5:2.5, v/v/v) – and mobile phase B – methanol/water/formic acid (92.5:5:2.5, v/v/v) under the following conditions: 50 μ L were injected at continuous flow of 0.5 mL/min, gradient elution starting at 100% mobile phase A for 50 min, then gradient reset at 45% A and 55% B between 50 to 55 min. Finally, the mobile phase A returns to 100% and remains at this percentage for 4 min (until 59 min). Detection was achieved at wavelengths ranging from 200 to 600 nm and, data acquisition and analysis were

accomplished with Software Empower 3. Polyphenolic compounds were identified and quantified by external calibration curve by comparison with pure standards, comparing retention times, UV absorption spectra and peak areas. All determinations were made in triplicate and the results were expressed as mg of phenolic compounds/100 g of DE.

5.2.8. Identification and quantification of sugars and organic acids by HPLC

The chromatographic separation was carried out using a Beckman Coulter HPLC equipment coupled to IR (K-2301) and UV detector (K-2501) (Knauer, Berlin, Germany). The aliquots taken from the GIT process at before mouth, mouth, stomach, small intestine and after dialysis were filtered (0.45 µm cellulose acetate membrane) and then 30 µL of sample were analyzed using an Aminex HPX-87H column (Bio-Rad, Hercules, CA, USA) operated at 40 °C with 13 mM H₂SO₄ as mobile phase at constant flow of 0.6 mL/min. Data acquisition and analysis were accomplished using Clarity software. The detection was accomplished with an infrared detector and peaks from samples were identified and quantified by comparison of retention time and by using calibration curves of each standard of lactic, formic, acetic, succinic, and propionic acids. All determinations were made in triplicate.

5.2.9. Prebiotic potential

The MPJ powder before and after GIT passage was tested for potential of prebiotic activity using the *in vitro* methods reported by Gullon et al. (2015) and Costa et al. (2019) using pure probiotic through the evaluation of growth curves using microplate assay.

5.2.9.1. Growth curves via microplate assay

Potential prebiotic effect of MPJ powder was determined for *Bifidobacterium animalis* Bo (CSK, Ede, Netherlands), *Bifidobacterium animalis* spp. *lactis* Bb12, *Lactobacillus casei* 01 (Chr. Hansen, Hørsholm, Denmark) and *Lactobacillus acidophilus* LA-5 (Lallemand, Montreal, Canada). Strains were stored at -80 °C in de Man–Rogosa–Sharpe (MRS) broth (Biokar Diagnostics, Beauvais, France) with 30% (v/v) glycerol. *L. casei* 01 and *L. rhamnosus* R11 inoculum were prepared by suspending each bacterial colony into De Man, Rogosa and Sharpe (MRS) broth, achieving a turbidity equivalent to 0.5 McFarland standard, and then diluting to reach the recommended concentration of probiotic bacteria in wells, 5x10⁵ CFU/mL. Twenty microliters of inoculum was transferred to 96-well microplate and a final volume of 200 µL completed with MRS broth without glucose with MPJ at concentrations of 1 and 2% (w/v). Microplate was incubated at 37 °C for 24 h with agitation. *B. animalis* Bo and *B. lactis*

BB12 inoculums were prepared under anaerobic atmosphere, in MRS broth supplemented with 0.05% (v/v) *L*-cysteine-HCl, achieving a final turbidity equivalent to 0.5 McFarland standard (1×10^8 CFU/mL), and then diluted to reach the recommended concentration of probiotic bacteria in wells (5×10^5 CFU/mL). Twenty microliters of each inoculum were transferred to a 96-well microplate and every well was fulfilled (to final volume of 200 μ L) with the MPJ diluted in basal MRS broth without glucose at concentrations of 1 and 2% (w/v). Microplates was sealed with paraffin and incubated at 37 °C for 48 h with agitation, with absorbance measurements at 660 nm registered every hour. Three samples were performed: i) Positive control, containing inoculum and MRS broth, ii) Sample containing the solubilized MPJ in MRS broth without glucose and iii) Negative control; containing only MRS broth.

5.2.10. Evaluation of cytotoxicity: Metabolic activity assay

5.2.10.1. Cell line growth conditions

Human epithelial cells obtained from European Collection of Authenticated Cell Cultures (ECACC), Caco-2 (ECACC 86010202) were cultured at 37 °C in a humidified atmosphere of 95% air and 5% CO₂, as monolayers using Dulbecco's Modified Eagle's Medium (DMEM) with 4.5 g/L glucose, L-glutamine without pyruvate (Gibco, Thermo Scientific, Waltham, MA, USA) containing 10% (v/v) of fetal bovine serum (FBS, Biowest, Nuaille, France), 1% (v/v) of Penicillin-Streptomycin-Fungizone (Lonza, Verviers, Belgium) and 1% (v/v) of non-essential amino acids (Gibco, Thermo Scientific, Waltham, MA, USA).

5.2.10.2. Prestoblue assay

Prestoblue assay was performed according to the Thermo scientific guidelines. In brief, cells were seeded at 1.0×10^5 cells/mL into wells of 96-well tissue culture plates. After 24 h, the media was removed and replaced by 90 μ L of the sample in the correspondent dilution. DMSO (dimethyl sulfoxide) was used as a negative control and the fresh media was used as a positive control (cell in normal growth conditions). After 24 h, 10 μ L of prestoblue reagent was added, and the plates were incubated for 1h in the dark at 37 °C. The plate content was transferred to a black microplate and the fluorescence was read. The metabolic inhibition was calculated accordingly to the equation (5.3):

$$\% \text{ Metabolic Inhibition} = \frac{\text{Absorbance positive control} - \text{Absorbance sample}}{\text{Absorbance positive control}} * 100 \quad (5.3)$$

5.2.11. Statistical analysis

SPSS Statistics (version 23) was used to carry out the statistical analyses. All experiments were carried out in triplicates, and data were reported as mean \pm standard deviation. Shapiro - Wilk test tested the normality of data distribution ($p < 0.05$). The differences of mean values among a concentration of bioactive compounds or bioactivities obtained in each phase of the *in vitro* GIT were analysed by one-way analysis of variance (ANOVA). The homogeneity of variances was assessed by Levene's test, and the multiple comparisons were made at those statistically significant variables using the Tukey's posthoc test at the $p < 0.05$ significance level.

5.3. Results and discussion

5.3.1. Stability and accessibility of bioactive compounds of melon peel juice during *in vitro* GIT digestion

5.3.1.1. Soluble Sugars

Soluble sugars changed after the GIT digestion, where fructose (47.70 g/100 g DM) was the most representative sugar, followed by glucose (33.12 g/100 g DM) and sucrose (3.22 g/100 g DM) (**Figure 5.1a**). At the mouth stage, the content of fructose, glucose and sucrose was not significantly affected, exhibiting a stable recovery index (RI%) (98.22%, 94.19% and 73.09%, respectively) while at stomach, fructose and glucose showed a substantial decrease to 72.61% and 68.23%, respectively. All the sugars, fructose, glucose and sucrose exhibited a significant reduction in the small intestine (47.14%, 43.46% and 37.28%, respectively) and then reaching 42.67%, 37.66% and 35.39%, respectively, during the simulated intestinal absorption (bloodstream) (**Table 5.1**). On the other hand, the accessibility index (%ACI) for all three sugars was around 85-90% (%ACI), becoming accessible for absorption to be used by the body (**Table 5.1**). Carbohydrates ingested can be absorbed in intestinal mucosa, metabolized by the liver and, finally transported to working muscles for oxidation (Malone et al., 2021). The changes in the RI% values could be explained due to several factors, including enzymatic action and pH changes, which can cause chemical modifications in the carbohydrates. The isomerisation of glucose into fructose also could justify the higher RI% of fructose than glucose (Ribeiro et al., 2020). Similar decrease behaviours during GIT simulation were observed on sugars (fructose and glucose) from olive pomace powder, starting from 59-62% in the mouth, then 36-47% at stomach and 30-40% in the small intestine, respectively (Ribeiro et al., 2020).

Despite the significant variations of sugar contents of MPJ powder throughout the GIT phases, these compounds still exhibited good percentages of recovery and accessibility, which could remark their importance as natural resource of bioactive compounds with great stability after their consumption. In this regard, fructose has been recommended for diabetics due to its low glycaemic index compared to that of glucose and combinations of glucose and fructose intake have indeed been reported to increase performance during exercise. Traditionally, the effects of ingested carbohydrates on exercise capacity have been attributed to the prevention of hypoglycaemia, muscle oxidation and central stimulation (Rosset et al., 2017). Usually, only about of 5-30% of the ingested sugars and sweeteners reach the large intestine due to the absorption of these molecules in the small intestine through sugar transporters. Hence, compared to the large intestine, the small intestinal is enriched ten times higher in sugars and sweeteners. These sugars are important substrates for microbes as they possess carbohydrate uptake and utilization genes and transcripts with respect to microbes in the large intestine (Di Rienzi and Britton, 2020). Fructose, sugar alcohols, and some sweeteners (e.g., sucralose) are passively, slowly, or very poorly absorbed in the small intestine. Up to 30-90% of these sugars and sweeteners pass into the large intestine. The exact amounts of sugars/sweeteners that reach the large intestine, however, is difficult to generalize across individuals, because between females and males display considerable variation in their absorptive capacity for a sweetener or sugar. Thus, assessing simple sugars behaviors from MPJ at each stage of the GIT phases could allow to find significant indicators to be exploited as prototype of functional powder rich in natural compounds, which have beneficial effects to the human health.

5.3.1.2. Organic acids

Results of the organic acids profile of MPJ through GIT simulation are depicted in **Figure 5.1b**. Three organic acids were identified by HPLC-UV, where citric acid was the most prominent organic acid with a value of 23.72 g/100 g DM followed by succinic (16.04 g/100 g DM) and malic acid (12.44 g/100 g DM). The content of all these organic acids decreased significantly during the GIT digestion (**Figure 5.1b**). The highest reduction of organic acids took place in the stomach and small intestine because of severe acidic conditions, reaching RI% values of 89.44%, 90.62% and 85.29%, following a decrease in the small intestine of 57.00%, 56.66% and 54.02%, and at the end, having values for intestinal absorption of 51.63%, 53.10% and 52.11% for citric, malic and succinic acids, respectively (**Table 5.1**). These results are in concordance with previous reports indicating that melon fruit and its parts possess organic

acids, highlighting their relevant presence for fruit sweetness and quality at sugar levels ranging from 1.5 to 3.5 g/100 g Fresh Weight (FW), as well as 0.25 to 9.89 g/100 g FW for organic acids contents (Obando-Ulloa et al., 2009; Tang et al., 2010; Huang et al., 2017). Despite the significant changes of the organic acids' contents of MPJ powder during the GIT phases, these compounds still exhibited stable percentages of recovery and accessibility, which could remark melon peels as an important natural resource of bioactive compounds with great stability after their intake. For example, citric acid is a natural antioxidant with high industrial value, which around 70% of its total production is used in the food and beverage industry for various purposes, 12% in pharmaceuticals and about 18% for other industrial uses (Di Rienzi and Britton, 2020). Moreover, citric acid extract from *Garcinia cambogia* was used as a plant-based drug to treat non-alcoholic fatty liver, which is the most common liver disease worldwide, which has the potential to progress to fibrosis cirrhosis and hepatocellular carcinoma (Nomi-Golzar et al., 2021). Also, succinic acid and its salts (succinates) are important organic compounds that have been shown several health benefits that positively affect the oxygenation of the internal environment, stabilize the structure and functional activity of mitochondria, and normalize the ion metabolism in the cell and having low toxicity succinic acid has well-manifested antioxidant, immunostimulating, adaptogenic properties (Lieschova et al., 2020). Hence, measuring organic acids stability and accessibility from MPJ at the different physiological phases of the GIT could allow the identification of key markers for the evaluation as a prototype of functional ingredient rich in molecules that promote health and well-being.

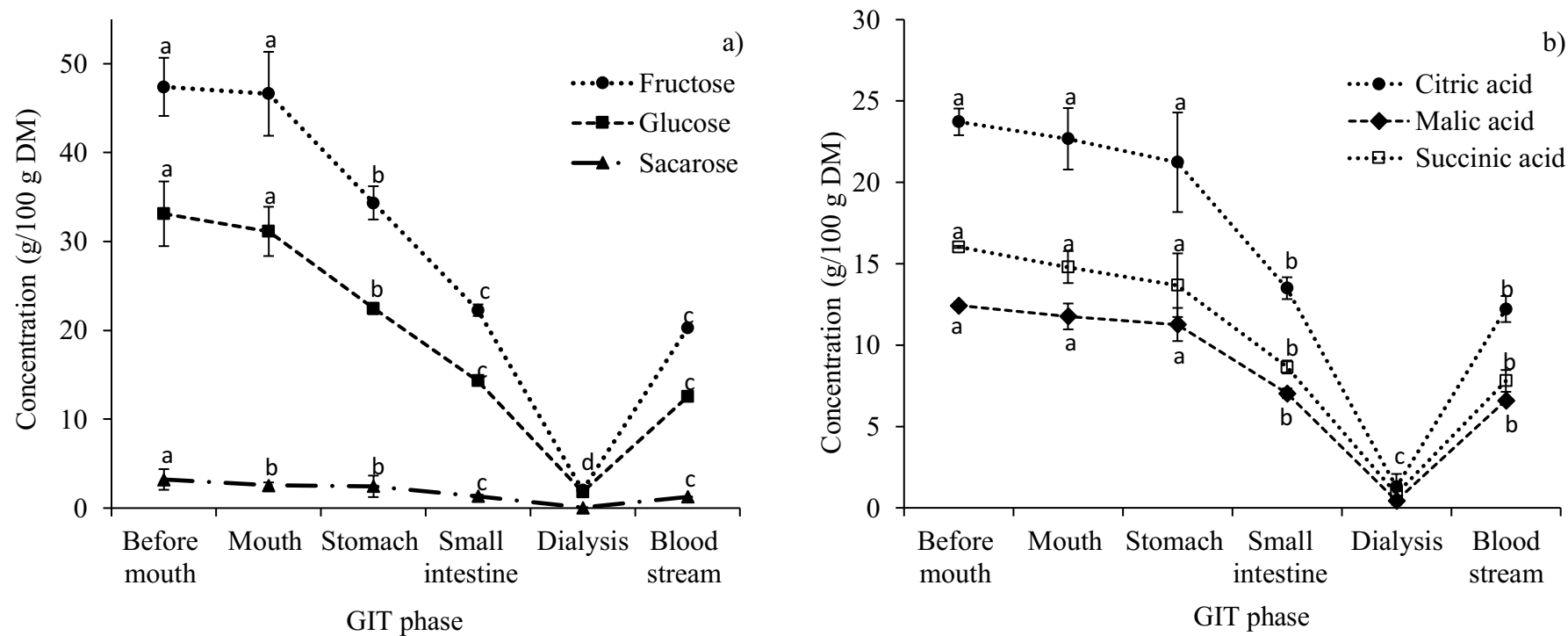


Figure 5.1. Concentrations (g/100 g DM) (\pm standard deviation) of a) soluble sugars and b) organic acids obtained after each phase of the *in vitro* gastrointestinal tract simulation (GIT) (n=3). DM: dry matter . Values with different letters indicate significant differences between each GIT stage, as determined by one-way ANOVA test and Tukey’s test ($p < 0.05$).

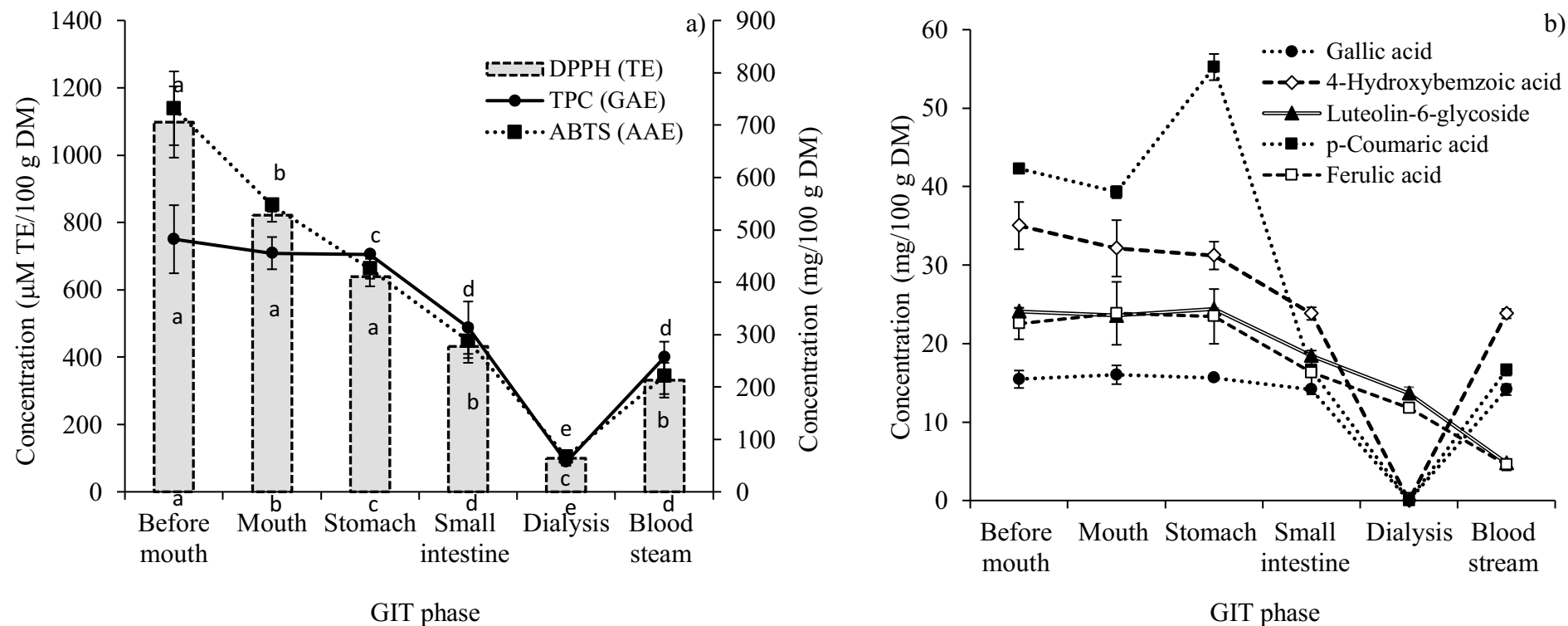


Figure 5.2. a) Total phenolic content (TPC) and antioxidant activity behaviours and b) concentrations of the main individual phenolic compounds identified by HPLC after each phase of the *in vitro* gastrointestinal tract (GIT). DM: dry matter; TPC: total phenolic content; GAE: gallic acid equivalents; AAE: ascorbic acid equivalents; TE: trolox equivalents. Results are the means of three independent determinations \pm standard deviation. Values with different letters indicate significant differences between each GIT stage, determined by one-way ANOVA test and Tukey's test ($p < 0.05$).

5.3.1.3. *Polyphenols and antioxidant activity along in vitro gastrointestinal digestion*

Figure 5.2a represents the TPC and antioxidant activity of the MPJ along GIT. Total phenolic compounds of the MPJ progressively decreased after each step of GIT simulation. The TPC of MPJ was slightly kept from before mouth until the stomach with RI of 90-95% and then a significant decrease was observed after the small intestine phase, exhibiting RI of 65%. On the other hand, the TPC showed to be more accessible for absorption in the bloodstream (80.14 % ACI) (**Table 5.2**). Similar negative decreases were observed on olive pomace TPC when exposed to GIT digestion at gastric and intestinal phases (Ribeiro et al. 2020). Additionally, during GIT conditions, pH has a key role as a protector of polyphenols against degradation in the stomach (acidic conditions) and as a promotor of degradation in the small intestine (mild alkaline conditions). On the other hand, the antioxidant activity determined by ABTS ($r = 0.85$) and DPPH ($r = 0.80$) was correlated with the TPC and significantly decreased from initial value of 738.18 to the lowest value 287.73 mg AEE/100 g DM and 1098.27 to 431.59 $\mu\text{M TE}/100$ g DM at small intestine phase, respectively (**Figure 5.2a**). These behaviours are in agreement with the TPC decrease in this phase where the conditions are more susceptible to polyphenols degradation and chemical modifications, losing the potential bioactivity (Laveffe et al., 2019). Likewise, some reports on TPC and antioxidant activity decreases have been associated to a direct connection between phenolics inhibition/degradation during GIT and loss of their bioactive properties. For example, *F. vesiculosus* phlorotannins extracts exhibited a significative decrease of the TPC from the undigested sample to the small intestine (9.93 to 5.15 mg PGE/g extract, respectively) (Catarino et al., 2021). Date pits and apple bagasse flours also showed decreases in their TPC, obtaining 80.49% and 89.64% at mouth phase followed by 66.90% and 83.38% at gastric phase and finally after intestinal 46.02% and 80.05% of recovery index, respectively (Gullon et al., 2015a). Regarding antioxidant properties, the same authors reported a slight increase (higher than undigested sample) at mouth step for ABTS (10.1% and 1.09%) and DPPH (16.4 and 2.8%), but a significative decrease (below than initial value) was observed at gastric (ABTS = 18.5% and 4.72%; DPPH = 8.2% and 6.27%) and intestinal digestion (ABTS = 38.5 and 36.8%; DPPH = 5.6% and 2.7%) for date pits and apple bagasse, respectively. The drop in TPC of the samples after the mouth digestion could be explained by possible interactions occurring between polyphenols and the salivary proteins. Indeed, such interactions are very well described for plant polyphenols

and very relevant for the development of important sensory characteristics of certain foods and beverages (Wojtunik-Kulesza et al., 2020). Furthermore, these behaviours could be explained by the fact that polyphenols are not protected or mixed within a complex matrix, being more exposed and therefore more susceptible to modification, losing their bioactive properties. Similar behaviours have been previously reported for phenolics and are on the basis of the development of delivery strategies such as phenolic compounds loaded in solid micro- or nano- carriers (encapsulation), to protect from GIT conditions (Campos et al., 2015; Madureira et al., 2016).

On the other hand, individual phenolic compounds of MPJ powder before and after *in vitro* GIT digestion were assessed (**Figure 5.2b**). In this context, *p*-coumaric acid, 4-hydroxybenzoic and luteolin-6-glycoside were the most distinguishable compounds in MPF (42.27, 35.02 and 24.09 mg/100 g DM, respectively) (**Table 5.2**). Only *p*-coumaric showed a substantial increment to 55.2 mg/100 g DM (130% RI) at the stomach phase, being more accessible for absorption in the bloodstream, and exerted its antioxidant properties, reaching 80.35% ACI, in contrast with the others phenolics (**Table 5.1**). Similar results were described for coffee phenolic extracts, where chlorogenic and cryptochlorogenic acids exhibited 50% and 80%, respectively, and Di-O-caffeoylquinic acids derivatives at intestinal phase exhibited very low RI % (less than 10%) (Vilas-Boas et al., 2020). Moreover, phenolics such as gallic, *p*-coumaric acid, 4-hydroxybenzoic, and ferulic acids have been widely studied, due to their high associated antioxidant activity feature: (i) ability to scavenge free radical, (ii) reduction or chelation of transition metal ions or (iii) inhibition of lipid peroxidation (Govea-Salas et al., 2016; Morais et al., 2015; Olubunmi et al., 2019). Also, gallic, 4-hydroxybenzoic, luteolin-6-glycoside ferulic acids presented stable RI% at intestinal absorption (blood stream) (73.30%, 55.10%, 57.20% and 16.60%, respectively) and ACI% (80.14%, 80.35%, 74.75% and 22.74%, respectively) (**Table 5.2**). The present findings suggest that most of the phenolics and their related antioxidant activity present in MPJ powder decreased throughout the GIT process.

Table 5.1. Recovery index (RI%) and Accessibility index (ACI%) of phenolic compounds and antioxidant activity throughout GIT simulation from melon peel juice (MPJ) powder.

Bioactive compound	Recovery index (RI %)					Accessibility index (ACI %)
	Mouth	Stomach	Small Intestinal	Dialysis	Blood stream	
Sugars						
Fructose	98.22 ± 3.15 ^a	72.61 ± 3.55 ^b	47.14 ± 3.79 ^c	4.47 ± 0.87 ^d	42.67 ± 3.26 ^c	90.56 ± 1.48 ^a
Glucose	94.19 ± 3.71 ^a	68.23 ± 5.38 ^b	43.46 ± 4.73 ^c	5.98 ± 2.14 ^d	37.66 ± 2.97 ^c	86.51 ± 3.59 ^a
Sucrose	73.09 ± 7.31 ^a	71.01 ± 5.70 ^a	37.28 ± 2.68 ^b	1.88 ± 0.16 ^c	35.39 ± 3.74 ^b	91.91 ± 0.81 ^a
Organic acids						
Citric acid	95.82 ± 4.02 ^a	89.44 ± 9.98 ^a	57.00 ± 1.66 ^b	5.36 ± 0.82 ^c	51.63 ± 2.46 ^b	90.56 ± 1.73 ^a
Malic acid	94.76 ± 4.20 ^a	90.62 ± 6.49 ^a	56.66 ± 1.18 ^b	3.56 ± 0.64 ^d	53.10 ± 0.55 ^c	93.73 ± 1.01 ^a
Succinic acid	92.51 ± 5.74	85.29 ± 11.02	54.02 ± 0.82	5.19 ± 3.73	52.11 ± 11.61	92.95 ± 10.79 ^a
Phenolics						
Gallic acid	103.72 ± 1.92 ^a	101.09 ± 1.18 ^a	91.48 ± 0.69 ^a	18.17 ± 1.98 ^c	73.30 ± 1.58 ^b	80.14 ± 2.07 ^a
4-Hydroxybenzoic	91.08 ± 11.58 ^a	89.56 ± 15.36 ^a	68.32 ± 7.54 ^{ab}	13.22 ± 1.68 ^c	55.10 ± 8.85 ^b	80.35 ± 4.52 ^a
Luteolin-6-glycoside	97.77 ± 1.95 ^a	101.30 ± 0.74 ^a	76.54 ± 1.42 ^b	57.20 ± 1.00 ^d	57.20 ± 1.00 ^c	74.74 ± 0.07 ^b
<i>p</i> -Coumaric acid	92.99 ± 2.85 ^b	130.85 ± 10.76 ^a	39.28 ± 3.35 ^c	UQ	15.96 ± 1.06 ^d	40.84 ± 4.65 ^c
Ferulic acid	106.41 ± 10.71 ^a	104.58 ± 9.40 ^a	72.67 ± 5.26 ^b	52.50 ± 4.73 ^c	16.60 ± 2.81 ^d	22.74 ± 2.27 ^d
TPC (mg GAE/100 g DM)	94.56 ± 7.51 ^a	93.99 ± 2.22 ^a	65.31 ± 1.60 ^b	12.54 ± 2.20 ^c	55.35 ± 3.43 ^b	81.89 ± 2.36 ^a
DPPH (µM TE/100 g DM)	62.71 ± 18.15 ^a	59.65 ± 11.69 ^a	45.91 ± 14.77 ^{ab}	17.31 ± 4.51 ^b	36.02 ± 11.07 ^{ab}	54.07 ± 6.96 ^b
ABTS (mg AAE/100 g DM)	75.26 ± 8.31 ^a	58.67 ± 7.90 ^a	39.77 ± 7.67 ^b	12.20 ± 0.64 ^c	44.32 ± 18.73 ^b	76.55 ± 3.62 ^a

UQ: under quantification limit. All determinations were carried out in triplicate and results are shown as mean value ± standard deviation. Results are the means of three independent determinations ± standard deviation.

Results are the means of three independent determinations ± standard deviation. Values with different letters in the same line to RI% and the same column to BI % indicate significant differences between each GIT stage, as determined by one-way ANOVA test and Tukey's test ($p < 0.05$).

Table 5.2. Main polyphenols identified and quantified by HPLC-DAD and antioxidant activity during the *in vitro* gastrointestinal tract simulation of melon peel juice (MPJ) powder.

No.	Phenolic compound	Gastrointestinal phase (concentration mg/100 g DM)					
		Undigested sample	Mouth	Stomach	Small Intestinal	Dialysis	Blood stream
1	Gallic acid	15.45 ± 0.11 ^a	16.02 ± 0.20 ^a	15.62 ± 0.28 ^a	14.13 ± 0.01 ^b	2.81 ± 0.29 ^d	11.03 ± 0.29 ^c
2	Hydroxytyrosol	UQ	UQ	ND	UQ	UQ	UQ
3	Tyrosol	UQ	UQ	ND	UQ	UQ	UQ
4	4-hydroxybenzoic	35.02 ± 3.01 ^a	32.13 ± 6.59 ^{ab}	31.21 ± 4.94 ^{ab}	23.81 ± 1.77 ^{bc}	4.63 ± 0.75 ^c	17.18 ± 2.37 ^d
5	Luteolin-6-glycoside	24.09 ± 0.39 ^a	23.55 ± 0.11 ^{ab}	24.41 ± 0.57 ^b	18.44 ± 0.11 ^c	13.78 ± 0.07 ^d	1.13 ± 0.68 ^d
6	7-hydroxycoumarin	NQ	NQ	NQ	NQ	NQ	NQ
7	<i>p</i> -Coumaric acid	42.27 ± 1.36 ^b	39.29 ± 0.77 ^b	55.23 ± 3.05 ^a	16.62 ± 1.67 ^c	UQ	9.74 ± 0.26 ^d
8	Luteolin-7-glycoside	NQ	NQ	NQ	NQ	NQ	NQ
9	Ferulic acid	22.56 ± 2.16 ^a	23.85 ± 0.23 ^a	23.46 ± 0.27 ^a	16.32 ± 0.50 ^b	11.77 ± 0.08 ^c	3.78 ± 0.31 ^d
10	Apigenin	UQ	UQ	ND	ND	NQ	NQ
Total by HPLC		139.39 ± 4.97	134.84 ± 7.42	149.92 ± 7.77	89.32 ± 3.26	32.99 ± 1.18	54.73 ± 4.73
TPC (mg GAE/100 g DM)		482.27 ± 65.32	455.70 ± 30.79	453.15 ± 20.83	313.37 ± 51.64	56.74 ± 6.87	256.63 ± 25.46

DM: dry matter; NQ: non-quantified; ND: non-detected; UQ: under quantification limit. Results are the means of three independent determinations ± standard deviation.

however, they kept stable percentages of ACI (50-80%), which could reinforce its application as functional powder with health promoter properties.

5.3.2. Prebiotic potential

The prebiotic potential of MPJ powder was studied on four strains in basal MRS medium without glucose, at concentrations of 1 and 2% w/v (10 and 20 mg/mL, respectively). Further, fructooligosaccharides (FOS) and glucose (Glu) were used as positive controls during 48 h of incubation. **Figure 5.3** reflects the growth profile of *Bifidobacteria* and *Lactobacillus* strains as measured by turbidity at 660 nm of optical density (OD), increasing their biomass concentrations along the first 20 h of incubation in most cases. The maximum OD at 660 nm is described in **Figure 5.4**, and the top growth rates are listed in **Table 5.3**. As expected, Glu demonstrated to be the best carbon source for both *Bifidobacteria* and *Lactobacilli* strains, showing the maximum μ_{\max} values among all the strains followed by FOS (see **Figure 3** and **Table 5.3**). Moreover, the MPJ powder influenced the growth of all the probiotic bacteria positively as compared to FOS and Glu, increasing their growth (OD at 660 nm) along the first 12-15 h of incubation for *Lactobacilli* and 10-12 h for *Bifidobacteria*, achieving very similar growth rates when compared to Glu and FOS. The MPJ at 2% (w/v) stimulated growth on tested bacteria than 1% (w/v). Comparing with MRS medium supplemented with Glu, no significant differences were found on the growth of both *Bifidobacteria* strains, but higher growth values were obtained when compared to the FOS. In this regard, the growth of *L. casei* 01 on MPJ powder (2%) showed a maximum OD value at 27 h, lower than Glu, but higher value than FOS (1.30, 2.26 and 0.92, respectively) and lower growth rates (0.09 h^{-1}) than most of the tested substrates. The strain *L. acidophilus* LA-5 was also able to ferment all the substrates tested, showing higher maximum OD values on MPJ than FOS (0.93 and 0.80, respectively). Using MPJ as substrate, *B. animalis* spp. *lactis* Bb12 and *B. animalis* Bo growth was lower than the observed when using Glu and higher than FOS, obtaining very similar μ_{\max} of 0.18 h^{-1} for both strains, which means that MPJ at 2% (w/v) could be used as carbon source and therefore as a prebiotic enhancer. Beyond, to evaluate the suitability of MPJ as food ingredient rich in beneficial compounds such as fermentable carbohydrates for probiotic bacteria growth, it was assessed the stability of its prebiotic effect upon gastrointestinal physiological conditions, most specifically after small intestine. Results (depicted in **Figure 3** - continuous line with a circle in the middle)

indicated that the gastrointestinal conditions negatively affect the prebiotic effect of MPJ when compared to the non-digested/intact melon sample (20 mg/mL), however, despite the negative decrease of its prebiotic potential, it still exhibited stable growth values for the four probiotic strains, achieving similar growth rates (μ_{\max} , h^{-1}) when compared to FOS (**Table 5.3**). The prebiotic effect of MPJ exhibited for *Bifidobacterium* and *Lactobacillus* strains could be attributed to the content of simple sugars such as glucose and fructose (as described previously in section 3.1.1), which could be used as a carbon source by the probiotic bacteria for their metabolism and growth enhancement. These probiotic bacteria are heterofermentative, which can ferment monosaccharides such as glucose and fructose (among other carbohydrates) for their metabolism/growth through the conversion of these simple sugars into intermediates of the hexose fermentation pathway, also called fructose-6-phosphate shunt or ‘bifid’ shunt and subsequently converted to short-chain fatty acids (SCFAs), which may be beneficial to the host (Pokusaeva et al., 2011; Zareba et al., 2012). These results indicate that melon substrates can promote the growth of all tested strains, with the exception of LA-5. The results obtained for the LA-5 are somehow different from the results obtained for *L. acidophilus* La3 using glucose and citric pectin, having similar OD (1.78 and 1.27, respectively) and μ_{\max} , h^{-1} (0.21 and 0.09, respectively) (Hurtado-Romero et al., 2021). Overall, the results here discussed indicate that MPJ can stimulate a fast growth of different probiotic strains, possibly due to the presence of glucose and other compounds. These growth enhancement effects of MPJ on probiotic bacteria are related to the improvement of gastrointestinal functions as well as increase or change in the composition of short-chain fatty acids, increased faecal weight and mineral absorption, immune stimulation and decreased colonic pH values.

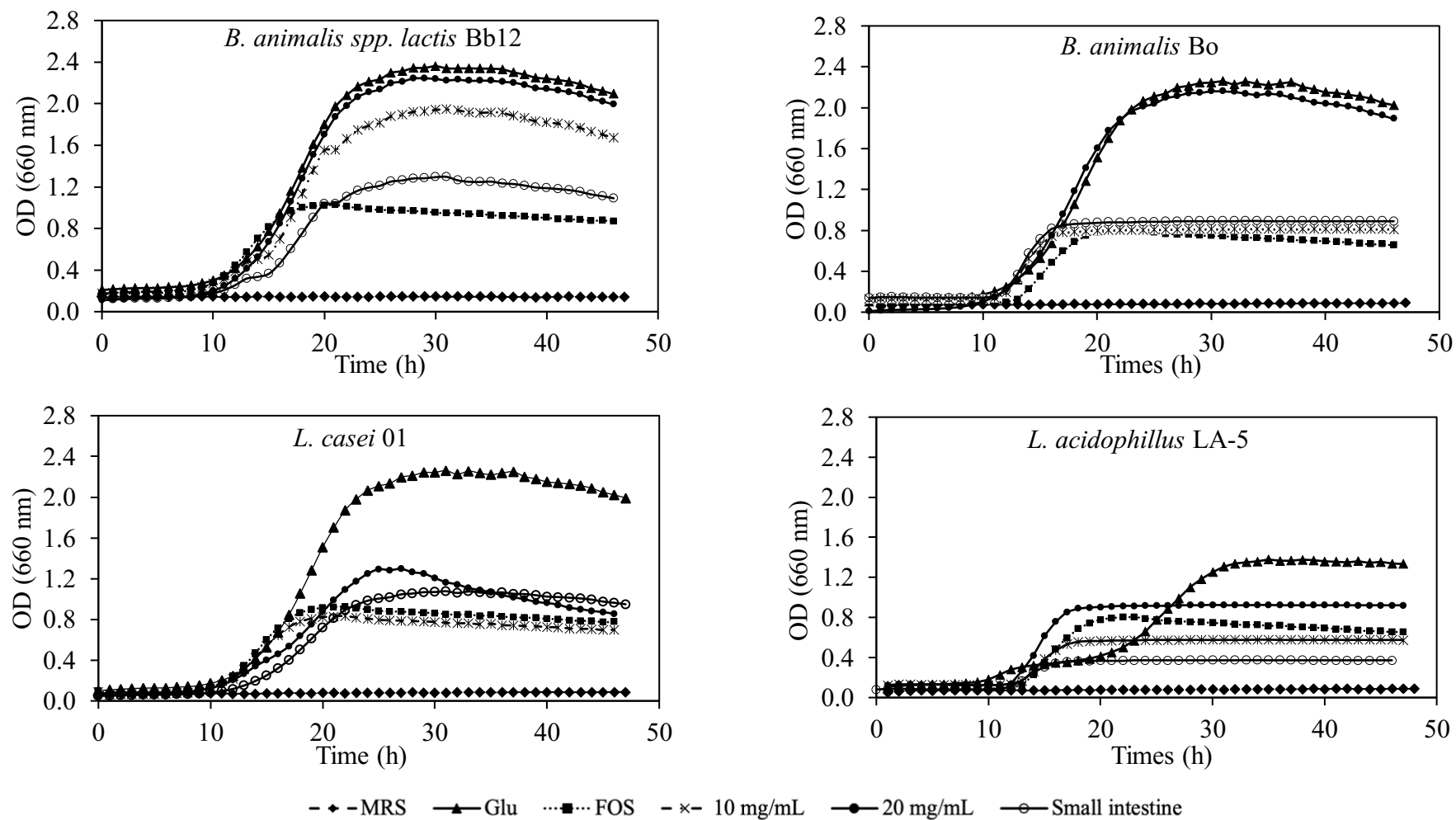


Figure 5.3. Optical cellular densities of *Bifidobacterium* and *Lactobacillus* probiotic strains in MRS media containing glucose (Glu), fructooligosaccharides (FOS) or melon peels juice (MPJ) powder at 10 and 20 mg/mL (1 and 2% w/v, respectively) during 48 h.

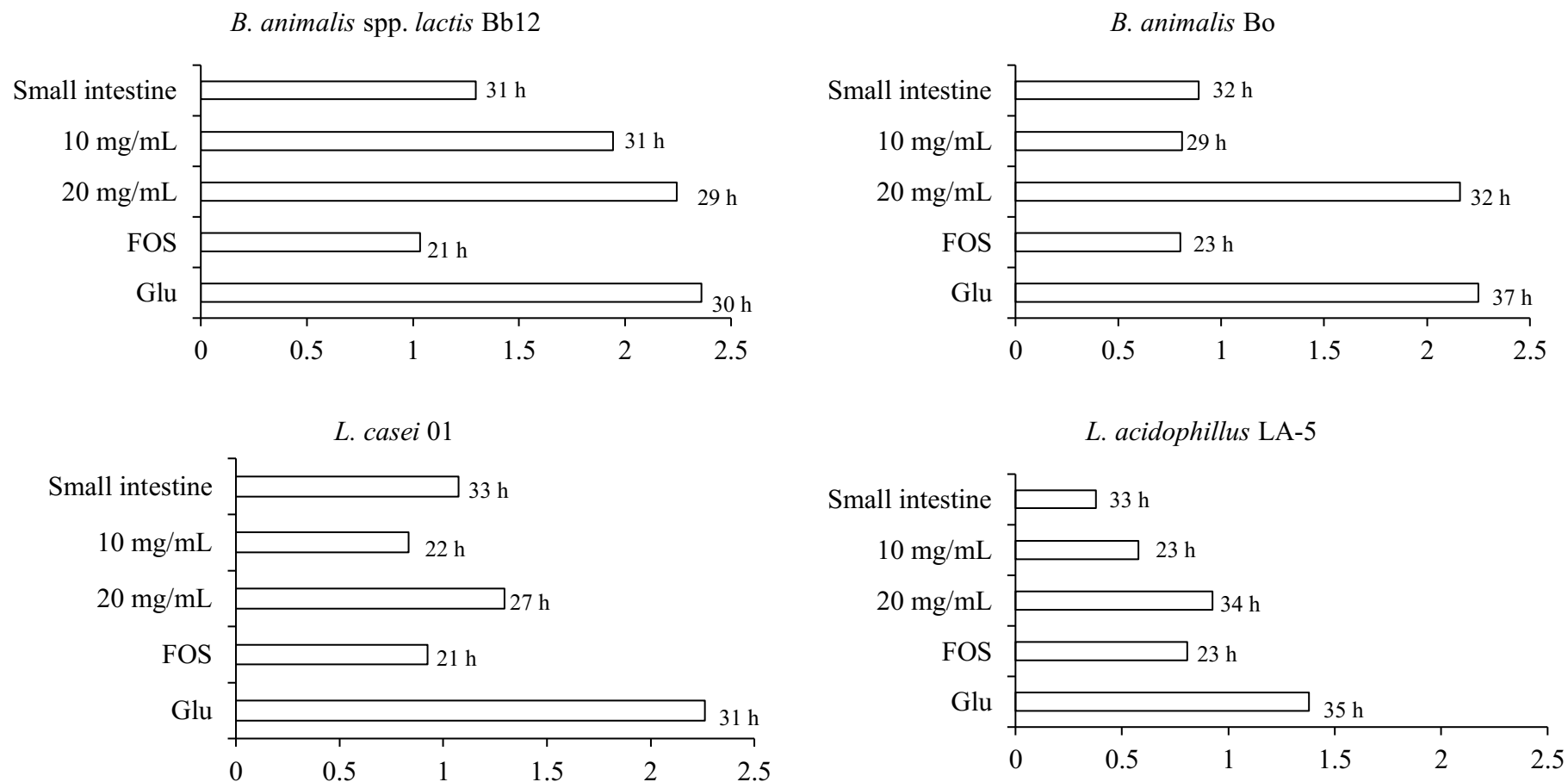


Figure 5.4. Maximum optical densities (OD at 660 nm) at the corresponding incubation times in experiments with *Bifidobacterium* and *Lactobacillus* probiotic strains grown in media containing glucose (Glu), fructooligosaccharides (FOS) or melon peels juice (MPJ) powder at 10 and 20 mg/mL (1 and 2% w/v, respectively) during 48 h.

Table 5.3. Maximum growth rates (μ_{\max} , h^{-1}) of the tested probiotic bacteria strains grown in media containing MRS media containing glucose (Glu), fructooligosaccharides (FOS) or melon peels juice (MPJ) powder at 10 and 20 mg/mL (1 and 2% w/v, respectively).

Probiotic strains	Maximum growth rate (μ_{\max} , h^{-1})				
	Positive Control (w/v)		MPJ powder (w/v)		
	GLU 2%	FOS 2%	2%	1%	SI
<i>Bifidobacterium animalis</i> ssp. <i>lactis</i> Bb12	0.18	0.18	0.18	0.14	0.08
<i>Bifidobacterium animalis</i> Bo	0.18	0.11	0.18	0.13	0.10
<i>Lactobacillus casei</i> 01	0.18	0.10	0.09	0.09	0.08
<i>Lactobacillus acidophilus</i> LA-5	0.10	0.11	0.15	0.09	0.06

The expressed values are the equation slope, which (m) means maximum growth rate.

5.3.3. Cytotoxicity

In order to obtain a cytotoxic profile of the MPJ and fulfil with the trend and demand of non-toxic and safe plant-based ingredients, the toxicity of MPJ powder before and after intestinal digestion was evaluated through cell proliferation assay upon Caco-2 intestinal cells, using extracts concentrations of 1 and 2% (w/v), as these were the concentrations that showed potential bioactivities. The **Figure 5.5** presents the metabolism inhibition of Caco-2 cells in the presence of MPJ and the sample from intestinal digestion. The prestobblue cell proliferation assay effectively measures cell growth and drug sensitivity in tumor cell lines. The sample of MPJ at 1% promoted Caco-2 cells metabolism by $12.34 \pm 2.45\%$, while for 2% by $17.53 \pm 3.12\%$. After the digestion of MPJ powder, it is possible to observe a slightly inhibition of cell metabolism, corresponding to $5.36 \pm 1.97\%$ and $8.09 \pm 0.76\%$ for samples after intestinal digestion at concentrations of 1% and 2%, respectively. It is possible to conclude that MPJ powder is safe to be used as food ingredient/additive at concentrations up to 2% w/v (20 mg/mL) but being limited to 3.5% w/v, where toxicity was observed (data not shown). It is also important to correlate the Caco-2 cells viability with the prebiotic potential when 2% (w/v) of MPJ powder was enough to proliferate probiotic bacteria strains as described in section 3.2.

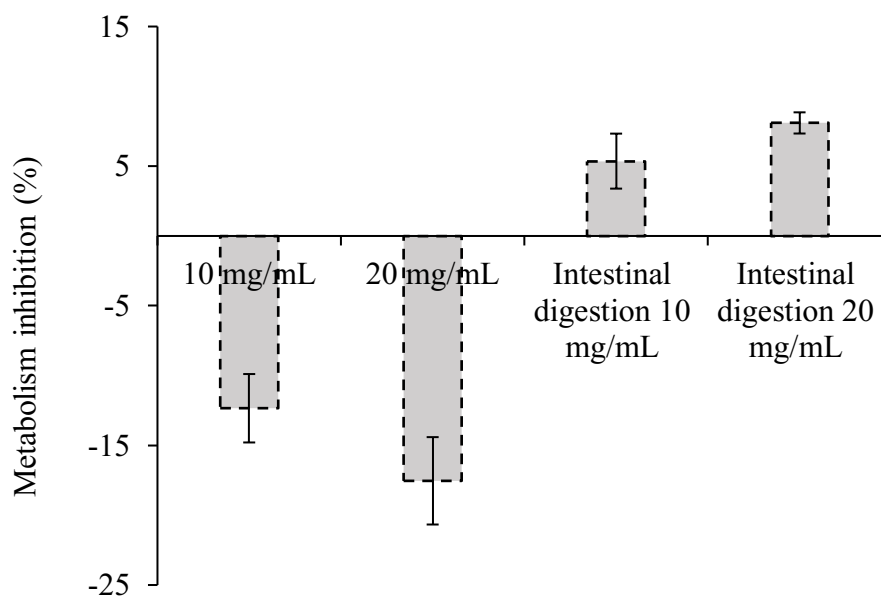


Figure 5.5. Metabolism of Caco-2 intestinal cells upon the presence of MPJ powder at concentrations of 10 and 20 mg/mL (1% and 2% (w/v), respectively) and after intestinal digestion.

5.4. Conclusions

These findings suggest that the melon peels juice powder might be used as potential food additive due to its high contents of bioactive compounds, including sugars, organic acids and phenolic acids as well as antioxidant properties that despite they decrease during the gastrointestinal tract (GIT) digestion, they showed good accessibility index 85-90% (sugars), 90-93% (organic acids) 80% (phenolics) and 54-76% (antioxidant activity), which allow to exert their related health benefits in the different steps of GIT for preventing some diseases caused by oxidative stress. In addition, this melon powder could be used as a prebiotic ingredient at 2% (w/v) establishing a potential carbon source that can be fermented by *Bifidobacterium* and *Lactobacillus*. However, profound studies are necessary to determine the possible synergic interactions of these melon by-products components, which could improve their related health benefits.

CHAPTER 6 – Prebiotic effect, bioactive compounds and antioxidant activity of melon peel (*Cucumis melo* L. *inodorus*) flour subjected to *in vitro* gastrointestinal digestion and human faecal fermentation

Ricardo Gómez-García^{a,c}, Mónica Sánchez-Gutiérrez^b, Célia Freitas-Costa^a, Ana A. Vilas-Boas^a, Débora A. Campos^a, Cristóbal N. Aguilar^c, Ana R. Madureira^a and Manuela Pintado^{a*}

^a*Universidade Católica Portuguesa, CBQF - Centro de Biotecnologia e Química Fina – Laboratório Associado, Escola Superior de Biotecnologia, Rua Diogo Botelho 1327, 4169-005 Porto, Portugal.*

^b*Food Science and Technology Department, Universidad de Córdoba, Spain.*

^c*BBG-DIA. Bioprocesses and Bioproducts Group. Food Research Department, School of Chemistry, Autonomous University of Coahuila, Saltillo, Coahuila, México.*

*This chapter has been submitted:
Journal of Food Research International*

Abstract

Melon peels are by-products derived from food processing industries, representing potential sources of new ingredients in particular rich sources of dietary fibre and phenolic compounds, which in synergy both could exert beneficial effects on human health. The objective of this study was to evaluate the accessibility of bioactive compounds from melon peels, throughout gastrointestinal digestion and evaluate their prebiotic effect when submitted to *in vitro* human faecal fermentation. Melon peels flour obtained from solid fraction showed an increase in antioxidant activity at the gastric and intestinal phase, which was corroborated by the total phenolic content (126.91%) increase and the identified individual phenolics (tyrosol, luteolin-6-glycoside, chlorogenic and caffeic acids). Also, melon peels flour exhibited a positive impact on the gut microbiota diversity, showing a similar ratio of *Firmicutes/Bacteroidetes* compared to the positive control Fructooligosaccharides (FOS) and promoted the production of short-chain fatty acids (SCFA) mainly acetate > propionate > butyrate. Thus, these findings demonstrate that melon peels flours have antioxidant and prebiotic potential attributed to the phenolic compounds and the production of beneficial SCFA, which could improve human gut health.

Keywords: Functional ingredients, dietary fiber, polyphenols, antioxidants, simulated digestion, gut health.

6.1. Introduction

Every year, 1.3 billion tonnes of food by-products are produced primarily by the food producers and processing industries with an estimated economic cost of 838 billion euros (FAO 2019). Fruits and vegetables represent ca. 30% of all food by-products (Campos et al., 2020a), but beyond huge problems always stands huge opportunities, which have been exploited by the scientific community focused on finding new and sustainable applications. Fruit by-products coming from processing industries occupy an ever-increasing space in the waste treatment facilities and in the landfills, which nowadays due to their poor usage and null suitable strategies for their management are causing environmental and economic issues (Oldfields et al., 2016). These biowastes represent a valuable resource with high content in organic matter that is rich in diverse compounds, including dietary fibre, proteins, lipids and polyphenols, which could be directed for human consumption (Esparza et al., 2020). Fruit waste reduction and valorisation to obtain value-added ingredients could have the capacity of increasing the efficiency of waste management and reducing their associated costs attributed to their transportation and disposal. In this context, there is a great increasing demand for products with health-beneficial properties focused on good nutritional and health claims, ensuing from the present diet needs and modern lifestyle based on plant-based foods and clean label ingredients. The development of novel functional food ingredients from fruit waste towards a circular bioeconomy implementation, could allow sustainable benefits such as the generation of economic revenue and possible jobs within the food value chain (Torres-Leon et al., 2018; Panchal et al., 2021). The study of biological properties of diverse fruit waste and by-products has increased, bringing to the market a huge knowledge upon the positive application for human and animal feed. Also, nowadays consumer claims/demands for natural, safe, and clean label food products, with beneficial and health-promoting characteristics have been increased. All this has contributed to diverse research studies on the development of novel functional food ingredients rich in bioactive compounds, especially dietary fibre and polyphenols, through an integral transformation of fruit by-products within the framework of circular economy and environmental pollution prevention (Guzel and Akpınar, 2019; Vella et al., 2019). Recently, the biological activities of some fruit by-products have been well described, but their use as

nutraceuticals with benefits upon human health and well-being are still lacking (Rolim et al., 2020; Silva et al 2020; Veiga et al., 2020). It is also known that the impact of the molecules can differ significantly between isolate form or when it is integrated in a complex system and is highly affected by environments such as gastrointestinal system (Rtibi et al., 2017). The simulation of gastrointestinal tract (GIT) has been applied to better understand the interaction of novel foods, ingredients or nanocarriers upon the human, and the same is happening to the human gut microbiota (Connolly et al., 2010; Lucas-González et al., 2018; Ribeiro et al 2021). Currently, an increasing interest has arose in plant fibre-rich by-products, due to their exhibited positive modulatory effect upon gut microbiota composition, which gives them prebiotic potential (Ayar et al., 2018; De Andrade et al., 2020). A prebiotic can be defined as a substrate that is selectively utilized by host microorganisms to confer a health benefit (Gibson et al., 2017). Dietary fibre and other non-digestible carbohydrates that reach the intestine can be used as a carbon source by bacteria and thus may influence the composition and metabolic activities of gut microbiota (Holscher, 2017). The recommended daily amount of fibre is 28 g/day, based on 2000 kcal/day diet. (Gibson et al., 2017). Short-chain fatty acids (SCFA) such as acetate, butyrate, and propionate are fermentation end-products derived from carbohydrates hydrolysis that may have beneficial local and systemic effects upon host health when they are produced in the intestine, having anti-carcinogenic properties, and thereby reduce the risk of colonic disorders (Markowiak-Kopeć and Śliżewska, 2020). In this regard, melon peels are by-products highly produced during fruit processing, representing around 20-30% of the total fresh weight. These by-products are rich in dietary fibre divided in insoluble (35-40%) and soluble (4-5%) dietary fibre, which also contain polyphenols (250-330 mg/100 g), mainly composed by hydroxycinnamic, benzoic acids and flavonoids (gallic, caffeic, ferulic, luteolin and tyrosol) (Mallek-Ayadi et al., 2017; Gómez-García et al., 2021b). Considering the richness in fibre and bioactives, these fractions have a high potential to be processed for the development of nutraceuticals, e.g., prebiotics. All these phenolics have been reported with biological beneficial properties, such as antimicrobial, anti-inflammatory, anti-diabetic and antioxidant activity, which are well-attributed to their high free radical-scavenging capacity (Martins et al., 2011; Govea-Salas et al., 2013; Oliveira et al., 2021). However, the development of functional ingredients from melon by-products has not been extensively studied or reported regarding the bioactivity changes during the GIT and the

impact on the human gut microbiota. It is important to understand how the combination between dietary fibre and polyphenols modulates the composition and metabolic functions of the microbial communities from human gut microbiota, since the positive modulation may help to prevent or reduce the risk of certain chronic illnesses like cancers, diabetes, cardiovascular and inflammatory disorders (Karlsson et al., 2013; Wan et al., 2021).

Therefore, owing to richness of melon peels in dietary fibre and phenolics, the specific aims of this research work were to evaluate the stability of phenolics and antioxidant activity from melon peels when crossing the GIT, as well as their potential prebiotic effect evaluated using an *in vitro* human gut microbiota fermentation model and monitoring the different representative microbial groups and the production of short-chain fatty acids (SCFA). Also, increase research interest for the melon by-products valorisation, describing their positive contribution on gut microbiota and consequently on health.

6.2. Material and methods

6.2.1. Chemicals and reagents

Chemicals used in this study such as ABTS - diammonium salt (2,2-azino-bis (3-ethylbenzothiazoline-6-sulphonic acid)), DPPH - (2,2-diphenyl-1-picrylhydrazyl), Folin-Ciocalteu's reagent, HCl - hydrochloric acid and Na₂CO₃ - anhydrous sodium carbonate were purchase from Merck (Algés, Portugal). α -amylase, bile salts pancreatin, CaCl₂•2H₂O - calcium chloride dihydrate, MgCl₂•6H₂O - magnesium chloride hexahydrate, NaHCO₃ - sodium hydrogen carbonate, pepsin and standards of gallic acid, caffeic acid, β -carotene (HPLC \geq 95%, synth., cryst.), ferulic acid, 4-hydroxybenzoic, protocatechuic acid, vanillic acid as well as ammonium acetate, D-(+)-glucose, KH₂PO₄ - potassium dihydrogen phosphate, NaOH – sodium hydroxide, H₂SO₄ - sulphuric acid, formic acid, hexane and methanol (HPLC grade) were purchased from Sigma-Aldrich (Sintra, Portugal), while hydroxytyrosol, luteolin, luteolin-7-glycoside, luteolin-6-glycoside, naringenin-7-glycoside, naringenin, tyrosol, from Extrasynthese (Lyon, France).

6.2.2. Melon peel material

According to the Nuvi Fruits S. A. Company Torres Vedras (Portugal), the melon fruits (*Cucumis melo* L. *inodorus*) were harvested (ripening stage was not controlled) from the Alentejo region in Portugal during the season of summer in August – September 2019. Fresh melon peels were generated as processing fruit by-products and then transported to the Centro de Biotecnologia e Quimica Fina (CBQF) at -20 °C. The melon peels were stored at -20 °C until their *in vitro* processing and pretreatment.

6.2.3. Preparation of melon peel flour (MPF)

Fresh melon peels were treated as described previously by Gómez-García et al. (2021b), they were milled employing a commercial juice machine (HR1869/8, 900 W, Philips) to separate the solid fraction (SF) from the liquid. The SF was collected and manually pressed using a fiber gauze to remove the excess of liquid and then oven-dried for 48 h at 55 °C. After, the dried SF was ground, and the obtained fine powder was called melon peel flour (MPF). The MPF was stored in plastic bags, avoiding humidity and sunlight.

6.2.4. *In vitro* simulated gastrointestinal digestion

To study the impact of simulated gastrointestinal (GIT) digestion upon the stability of bioactive compounds of melon peel extract, *in vitro* simulation of GIT was performed according to Madureira et al. (2011) with some modifications. Samples were prepared in three independent experiments by mixing 1 g of SF in 20 mL of ultra-pure water. Digestion was simulated by the action of different enzymes, while the intestinal absorption process was simulated by dialysis. All enzyme solutions were prepared immediately before usage and kept in an ice bath during the process of gastrointestinal digestion until addition. A water bath at 37 °C was used to simulate the temperature of the human body whereas peristaltic movements were imitated by mechanical agitation using intensities like those observed *in vivo* at each digestive phase. At the end of each GIT phase (oral, stomach and small intestine), aliquots of the digestion mixtures were taken and frozen stored until their analysis of bioactive compounds and antioxidant activity. The TPC as well as antioxidant activity (ABTS and DPPH) was measured before and after exposure to the simulated digestion conditions using the methodologies described above.

6.2.4.1. Mouth simulated digestion

The initial pH of the samples was adjusted between 5.6 and 6.9 using NaOH 0.1 M. The oral digestion was performed with 0.6 mL of α -amylase solution (100 U/mL) and the incubation took place for 2 min at 37 °C and 180 rpm.

6.2.4.2. Stomach simulated digestion

For gastric digestion, the pH of the samples was adjusted to 2.0 using HCl 1M. Pepsin at 25 mg/mL was added at a rate of 0.05 mL/mL of sample to simulate the gastric juice. The mixture was incubated during 1 h in a shaking bath at 37 °C and 130 rpm.

6.2.4.3. Gut simulated digestion

Small intestinal digestion was performed by adjusting pH to 6.0 with NaHCO₃ 1 M. The intestinal juice was simulated by dissolving and mixing 2 g/L of pancreatin and 12 g/L of bile salts; the mixture was added at a concentration of 0.25 mL/mL of sample. The solution was then incubated for 2 h, at 37 °C and 45 rpm to mimic long intestine digestion.

6.2.4.4. Small intestine absorption – Dialysis

In the last phase of intestinal digestion, the digested sample was transferred into a cellulose acetate dialysis membrane with a molecular weight of 3 kDa (Spectra/Pro, Spectrum Lab, Breda, Netherlands) to reproduce the natural absorption step in the small intestine. Then, the membranes were immersed in regularly renewed distilled water at room temperature, during 24 h and stirred at 1000 rpm to maintain homogeneity. At the end of the process, the solution that managed to diffuse the dialysis tubing represents the sample that is accessible for absorption (bloodstream), and the solution left inside the dialysis tubing represented the non-absorbable sample (colon-available), which is fermented by the gut microbiota.

6.2.5. Stability and accessibility of melon polyphenols along in vitro gastrointestinal digestion

6.2.5.1. Recovery and Accessibility index

To examine the effect on the MPF sugar, organic acid and phenolic contents along *in vitro* digestion, two different percentage indexes were studied: recovery (RI%), accessibility

indexes (ACI%). The %RI measures the amount of phenolic compounds present in the digested food material after mouth, gastric and intestinal digestion, according to the equation 6.1:

$$\text{Recovery index (RI\%)} = \frac{BC_{DS}}{BC_{BD}} * 100 \quad (6.1)$$

where BC_{DS} is the bioactive content (mg/100 g DM) in the digested sample (DS) and BC_{BD} is the bioactive content (mg/100 g DM) quantified in the sample before digestion (BD) (undigested). Bioactive compounds, to exert their effects must be accessible and released from the food matrix and maintain their bioactive form, despite the reactions that might take place in the GIT. Accessibility is defined as the percentage of the bioactive compound solubilized after intestinal dialysis step; this index is the fraction of the bioactive compound that could become available for absorption into the blood system:

$$\text{Accessibility index (ACI\%)} = \frac{BC_{BS}}{BC_{DS-IP}} * 100 \quad (6.2)$$

where BC_{BS} is the bioactive content (mg/100 g DM) at the intestinal absorption phase (bloodstream (BS)) and BC_{DS-IP} is the bioactive content (mg/100 g DM) in the digested sample at the intestinal phase (DS-IP).

6.2.6. *In vitro* faecal fermentation assay - Prebiotic effect

In this work, the potential prebiotic activity of MPF was evaluated by *in vitro* human gut microbiota fermentation assay. The human faecal samples were collected into sterile plastic boxes and kept under anaerobic conditions until their usage in fermentation (maximum of 2 h post-collection). The samples were obtained fresh, from healthy human adults (donors), with the request of not having any known metabolic or gastrointestinal disorder. Besides, the donors confirmed not to be taking any probiotic or prebiotic supplements, as well as any form of antibiotics during the last 3 months. The basal medium was prepared as reported previously by Madureira et al. (2016) the nutrient base medium comprised 5.0 g L⁻¹ trypticase soya broth (TSB) without dextrose (BBL, Lockesville, USA), 5.0 g L⁻¹ bactopectone (Amersham, Buckinghamshire, UK), 0.5 g L⁻¹ cysteine-HCl (Merck, Germany), 1.0% (v/v) of salt solution A (100.0 g L⁻¹ NH₄Cl, 10.0 g L⁻¹ MgCl₂·6H₂O, 10.0 g L⁻¹ CaCl₂·2H₂O) and a trace mineral solution, 0.2% (v/v) of salt solution B (200.0 g L⁻¹ K₂HPO₄·3H₂O) and 0.2% (v/v) of 0.5 g L⁻¹ resazurin

solution, prepared in distilled water and then adjusted at pH 6.8. The basal medium was dispensed into airtight glass anaerobic bottles, sealed with aluminium caps before sterilization by autoclave. Stock solutions of Yeast Nitrogen Base (YNB) were sterilized with 0.2 µm syringe filters (Chromafils, Macherey-Nagel, Düren, Germany) and inserted into the bottles. The serum bottles were incorporated with MPF at a final concentration of 2% (w/v) and inoculated with faecal slurries of 2% (v/v) at 37 °C for 48 h without shaking. Also, the human faeces of the five donors were supplemented with FOS at a final concentration of 2% (w/v), as a positive control. Samples were taken at 0, 12, 24 and 48 h of fermentation. All the experiments were carried out inside an anaerobic cabinet with 5% of H₂, 10% of CO₂ and 85% of N₂.

6.2.7. Gut microbiota evaluation

6.2.7.1. DNA extraction

Genomic DNA was extracted and purified from stool samples using NZY Tissue gDNA Isolation Kit (Nzytech, Lisboa, Portugal), with some modifications and previously described by Madureira et al. (2016) and later reported by Campos et al. (2020c). Briefly, the samples were centrifuged at 11,000 g during 10 min, to separate the supernatant from the pellet. Around 170–200 mg of pellet was taken from control and test samples for all times. After, the pellets were homogenized in TE buffer (10 mM Tris/HCl; 1 mM EDTA, pH 8.0) and centrifuged again at 4000 g for 15 min. The supernatant was discarded, and the pellet was resuspended in 350 µL of buffer NT1. After an incubation step at 95 °C for 10 min, samples were centrifuged at 11 000 g for 1 min. Then, 25 µL of proteinase K was added to 200 µL of supernatant for incubation at 70 °C for 10 min. The remaining steps followed the manufacturer's instructions. The DNA purity and quantification were assessed with a NanoDrop spectrophotometer (Thermo Scientific, Wilmington, DE, USA). Real-time PCR for microbial analysis at stool: real-time PCR was performed as described before by Madureira et al. (2016), in sealed 96-well microplates using a LightCycler FastStart DNA Master SYBR Green kit and a Light Cycler instrument (Roche Applied Science, Indianapolis, ID, USA). PCR reactions mixtures (total of 10 µL) contained 5 µL of 2 × Faststart SYBR Green (Roche Diagnostics Ltd), 0.2 µL of each primer (final concentration of 0.2 µM), 3.6 µL of water and 1 µL of DNA (equilibrated to 20 mg). Primer sequences (Sigut microbiota-Aldrich, St. Louis, MO, USA) were used to target the 16S rRNA gene of the bacteria and the conditions for PCR amplification

reactions are reported in **Table 6.1**. To verify the specificity of the amplicon, a melting curve analysis was performed via monitoring SYBR Green fluorescence in the temperature ramp from 60 to 97 °C. Data were processed and analysed using the LightCycler software (Roche Applied Science). Standard curves were constructed using serial tenfold dilutions of bacterial genomic DNA, according to the following webpage <http://cels.uri.edu/gsc/cbdna.html>. Bacterial genomic DNA used as a standard (**Table 6.1**) was obtained from DSMZ (Braunschweig, Germany). Genome size and the copy number of the 16S rRNA gene for each bacterial strain used as a standard was obtained from NCBI Genome database (<http://www.ncbi.nlm.nih.gov>). Data are presented as the mean values of duplicate PCR analyses. The F:B ratio was obtained by dividing the number of copies of *Firmicutes* divisions by the number of copies of *Bacteroidetes* divisions. Moreover, the relative differences to negative control percentage (only faeces fermentation) were calculated using the following equation (6.3):

$$\text{Relative difference to control (\%)} = \frac{SMC - CMC}{CMC} * 100 \quad (6.3)$$

where SMC is the mean copy numbers of the sample at a certain time (12, 24 and 48 h) and CMC is the mean copy numbers of the control sample at the same time as SMC. Positive % values mean the occurrence of an increase in the number of copies relative to the control sample at that certain time. Higher the value, the higher increase.

6.2.8. Total phenolic content (TPC)

The total phenolic content of MPF suspension before and after GIT was determined by the Folin-Ciocalteu method with some modifications (Singleton and Rossi, 1965). In a 96-well plate, aliquots of 20 µL of samples were mixed with 80 µL of Folin–Ciocalteu reagent previously diluted 1:10 (v/v) in water and 100 µL of 7.5% (w/v) sodium carbonate. After 1 h of incubation at room temperature in darkness, the absorbance was measured at 750 nm using a microplate reader (Synergy H1, Vermont, USA). Gallic acid was used as standard and the results were expressed as mg gallic acid equivalents (GAE)/100 g of dry matter (DM). All measurements were performed in triplicate for each experiment.

6.2.9. Antioxidant activity determination by ABTS and DPPH

The ABTS scavenging activity of MPF before and after GIT digestion was determined as described by Arnao, Cano and Acosta (2001). Briefly, the ABTS⁺ radical stock solution was prepared by combining ABTS⁺ (7 mM) with potassium persulfate (2.5 mM) in ultra-pure water and kept stirring at room temperature for 16 h for total homogenization. Then, the solution ABTS⁺ was diluted with water until reach an absorbance of 0.700 ± 0.020 at 734 nm (Synergy H1 microplate reader, Vermont, USA). After, in a 96-well plate 15 μ L of the sample extract were allowed to react with 200 μ L of ABTS⁺ solution for 6 min in the dark and the absorbance was immediately recorded at 734 nm. The standard curve was made with L-ascorbic acid (AA) (0.05-0.5 mg/mL). All experiments were in triplicate and expressed in mg ascorbic acid equivalents (AAE)/100 g DM.

The DPPH⁺ assay was performed according to the method of Brand-Williams, Cuvelier and Berset, (1995) with some modification. A starting solution (600 μ M) was made using 24 mg of DPPH and 100 mL of pure methanol. The DPPH solution of 60 μ M and adjusted to a final absorbance of 0.600 ± 0.100 at 515 nm (Synergy H1 microplate reader, Vermont, USA). After, in a 96-well plate 25 μ L of sample were mixed with 175 μ L of DPPH solution. The reaction mixture was kept at room temperature for 30 minutes in the dark and the absorbance was then measured at 515 nm. Standard of trolox was used for the preparation of a calibration curve (0.005-0.08 mg/mL). The measurements were made in triplicated and were expressed in μ M of trolox equivalents (TE)/100 g DM.

6.2.10. Identification and quantification of polyphenols by HPLC

Phenolic compounds profile of MPF before and after GIT was obtained by High Performance Liquid Chromatography coupled to diode-array detector (HPLC-DAD), according to the method described by Campos et al. (2020b) with some modifications. The aliquot samples taken from the GIT process at each phase (before mouth, mouth, stomach, small intestine and after dialysis) and during the faecal fermentation (at 0, 12, 24 and 48 h) were filtered (0.45 μ m cellulose acetate membrane) into a glass vial and then placed into a Waters Series e2695 Separation Module System (Mildford MA, USA) interfaced with the UV/Vis photodiode array detector (PDA 190-600 nm). Separation was achieved in a reverse-phase column (COSMOSIL 5C1 8-AR-II Packed Column – 4.6 mm I.D. \times 250 mm: Dartford, UK). Chromatographic separation of phenolic compounds was carried out using water/methanol/formic acid (92.5:5:2.5, v/v/v) as mobile phase A and

methanol/water/formic acid (92.5:5:2.5, v/v/v) as mobile phase B under the following conditions: 50 µL of sample was injected at continuous flow of 0.5 mL/min, gradient elution starting at 100 % mobile phase A for 50 min, then gradient reset at 45% A and 55% B between 50 to 55 min. Finally, mobile phase A returns to 100% and remains at this percentage for 4 min, reaching 59 min total run. Data acquisition and analysis were carried out using Software Empower 3. Detection was achieved at wavelengths ranging from 200 to 600 nm. Individual phenolic compounds were identified and quantified by using a calibration curve by comparison with pure standards, comparing retention times, UV absorption spectra and peak areas. All determinations were made in triplicate and the results were expressed as mg of phenolic compounds/100 g of DM.

6.2.11. Identification and quantification of sugars and organic acids – short chain fatty acids by HPLC

The chromatographic separation was carried out using a Beckman Coulter HPLC equipment coupled to IR (K-2301) and UV detectors (K-2501) (Knauer, Berlin, Germany). The aliquots taken from the GIT process at each phase (before mouth, mouth, stomach, small intestine and after dialysis) and during the faecal fermentation (at 0, 12, 24 and 48 h) were filtered (0.45 µm cellulose acetate membrane) and then 20 µL of sample were analysed through an Aminex HPX-87H column (Bio-Rad, Hercules, CA, USA) operated at 40 °C with 5 mM H₂SO₄ as mobile phase at constant flow of 0.6 mL/min during 30 min. Data acquisition and analysis were accomplished using Clarity software. The detection for individual sugars and organic acids was accomplished with an IR and UV detector, respectively, and peaks from samples were identified and quantified by comparison of the retention time using calibration curves of each standard for fructose and glucose as well as for lactic, formic, acetic, succinic, and propionic acids. Acquisitions were made in triplicate and the results were expressed as g of sugars and/or organic acid/100 g of DM.

6.2.12. Statistical analysis

The statistical analyses were carried out using SPSS Statistics version 23. The significance of the differences between different stages of GIT digestion was determined by one-way analysis of variance (ANOVA) according to the normality of data distribution (Shapiro-Wilk test) at the ($p < 0.05$). The homogeneity of variances was assessed by

Table 6.1. Primer sequence and real-time PCR conditions applied for gut microbiota analysis

Target group	Maximum growth rate (μ_{\max} , h ⁻¹)	Primer sequence	Genomic DNA standard	PCR product size (bp)	AT (°C)
<i>Universal</i>		AAA CTC AAA KGA ATT GAC GG CTC ACR RCA CGA GCT GAC	<i>Bacteroides vulgatus</i> ATCC 8482 (DSMZ 1447)	180	45
<i>Firmicutes</i>		ATG TGG TTT AAT TCG AAG CA AGC TGA CGA CAA CCA TGC AC	<i>Lactobacillus gasseri</i> ATCC 33323 (DSMZ20243)	126	45
<i>Clostridium leptum</i>		GCA CAA GCA GTG GAG T CTT CCT CCG TTT TGT CAA	<i>Clostridium leptum</i> ATCC 29065 (DSMZ 753)	239	45
<i>Lactobacillus</i> spp.		GAG GCA GCA GTA GGG AAT CTT C GGC CAG TTA CTA CCT CTA TCC TTC TTC	<i>Lactobacillus gasseri</i> ATCC 33323 (DSMZ 20243)	126	55
<i>Bacteroidetes</i>		CAT GTG GTT TAA TTC GAT GAT AGC TGA CGA CAA CCA TGC AG	<i>Bacteroides vulgatus</i> ATCC 8482 (DSMZ 1447)	126	45
<i>Bacteroides</i> spp.		ATA GCC TTT CGA AAG RAA GAT CCA GTA TCA ACT GCA ATT TTA	<i>Bacteroides vulgatus</i> ATCC 8482 (DSMZ 1447)	495	45
<i>Actinobacteria</i> <i>Bifidobacterium</i> spp.		CGC GTC YGG TGT GAA AG CCC CAC ATC CAG CAT CCA	<i>Bifidobacterium longum</i> subsp. <i>Infantis</i> ATCC 15697 (DSMZ 20088)	244	50

AT: annealing temperature; bp: base pairs; PCR: polymerase chain reaction

Levene's test, and the multiple comparisons were made at those statistically significant variables using the Tukey's posthoc test at the $p < 0.05$ significance level. In case of the significance difference analysed between only two samples was used t-test or Mann-Whitney according to the normality of data distribution (Shapiro-Wilk test) at the $p < 0.05$ significance level.

6.3. Results and discussion

6.3.1. Effects of GIT simulation on melon peel flour compounds: Stability and accessibility

6.3.1.1. Simple sugars and organic acids

Results of soluble sugars and organic acids of MPF through GIT simulation are depicted in **Figure 6.1a** and **b**, respectively. Soluble sugars changed significantly after the GIT digestion ($p < 0.05$), where fructose (3.10 g/100 g DM) was the most representative sugar followed by glucose (1.39 g/100 g DM), as expected. Fructose was the sugar most positively affected with %RI higher than 100%. In the mouth, a higher content of fructose was verified (3.17 g/100 g DM), when compared with respect to the undigested sample ($p < 0.05$), reaching 105.24% of RI. Both fructose and glucose exhibited a significative reduction after stomach (76.73 and 50.81%, respectively), small intestine (47.31 and 28.46%, respectively) reaching 33.75 and 17.79%, respectively, during the simulated intestinal absorption (blood stream) (**Table 6.2**). Exogenous carbohydrates can pass through the GIT up to intestinal absorption, then are transported to the liver by the portal circulation, reaching muscles for oxidation process (Malone et al., 2021). In this regard, around 60-70% (ACI) of fructose and glucose became accessible for absorption to be used by the body (**Table 6.2**). These changes in the RI% values could be explained due to several factors, including enzymatic action and pH changes, which can cause chemical modifications in the carbohydrates. The isomerisation of glucose into fructose also could justify the higher RI% of fructose than glucose (Ribeiro et al., 2020). On the other hand, three organic acids were identified by HPLC-UV, where citric acid was the most prominent organic acid with value of 7.17 g/100 g DM followed by succinic (4.90 g/100 g DM) and malic acid (1.29 g/100 g DM). The concentration of these organic acids decreased along the GIT digestion stages ($p < 0.05$) (**Figure 6.1b**). The highest reduction of organic acids had place in the stomach because of acidic conditions (pH=2) and at the end of GIT simulation they were accessible for absorption with percentages about 46, 39

and 24% for citric, malic, and succinic acids, respectively (**Table 6.2**). These results are in concordance with previous reports indicating that melon fruit and its parts possesses soluble sugars and organic acids originally in its composition, highlighting their relevant presence for fruit sweetness and quality at sugar levels ranging from 1.5 to 3.5 g/100 g Fresh Weight (FW), as well as 0.25 to 9.89 g/100 g FW for organic acids contents (Obando-Ulloa et al., 2009; Tang et al., 2010; Huang et al., 2017). Despite the significant changes of sugars and organic acids contents of MPF throughout the GIT phases, these compounds still exhibited good percentages of recovery and accessibility, which could remark its importance as natural resource of nutrients and bioactive compounds with great stability after their intake. For instance, fructose has been recommended for diabetics due to its low glycaemic index compared to that of glucose and combinations of glucose-fructose intake have indeed been reported to specifically increase performance during exercise. The effects of ingested carbohydrates on exercise capacity have been traditionally attributed to several mechanisms, including prevention of hypoglycaemia and direct muscle oxidation, as well as central stimulatory effects (Rosset et al., 2017). Citric acid has a fundamental function in the cellular energy metabolism and biosynthesis of macromolecules in the mitochondrial matrix. It is implicated that the abnormal function of the citric acid cycle can lead to pathological conditions (Cho et al., 2020). In this study, succinic acid showed the highest recovery index (45.96%) retained in the colon-available sample, which could be used by gut microbiota. In this regard, succinic acid in living organisms takes the form of an anion, succinate, which has multiple biological roles as a catabolic metabolite of microbial polysaccharide fermentation, intermediate in the microbial production of propionate and a common end-product of some bacteria (e.g., *Prevotella* and *Bacteroides*) (Medina et al., 2021). Succinate is considered as a primary cross-feeding metabolite between gut host microbes because it is produced by some primary fermenters and consumed by secondary fermenters (e.g., *Bacteroides thetaiotaomicron*). Moreover, some evidence proved to be effective for improving metabolic abnormalities associated with obesity (Fernández-Veledo et al., 2021). Therefore, measuring sugars and organic acids accessibility from MPF at the different physiological phases of the GIT could allow the identification of important markers to demonstrate its potential as clean label functional ingredient rich in molecules that promote gut health and well-being.

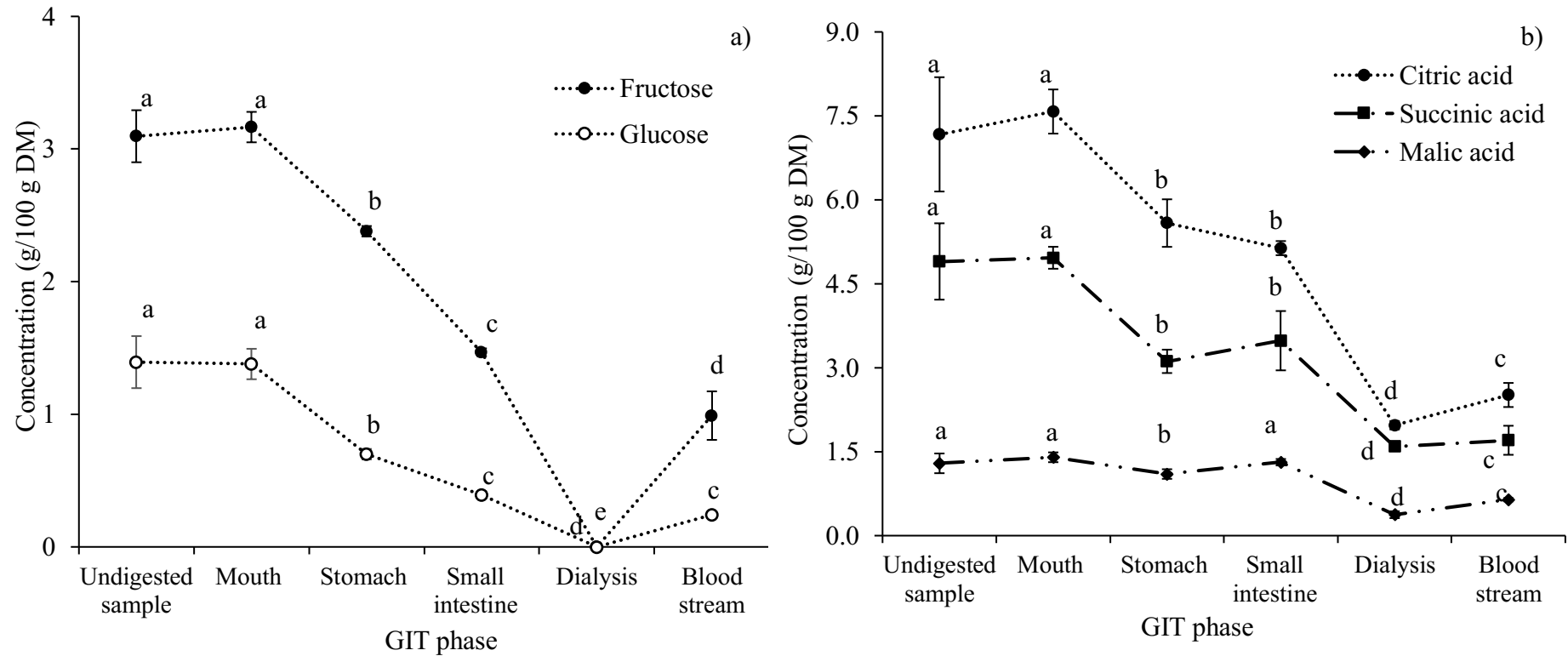


Figure 6.1. Concentrations of a) soluble sugars and b) organic acids obtained after each phase of the *in vitro* gastrointestinal tract simulation (GIT). DM: dry matter. Results are the means of three independent determinations \pm standard deviation. Values with different letters indicate significant differences between each GIT stage, as determined by one-way ANOVA test and Tukey's test ($p < 0.05$).

6.3.1.2. Phenolic compounds and antioxidant activity throughout the GIT phases

It has been reported that phenolic compounds can be released from food matrix in the upper area of GIT by direct solubilization in the intestinal liquids at physiological conditions (37 °C, pH 1-7.5) together with the action of digestive enzymes, being more accessible to exert their bioactivities and later becoming available for absorption (Costa et al., 2019; Vilas-Boas et al 2020). This behaviour was observed in this study when MPF was subjected to each phase of the GIT digestion, the total phenolic content (TPC) increased from 183.41 mg GAE/100 g DM (undigested sample) to 220.91 mg GAE/100 g DM at the intestinal phase ($p < 0.05$) (**Figure 6.2**), being significantly more accessible (126.91 %RI) for absorption in the bloodstream (85.57 ACI%) (**Table 6.2**). On the other hand, the antioxidant activity determined by DPPH ($r = 0.90$) and ABTS ($r = 0.95$) was correlated with the TPC and significantly increased from initial value of 42.49 to the highest value at stomach phase with 227.77 $\mu\text{M}/100$ g DM and 84.99 to 568.43 mg AEE/100 g DM at small intestine phase, respectively (**Figure 6.2**). These behaviours could be explained by polyphenols hydrophobic aromatic rings and hydrophilic hydroxyl units that can be linked to polysaccharides and some of them can exert antioxidant capacity once they are hydrolysed and released by enzymatic activity and pH value changes. (Quirós-Sauceda et al., 2011; Ullah et al., 2014). Similarly, some authors reported similar TPC, and antioxidant values increment, concluding the existence of a direct correlation with the release of certain families of phenolic compounds (hydroxycinnamic and hydroxybenzoic acids) from fibres. For example, tomato flour showed an increase in the TPC (RI 172.186%), DPPH (RI 134.35%) and ORAC (RI 121.65%) at the stomach phase (Coelho et al., 2021); mango by-products subjected to *in vitro* intestinal conditions showed an increase in TPC two times greater than the control (Bertha et al., 2019); apple pomace exhibited enhanced antioxidant activity upon *in vitro* intestinal digestion (from 78.2 to 400–500 $\mu\text{mol TE}/\text{mL}$ at the ileal phase) attributed in part to the increased release of individual polyphenols mainly flavanols, phenolic acids and dihydrochalcones (Liu et al., 2019). The redox properties of polyphenols from fruits are under increasing interest due to their role in the prevention of several chronic diseases associated with oxidative stress, such as cardiovascular diseases, cancers, type 2 diabetes, neurodegenerative diseases or osteoporosis (Cervantes-Paz et al., 2014; Dey et al., 2016). Some phenolics are also known for their potential inhibitory effects on obesity and their underlying molecular signalling mechanisms (Gómez and Martínez, 2018).

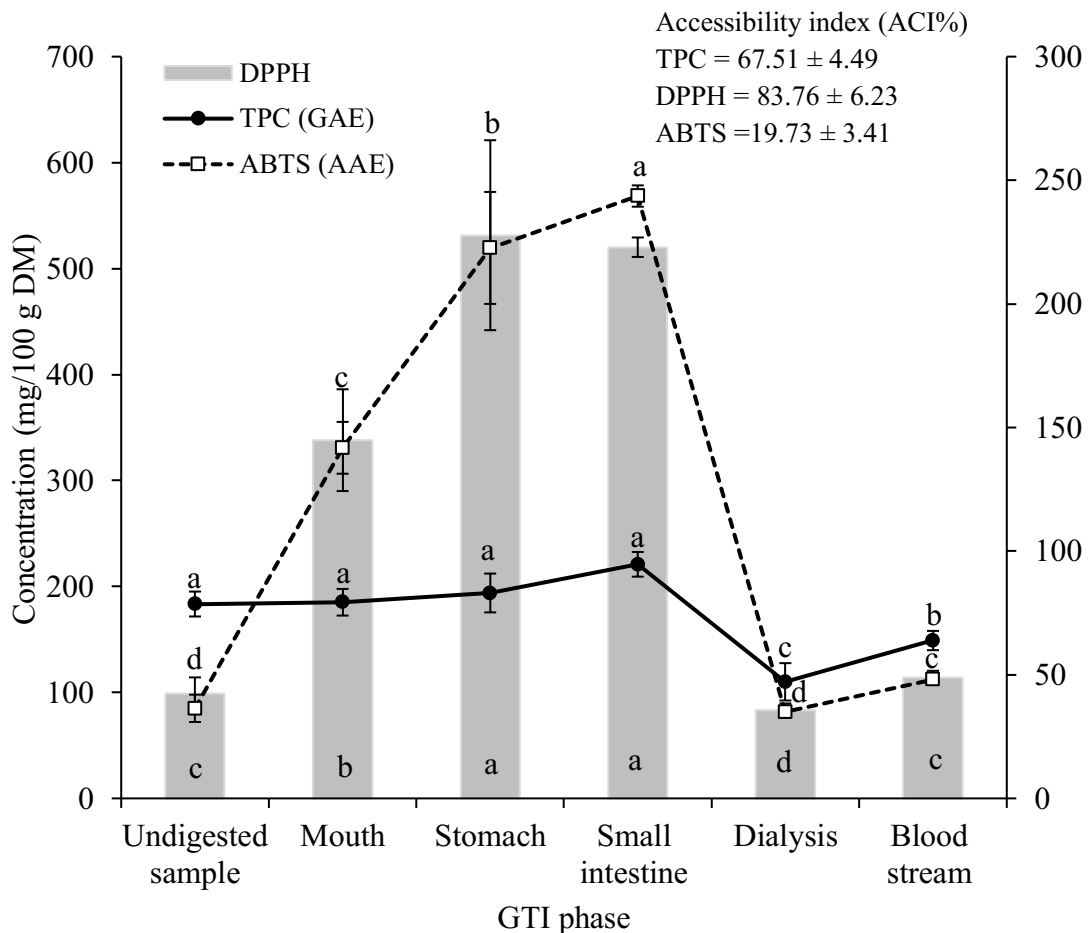


Figure 6.2. Total phenolic content (TPC) and antioxidant activity stability after each phase of the *in vitro* gastrointestinal tract (GIT). DM: dry matter; TPC: total phenolic content; GAE: gallic acid equivalents; AAE: ascorbic acid equivalents; TE: trolox equivalents. Results are the means of three independent determinations \pm standard deviation. Values with different letters indicate significant differences between each GID stage, as determined by one-way ANOVA test and Tukey's test ($p < 0.05$).

In this context, fourteen individual phenolic compounds were identified and at least nine were quantified before and after GIT digestion (**Table 6.3**), where luteolin-6-glycoside, tyrosol and chlorogenic acid were the most prominent compounds found in MPF (26.57, 19.25 and 18.95 mg/100 g DM, respectively). Only tyrosol showed a substantial increment ($p < 0.05$) until 73.81 mg/100 g DM at the intestinal phase, being more accessible for absorption in the blood stream and exert its antioxidant properties, reaching 97.29%. Phenolics such as chlorogenic, caffeic acid, and tyrosol have been associated with the prevention of cardiovascular diseases due to their capacity to inhibit low-density lipoproteins oxidation or platelet aggregation, especially cardio and neuro protective

Table 6.2. Recovery index (RI%) and Accessibility index (ACI%) of phenolic compounds throughout GIT simulation from melon peel flour (MPF).

Bioactive compound	Recovery index (RI %)					Accessibility index (ACI%)
	Mouth	Stomach	Small Intestinal	Dialysis	Blood stream	
Sugars						
Fructose	105.24 ± 1.42 ^a	76.73 ± 3.96 ^b	47.31 ± 0.93 ^c	UQ	33.75 ± 1.19 ^d	71.34 ± 1.83 ^b
Glucose	90.95 ± 10.51 ^a	50.81 ± 7.05 ^b	28.46 ± 3.51 ^c	UQ	17.79 ± 2.52 ^d	62.47 ± 2.86 ^b
Organic acids						
Citric acid	107.53 ± 19.62 ^a	78.86 ± 11.32 ^b	72.64 ± 10.73 ^b	27.85 ± 3.60 ^d	33.80 ± 6.79 ^d	46.30 ± 2.36 ^c
Malic acid	110.21 ± 20.63 ^a	86.07 ± 11.01 ^b	102.49 ± 10.89 ^a	28.97 ± 3.13 ^c	39.69 ± 5.50 ^c	38.64 ± 1.51 ^c
Succinic acid	102.49 ± 10.89 ^a	64.35 ± 8.98 ^b	71.78 ± 12.05 ^b	45.95 ± 1.38 ^d	17.33 ± 4.99 ^c	23.76 ± 4.34 ^{c,d}
Phenolics						
Gallic acid	102.40 ± 2.84 ^a	96.85 ± 2.19 ^{ab}	96.32 ± 2.43 ^b	20.17 ± 0.67 ^d	82.48 ± 2.10 ^c	85.62 ± 0.05 ^a
Hydroxytyrosol	11.22 ± 4.88 ^b	57.43 ± 13.62 ^a	UQ	UQ	UQ	UQ
Tyrosol	88.93 ± 11.09 ^b	88.36 ± 6.25 ^a	383.54 ± 12.51 ^a	18.27 ± 8.71 ^c	373.15 ± 13.37 ^a	97.29 ± 0.06 ^a
Chlorogenic acid	97.26 ± 0.63 ^a	86.80 ± 1.19 ^b	88.93 ± 1.52 ^b	UQ	78.37 ± 1.38 ^c	88.13 ± 0.05 ^a
4-hydroxybenzoic	103.25 ± 2.01 ^a	87.33 ± 2.81 ^b	85.35 ± 2.33 ^b	UQ	70.53 ± 2.27 ^c	82.63 ± 0.42 ^a
Caffeic acid	101.15 ± 0.52 ^a	100.82 ± 1.06 ^a	99.32 ± 9.34 ^a	UQ	84.38 ± 9.18 ^b	84.88 ± 1.20 ^a
Luteolin-6-glycoside	104.25 ± 3.38 ^a	100.44 ± 2.88 ^a	69.07 ± 1.60 ^b	59.88 ± 1.08 ^c	9.19 ± 1.74 ^d	13.28 ± 2.26 ^f
<i>p</i> -coumaric acid	111.84 ± 11.14 ^a	94.18 ± 10.30 ^b	29.40 ± 10.31 ^c	UQ	15.22 ± 10.72 ^d	47.95 ± 16.78 ^c
Ferulic acid	101.29 ± 0.44 ^a	98.38 ± 1.56 ^a	92.95 ± 1.55 ^b	UQ	77.67 ± 1.40 ^c	83.56 ± 0.12 ^a
TPC (mg GAE/100 g DM)	106.34 ± 7.22 ^{ab}	111.36 ± 10.53 ^a	126.91 ± 6.69 ^a	63.20 ± 10.12 ^c	85.57 ± 5.23 ^b	67.51 ± 4.49 ^b

UQ: under quantification limit. All determinations were carried out in triplicate and results are shown as mean value ± standard deviation. Results are the means of three independent determinations ± standard deviation. Values with different letters in the same line to RI% indicate significant differences between each GIT stage and in the same column to ACI% indicate significant differences of accessibility as determined by one-way ANOVA test and Tukey's test ($p < 0.05$).

Table 6.3. Main phenolics identified and quantified by HPLC-DAD during the *in vitro* gastrointestinal tract simulation of melon peel flour (MPF).

No.	Phenolic compound	Gastrointestinal phase (concentration mg/100 g DM)					
		Undigested sample	Mouth	Stomach	Small Intestinal	Dialysis	Blood stream
1	Gallic acid	14.45 ± 0.34 ^a	14.79 ± 0.26 ^a	13.99 ± 0.20 ^b	13.91 ± 0.05 ^b	2.91 ± 0.05 ^d	11.91 ± 0.08 ^c
2	Hydroxytyrosol	2.20 ± 0.09 ^a	0.24 ± 0.10 ^c	1.26 ± 0.27 ^b	UQ	UQ	UQ
3	Tyrosol	19.25 ± 0.33 ^a	17.11 ± 2.03 ^a	17.01 ± 1.22 ^b	73.81 ± 1.64 ^b	3.51 ± 1.64 ^d	71.81 ± 1.94 ^c
4	Chlorogenic acid	18.95 ± 0.25 ^a	18.43 ± 0.30 ^b	16.44 ± 0.18 ^c	16.84 ± 0.18 ^c	UQ	14.84 ± 0.08 ^d
5	4-hydroxybenzoic	13.50 ± 0.10 ^a	13.94 ± 0.17 ^a	11.79 ± 0.18 ^b	11.52 ± 0.28 ^b	UQ	9.52 ± 0.28 ^c
6	Caffeic acid	13.39 ± 0.15 ^{ab}	13.54 ± 0.17 ^a	13.50 ± 0.01 ^a	13.29 ± 1.10 ^{ab}	UQ	11.29 ± 1.10 ^b
7	Luteolin-6-glycoside	26.57 ± 0.54 ^a	27.69 ± 0.94 ^a	26.67 ± 0.23 ^a	18.34 ± 0.07 ^b	15.91 ± 0.41 ^c	2.44 ± 0.42 ^d
8	Luteolin derivative	NQ	NQ	NQ	NQ	NQ	NQ
9	Luteolin derivative	NQ	NQ	NQ	NQ	NQ	NQ
10	7-hydroxycoumarin	NQ	NQ	NQ	NQ	NQ	NQ
11	<i>p</i> -Coumaric acid	14.14 ± 0.85 ^a	15.79 ± 1.49 ^a	13.37 ± 1.59 ^a	4.18 ± 1.59 ^b	UQ	2.18 ± 1.59 ^b
12	Luteolin-7-glycoside	NQ	NQ	NQ	NQ	NQ	NQ
13	Ferulic acid	13.09 ± 0.13 ^{ab}	13.26 ± 0.18 ^a	16.42 ± 6.12 ^b	12.17 ± 0.09 ^c	UQ	10.17 ± 0.09 ^d
14	Apigenin	NQ	NQ	NQ	NQ	NQ	NQ
Total by HPLC		134.39 ± 1.16	134.79 ± 5.01	118.66 ± 9.18	163.67 ± 3.09	22.33 ± 1.83	134.16 ± 3.04
TPC (mg GAE/100 g DM)		183.41 ± 11.77 ^{ab}	185.11 ± 12.57 ^{ab}	193.85 ± 18.32 ^a	220.1 ± 11.64 ^a	110.00 ± 17.61 ^c	148.95 ± 9.10 ^b

DM: dry matter; UQ: under quantification limit; NQ: non-quantified. Results are the means of three independent determinations ± standard deviation. Values with different letters indicate significant differences between each GID stage, as determined by one-way ANOVA test and Tukey's test ($p < 0.05$).

effects, anti-osteoporosis, anti-inflammatory, anti-diabetic capacities have been associated to tyrosol (Thielmann et al., 2017; Nunes et al., 2018). Similar behaviours in the release of phenolic compounds were reported for bamboo leaves hydroxycinnamic acids, showing an increase of neochlorogenic, chlorogenic, cryptochlorogenic acids and isoorientin at gastric digestion phase, 1.88%, 17.16%, 12.91% and 5.47% higher than the control, respectively. DPPH radical scavenging activity and FRAP increased by 76.61% and 2.97% compared with the control, respectively (Ma et al., 2020). The TPC and antioxidant increment of MPF could be justified with the long interaction time of the material with the intestinal fluids and digestive enzymes mainly composed by proteolytic, lipolytic, amylolytic, and nucleic acid splitting enzymes, leading a release of polyphenols associated to the plant matrix (Coelho et al., 2021). Moreover, other compounds such as caffeic, gallic and ferulic acids presented stable RI% (84.38, 82.48 and 77.67%, respectively) and ACI% (84.88, 85.62 and 83.57%, respectively) (**Table 6.2**). The present findings could suggest that most of the melon flour phenolics slightly decreased throughout the GIT process, but keeping stable percentages of ACI (80-90%). On the other hand, the phenolics that were released during gastric and intestinal phases may be due to linkages breakdown between structural carbohydrates and/or proteins with polyphenols, improving the TPC and subsequently the antioxidant activity of MPF, which could promote an antioxidant environment and therefore physiological protection.

6.3.2. Human gut microbiota fermentation

6.3.2.1. Evaluation of the gut microbiota profile groups

The MPF sample after GIT process was freeze-dried and subjected to human faeces fermentation during 48 h to study the effect on the human microbiota. To understand the growth behaviour of the microorganisms and their metabolic activities modulation during fermentation, samples were taken at 0, 12, 24 and 48 h and analysed. In the **Table 6.4** are depicted the compositional average of copy numbers obtained by PCR real time of the main groups of human gut microbiota as described by Madureira et al. (2016). Three of the four dominant phyla in the human gut were evaluated, viz. *Firmicutes*, *Bacteroidetes* and *Actinobacteria*. Numbers were in accordance with the ones found in healthy human volunteers' faeces, e. g., *Lactobacillus* spp. which is usually found in lower numbers in normal gut microbiota (De Carvalho et al., 2019). In **Figure 6.3** are shown the relative differences percentages between the microbiota groups of the tested melon sample against control throughout the faecal fermentation at 12, 24 and 48 h of fermentation. Fructooligosaccharides

(FOS) were used as positive control, which is a well-known and recognized natural polymer with prebiotic effect (Samanta et al., 2012). As expected, FOS promoted the growth of all phyla analysed, while the MPF also showed a positive effect on *Lactobacillus* spp > *Bifidobacterium* > *Prevotella* spp. and relative lower effect on *Clostridium leptum*. Notably, *Lactobacillus* spp. and *Bifidobacterium* are two of most abundant bacteria living in the gut. These particular bacteria are vital for the health and well-being of their host, having a helpful function in the reduction of disease or in the maintenance of the immunological activity, energy consumption and even in the brain activity (Dinan and Cryan, 2013; Mota de Carvalho et al., 2018). These findings could suggest that MPF may possess prebiotic effect, promoting the growth of the probiotic bacteria present in the donor samples. Moreover, in a healthy adult, the Gram-positive *Firmicutes* (*Clostridium leptum* and *Lactobacillus* spp.) and the Gram-negative *Bacteroidetes* (*Bacteroides* spp. and *Prevotella* spp.) are the main phyla in the human gut microbiome (Abenavoli et al., 2019). During the time of fermentation, high percentage values were found for *Lactobacillus* spp. (61%) and *Prevotella* spp. (10%) after 12 h for MPF, while in the end of faecal fermentation statistical differences were noted ($p < 0.05$) after 24 and 48 h, however significant values were still observed on the growth of these beneficial bacteria with 35% and 3% after 48 h, respectively, especially for *Lactobacillus* without statistical differences ($p < 0.05$) with respect to the FOS (36%). This result was expected due to the high content of dietary fibre of melon peels. Previous studies showed that diets low in fat and high in dietary fibre were associated with higher *Firmicutes* percentages (Holscher, 2020).

Table 6.4. Faecal microbiota composition of volunteer sample donors.

Division (genus)	Number of copies (n=5)
<i>Universal</i>	7.24 ± 0.9
<i>Firmicutes</i>	6.48 ± 1.3
<i>Clostridium leptum</i>	5.40 ± 0.4
<i>Lactobacillus</i> spp.	1.90 ± 0.6
<i>Bacteroidetes</i>	6.94 ± 0.9
<i>Prevotella</i> spp.	4.27 ± 1.6
<i>Actinobacteria</i>	
<i>Bifidobacterium</i> spp.	3.22 ± 1.0
F:B ratio	0.93 ± 1.5

Values are expressed as mean ± of standard deviation and expressed as log₁₀ 16S rRNA copies per 20 ng of DNA.

On the other hand, the relative abundance between *Firmicutes* and *Bacteroidetes* is an important parameter to be analysed. Naturally, healthy people display a nearly 1:1 ratio of

Firmicutes to *Bacteroidetes* (F:B) and its increase (e.g., to 20:1) or decrease have been associated with obesity or weight loss (Karlsson et al., 2013; Giuliani et al., 2019). In this study, the F:B ratio for FOS (1.17) was statistically lower ($p < 0.05$) than the MPF (1.80) during the first 12 h of fermentation and a slight decrease was exhibited between the next 24 and 48 h, reaching very normal levels and no statistical differences ($p < 0.05$) with regard of the FOS. In general, FOS and MPF samples maintained the ratio of F:B stable and near to one (**Figure 6.4**). *Bacteroides* and *Prevotella* are the main genera found belonging to the Bacteroidia class and *Bacteroidetes* phylum. Both genera have been reported with reciprocal patterns of abundance. *Bacteroides* correlated well with consumption of choline, fats and amino acids, while *Prevotella* correlated with the composition of carbohydrates (Connolly et al., 2010; Gutierrez-Sarmiento et al., 2020). Several studies have suggested that *Prevotella* spp. is a microbial group associated with beneficial gut microbiota particularly in the improvement of glucose metabolism (Saffouri et al., 2019). The related bacterial growth in number of DNA copies during the fermentative process is shown in **Figure 6.5**. The positive control showed the highest number of copies, indicating the proliferation for *Bifidobacterium*, *Lactobacillus* spp, *Prevotella* spp and *Clostridium leptum* followed by the MPF, which show slightly higher differences compared to the negative control, following similar behaviours between 24 and 48 h. In the case of the negative control, it seems that no bacterial growth occurred after the first 12 h, while FOS control seemed to continue the growth of all phyla, which was to be expected. Results showed that melon flour and FOS did not promote the *Clostridium leptum* growth (**Figure 6.5**). The growth for positive control was maintained until 12 h of fermentation and then reduced after 48 h, suggesting that *Clostridium leptum* did not use FOS as energy source. Therefore, MPF sample presented stable F:B ratio values similar to the reported for pineapple flour by-products accounting from 1.25 to 2 (Campos et al., 2020c), confirming the possibility that melon sample was used as carbon source by the faecal bacteria, which means high content of potential beneficial microbiota. The digested melon flour allowed to promote the growth of phyla of good microbiota, highlighting its potential employment as functional ingredient with prebiotic health-promoting effect.

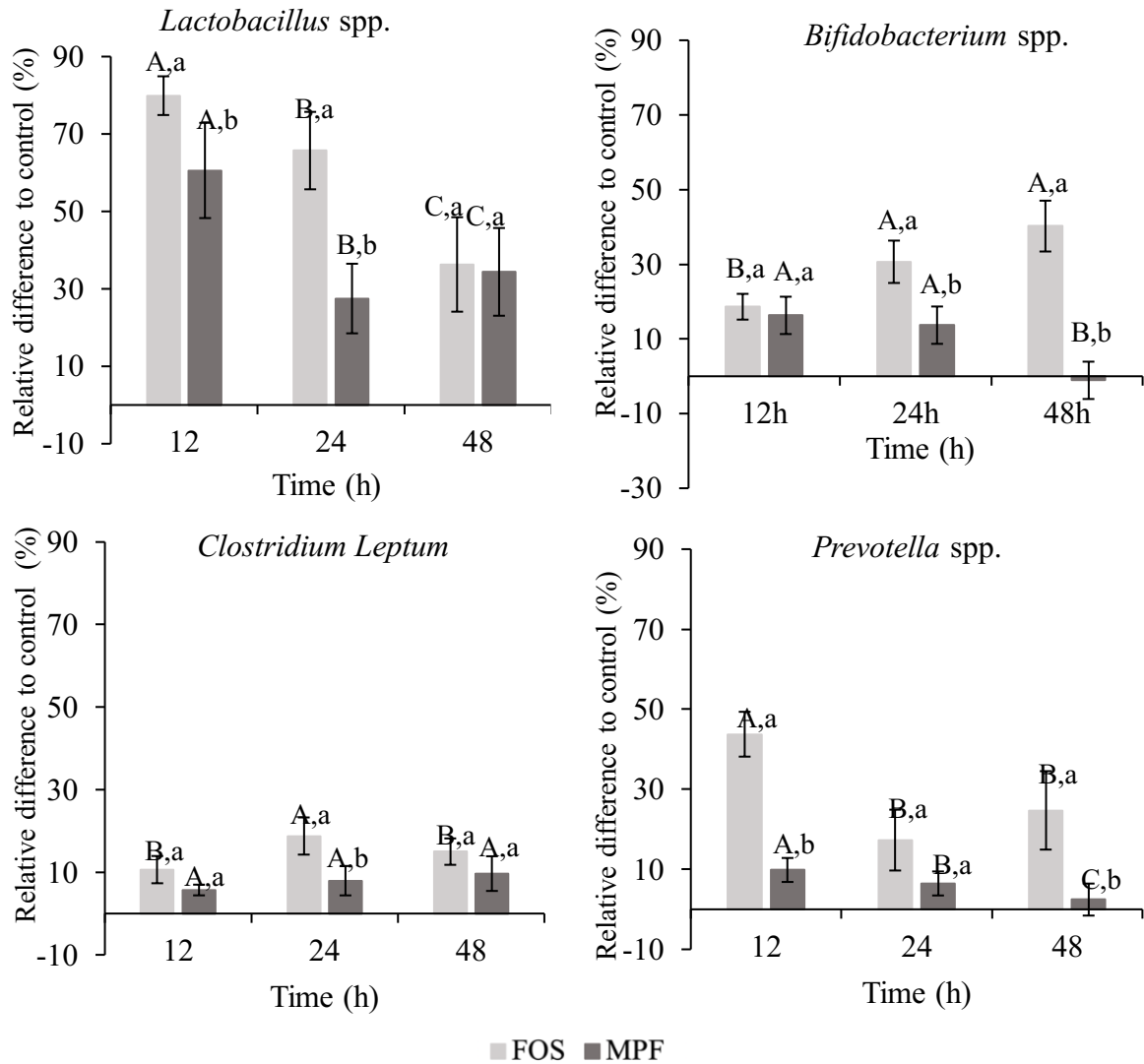


Figure 6.3. Relative differences to negative control throughout *in vitro* fecal fermentation. FOS: positive control (2% w/v); MPF: melon peel flour (2% w/v). Data is presented in percentage during fermentation time. Results are the means of five independent determinations \pm standard deviation. Different letters indicate significant differences ($p < 0.05$). The capital letters indicate the differences among the time (12, 24 and 48 h) for the same sample for each microbial genus and small letters indicate the differences between samples (FOS and MPF) for the same microbial genus in same point of time.

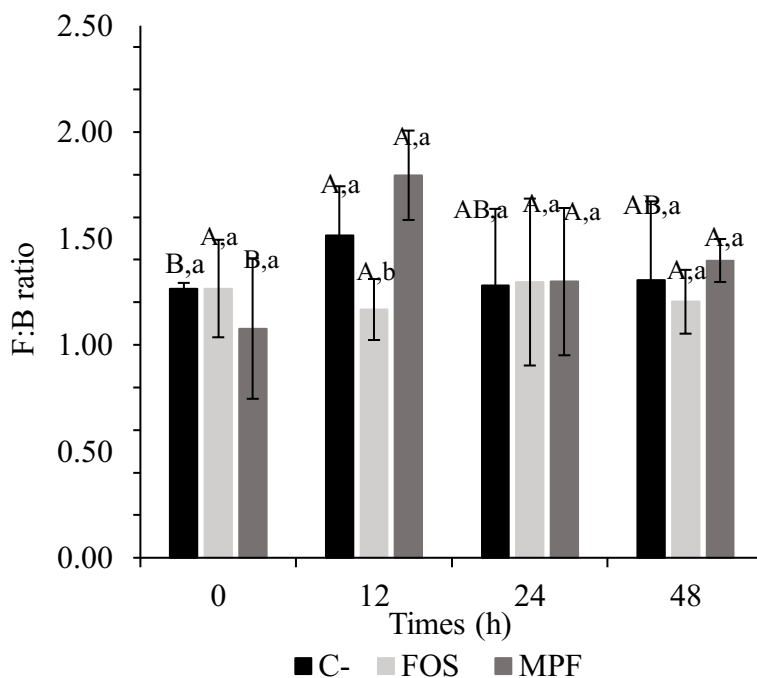


Figure 6.4. *Firmicutes*:*Bacteroidetes* (F:B) ratio evaluation during fermentation with human faeces. FOS: positive control (2% w/v); MPF: melon peel flour (2% w/v). Data is presented in percentage during fermentation time. Results are the means of five independent determinations \pm standard deviation. Different letters indicate significant differences ($p < 0.05$). The capital letters indicate the differences among the time (12, 24 and 48 h) for the same sample for each microbial genus and, small letters indicate the differences between samples (FOS and MPF) for the same microbial genus in same time point.

6.3.2.2. Short-chain fatty acids (SCFAs) during *in vitro* faecal fermentation

The changes in the concentration of SCFAs throughout the fermentation process of MPF (2%) negative control (C-) and FOS (2%) with human faeces analysed by HPLC are illustrated in **Figure 6.6a**. Five organic acids were identified during the fermentation of the samples, such as succinate, acetate, propionate, butyric, and lactic acids. Acetate, succinate, and propionate were the organic acids in higher concentrations for MPF and FOS samples. Lactate and acetate were presented in very lower concentrations before fermentation, which means that they were produced after 12 h of fermentation through the metabolization of carbohydrates. Acetate presented a gradual increase statistically significant ($p < 0.05$) between 0 and 24 h, followed by a decrease until the 48 h. The SCFA are generally produced by intestinal bacteria through fermentation of non-digestible carbohydrates. Acetate, propionate, butyrate and gas (H_2 and CO_2) are the main bacteria fermentative end-products from the hydrolysis of complex carbohydrates (Kawabata et al., 2019), thus, indicating a positive fermentative process on the MPF and FOS samples by the colon bacteria. The changes of the SCFAs concentrations

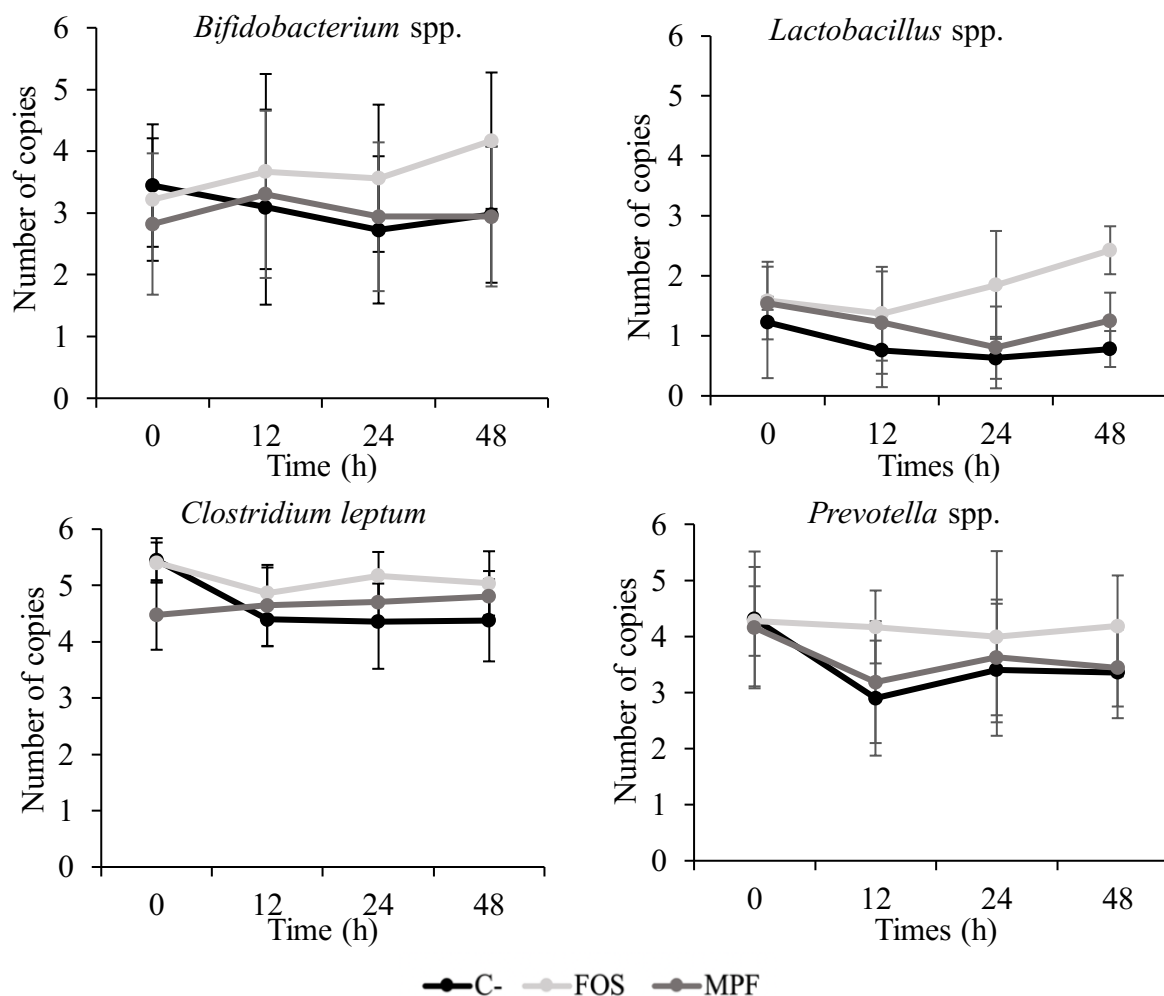


Figure 6.5. Number of DNA copies measured by PCR from the *in vitro* fecal fermentation of melon peel flour (MPF), positive (FOS: 2% w/v) and negative controls (C-). Results are the means of five determinations \pm standard deviation.

occurred along GIT, with the highest concentration near to the colon, which is the zone of the GIT with the biggest concentration of microbes and lower concentrations in the distal colon (Aoe et al., 2019). Moreover, the SCFAs concentration values found in the FOS were strongly related with the decrease of pH values and slightly correlated with the MPF, while for negative control (C-) the pH was increased (**Figure 6.6b**). An increase of SCFAs production within gut microbiota reduces luminal pH, which helps to prevent colonization and infections from pathogenic bacteria (Holscher, 2020). Acetate was the SCFA with the highest concentration with 2.76 and 1.50 mg/mL, after 12 h of fermentation for FOS and MPF ($p < 0.05$), respectively, being in concordance with the reported values for pineapple peel flour (1.85 mg/mL) and FOS (2.30 mg/mL) and for olive pomace (2.20 mg/mL) and FOS (2.30 mg/mL) (Campos et al., 2020a; Ribeiro et al., 2021), but lower from the reported from olive pâtre (3.01

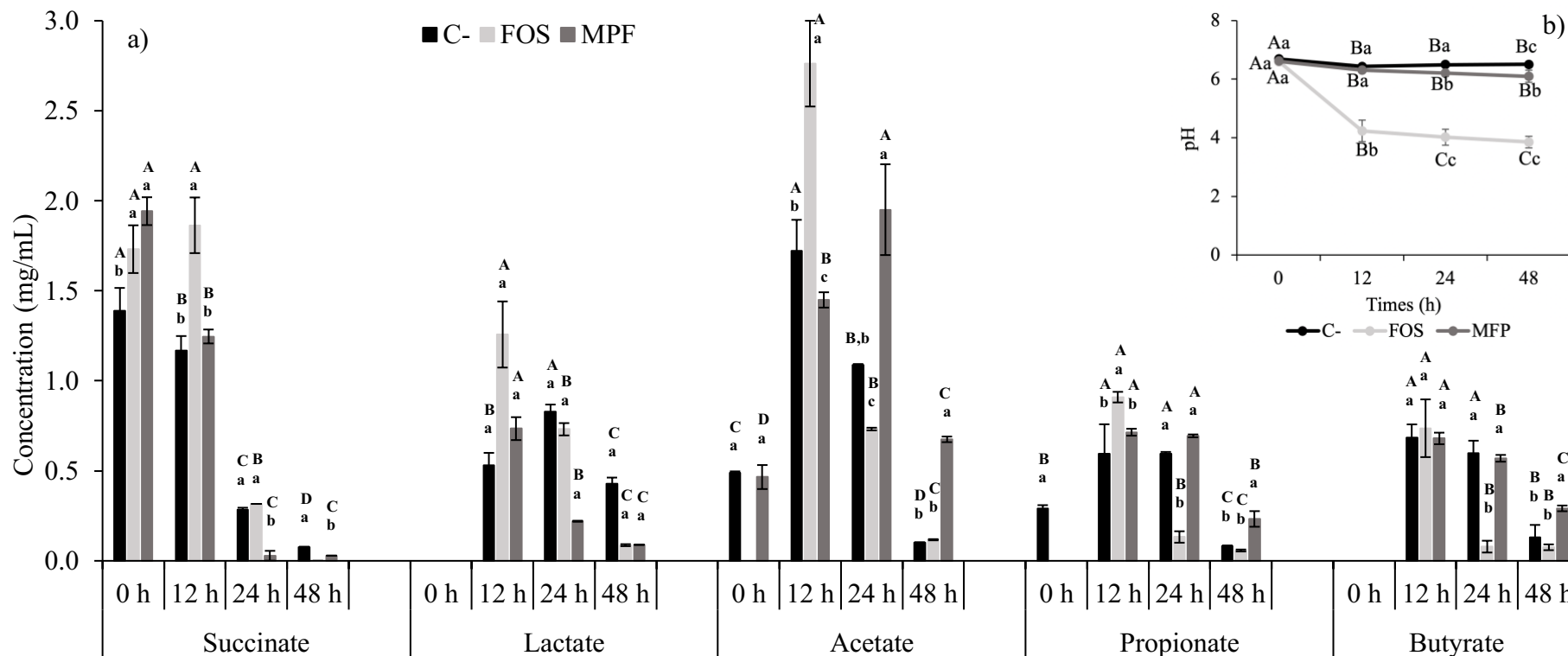


Figure 6.6. a) Concentration variation of organic acids and b) pH through the *in vitro* faecal fermentation. C-: negative control; FOS: positive control (2% w/v); MPF: melon peel flour (2% w/v). Results are the means of five determinations \pm standard deviation. Results are the means of five independent determinations \pm standard deviation. Different letters indicate significant differences ($p < 0.05$). The capital letters indicate the differences among the time (0, 12, 24 and 48 h) for the same sample for each microbial genus and, small letters indicate the differences between samples (control, FOS and MPF) for the same microbial genus at the same time point.

mg/mL) and pomegranate (3.32 mg/mL) (Giuliani et al., 2019). In this regard, acetate is the most prominent SCFA, which has been shown to cross the blood-brain barrier and despite acetate be an essential co-factor/metabolite for the growth of bacteria, it provides the capacity of bifidobacteria to inhibit enteropathogens and reduce the appetite of the host through the interaction with the central nervous system (Ríos-Cavián et al., 2016; De Carvalho et al., 2019). The SCFAs are volatile fatty acids produced by the gut microbiota in the colon as fermentation products from food components that are unabsorbed/undigested in the small intestine, which can be produced during growth phases, be present in medium composition (presence and absence of amino acids) and be produced by metabolic cross-feeding (e.g., consumption of lactate or formate to produce acetate) (Fu et al., 2019; Aoe et al., 2019). As previously stated in section 6.3.1.1, succinate was present in the MPF even before the fermentation started and a significant decrease was observed ($p < 0.05$) during fermentation time. This could suggest that the microbiota metabolized this organic acid by the different pathways for propionate and energy production by some strains present in the human gut microbiota (Kawabata et al., 2019; Ikeyama et al., 2020). This trend was observed when succinate concentration at 24 h was reduced to 0.03 mg/mL from 1.94 mg/mL at 0 h of fermentation. Also, propionate increased, reaching concentrations of 0.70 mg/mL at 12 h and 0.69 mg/mL at 24 h of fermentation ($P > 0.05$). Careful attention must be given to the higher concentration of lactate, since this SCFA is present at in high concentrations in faeces from individuals who have undergone gut resections (short bowel syndrome) or that suffer from ulcerative colitis (Kowlgi and Chhabra, 2015; Madureira et al., 2016). Nevertheless, the abundance of this fatty acid is positive as an intermediate to produce butyrate, a beneficial fatty acid. Butyrate is the key energy source of colonocytes and enterocytes. Propionate can be employed through conversion into glucose by intestinal gluconeogenesis or diffuse into the portal vein to be consumed as substrate for hepatic gluconeogenesis (Moco et al., 2012). Butyrate and propionate derive exclusively from bacterial metabolism, but acetate could also have an endogenous origin (Saffouri et al., 2019). Propionate and butyrate were the acids with similar expression profiles after 24 and 48 h. The MPF enhanced the production of the acetate, propionate, and butyrate. In this regard, the acetate-to-propionate ratio for FOS and MPF correspond to 3 and 2.10, respectively, at 12 h, such values decreased along fermentation process and were in concordance to the reported for pineapple flour and olive pomace (Campos et al 2020a; Ribeiro et al. 2021). Low acetate-to-propionate ratios have been proposed as a positive indicator of a hypolipidemic effect, resulting from an inhibited biosynthesis of cholesterol and fatty acids in liver, which finally results in

decreased blood lipid level (Gullón et al., 2014). Therefore, the *in vitro* fermentation with human faecal inoculum in the presence of melon by-product flours exhibited interesting similar SCFAs profiles when compared to the FOS, stimulating the production of the beneficial compounds, such as acetate, propionate, and butyrate. The production of these SCFAs could exert health benefits not only in the colon and gut microbiota, but also in other organs, which could highlight melon peel by-products as health-promoting ingredients.

6.3.2.3. Phenolic compounds throughout *in vitro* faecal fermentation

The individual phenolic compounds were evaluated by HPLC during the MPF fermentation at 0, 12, 24 and 48 h (**Table 6.5**). Results, in general, allowed the identification of seven phenolics and at least four were quantified, such as gallic, chlorogenic, caffeic and ferulic acids. After 12 h of fermentation, the content of chlorogenic and caffeic acids was significantly increased ($p < 0.05$) and kept constant until 48 h, while the appearance of ferulic acid was detected after 24 and 48 h concerning the initial time. These phenolic compounds are hydroxycinnamic acids, which generally are linked to insoluble fibre and possess antioxidant properties, thus the human microbiota was able to break the linkage between fibre and other molecules, leading to the release of these bioactive compounds (Quirós-Sauceda et al., 2011). For example, caffeic and ferulic acids are associated to the hemicellulose-lignin complex polymers of plants and could be released by hydrolytic enzymes (cellulase and xylanases), which gut bacteria can produce during their growth. In our previous reported work (Gómez-García et al., 2021b), the MPF was found to be constituted mainly by insoluble dietary fibre (40%), which in turn is composed by cellulose, hemicellulose, and lignin, and after its alkaline hydrolysis, caffeic and ferulic acids were liberated by the breakdown of hemicellulose-lignin complex, confirming the presence of both phenolics within the MPF sample after GIT process and then possibly liberated during the *in vitro* fermentation by gut microbiota. In this context, monitoring melon phenolics throughout the fermentative process is an important task because it could provide different insights to better understand their growth-promoting effect of certain bacteria. In this regard, polyphenols have been reported with the capability to alter the composition of microbial bacteria in the gut, due to their ability to inhibit the growth of specific bacteria, especially pathogenic, such as *E. coli*, *S. aureus* and *C. albicans*, while beneficial bacteria are stimulated and are not affected by polyphenols (Moco et al., 2012). For example, berry polyphenols, especially hydroxybenzoic (gallic, vanillic and *p*-hydroxybenzoic acids), hydroxycinnamic (caffeic and ferulic acids) and flavonoids (anthocyanins) have been reported to exhibit potential antimicrobial effect on

Table 6.5. Phenolic compounds identified and quantified by HPLC throughout *in vitro* faecal fermentation of melon peel flour (MPF) subjected previously to *in vitro* GIT digestion.

No.	Phenolic compound (mg/100 g DM)	Time (h)			
		0	12	24	48
1	Gallic acid	3.89 ± 0.2 ^a	ND	ND	ND
2	Hydroxytyrosol	UD	UD	ND	ND
3	Chlorogenic acid	4.81 ± 0.1 ^c	7.26 ± 0.1 ^a	6.29 ± 0.1 ^b	5.55 ± 0.9 ^b
4	4-hydroxybenzoic acid	UD	ND	ND	ND
5	Caffeic acid	3.82 ± 0.1 ^d	4.38 ± 0.1 ^a	4.21 ± 0.1 ^b	4.03 ± 0.6 ^c
6	Luteolin-6-glycoside	9.09 ± 2.4 ^a	4.69 ± 0.3 ^b	ND	ND
7	Ferulic acid	ND	ND	3.77 ± 0.2 ^a	3.35 ± 0.1 ^b
Total by HPLC		21.61 ± 2.0	20.33 ± 0.3	14.26 ± 0.1	12.94 ± 1.5

Results are the means of five determinations ± standard deviation. UD: under detection limit; ND: non-detected. Results are the means of five independent determinations ± standard deviation. Values with different letters indicate significant differences in fermentation time-points, as determined by one-way ANOVA test and Tukey's test ($p < 0.05$).

human intestinal pathogens, showing better inhibitory effect in Gram-negative than Gram-positive bacteria particularly, *Staphylococcus* and *Salmonella* were the most sensitive to the berries, while showed an increase in beneficial bacteria such as *Roseburia*, *Bacteroides*, *Prevotella* and *Bifidobacterium* (Lavefve et al., 2019). Ribeiro et al. (2021) reported the health promotion potential on the gut microbiota of phenolics (caffeic, *p*-coumaric and ferulic acids, among others) and insoluble dietary fibre (46%) from olive pomace by-products as antioxidant, antimicrobial and prebiotic ingredient, finding from an *in vitro* faecal fermentation a positive effect in *Prevotella* spp./*Bacteroides* spp. bacteria and the production of SCFA, mainly acetate > butyrate > propionate. Catarino et al. (2021) evaluated the prebiotic potential of phlorotannins a type of polyphenols from red algae, reporting a positive effect on gut microbiota growth, especially on the phyla *Firmicutes* and *Bacteroidetes*, which are representative of a healthy microbiota and the production of butyrate > propionate > acetate. These findings on melon by-products, especially due to their high content of insoluble dietary fibre with phenolic compounds, could suggest a positive effect on human intestinal microbiota mainly promoting specific bacteria groups such as *Lactobacillus* and *Bifidobacterium*.

6.4. Conclusion

Melon by-products from fruit processing industries characterized by the co-presence of polysaccharides and phenolic compounds, were evaluated for the first time for their changes during GIT simulation and after interaction with human gut microbiota. The results showed that the *in vitro* simulated digestion had a significative effect on phenolic compound and antioxidant properties of MPF, however good accessibility index was exhibited in TPC (67.51%), ABTS (19.73%) and DPPH (83.76%), which demonstrate the great stability of those compounds and the possibility to exert their health-related benefits. The digested melon flour was used by human gut microbiota, assuring the maintenance and enhancement of the beneficial bacteria, being *Lactobacillus* spp. and *Bifidobacterium* spp. with the better growth results probably due to the high content of dietary fibre and simple sugars. Moreover, these growth behaviours could be correlated due to the production of SCFA, especially acetate > propionate > butyrate, which showed a closely equal profile to FOS during the *in vitro* faecal fermentation. Finally, caffeic and ferulic acids were the most relevant phenolics identified after fermentation, which also could have a positive effect on gut microbiota. The phenolic and antioxidant profiles together with the positive effects exhibited on gut microbiota of melon by-products could remark their potential applications as functional flour ingredient with health-enhancing benefits.

PART III – Industrial interest value-added ingredients

CHAPTER 7 – Valorisation of melon (*Cucumis melo* L. *inodorus* cultivar) industrial by-products as rich sources of high-methoxyl pectin: Improvement of hot-acid extraction and performance properties

Ricardo Gómez-García^{a,b}, Sérgio C. Sousa^a, Débora A. Campos^a, Cristóbal N. Aguilar^b,
Ana R. Madureira^a and Manuela Pintado^{a*}

^a*Universidade Católica Portuguesa, CBQF – Centro de Biotecnologia e Química Fina – Laboratório Associado, Escola Superior de Biotecnologia, Rua Diogo Botelho 1327, 42169-005 Porto, Portugal*

^b*BBG-DIA. Bioprocesses and Bioproducts Group. Food Research Department, School of Chemistry, Autonomous University of Coahuila, Saltillo, Coahuila, Mexico.*

*This chapter has been submitted:
Journal of Carbohydrate Polymers*

Abstract

Melon peels are by-products highly produced by the fruit processing industry, requiring a suitable management because they represent rich resources of value-added molecules such as pectin. In this study, the yields of melon pectin were higher when extracted with citric acid (PCA) (34%) followed by tartaric acid (PTA) (31%) and hydrochloric acid (PHCl) (20%). The extracted pectins were characterized by a degree of methyl esterification from 65 to 87%, a galacturonic acid content from 60 to 70% and a molecular weight from 70 to 146 kDa. Pectins PHCl, PCA and PTA showed emulsifying capacities of 41.04, 37.71 and 34.55%, respectively, with high stability at 80 °C. Gels produced with 1% (w/v) of *inodorus* melon pectins were stable at pH 3.5, Ca²⁺ 10 mM and 65% of sucrose, showing a higher elastic profile (G') than the viscous (G''). The present research strongly highlights melon by-products as suitable alternative for pectin obtention, which could respond its increasing demand as food and nutraceutical functional ingredient.

Keywords: Melon by-products, high-methoxyl pectin, circular economy, resource recovery, functional ingredients, rheology, emulsifying and gelling properties.

7.1. Introduction

Nowadays, industrial food by-products represent a social concern, an economic malfunction and an environmental issue (Martin-Rios, Hofmann, and Mackenzie, 2021). Such by-products are poorly managed, causing wastage and consequently emitting harmful greenhouse gas (GHG) emissions, being the food processing industry responsible for 26% of such GHG (Esparza et al., 2020). Based on these alarming concerns, in certain regions like Europe there are clear indications of a shift away from landfilling and animal feeding towards efficient waste management and valorisation approaches (Carmona-Cabello et al., 2020). Therefore, food waste management plays an important role in the food system due to food losses and wastes, which are highly produced globally (ca. 1.3 billion tonnes), and the pressure of EU to reduce them up to 50% until 2030. So, taking the increasing implementation of circular economy in agro-food sector considering food by-products as resources (new raw materials), there is being promoting for their reincorporation into the food value chain as well as into the industrial economy (Trigo et al., 2019). The circular economy has been focused on the revaluation of food by-products, which can be traded and employed as primary raw materials against traditional extractive resources, highlighting certain bioactive compounds with functional properties and potential industrial applications (Gómez-García et al., 2021a). The employment of these materials as novel resources could contribute not only to reduce food wastage and its environmental impacts, but also to prevent the depletion of natural resources (Imbert, 2017; Torres-Leon et al., 2018) and to bring value to the economy. However, because these food by-products are still being discarded by the food industry, research and biotechnological efforts have been increased in order to face the challenges related with food by-product management and valorisation through the application of environmental-friendly and eco-efficient methodologies, which could make the treatment and recycling systems economically attractive for the food industry (Teigiserova et al, 2021). Local conversion or treatment within industrial facilities together with tailored solutions can further reduce transportation and disposal costs, while sustainability and viability may increase (Campos et al., 2020c).

On the other hand, fruit processing industries such as melon (*Cucumis melo* L.) generally produce a significant amount of melon by-products, resulting from the production of commercial foodstuffs specially, juices, dehydrated fruit, jams, among other products. Such commercial activities also lead an overaccumulation of melon peels (by-products)

with an estimative of 8 to 20 million tonnes of melon by-products *per* year, which despite their richness in nutritional and biofunctional compounds are still rejected and disposed in landfills (Rolim, Seabra, and de Macedo, 2019; Gómez-García et al., 2020). For such reasons, research studies are needed to use melon by-products as sources of natural compounds (proteins and dietary fibres) specially to recover commercially valuable ingredients (generally recognized as safe; GRAS), such as pectins that could be exploited/used by different industries (Mellinas, Ramos, Jiménez, and Garrigós, 2020). In this regard, pectin polymer is a complex heteropolysaccharide present in the peels and skins of many fruits (apple, citrus peel, beet root) (Banerjee et al., 2018). Traditionally, pectin has been used in food industry as a thickener, emulsifier, texturizer, stabilizer, gelling agent, confectionery and fat substitute in spreads, ice-cream and meat products (Thirugnanasambandham et al., 2014; Minjares-Fuentes et al., 2014). Also, this polysaccharide has been associated with human health benefits, it was used to prevent or control high blood cholesterol level, heart disease, hypoglycemia, gallstones, cancer or stimulate macrophage induction to prevent infection (Zhang et al., 2015; Thirugnanasambandham et al., 2014). Pectin polymer is constituted by *D*-galacturonic acid (GalA) and monosaccharides, including *L*-rhamnose, *L*-arabinose, *D*-galactose, and *D*-xylose. In addition, GalA residues can be partially methyl esterified, this characteristic is known as the degree of methyl esterification (DM), which its percentage depends on the source and conditions of pectin extraction and also DM can confer regulation properties on gel strength, gelling time and sensitiveness to metal ions (Chen et al., 2021). Based on the DM percentage, pectins are categorised as high-methoxyl pectins (HMP) or low-methoxyl pectins (LMP). When degree of methylation of pectin correspond to 50% or higher, they are consider as HMP, which can form gels in presence of sugars with fast gelling time of 20–70 s. Pectins below 50% of DM fall under LMP classification, which also describes low concentration sugar gels, having slow set time of 180–250 s (Abboud et al., 2020; Zheng et al., 2020). Furthermore, pectin is usually extracted at hydrothermal conditions with water acidified by sulfuric acid or hydrochloric acid as a catalyst. For the acidification of water, the use of these mineral acids can cause corrosion of the equipment as well as can be harmful to the environment (Hosseini et al., 2016; Freitas, Sousa, Dias, and Coimbra, 2020). Instead of mineral acid, the use of organic acid is a more proper approach, environmentally, and due to the low dissociation capacity, it causes less depolymerisation of the pectin (Oliveira et al., 2016).

Hence, the main purposes of this research study were to investigate for the first time the potential use of *inodorus* melon industrial by-products as a suitable alternative for pectin obtention, following its improved extraction method by hot-acid treatment using three different acid agents and to further increase the complete value of this melon resource, a full-detailed physicochemical and structural characterisation of the melon peel pectins was assessed. Finally, the performance of the pectins extracted as emulsifier and rheology modifiers ingredients was evaluated. This study also aims to provide a future view of melon by-products valorisation within industrial facilities as rich sources of pectin.

7.2. Materials and methods

7.2.1. Chemicals

Reagents as boric acid, citric acid (99%), 3,5-dimethylphenol, *D*-galacturonic acid, glacial acetic acid, hydrochloric acid (HCl), pectin from citrus peel $\geq 74.0\%$, sodium chloride (NaCl), sodium hydroxide (NaOH), sulphuric acid (H₂SO₄) were obtained from Sigma-Aldrich (Sintra, Portugal), vegetable soy oil were all purchased from Acoforma (Madrid, Spain) and tartaric acid from LABCHEM (USA).

7.2.2. Melon peel by-products

Melon fruits (*Cucumis melo* L. *inodorus*) were harvested (ripening stage was not controlled) from the Alentejo region in Portugal and processed by Nuvi Fruits S. A. Company Torres Vedras (Portugal), during the season of summer in August – September 2020. Fresh melon peels were generated as by-products and then transported to the Centro de Biotecnologia e Quimica Fina (CBQF) at -20 °C. The melon peels were thawed at room temperature and then processed as previously reported by Gómez-García et al. (2021b). They were milled employing a commercial machine (HR1869/8, 900 W, Philips) in order to obtain a fibre rich solid fraction (SF) with low liquid content. The SF was collected and manually pressed using a fibre gauze to eliminate the remaining liquid and facilitate its drying process in a convection oven at 55 °C for 48 h. Afterwards, the dried SF was grinded to obtain a fine powder with estimative particle size of ≤ 250 μm . Finally, this powdered fraction was labelled as melon peel flour (MPF) and stored in hermetic-zip plastic bags, avoiding humidity and sun light.

7.2.3. Hot acid extraction of pectin methodology

Extractions were performed using three different acids, two organic (citric and tartaric acid) and one mineral (hydrochloric acid) and the effect on the pectin yield and its physicochemical and structural properties were investigated. The flow process chart for pectin extraction is shown in **Figures 7.1** and **7.2**. Pectin extraction was carried out following the methodology reported by Raji et al. (2017) with slightly modifications, acidity was set at pH 2, distilled water at 90 °C for 60 min with a mass-solvent ratio (MSR) of 1:50. Then, the sample was filtered using two layers of muslin cloth and the filtrate was centrifuged at 2353 g for 20 min to remove insoluble particles from the pectin slurry. Later, pectin slurry was subjected to ultrafiltration, through membrane of 3 kDa to achieve higher purification levels by the elimination of smaller particles, particularly monosaccharides. Then, pectin precipitation was conducted by mixing ethanol (96%) in a 2:1 ratio (v/v) with the supernatant and incubated at 4 °C overnight (18-20 h), the polysaccharides were collected by filtration (muslin cloth) and repeatedly washed two times with ethanol. Finally, the precipitated pectins were freeze-dried and labelled as pectin extracted by hydrochloric acid (PHCl), citric acid (PCA) and tartaric acid (PTA). The yield of pectin extraction (EY) was calculated according to the following equation 7.1:

$$\%EY = \frac{\text{weight of dried extracted pectin (g)}}{\text{weight of dried MPF (g)}} * 100 \quad (7.1)$$

7.2.4. Physicochemical properties evaluation

The moisture content of the extracted pectins from melon peels (PHCl, PCA and PTA) was calculated by drying pectin samples in an oven at 105 °C for 24 h until constant weight. The ash content was measured using a muffle at 550 °C for 24 h and total crude protein ($N \times 6.25$) was determined using the Kjeldahl method. The results were described as a percentage of dry weight (DW). Total carbohydrate content (TC) was determined by the spectrophotometric method of phenol-sulfuric acid technique (Kazemi et al., 2021). The galacturonic acid content was determined according Deng, Penner, and Zhao (2011) and later described by Gómez-García et al., (2021b) with small modifications. Briefly, 250 µL of a solution of boric acid (30 g/L) and sodium chloride (20 g/L) were added into a glass tube containing 250 µL of sample and then mixed with 4 mL of H₂SO₄ (96%). The mixture was homogenised in a vortex and then incubated at 70 °C for 40 min. Later, the

mixture tubes were put under cool water bath for 1 h. Afterwards, 200 μ L of dimethylphenol solution (100 mg of 3,5-dimethylphenol in 100 mL of glacial acetic acid) were added to the mixture and carefully homogenized in a vortex. Finally, the absorbance

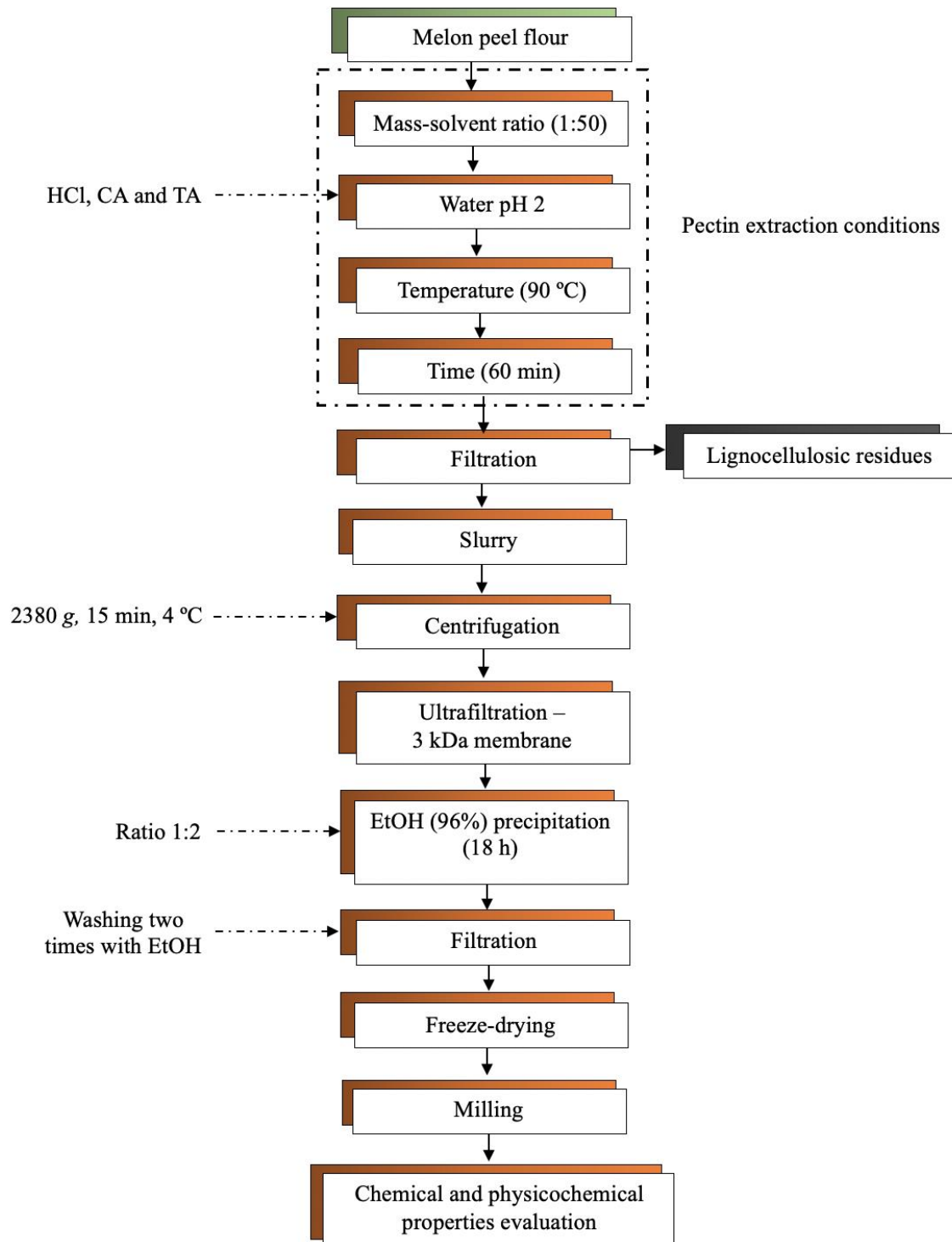


Figure 7.1. Extraction conditions of pectin from melon peels with different acid agents. HCl – Hydrochloric acid; CA – Citric acid; TA – Tartaric acid.

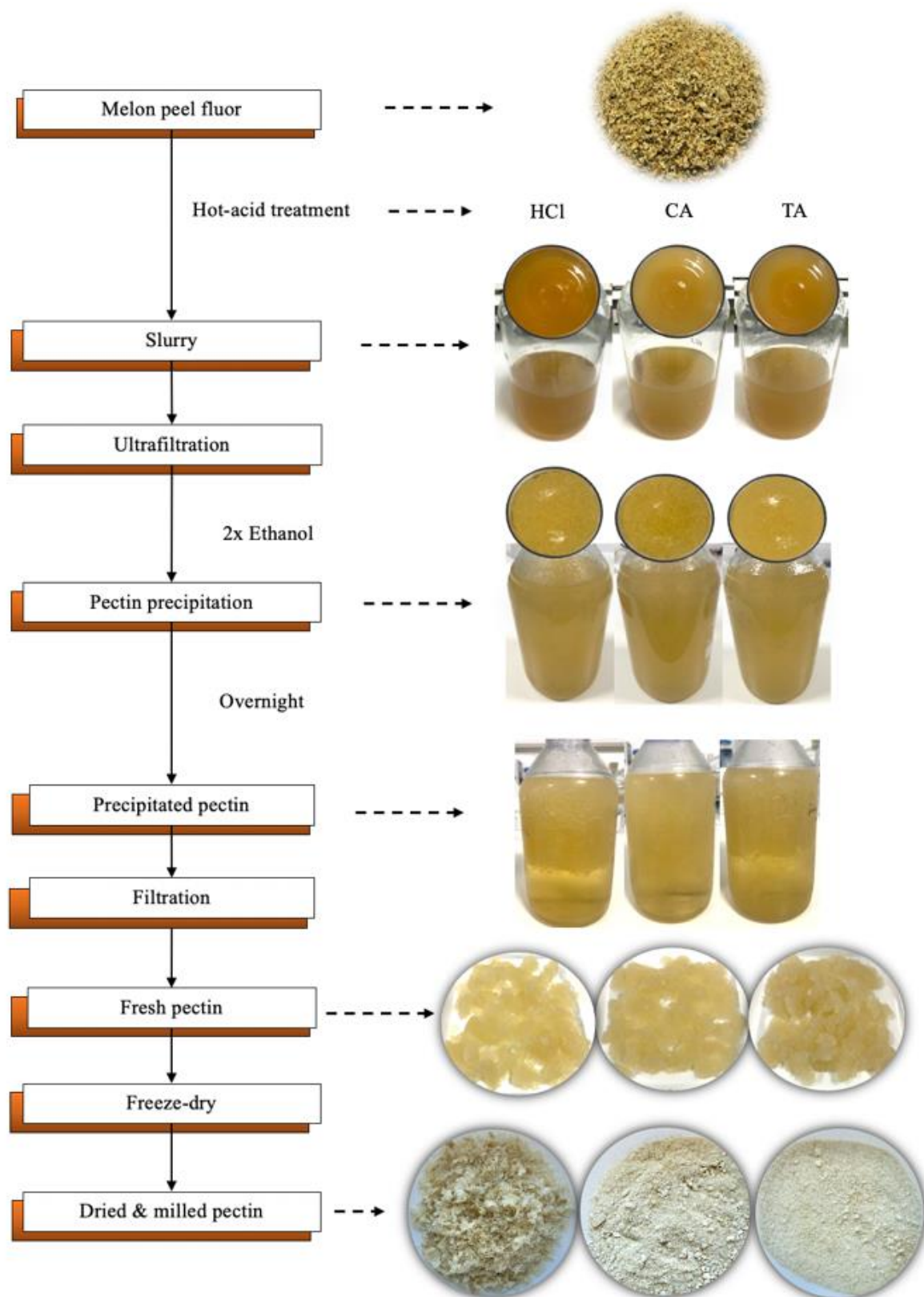


Figure 7.2. Flow diagram of the process to extract pectin from melon peels through hot-acid treatment. HCl – Hydrochloric acid; CA – Citric acid; TA – Tartaric acid.

was recorded at 400 and 450 nm (Synergy H1 microplate reader, Vermont, USA). *D*-galacturonic acid was used as calibration curve standard (0.005 – 0.15 mg/mL) and the results were assessed as g of galacturonic acid equivalents (GalA)/100 g DW employing the equation 7.2:

$$GalA = \frac{A(t) \times V(t) \times DF \times C \times 0.91 \times 100}{A(s) \times W(t)} \quad (7.2)$$

where: A(t) is the difference in absorbance (between Abs₄₀₀ – Abs₄₅₀ nm) of the sample; V(t) is the total volume; DF is the dilution factor; C is the concentration of the standard (0.1 mg/mL); A(s) is the difference in absorbance of the 0.1 mg/mL standard; W(t) is the weight of the sample (mg) and 0.91 is the factor for converting experimentally determined values for monosaccharides to polysaccharides. All of the extracts were performed in triplicate.

7.2.5. Determination of the degree of methyl esterification (DM)

The degree of methyl esterification (DM) of melon pectins (PHCl, PCA and PTA) was determined by a titrimetric method commonly used and described by Raji et al., (2017). An amount of 20 mg of the dried pectin was humidified with 2 mL of 96% ethanol and then mixed with 20 mL of distilled water, the solution was kept at continuous stirring until total pectin dissolution. After, five drops of phenolphthalein (0.1% w/v) were added to the solution and then the solution was titrated with 0.5 M NaOH and the volume of NaOH used until colour change was recorded as the initial titter (V1). Subsequently, 10 mL of 0.5 M NaOH was added and then the solution was stirred intensely. Each solution was let rest for 15 min. Next, 10 mL of 0.5 M HCl was added, and the solution was stirred until the pink colour disappeared. The solution was titrated again with 0.5 M NaOH for the last step, and the volume used was recorded as the final titter (V2). The DM was calculated according to the equation 7.3:

$$\%DM = \frac{V2}{V1 + V2} * 100 \quad (7.3)$$

7.2.6. Chemical groups evaluation by FTIR spectroscopy

Fourier transform infrared (FTIR) spectrums of the extracted melon pectins with the three tested acids (PHCl, PCA, PTA and PCP) were obtained using an ABB MB3000 FTIR spectrometer (ABB, Zürich, Switzerland) equipped with a horizontal attenuated total reflectance (ATR) sampling accessory (PIKE Technologies, Madison, WI, USA) with a diamond/ZnSe crystal. The spectrum was recorded in the range from 400 to 4000 cm^{-1} with a resolution of 4 cm^{-1} using 32 co-added scans per sample.

7.2.7. Pectins molecular weight determination by HPLC-SEC

The molecular weight (MW) of *Inodorus* melon pectins (PHCl, PCA and PTA) and PCP were measured using size exclusion chromatography (SEC) coupled with a chromatographic system using a Beckman and Coulter 168 series HPLC system with refractive index - RI detector (Knauer, Berlin, Germany) according to Campos et al. (2020a) with slightly modifications. Molecular separation was carried out using columns packed with hydroxylated polymethacrylate-based gel from Waters Ultrahydrogel SEC Columns (Waters, Milford, Massachusetts, USA) serially coupled as follows: UltraHydrogel Guard column (6x40 mm), 120 Å, 250 Å and 2000 Å (7.8x300 nm). A dispersions of 5 mg/mL melon pectin samples were prepared in ultrapure water (Milli-Q, Merck, Darmstadt, Germany) and allowed to hydrate overnight at room temperature (25 °C). After, pectin solutions were filtered through a 0.22 μm nylon membrane filters and transferred into glass vials and 30 μL of sample were injected into the HPLC-SEC system eluted with mobile phase (previously filtered and degassed) composed by sodium nitrite (NaNO_2 ; 0.1 M) and sodium azide (NaN_3 ; 0.2 g/L) in ultrapure water under an isocratic gradient at a continuous flow of 0.5 mL/min during 90 min at room temperature. Data acquisition and analysis were accomplished using Karat32 software. The average MW of the displayed peaks were analysed and quantified by comparison to the retention times using a calibration curve made with Shodex Pullulan P-82 standards (Showa Denko K. K., Tokyo, Japan) ranging from P-5 (5.9 kDa) to P-800 (708 kDa).

7.2.8. Emulsifying capacity (EC) assessment

Emulsifying capacity of pectin samples and the stability of prepared emulsions were assessed according to the method described by Roman et al. (2021). Determination of EC is based on the ratio of the emulsified layer volume and the whole volume of the solution.

Emulsions were prepared in triplicate by mixing equal volumes, 5 mL of vegetable oil with 5 mL of pectin solution at 5 mg/mL. The oil-water mixtures were homogenized at 12000 rpm for 3 min at room temperature with an Ultra-Turrax apparatus (IKA Ultra-turrax T18, Wilmington, USA). Samples were centrifuged at $1100 \times g$ for 5 min at room temperature. After centrifugation, the EC was calculated according to the equation 7.4.

Emulsion stability (ES) of the emulsion prepared for EC was also analysed through heating at 80 °C during 30 min, cooled to room temperature and centrifuged at 1100 g for 5 min at room temperature. The ES was calculated using the following equation 7.5, where ELHA is the height of the emulsified layer after heating and TELHA is the total height emulsion layer.

$$\%EC = \frac{ELHA \text{ (cm)}}{TELHA \text{ (cm)}} * 100 \quad (7.5)$$

7.2.9. Gel preparation

Gelling capacity of melon pectins (PHCl, PCA, and PTA) and commercial PCP were carried out according to the standard method for gel preparation reported by Han et al. (2017) with slightly modifications. Gels were made with pectin samples at 1% (w/v) and two different sucrose concentrations (40 - 65% w/v) dissolved in ultrapure water in a 10 mL beaker at constant stirring. The pectin solutions were adjusted to pH 3.5 and heated to 80 °C during 15 min and then calcium chloride ($CaCl_2$) was added with constant stirring, reaching a final concentration of 10 mM. Beakers with the viscous solution were removed from heating and stored in dark conditions at room temperature during 24 h.

7.2.10. Rheological measurements

Rheological analysis was performed on a Gemini Advanced Rheometer (Bohlin Instruments, Bristol, UK), coupled with a peltier unit for temperature control. Oscillatory tests on pectin gels samples (PHCl, PCA, PTA and PCP) were performed using a cone and plate geometry ($d = 40$ mm, 4° angle) at 25 °C. Frequency sweeps were performed between 0.01 and 100 Hz, using a constant stress of 0.05 Pa, which was previously determined to be within the linear viscoelastic region.

7.3. Results and discussion

7.3.1. Effect of different acids on pectin extraction yield and chemical composition

7.3.1.1. Extraction yield

Selection of a acid type is an critical aspect in the pectin extraction process, mainly because it has considerable influences in the final pectin products, it not only affects its yield and purity, but also determines its chemical and functional properties such as methylation degree (DM), average molecular weight (MW), emulsifying capacity (EC), and gel strength (Freitas, Sousa, Dias, and Coimbra, 2020). In this study, pectin extraction from melon peel by-products was performed using three types of acids (two organic acids: citric and tartaric and one mineral acid: hydrochloric). The effect on extraction yield regarding acid type, when the conditions of temperature (90 °C), extraction time (60 min,) acidity (pH 2), and MSR (1:50 w/v) were constant, was found as follows (**Table 7.1**): citric acid (CA) (34.58%) > tartaric acid (TA) (31.10%) > hydrochloric acid (HCl) (20.90%). As can be observed, organic acids showed better extraction yields because of their less severe dissociation power, and among the three tested acid types, citric acid was the best one. The low yield of extraction by HCl could be explained by its stronger power that leads to higher dissociation capacity than the organic acids, which can cause higher depolymerisation of the pectin into small sugars that could be removed during the ultrafiltration process. Therefore, the use of organic acids could lead to a more effective and environmentally-friendly pectin extraction process. Several researchers have described the use of organic acids as suitable alternatives against mineral acids, since they could improve the yield and quality of pectin, decreasing environmental impact and providing financial benefits (Chen and Lahaye, 2021). In this context, the use of citric acid coupled to the ultrafiltration step allowed higher yields than that reported from *cantalupensis* melon peels (32.81%) using microwave assisted extraction (Golbargi et al., 2021), acid treatment on Iranian melon peels (29.48%) (Reji et al., 2017) and enzymatic hydrolysis on red beet (20.7%) (Fissore, Rojas, and Gerschenson, 2012). Nevertheless, the use of tartaric and hydrochloric acids also exhibited higher values than the reported for *reticulatus* melon peels (6.54%) and apple pomace (13.30%) extracted with different conditions of temperature and pH (95 °C, pH 1) (Güzel and Akpınar, 2019). Thus, the present study clearly suggests that food-grade organic acids can be employed to recover pectin, with higher extraction yield compared with microwave and enzymatic assisted extraction, avoiding discharges of toxic chemicals (HCl), time consuming process (18-20

h of hydrolysis) and expensive equipment (microwave system).

7.3.2. Chemical characterization

Results of the chemical composition of pectins extracted from melon peel by-products are depicted in **Table 7.1**. In this study, the dry weight (DW) content of the pectin extracted from *inodorus* melon peels by PHCl, PTA and PCA was similar to the content of commercial pectin from citrus pectin (PCP) (ca. 90%) and higher than apple pectin (ca. 85%), but lower than melon peels (ca. 95%) extracted by CA (Güzel and Akpınar, 2019). The DW values of pectins are within the recommended value ($\geq 90\%$) established by the FAO. Total ash content is a significant physicochemical characteristic, which influences the gelling properties of pectin. According to FAO, an ash content lower than 10.0% is required for good-quality pectin. In the present study, for pectins extracted with CA and TA the ash contents were 1.13 and 2.05% respectively, and higher than PCP (0.51%) and PHCl (0.42%). Nonetheless, pectins from melon peels exhibiting lower ash content suggests higher purity. Also, the protein content is an important parameter, which positively affects the emulsifying capacity of pectin. It is widely reported that the hydrophobicity of proteins is responsible for a higher emulsification activity of pectin, and high content of protein could enhance the emulsifying properties (Kazemi et al., 2020). As shown in **Table 7.1**, the protein content of PHCl (5.50%) had the highest value followed by PTA (3.96%), and higher than PCP (2.71%) and PCA (2.66%) with the lowest content. Moreover, the results obtained for protein content from melon peel pectin correspond to pectin isolated from different sources, such as berry (2.9-3.1%) and citrus peels (2.8-3.8%) (Roman et al., 2021). The structure of pectin is comprised by at least seventeen different monosaccharides in which *D*-GalA is the most prominent molecule that is regularly used for measurement of pectin purity. A food-grade pectin should contain at least 65.00% of *D*-GalA, according to FAO and EU recommendations. In this concern, the *D*-GalA content of the three melon pectins were within the recommended limit. For instance, PTA had the lowest *D*-GalA content, accounting with 60.30% followed by 65.60% for PCA, and the highest value was for PHCl with 70.40%. These results are higher than the reported by Raji et al. (2017) and Muthukumaran et al. (2017) for melon peel (47-48%), berry (38-60%) and mango (56-66%), respectively, but lower than the PCP (74.34%), apple (79.78%) and citrus (86.4%) sources (Güzel and Akpınar, 2019). In general, pectins extracted from melon peels were found to be within the

recommended limit (60-70% GalA), which confirms that these samples have great potential food industrial applications. Concerning the degree of esterification (DM), PHCl, PCA and PTA were categorized into the group of high-methoxyl pectin (HMP) having higher than DE > 50% in each extracted pectin, for example PHCl had the highest value with 87.47% compared with PCP (85.57%), PCA (74.84%) and PTA (65.01%), and the reported of mango peel (77-89%) (Banerjee et al., 2018), apple (77.62%), carrots (24-49.9%) (Encalada et al., 2019) citrus peel (6.77%) (Hosseini, Khodaiyan, Kazemi, and Najari, 2019) and berry (76.90%) (Roman et al., 2021) and red beet (3.40%) (Fissore, Rojas, and Gerschenson, 2012). It has been described that pectin extracted through extreme conditions regarding high temperature, long time and low pH generally presents low DE due to the polygalacturonic polymer is damaged, causing high deesterification. However, the extraction conditions implemented in this study did not show these drawbacks on melon pectin. Previous studies found that the maturation stage of the fruits and extraction methods affect the esterification degree of pectins. These findings could be explained by the differences obtained in this study.

7.3.2. Structural analysis

FTIR spectroscopy was used to investigate the structural functional groups of the extracted melon pectins (PHCl, PCA and PTA) and to identify diverse structural differences in contrast to commercial pectin. FTIR spectrum was recorded over the wavenumber range of 400 to 4000 cm^{-1} . As can be observed in **Figure 7.3**, alike signals were found between PHCl, PCA and PTA by comparison with the signals showing for the commercial PCP spectrum. For example, in the spectrum, the intense signal between 3300 cm^{-1} to 3600 cm^{-1} , positioned at 3322.9 cm^{-1} is a characteristic stretching vibration of O–H groups due to inter and intra molecular hydrogen bonding of the GalA structure (Chen and Lahaye, 2021). A smaller peak in the region of 3000 to 2800 cm^{-1} , positioned at 2944.8 cm^{-1} represents the C–H absorption, including stretching vibrations of CH, CH₂ and methyl (CH₃) group of the methyl esters (Kalapathy and Proctor, 2001). Furthermore, the peak at 1740.1 cm^{-1} is originated from stretching vibration of methyl esterified carboxylic groups (C=O), while peak at 1693.8 cm^{-1} is resulting from carboxylate anion stretching vibration (C–O–O⁻). The strength of both peaks confirms that all pectin samples had a DE value higher than 50% and should be considered as HMP as demonstrated by the titration method. Moreover, the signals ranging from 1000 to 1250

cm^{-1} were attributed to stretching of glycoside bonds in the pectin structure (C-O-C) (Kazemi et al., 2021). The peaks near at 1440 and 1328 cm^{-1} maybe derived from the C-H, O-H or CH₂ bending and 1220.5 cm^{-1} from stretching of CH₃CO were followed by high absorption peaks between 800 to 1200 cm^{-1} , referred to the specific fingerprint region of each polysaccharide. The fingerprint region can be related to the difference in pectin's sugar structure due to the presence of vibration bands attributed to monosaccharide molecules (Thu Dao, Webb, and Malherbe, 2021). In this region, diverse peaks were detected at 1142.5, 1090.1, 1071.4, 1043, 1017 and 944.23 cm^{-1} for pectin samples (PHCl, PCA and PTA), including in PCP. Similar spectrum profiles were found in low (29%) and high (61%) methoxyl pectins extracted with citric acid from Iranian (Raji et al., 2017) and *reticulatus* melon peels (Muthukumaran et al., 2017), respectively. Peaks between 800 to 1140 cm^{-1} could be assigned to the presence of stretching vibrations of glycosidic bonds (C-O) and pyranoid rings (C-C). The several absorption peaks between 1017 to 1103 cm^{-1} indicated the presence of pyranoses and furanoses in pectin samples possibly due to glucose elimination during process (Golbargi et al., 2021).

7.3.3. Molecular weight (MW) of pectins

The MW of the extracted pectins (PHCl, PCA and PTA) and commercial PCP was estimated by size exclusion chromatography (SEC), with elution profiles of refractive index and average MW as shown in **Figure 7.4** and **Table 7.1**, respectively. The average MW for the HMP extracted from *Inodorus* melon peels corresponded to 70.86 kDa (PTA), 138.02 kDa (PCA) and 146.99 kDa (PHCl), being slightly lower than the PCP (155.60 kDa), but in agreement with some values reported in literature for pectin extracted from various sources such as melon peel, apple, citrus peel, mango and berries (67.6–384.5 kDa). In the case of *Inodorus* melon, pectic polysaccharide extracted with citric acid with average MW of 138.02 has been previously reported, while pectin from hydrochloric and tartaric acids (155.60 and 70.86 kDa, respectively) has not been reported yet. As can be observed, a change to higher retention times appeared in the elution profiles of PCA and PTA, together with a more prominent second peak at higher retention times of 57.3 and 58.8 min, respectively. This could be possible due to the appearance of pectic

Table 7.1. Composition of pectin polysaccharide extracted from inodorus melon peel by-products with different acid agents and comparison with commercial citrus pectin and different pectin sources.

Acid	Pectin source									
	<i>Inodorus melon peel</i>			PCP	Melon peel			Apple	Berry	Citrus
	CA	HCl	TA	HCl	CA	CA	CA	CA	CA	HCl
%EY	34.58 ± 3.8	20.90 ± 1.8	31.10 ± 3.3	-	29.48 ± 1.7	3.8	6.54 ± 0.02	13.30 ± 0.9	-	-
%DW	90.58 ± 0.3	89.19 ± 1.5	92.03 ± 0.3	93.87 ± 0.1	-	-	85.19 ± 0.5	95.33 ± 3.8	-	-
%M	9.42 ± 1.0	10.81 ± 0.3	7.97 ± 0.4	6.13 ± 0.1						
%Ash	1.13 ± 0.1	0.42 ± 0.1	2.05 ± 0.3	0.51 ± 0.2	3.5	-	1.35 ± 0.20	1.08 ± 0.1	-	-
%Protein	2.66 ± 0.6	5.50 ± 0.1	3.96 ± 0.1	2.71 ± 0.4	1.5	-	-		3.1 ± 0.0	2.8 ± 0.0
%TC	76.24 ± 5.1	80.57 ± 2.7	74.14 ± 8.6	86.08 ± 0.9	10	-	-	-	-	-
pH		2		-	1	1		1		2
%DM	74.84 ± 1.4	87.47 ± 0.7	65.01 ± 1.1	85.57 ± 0.7	29.33	61.38	71.98 ± 3.7	77.62 ± 0.8	76.9 ± 0.0	79.9 ± 0.1
%D-GalA	65.63 ± 1.2	70.42 ± 3.0	60.27 ± 1.0	74.34 ± 3.7	48	47	92.97 ± 1.4	79.78 ± 1.4	38.3 ± 2.5	86.4 ± 1.4
MW (kDa)	138.02 ± 2.5	146.99 ± 2.7	70.86 ± 2.4	155.60 ± 3.4	67.6	384.5	-	-	159.0 ± 2.8	234.5 ± 10.1
Reference	This study				Raji et al. (2017)	Chandrasekaran et al. (2017)	Güzel and Akpınar, (2019)		Roman et al. (2021)	

Extraction yield (EY); Dry weight (DW); Moisture (M); Total carbohydrates (TC); Degree of methyl esterification (DM); *D*-galacturonic acid (GalA); Molecular weight (MW); Hydrochloric acid (HCl); Tartaric acid (TA); Citric acid (CA); Pectin from citrus peel (PCP) – commercial. All determinations were carried out in triplicated and mean value ± standard deviation.

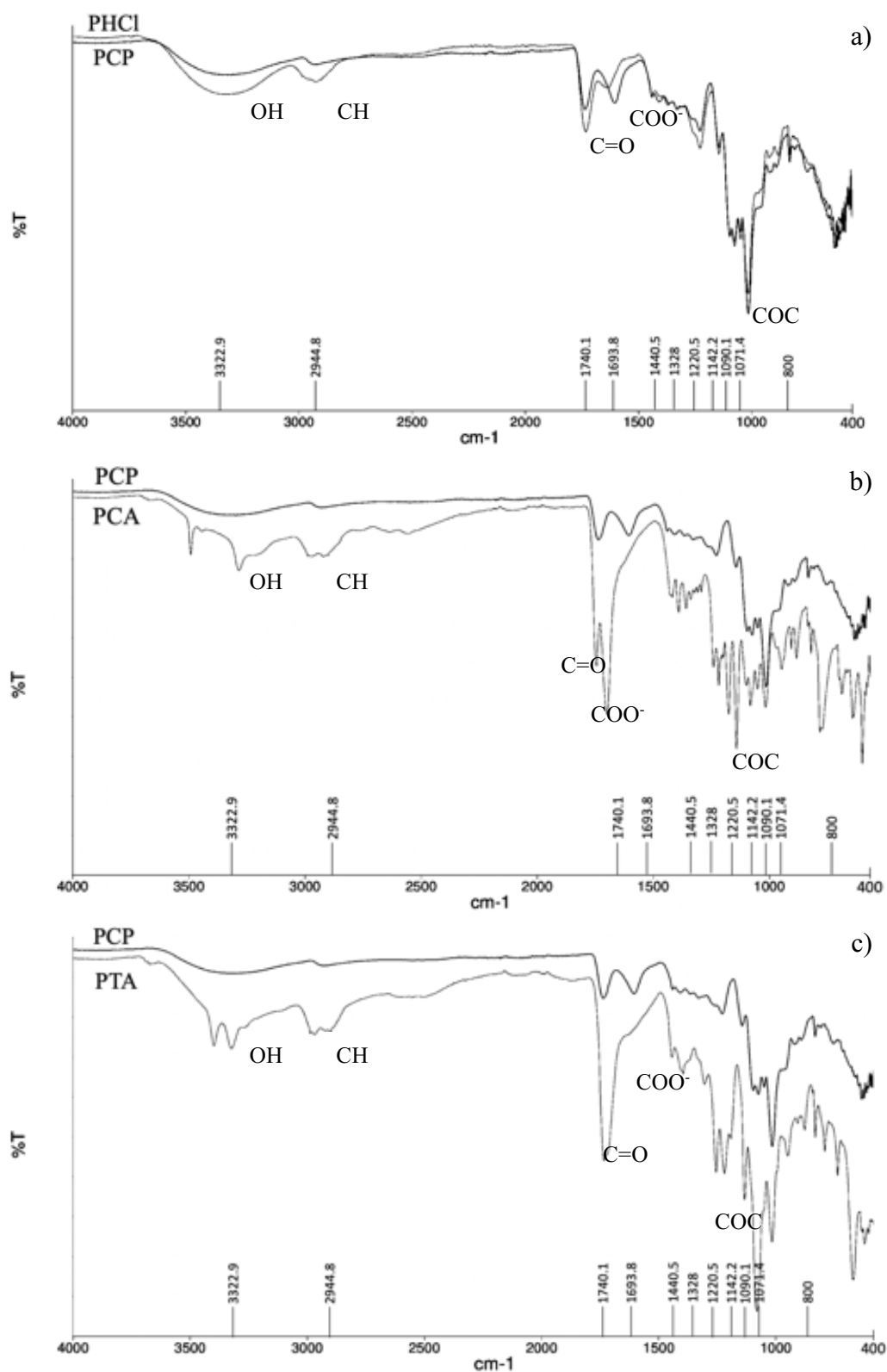


Figure 7.3. Fourier transform infrared (FTIR) spectrums of the high methoxyl pectin extracted, with hydrochloric acid (PHCl), citric acid (PCA) and tartaric acid (PTA) compared with commercial pectin from citrus peel (PCP).

oligosaccharides released during the hot-acid process. These behaviors in the elution profile with a thin peak appearing at higher retention times and resulting in a lower MW of extracted pectins could be attributed to the partial hydrolysis of the melon peel pectins or by a chemical degradation of pectins during the extraction process related with long extraction time, drastic pH values and temperatures. Indeed the chemical demethoxylation of pectin could be rapidly catalyzed by the acid environment resulting in pectin with lower DM and MW as well (Zhang et al., 2020). Several reports mentioned that at pH of ca. 4.5 and temperatures higher than 60 °C, acid hydrolysis occurs more rapidly, and this effect can be observed at basic pH values. Although pectin demethoxylation indirectly enhances its depolymerization reaction, the reaction rate of acidic demethoxylation is higher than that of acidic hydrolysis, especially of the homogalacturonan backbone (HG) (Einhorn-Stoll et al., 2019). Therefore, the extracted melon pectins under these conditions might result in chemical de-methoxylation, but without a drastic de-polymerization of the pectin backbone as suggested by the GalA content of the samples. Pectin is a natural polymer within a heterogeneous family and diverse MWs, depending on its source and the extraction methods. Previous studies suggested that this parameter could have significant effects on the functional properties of pectin samples such as emulsifying properties.

7.3.4. Emulsifying properties of pectins

The emulsifying capacity (EC) and emulsion stability (ES) of *inodorus* melon pectins (PHCl, PCA and PTA) were evaluated for the first occasion and the results are shown in **Figure 7.5**. The emulsifying capacity of pectin polymer is generated by several factors such as, structural characteristics, including MW, methyl and acetyl content, feruloyl, proportion of HG domain, conformation of rhamnogalacturonan (RG-I) side chains, and presence of attached protein groups (Grassino et al., 2018). In emulsions composed by oil in water, the hydrophobic protein molecules adsorb at the oil-water interface, serving as anchoring point with only a small fraction of the pectin molecules, being adsorbed at the interface. The oil droplets are also sterically stabilized by the hydrophilic carbohydrate moieties protruding into the aqueous phase (Medeiros et al., 2019). The remaining pectin molecules will also contribute to the decrease in the tendency of the dispersed oil droplets to approach each other by increasing the viscosity of the continuous phase. In this study, after centrifugation step of the pectin emulsions, three phases were observed in the rest

tubes conformed by a very tiny oil layer on top, an emulsified layer phase in the middle and in the bottom a pectin aqueous phase. Among all the melon pectin samples, PHCl (41.04%) resulted in higher EC than PCA (37.71), PTA (34.55%) and commercial PCP (36.36%). Pectin polysaccharides have been reported to form and stabilize emulsions. These higher results observed for melon pectins against commercial pectin could be explained with the ultrafiltration process performance before ethanolic precipitation, which allowed higher purity due to the removal of small impurities from the slurry, increasing the concentration of pectin extracted by enhancement of the pectin surfactant potential. For the ES of the resulted pectin emulsions, samples were subjected to drastic conditions of high temperature (80 °C) during 30 min to accelerate the union and creaming phenomena in the emulsions. A higher ES was observed for pectin samples with higher amount of protein, e.g., PHCl and PTA presented higher content of ca. 5.50 and 3.96% with a stability percentage of 38.36% and 32.35%, representing 94 and 93% of the initial formed emulsions, respectively.

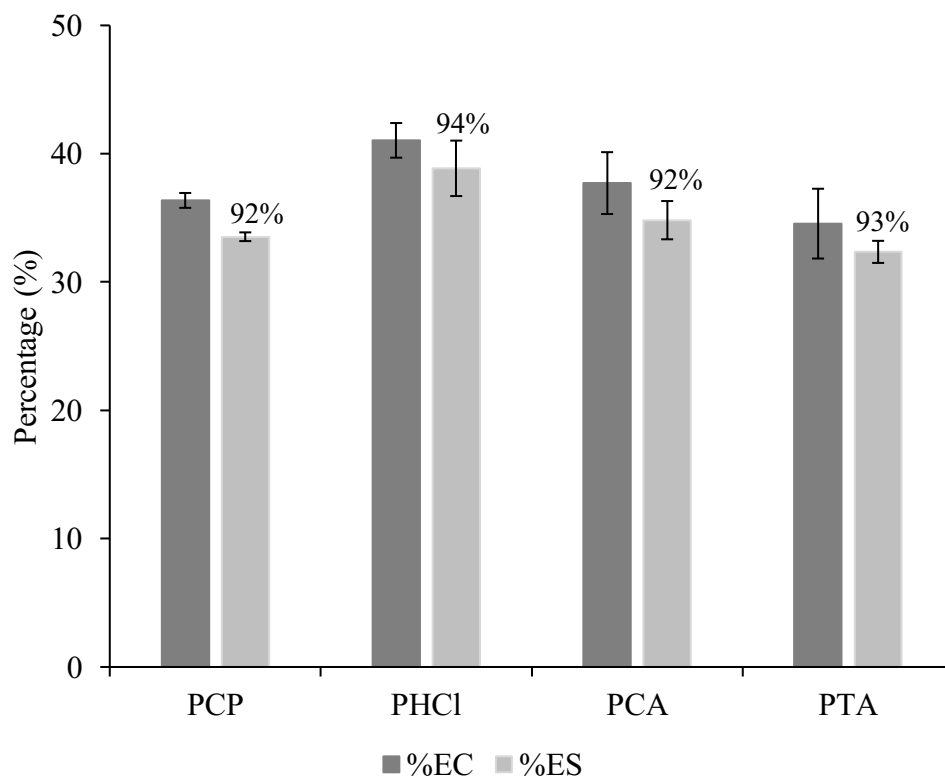


Figure 7.5. Emulsifying capacity (%EC) and emulsion stability (%ES) of *inodorus* melon pectins. Values in the graph are the percentage that %ES represents in regard to %EC. Pectin extracted by hydrochloric acid (PHCl), citric acid (PCA) and tartaric acid (PTA); Pectin from citrus peel (PCP) – commercial

The hydrophobic covalent bound proteins present in the pectin adsorb at the oil-water interface and has been reported to be a major determinant for the emulsifying potential of pectin. Thus, bonded-protein could enhance and facilitate the interfacial adsorption of large macromolecules in the oil-water interface, providing superior stability. In this regard, fast adsorption to the interface has been described as a critical step for emulsion stabilization (Jiang, Qi, Huang, Zhang, and Yang, 2020). A higher amount of protein content could also delay pectin desorption from the oil-water interface, making emulsions more stable. In this respect, some researchers have reported that beet and citrus pectins were capable of stabilizing oil-in-water emulsions, with the small amount of covalently-bound proteins playing a vital factor due to their adsorption at the oil-water interface and the creation and stabilization of smaller droplets (Teresa Pacheco, Villamiel, Moreno, and Moreno, 2019; Wang, Qiu, Chen, and Yan, 2021). It is noteworthy that the protein content of melon pectin was found different, but ES cannot be just explained by these content differences. Thus, results suggest that the combination of a higher protein content and structural properties of pectin domains, MW and DM of pectins all together might improve the emulsifying capacity of the melon pectin polysaccharide.

7.3.5 Rheological properties of pectin-gel samples

One of the most demanded properties of pectins to be used as a raw material for food or nutraceutical industrial purposes, is their capacity to form gels. In this context, rheological techniques, particularly oscillatory measurements, are mostly applied to evaluate gel strength and deformation properties against increasing frequencies, considering the relationship between of the storage modulus (G') and the loss modulus (G''), which are related to elastic and viscous behaviour of materials, respectively (Ström, Schuster, and Goh, 2014). Moreover, HMP dispersed in water usually demonstrated a liquid-like behaviour, where G'' is higher than G' in the whole frequency range analysed. There are several parameters that affects gelation properties such as pH, ionic strength (Ca^{2+}) and co-solute presence (sucrose) (Löfgren et al., 2005). **Figure 7.6** shows the behaviours of the gels, where at low frequencies the G' moduli were always higher than G'' (both being dependent on sweep frequency); this implies that the melon pectins were more elastic than viscous and all the solutions behaved as gels with all the pectin concentration (1%

w/v) tested at the established conditions of pH 3.5, Ca²⁺ (10 mM) and using both concentrations of sucrose (40 and 60% w/v). This positive gelling test could be attributed to the low pH range in which the carboxyl groups are protonated, transforming pectin from the double helix to a three-helix conformation by hydrogen cross-linking between carboxyl groups of the triple helix pectin chain (Han et al., 2017). Moreover, sucrose is typically used to promote gelation of HMPs, which generally are viscoelastic liquids in the absence of a co-solute. This expected gelling behaviour was observed on PCP and PHCl (**Figure 7.6a** and **b**), since sucrose increased the gel strength, helping to gel network organisation. The effect of further increase in sucrose concentration from 40 to 65% (w/v) in these both pectins progressively increase the elastic modulus, thereby increasing gel strength (G' was always higher than G'' in all the pectin gels). Similar results were reported by Banerjee et al. (2018) on mango pectin-gels, increasing gel strength by increasing sucrose content from 55 to 75% (w/v). The increase in the elastic moduli observed for PCP and PHCl also could be justified in this acid pH range, although the pectin charge density was low, the presence of Ca²⁺ promoted the gelation properties. On the other hand, a weaker gel behaviour was observed for PCA and PTA supplemented with 40% (w/v) of sucrose (**Figure 7.6c** and **d**, respectively), and a transition from solid to liquid-like behaviour (G' and G'' crossover) was observed at 0.2 and 1 Hz, respectively, being G'' higher than G' over the remaining frequency range. A high content of co-solute (65% w/v) allowed a gel-promoting effect of both pectins under these conditions. This promotion could be attributed to the Ca²⁺ ions, which link with the free dissociated carboxyl groups of pectin to generate a denser and more elastic gel network, a phenomenon reported to form “egg-box” junction zones (Li, Feng, Niu, and Yu, 2018). However, dramatically increases of G'' comparatively to G' with frequency increases (up to 2 Hz), almost crossing over each other by increasing the frequency sweep, which could suggest that low concentrated weak gel systems were less resistant and at higher frequencies there is unravelled in the gel network structure. Furthermore, the increase in the complex modulus (G^*) that increased with sucrose concentration, observed for all gel samples (**Figure 7.6e**), suggested that additional networks were formed as the sucrose content increased. This influence is ascribed to the abundant number of hydroxyl groups, stabilizing the structure of junction zones, promoting hydrogen bonding, and immobilizing free water (Zheng et al., 2020). There is no doubt that sucrose had a reinforcing effect on pectin gels at appropriate pectin content, pH and Ca²⁺ concentration

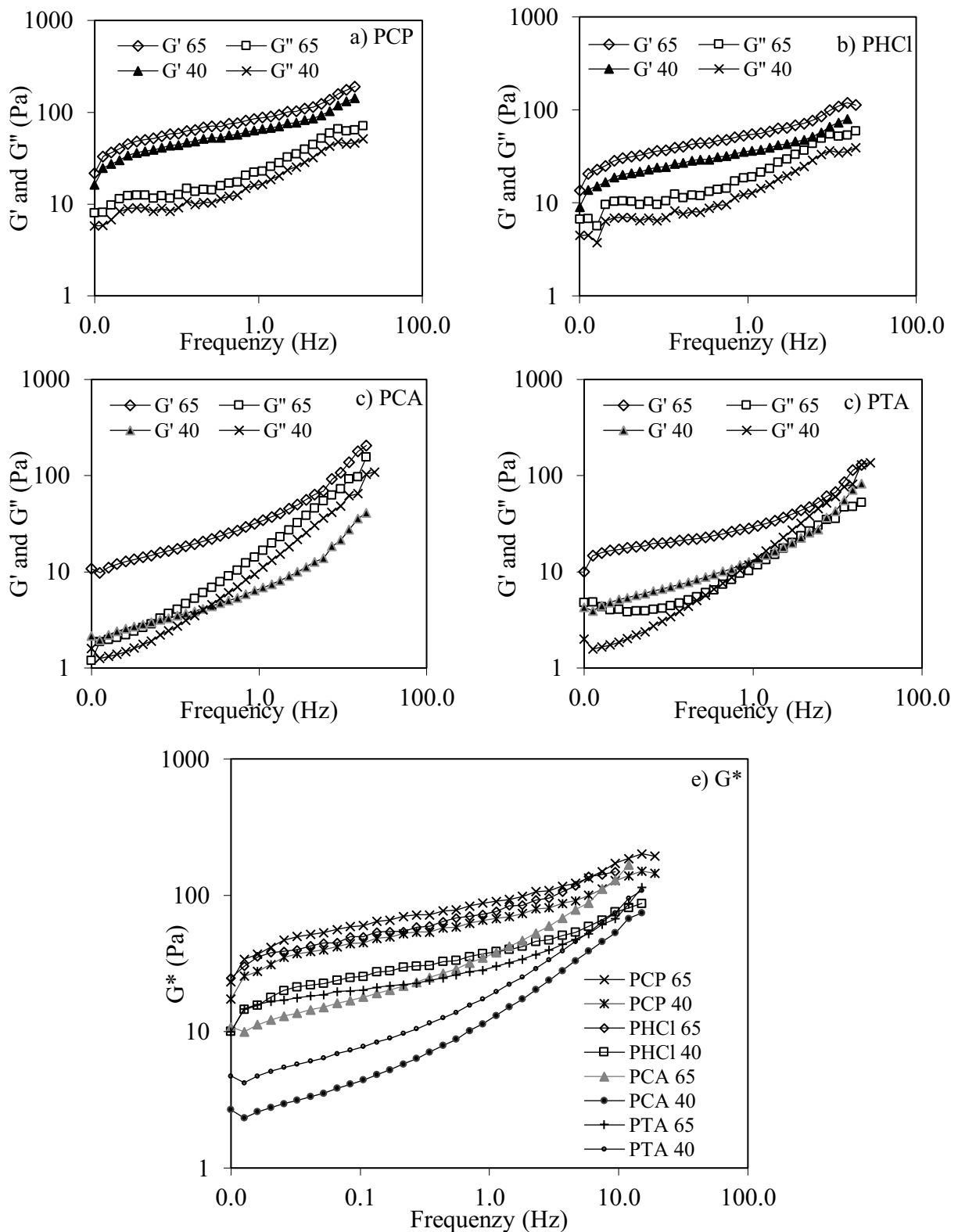


Figure 7.6. Effect of sucrose concentration (40 – 65% w/v) in pectin gels (1% (w/v), pH 3.50, CaCl₂ (10 mM)) storage modulus (G'), loss modulus (G''), and the complex modulus (G^*). Pectins extracted with hydrochloric acid (PHCl), citric acid (PCA) and tartaric acid (PTA) compared with commercial from citrus peel (PCP).

and these melon pectins behave as rigid solids, until the shear stress is exceeded and the material flows as shear-thinning fluid (liquid-like behaviour). These behaviours are in agreement to the reported for gels composed by HMP (2% w/v) extracted from passion fruit peel combined with sucrose at 20 and 50% (w/v) (Abboud et al., 2020). Since all melon pectins herein studied showed very similar chemical composition, it could be stated that some differences in the rheological performance of each pectin product come from the different molecular weight. Also, all the extracted melon pectins showed gelling properties with 65% (w/v) of sucrose, thus confirming high DE pectin.

7.4. Conclusions

In this study, a natural resource recovery approach on melon peel by-products valorisation as novel raw materials for pectin extraction was implemented. *Inodorus* melon pectins extracted by hot-acid treatment with different acid agents (HCl, TA and CA) allowed to obtain yields of 20.90, 31.10 and 34.58%, respectively, with low ash and high protein content. The *D*-GalA content and DE ranged from 60 to 70% and 74 to 87% respectively, which matches that of commercial pectin (PCP), and all of them are categorized as high-methoxyl pectins (HMP). The characterization by FTIR of the extracted pectins also showed similar patterns to commercial citrus pectin. The molecular weights of pectins were found similar to those reported in literature, ranging from 70 to 146 kDa. These melon pectins were strongly highlighted by their performance namely emulsifying and gelling properties. Melon pectins were capable to form very stable water-oil emulsions 34 to 42%, even higher than the commercial pectin (36%). This study revealed that pectins at low pH (3.5) and 65% of sucrose form strong gels in the presence of Ca^{2+} ions, showing consistency and organized polymer chains linking in ordered junction zones. The rheological characterization of the acid pectin samples extracted by citric and tartaric acids exhibited characteristics of a weak gel ($G' > G''$ frequency dependence) with G' and G'' values becoming similar at higher frequencies. Overall, *inodorus* melon peels can be emerging as low-cost resources/alternative for industrial pectin production, which could respond the increasing demand for thickening or gelling pectin in global markets, including the market needs of food and nutraceutical industries.

CHAPTER 8 – Production and characterisation of microcrystalline cellulose from industrial melon by-products residues using a biorefinery approach

Ricardo Gómez-García^{a,b}, Sérgio C. Sousa^a, Oscar L. Ramos^a, Débora A. Campos^a,
Cristóbal N. Aguilar^b, Ana R. Madureira^a and Manuela Pintado^{a*}

^a*Universidade Católica Portuguesa, CBQF – Centro de Biotecnologia e Química Fina – Laboratório Associado, Escola Superior de Biotecnologia, Rua Diogo Botelho 1327, 42169-005 Porto, Portugal*

^b*BBG-DIA. Bioprocesses and Bioproducts Group. Food Research Department, School of Chemistry, Autonomous University of Coahuila, Saltillo, Coahuila, Mexico.*

This chapter has been submitted to:

Journal of Bioresource Technology

Abstract

Residual melon by-products were explored for the first time as bioresource of microcrystalline cellulose (MCC). Two alkaline extraction methods were employed, the traditional (4.5% NaOH, 2 h, 80 °C) and a thermo-alkaline in the autoclave (2% NaOH, 1 h, 100 °C). The final MCC were characterized for their chemical groups by FTIR, crystallinity with X-ray diffraction and morphology analysed by SEM. FTIR spectra showed that the traditional protocol allows a more effective hemicellulose and lignin from the melon fibres than the thermo-alkaline process. The degree of crystallinity of MCC ranged from 51.51-61.94% and 54.80-55.07% for thermo-alkaline and traditional process, respectively. The peaks detected in X-ray diffraction patterns indicated the presence of Type I cellulose. SEM analysis revealed microcrystals with rough surfaces and great porosity, which could remark their high-water absorption capacity and drug carrier capacities. Thus, these findings could respond the need to valorise industrial melon by-products as raw materials for MCC obtention with potential applications as biodegradable materials.

Keywords:

Melon residues, bioresource recovery, circular bioeconomy, crystalline cellulose, X-ray diffraction.

8.1. Introduction

In the European Union, food waste residues (FWR) account for at least 180 M tonnes, representing 10 to 15% of total waste generated worldwide, with a huge associated management/treatment cost of up to 140 billion €. About 50% of FWR are semi-treated in a suitable way, accounting 29% for recycling and 20% destined for composting or anaerobic digestion treatments, while the remaining percentage is just disposed in landfills or incinerated (Oldfield et al., 2016; Gómez-García et al., 2021b). Nonetheless, these management strategies must change in the near future following the new European Directives currently launched (article 11 and article 5) commitment to decrease landfilling to 10%, while assuring sustainable managements of FWR to 65% by 2030. (Carmona-Cabello et al., 2020; Esparza et al., 2020). Therefore, the development of suitable strategies for food waste management under the biorefinery approach plays an important role in increasing sustainability and achieving the challenges that food processing industries may face in the future (Liguori and Faraco, 2016). Biorefinery approach combines simultaneously different processing treatments on the raw materials to maximize productivity and recovery of several high value-added products. In this context, a biomass-based biorefinery could produce fuels, electricity and power as well as several products (e.g., plastics, chemicals), analogously to petroleum refinery, maximizing the value derived from biomass components and intermediates (e.g., enzymes, bioactive compounds, biodegradable plastics, and nanoparticles among many other molecules) (Yusuf, 2017; Dahiya et al., 2018). Biomass-based biorefinery helps to reduce energy consumption and the greenhouse gas emissions, compared to traditional energy generation plants. Biorefineries are still under research, but they are expected to play a significant role in the future of energy, biochemicals and biomaterials generation (Bilal et al., 2017; Patel et al., 2019). Currently, fruit processing industries need a modernisation under biorefinery and circular economy concepts since 30-60% of the total fresh weight of fruit represent food waste (peels, seed, stems among others), emphasizing on bioresource recovery efficiency, circularity, and valorisation of their by-products of lignocellulosic nature. These kinds of biomasses have not yet existent industrial applications on a big scale nor in a real waste management case for the obtention of value-added compounds with high industrial interest, reducing the opportunities and benefits to develop new business, revenues streams and possible jobs, instead they are generally disposed in landfills as the most accessible treatment, where all their potential natural value is wasted and lost (Campos et al., 2020c; Vlachokostas et al., 2021).

Melon (*Cucumis melo* L.) processing industries within their lineal production business of foodstuff such as juices, salads, snacks, among others, generate high amounts of peels as by-products (8 to 20 M tonnes wasted/year). These by-products represent rich biomass composed by cellulose (20-35%), hemicellulose (10-25%), lignin (5-20%), pectin (15-30%) and proteins (5-15%) (Santos et al., 2018; Rolim et al., 2020; Rodríguez-Luna et al., 2020; Gómez-García et al., 2021b). Such compounds could be valorised and exploited under the approaches of biorefinery and circular bioeconomy, using this biomass as feedstock for the development of novel eco-friendly and value-added products such as cellulose polymer (Gómez-García et al., 2020; Panchal et al., 2021). Cellulose is the most abundant polymer in nature structured by β -(1-4) linked *D*-glycosidic units, which has mainly been used in paper making, adhesives, textiles, food and pharmaceuticals due to its outstanding features and properties such as biocompatibility, biodegradability, renewability, low-cost and null-toxicity (Liu et al., 2017; Zhao et al., 2018). The structure of cellulose polymer is mainly constituted of highly ordered regions (crystalline structure) and disordered regions (amorphous structure), contributing to the rigidity and flexibility of fibres, respectively (Jin et al., 2016; Naduparambath et al., 2018). Microcrystalline cellulose (MCC) is one of the main cellulose derivatives characterized as a fine, white, odourless, purified and partially depolymerized powder obtained after cellulose hydrolysis. In this regard, its obtention involves mechanical processes such as grinding, high-pressure homogenization or refining, using hydrochloric or sulphuric acids (the most frequently used) to hydrolyse the amorphous regions of cellulose (Zhang et al., 2016; Sosiati et al., 2017; Ventura-Cruz et al., 2020). This natural polymer is highlighted as valuable material because of its crystallinity, mechanical properties, high surface area/porosity and its ability to form hydrogen bonds, forming an organized network that make difficult molecules to pass through (Haldar and Purkait, 2020; Zhang et al., 2020). Thus, its incorporation for composite materials development is under intense research as a reinforcing and fence agent, focusing on water vapor and oxygen absorption properties, as well as a binder and filler agent in food and medical tablets. Beside, MCC also has functional properties such as water absorption, suspension stabiliser, viscosity controller and emulsifying (Ferreira et al., 2018; Kharismi et al., 2018; Haldar and Purkait, 2020). Some studies have shown that MCC can be obtained from lignocellulosic waste on a dry basis, e.g., corncobs and sugarcane bagasse (Harini and Chandra Mohan, 2020), Betung bamboo (Kharismi et al., 2018), esparto grass (Beroual et al., 2021), grape stalk (Vallejo et al., 2021), lemon seeds (Zhang et al., 2020), pineapple peels (Madureira et al., 2018),

rose stems (Ventura-Cruz et al., 2020), Sago seed shell (Naduparambath and Purushothaman, 2016) and tea waste (Zhao et al., 2018). In the current years, biocomposites and microcellulose materials have been a relevant natural key compound for researchers and industries because such materials are indeed better and sustainable alternatives due to their renewability and biodegradability against traditional petroleum products, which could allow a less environmental impact (Kargarzadeh et al., 2017; Rasheed et al., 2020).

However, to the best of our knowledge, studies on valorisation of cellulosic materials from melon peel by-products have not been extensively explored or reported yet. Thus, to further increase the overall value of this melon biomass, a full-detailed structural characterization of melon peel residues after pectin extraction was carried out to obtain MCC. This research study aimed to explore melon peel by-products as bioresource to recover value-added compounds, such as cellulose, under the context of biorefinery as a suitable strategy for their integral valorisation, following MCC obtention process and comparatively examined by its extraction yield, psychochemical structure and morphology.

8.2. Materials and methods

8.2.1. Chemicals

All reagents used in this study such as citric acid, *D*-(+)-glucose, *D*-(+)-xylose, *L*-(+)-arabinose, hexane, hydrochloric acid (HCl), hydrogen peroxide (H₂O₂, 30%) sodium hydroxide (NaOH), sulphuric acid (H₂SO₄, 98%) and tartaric acid were purchased from Sigma-Aldrich (Sintra, Portugal).

8.2.2. Biorefinery approach: Deconstruction of melon peels biomass in different fractions and value-added compounds

Three different melon peel residues were obtained after hot-acid extraction of pectin using hydrochloric acid (HCl), citric and tartaric acids (CA and TA, respectively). The processing of melon peels (on a fresh weight basis) were handled as described previously by Gómez-García et al. (2021c), the melon peels were fractionated using a commercial juicer (HR1869/8, 900 W, Philips) to separate the solid fraction (SF) from the liquid. The SF was collected and pressed using a muslin cloth to remove the remaining liquid and then drying in an oven-dryer at 55 °C for 48 h. The liquid fraction was used for cucumisin

enzyme recovery previously reported by Gómez-García et al., 2021a. Afterwards, the dried SF was grinded using a coffee machine to obtain a fine powder with an estimated particle size ≤ 250 μ m and this fraction was called as lignocellulosic melon by-products (LMB). Pectin extraction from LMB was carried out in acidified (pH 2) hot distilled water at 90 °C and 120 rpm during 60 min with a solid-liquid ratio of 1:50. Then, the sample was filtered using two layers of muslin cloth and the solid particles were collected and dried at 55 °C for 24 h. Later, the dried solids were ground (particle size ≤ 250 μ m) and labelled as RHCl, RCA and RTA residues from hydrochloric, citric and tartaric acids treatment, respectively. The residues were stored in plastic bags, avoiding humidity and sunlight. The flow chart for the melon peel fractionation process is shown in **Figure 8.1**.

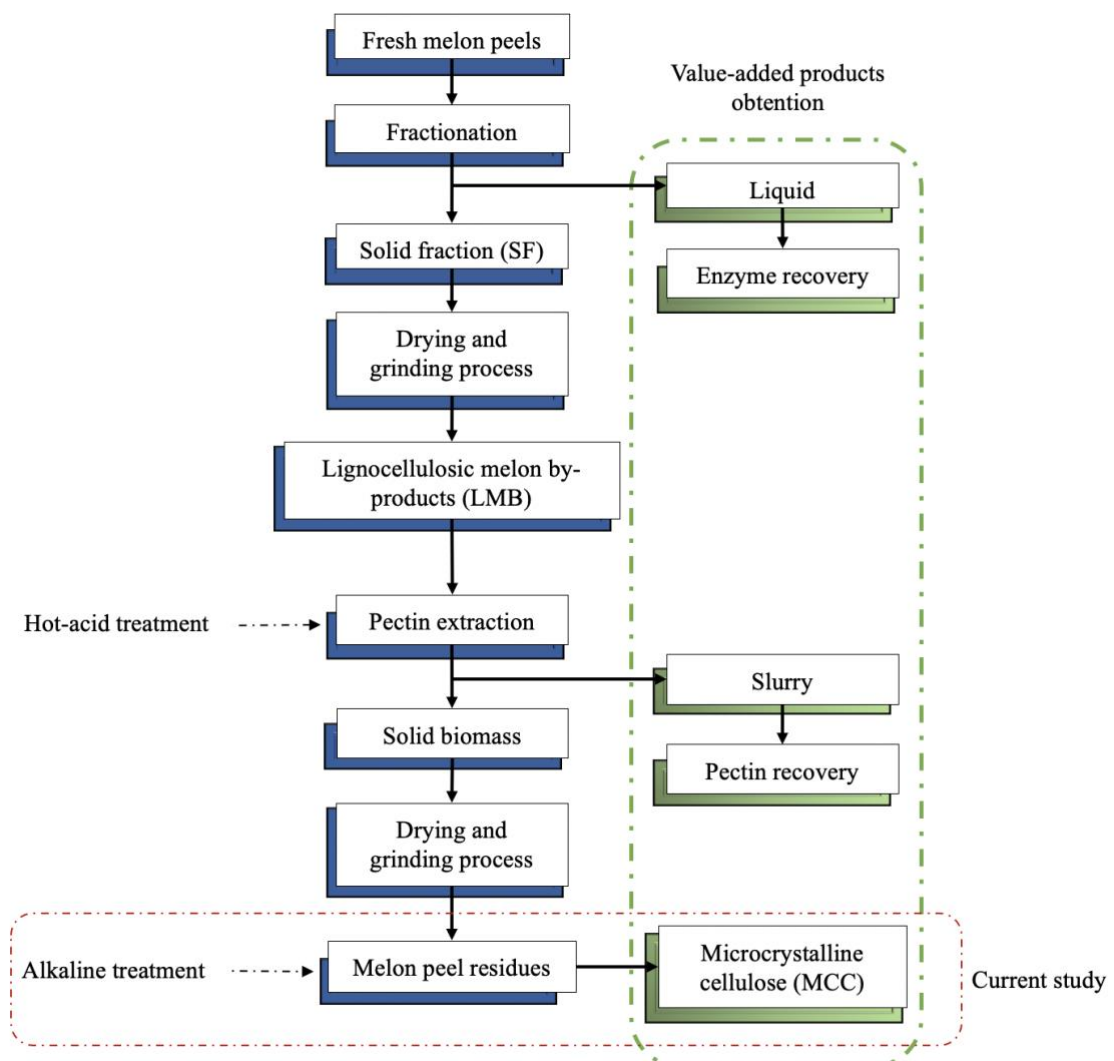


Figure 8.1. Process flow chart for melon peel by-products valorisation under biorefinery approach.

8.2.3. Chemical composition of melon peels residues

The content of dry matter (DM), moisture, ash, protein, dietary fibre, and carbohydrate constituents of the samples were made in triplicate according to standard procedures (AOAC) and described by Gómez-García et al. (2021c) as follows.

8.2.3.1. Dry matter and moisture content

The dry matter was calculated using the AOAC (1990) procedure. The moisture content was calculated by drying melon samples (1 g) at 105 °C for 24 h until constant weight (AOAC, 1997). The results were presented as percentage of %DM.

8.2.3.2. Ash content

Ash was measured by carbon removal of the dry residue samples from section 2.3.1, being incinerated in a muffle furnace at 550 °C for 24 h (AOAC, 1980). Total ash content was expressed as percentage of %DM.

8.2.3.3. Protein content

The total protein content of the melon samples was determined by Kjeldahl method (AOAC, 1997). Protein was estimated using the conversion factor of 6.25 for vegetables. The data was expressed as a percentage of %DM.

8.2.3.4. Determination of structural carbohydrates composition

Extractives and structural carbohydrates (cellulose and hemicellulose) and lignin of melon residues and samples were quantified accordingly to a laboratory analytical protocol reported by Sluiter et al. (2008). Briefly, 3 mL of H₂SO₄ (72%) were added to a glass tube containing 0.3 g of sample and incubated at constant agitation (120 rpm) in a shaking water bath at 30 °C for 1 h. The suspension was diluted to a final concentration of 4% by adding distilled water and then subjected to incubation for 1 h at 121 °C. The hydrolysed sample was cooled at room temperature and later vacuum-filtered (Pyrex® 50 mL M crucible, Corning, Inc., USA) and the solid residues were used for gravimetric analysis of acid-insoluble lignin and the filtrate was used for acid-soluble lignin and sugar quantification. The chromatographic separation of sugars was carried out using a Beckman Coulter HPLC equipment coupled to IR (K-2301) (Knauer, Berlin, Germany). The aliquots were filtered (0.45 µm) into a glass vial. Then 30 µL of sample were analysed using an Aminex HPX-87H column (Bio-Rad, Hercules, CA, USA) operated at 40 °C with 5 mM H₂SO₄ as mobile phase at constant flow of 0.6 mL/min during 30 min. Data

acquisition and analysis were accomplished using Clarity software. The peaks were examined and quantified using a calibration curve of each sugar standard (glucose, arabinose, and xylose) by comparing the retention time and areas. Total dietary fibre in each fraction was carried out using the enzymatic-gravimetric method described by Lee, Prosky, and Vries, (1992) and letter reported in our previous work (Gómez-García et al. 2021b). Three independent analyses were performed for each experiment.

8.2.3.5. Fat content

The total fat content was calculated using the Soxtec method (Soxtec 8000, Foss, Denmark). Fat was extracted from 1 g of sample packed in a cellulose thimble with 60 mL of hexane for 3 h at 90 °C. The analysis was conducted by triplicate and the results were expressed as a percentage of DM.

8.2.3.6. Total carbohydrates

Total carbohydrates content was calculated by the difference of mean values [100 – (% moisture + % ash + % protein + % fat)].

8.2.4. Extraction of cellulose from melon peel residues

8.2.4.1 Traditional method

An alkaline traditional treatment with NaOH (4.5% w/v) was carried out on the dried melon residues (RHCl, RCA and RTA) with a solid-liquid ratio of 1:10, during 2 h at 80 °C under agitation at 200 rpm in an orbital shaker (MaxQ 6000, Thermo Scientific). After, the reaction was cooled in an ice bath (15 min) and then vacuum-filtered using two layers of muslin cloth and washed until elimination of the dark alkaline liquor and reach neutral pH. The solids were oven-dried during 18 h at 55 °C and grinded (particle size \leq 250 mm). The dried residues were bleached according to the method reported by Ventura-Cruz et al. (2020) with a mixture (ratio 1:1) composed by NaOH (5% w/v) and H₂O₂ (16% w/v) and a solid-liquid ratio of 1:40 for 1.5 h at 55 °C under agitation at 200 rpm orbital shaker. The hydrolysed solids were carefully filtered using muslin cloth and washed two times with deionized water. The solid materials were oven-dried during 12 h at 55 °C and grinded (particle size \leq 250 mm).

8.2.4.2 Thermo-alkaline method

Melon peel residues were subjected to a thermo-alkaline treatment in an autoclave with

NaOH (2% w/v) in a solid-liquid ratio of 1:10 for 1 h at 100 °C. The hydrolysate was cooled (15 min) under water bath and then vacuum-filtered using two layers of muslin cloth and the remaining solids were washed with distilled water until the elimination of the dark alkaline liquor and reach neutral pH. The solids were oven-dried during 12 h at 55 °C and grinded (particle size ≤ 250 μm). Bleaching step was carried out twice as described above in section 8.2.4.1.

8.2.5. Microcrystalline cellulose (MCC) from cellulose of melon residues

The MCC was obtained by acid hydrolysis of the bleached cellulose obtained from each melon residues using H_2SO_4 (30% w/v) in a solid-liquid ratio of 1:20 for 2 h at 80 °C under agitation at 200 rpm in orbital shaker. After, the mixture was diluted 10-fold with water at room temperature to stop the reaction and vacuum-filtered using muslin cloth and the hydrolysed solids were washed with deionized water until the excess of acid was removed. Afterward, the resulting mixture was put under ice-water bath and sonicated at 70% intensity in a VCX 130 ultrasonicator (Sonics and Materials, Newtown, USA) for 5 min. The colloidal sample was stored at -80 °C until its freeze-drying process. The yield of MCC extraction (YMCC) was calculated according to the equation 8.1. The graphic flow chart for the obtention of MCC from melon peel residues is displayed in **Figure 8.2**.

$$\%YMCC = \frac{\text{mass of the freeze dried MCC (g)}}{\text{mass of the melon residues after cellulose bleaching (g)}} * 100 \quad (8.1)$$

8.2.6. X-Ray Diffraction

Tests were run in a Powder X-Ray Diffraction Analyses (PXRD), performed on Rigaku MiniFlex 600 diffractometer with Cu $\text{K}\alpha$ radiation, with a voltage of 40 kV and a current of 15 mA ($3^\circ \leq 2\theta \leq 60^\circ$; step of 0.01 and speed rate of 3.0°/min). The degree of crystallinity (DC) was calculated as the ratio of the areas under the crystalline peaks to the total area.

8.2.7. FTIR

Tests were performed in a spectrometer (Spectrum 400 Perkin- Elmer FTIR/FIR, USA). The spectra were collected in the range of 500 to 4000 cm^{-1} , with a resolution of 4 cm^{-1} and 64 scans per sample.

8.2.8. Scanning Electron Microscopy (SEM)

Morphology of melon MCC was evaluated by scanning electron microscopy (SEM) using a JEOL-5600 LV microscope (Tokyo, Japan). Briefly, a small amount of freeze-dried sample was placed over an observation stub covered with double-sided adhesive carbon tape (NEM tape; Nisshin, Japan) and then coated with gold/palladium (Au/Pd) using a Sputter Coater (Polaron, Bad Schwabach, Germany). SEM was operated at high-vacuum mode, using an accelerating voltage of 15-20 kV.

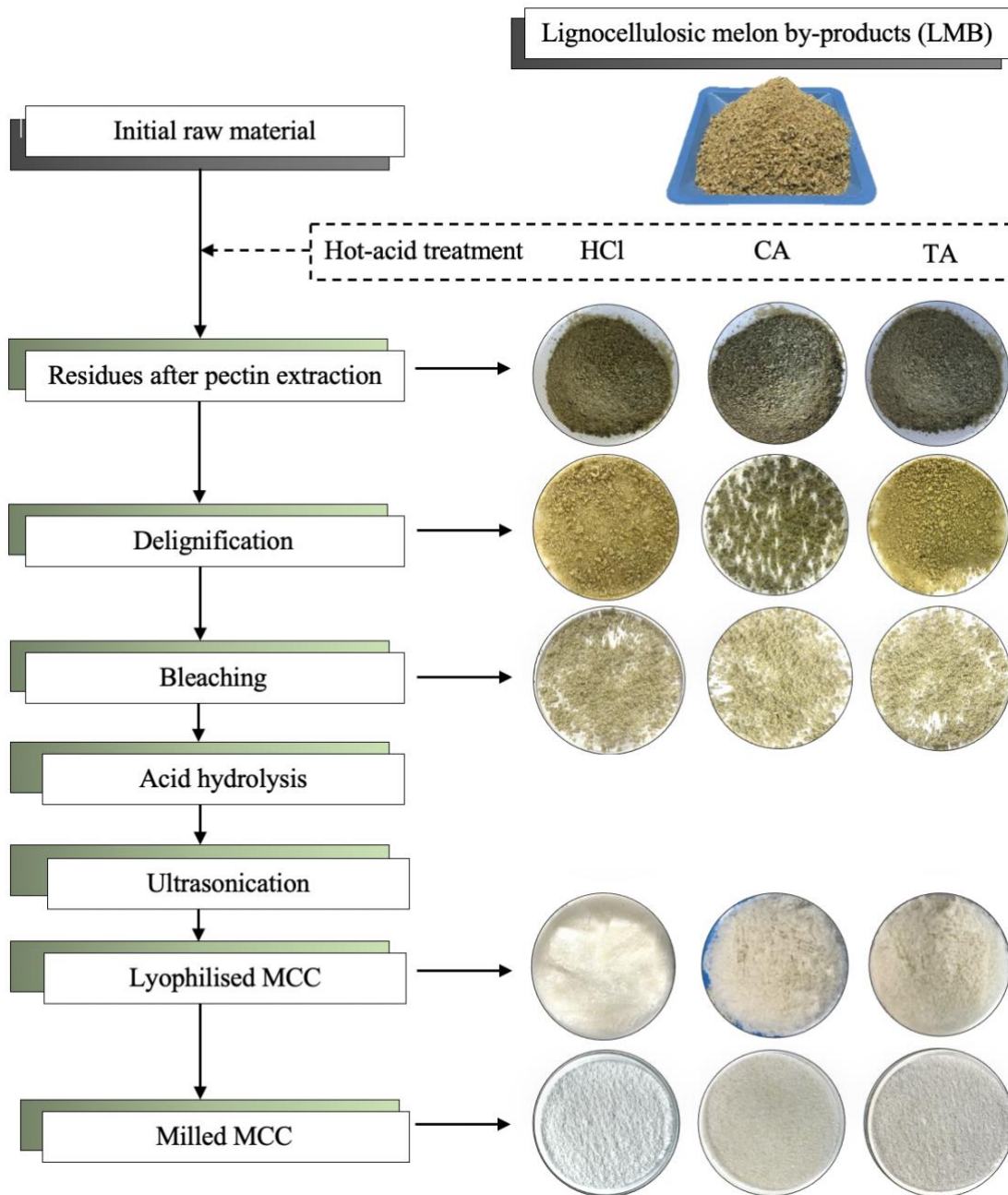


Figure 8.2. Flow diagram of the process to obtain microcrystalline cellulose (MCC) from melon residues through thermo-alkaline double-bleaching process. HCl: hydrochloric acid; CA: citric acid; TA: tartaric acid.

Results and discussion

8.3.1. Chemical composition and structural changes of lignocellulosic melon by-products (LMB) after pectin extraction

The chemical composition of the melon peel (LMB) before and after the pectin extraction process is depicted in **Table 8.1**. As can be seen, the content of protein, fat and ash in RHCl, RCA and RTA decreased during the hot-acid treatment since most of these compounds are solubilized/dragged in the liquid medium during the treatment, demonstrating a higher solubility by the delocalization of electrons in the complex polysaccharide matrix. These electrons increase the interface with the liquid medium in hydrothermal conditions and therefore increments the total fibre content from 37.10% in LMB to 49.60%, 55.51% and 77.71% for RCA, RTA and RHCl, respectively. Dietary fibre is classified as water-soluble (pectin) and water-insoluble fibres structured by cellulose, hemicellulose and lignin. In this regard, LMB showed a composition of 24.24% of cellulose, 12.05% of lignin and 11.04% of hemicellulose, which was incremented after pectin extraction, ranging from 40.13-58.84%, 21.33-27.50% and 18.39-29.46% for cellulose, hemicellulose and lignin, respectively (**Table 8.2**). These increments were observed since pectin was successfully removed from the melon peel by-products (data not shown) by the combination of elevated temperature and vigorous thermal agitation, which result in the breakdown of hydrogen bonds and other intermolecular interaction. These interactions enhance the dissolution of pectin in water (Banerjee et al., 2018), resulting in lignocellulosic melon biomass free of impurities for the extraction of MCC. Cellulose contents are comparable to that of some different sources, for example, natural wood (48.30%) (Wu et al., 2019) and higher than banana peels (23.37%) (Palacios et al., 2017), citrus peels (34.80%) (John et al., 2017) and mango seed (39.00%) (Banerjee et al., 2018). Cellulose, hemicellulose and lignin contents are high owing also to the removal of pectin from the initial sample (LMB), which concentrates the structural components. The removal of extractives could allow an easier and fast cellulose extraction from the plant matrix with less usage of corrosive agents. Also, lignin seems to be slightly removed during pectin extraction helping in extraction a purified cellulose.

Table 8.1. Chemical composition of the melon peel residues after pectin extraction.

Component (%)*	LMB	RHCl	RCA	RTA
Moisture	7.89 ± 0.51	11.12 ± 1.13	11.46 ± 0.46	12.16 ± 0.63
Total protein	8.80 ± 0.19	4.76 ± 0.24	2.77 ± 0.96	2.98 ± 0.13
Fat	1.74 ± 0.92	0.46 ± 0.16	0.67 ± 0.11	0.87 ± 0.47
Ash	1.67 ± 0.82	0.99 ± 0.11	1.16 ± 0.43	1.04 ± 0.19
Total carbohydrates**	79.90 ± 0.55	82.76 ± 1.29	83.94 ± 1.53	82.95 ± 1.89
Total fibre	37.10 ± 0.15	77.71 ± 0.56	49.60 ± 0.26	55.51 ± 0.34
Insoluble dietary fibre	35.51 ± 0.19	73.24 ± 0.45	46.67 ± 0.21	49.55 ± 0.47
Soluble dietary fibre	1.60 ± 0.10	4.47 ± 0.95	2.99 ± 1.33	5.96 ± 0.16

LMB: Lignocellulosic melon by-products; Residues from HCl: hydrochloric acid; CA: citric acid; TA: tartaric acid. All determinations were carried out in triplicated and mean value ± standard deviation. *Results are expressed in % of dry matter basis (g/100 g DM). **Total carbohydrates content was obtained by difference.

Table 8.2. Proximal structural composition of melon peels residues after pectin extraction with different acid agents.

Component (g/100 g DM)	LMB	RHCl	RCA	RTA
Cellulose	24.24 ± 3.01	58.84 ± 6.00	40.13 ± 6.47	42.74 ± 7.03
Hemicellulose	11.04 ± 1.92	27.50 ± 2.24	21.33 ± 1.88	22.81 ± 3.08
Lignin	12.05 ± 1.53	29.46 ± 2.14	18.39 ± 0.72	20.4 ± 0.76

LMB: Lignocellulosic melon by-products; Residues from HCl: hydrochloric acid; CA: citric acid; TA: tartaric acid; DM: dry matter. All determinations were carried out in triplicated and mean value ± standard

8.3.2. Microcrystalline cellulose (MCC) extraction and structural composition

As can be appreciated in **Figure 8.2**, the untreated dry melon fibres (LMB) presented an initial light yellow-brown colour that changed to dark green after hot-acid treatment, yellow-like after delignification process by thermo-alkaline method and became white after acid hydrolysis. The change in colour of the LMB from dark green to white indicates the effective removal of lignin from the melon fibres. The mass yield of the LMB through each step of both extraction process indicates the successive recovery of the biomass throughout the obtention of MCC (**Table 8.3**). Samples treated by the thermo-alkaline process obtained the highest value of bleached fibres for RHCl (53.67%) followed by RCA (49.81%) and RTA (43.39%). However, RCA sample treated by the traditional process (4.5% NaOH) had the highest bleaching yield 77.84% followed by RTA (77.04%) and RHCl (71.59%). After freeze-drying, a cellulose biomass visualised as white-spongy fibres were obtained (**Figure 8.2**.) In this step, the maximum yields obtained were 13.04% and 23.81% for HCl by thermo-alkaline and traditional process, respectively. These yields are similar with some already described in literature for acid hydrolysis of cellulose from other sources, e.g., 12.10% from tea waste (Zhao et al., 2018), 14.60% from lemon seeds (Zhang et al., 2020) and 26.10% from corncob (Vallejo et al., 2021), but lower compared to 27.24 and 32.12% from corn and sugarcane,

respectively (Harini and Chandra Mohan, 2020) and 53.60% from bamboo (Kharismi et al., 2018). Factors such as concentration of acid, temperature and reaction time are critical parameters to keep under constant control during the acid hydrolysis because such hydrolysis in many cases depends on the plant material, for example high acid concentrations can destroy cellulose fibres, for this, it is preferably performed it under mild conditions at low temperature (<90 °C) and low acid concentrations (<70%) to avoid cellulose deterioration, but in other cases these conditions are not able to complete the dissolution of amorphous cellulose region. In our particular case, all the conditions used in this study were implemented based on these reported factors, employing 80 °C and 30% of acid concentration as improved conditions for melon fibres hydrolysis. Therefore, to the best of our knowledge, these results on melon MCC were for the first time obtained from melon peels residues after pectin extraction, within the framework of biorefinery approach. **Table 8.4** shows the structural composition, ash and moisture content of MCC obtained from the treatment of melon peel residues (RHCl, TCA and RTA) by thermo-alkaline and traditional processes. Microcrystalline cellulose-RHCl had the highest content in cellulose (48.34% and 55.03%), followed by MCC-RTA (46.31% and 52.51%) and MCC-RCA (44.89% and 51.40%). Lignin content was highly reduced in all the MCC samples, reaching values below 4.00% and even lower than 3.00% by thermo-alkaline and traditional processes, respectively. This indicates that the mixture between NaOH and H₂O₂ effectively removed most of the lignin present in the untreated LMB fibres. The moisture content is an important parameter that should be considered, when determining if a natural material is an appropriate filler for polymer composites, as it influences the functionality and mechanical properties of MCC. The permissible maximum moisture content is estimated at <7.00%, according to the United States Pharmacopoeia (USP), since larger contents could negatively affect the fibres and the properties of the polymer composites or material where MCC could be incorporated (Beroual et al., 2021). Thus, these melon MCC samples obtained by both processes that presented lower moisture content (3.90 to 5.23%) are within the limit recommended and are comparable to 5.80% reported for MCC from *Posidonia oceanica* algae, obtained by acid hydrolysis. Also, ash content was comparable to 2.00% for pineapple peels (Madureira et al., 2018) and lower than 8.80%, 11.85% and 14.30% for walnut shell, corncob and sugarcane bagasse, respectively (Harini and Chandra Mohan, 2020).

Table 8.3. Mass yields (%)* obtained after each successive chemical treatment.

Step	Treatment					
	Thermo-alkaline (2% NaOH-DB)			Traditional (4.5% NaOH)		
	RHCl	RCA	RTA	RHCl	RCA	RTA
Residues after pectin extraction	39.21 ± 1.52	63.12 ± 3.88	57.83 ± 5.32	39.21 ± 1.53	63.12 ± 3.90	57.83 ± 5.34
Delignification	77.50 ± 4.21	83.54 ± 4.01	69.42 ± 5.41	53.66 ± 3.84	41.74 ± 5.31	40.18 ± 7.65
Bleaching	53.67 ± 1.94	49.81 ± 2.63	43.39 ± 1.25	71.59 ± 1.42	77.85 ± 3.73	77.04 ± 2.28
Acid hydrolysis (L-MCC)	13.04 ± 0.86	8.02 ± 0.53	10.15 ± 0.94	23.81 ± 1.07	19.23 ± 1.33	14.66 ± 1.75

Residues from HCl: hydrochloric acid; CA: citric acid; TA: tartaric acid; L-MCC: lyophilised microcrystalline cellulose; DB: double-bleaching. *Results are expressed in % of dry matter basis (g/100 g DM).

Table 8.4. Proximal structural composition of microcrystalline cellulose (MCC) from melon residues.

MCC component (g/100 g DM)	Treatment					
	Thermo-alkaline (2% NaOH-DB)			Traditional (4.5% NaOH)		
	RHCl	RCA	RTA	RHCl	RCA	RTA
Cellulose	48.34 ± 4.15	44.89 ± 6.19	46.31 ± 3.32	55.03 ± 3.12	51.40 ± 5.4	52.51 ± 4.61
Hemicellulose	27.21 ± 2.63	23.45 ± 3.87	25.83 ± 3.13	36.21 ± 1.36	29.20 ± 3.9	33.31 ± 5.18
Lignin	2.53 ± 1.18	3.54 ± 3.05	2.24 ± 5.45	1.76 ± 0.81	2.71 ± 0.32	1.84 ± 0.56
Ash	1.21 ± 0.66	2.22 ± 0.51	1.93 ± 0.25	0.94 ± 0.41	1.74 ± 0.77	1.32 ± 0.22
Moisture	4.43 ± 0.63	5.23 ± 0.72	4.10 ± 0.93	3.90 ± 0.21	4.14 ± 1.41	4.06 ± 1.08

Residues from HCl: hydrochloric acid; CA: citric acid; TA: tartaric acid; DB: double-bleaching.

8.3.3. X-ray diffraction

Figure 8.3 shows the diffraction profiles of the LMB, melon residues (RHCl, TCA and RTA) and MCC samples obtained by both processes. The untreated LMB fibres had a less concentrated cellulose (please see **Table 8.2**), showing thicker and less defined peaks, while the RHCl showed a pattern typical of cellulose and an increment in the intensity of the peaks, suggesting that the cellulose became more available after the hot-acid treatment with this acid (**Figure 8.3A**). As for the RCA and RTA samples, showed irregular profiles with small peaks, which could be attributed to the presence of some salts or minerals embedded in the fibres of these residues derived from the hydrolysis with citric and tartaric acids (**Figure 8.3C and E**, respectively). The individual diffraction patterns of the MCC from alkaline treatments and untreated LMB fibres occurred at 2θ angles of 15.70 , 22.31 and 34.98° , and can be ascribed to the crystallographic planes (101), (002) and (040), respectively (**Figure 8.3B, D and F**), which are consistently characteristic of Type I cellulose (native cellulose) (Hajlaoui et al., 2020; Abu-Thabit et al. 2020). All related diffraction angles in all the samples from the delignification until the bleaching processes might indicate that the cellulose kept its structure intact. In this case, the diffraction peak at 22° showed sharper and its intensity increased as well, which indicates an improved crystallinity in the structure of MCC regarding the starting material (LMB). For example, all the MCC samples obtained from RHCl, RCA and RTA showed an intensity increment in their profiles and better-defined peaks (without impurities) after the bleaching step (**Figure 8.3B, D and F**), evidencing the crystalline nature of the treated melon cellulose fibres. The presence and defined patterns in the MCC samples could suggest that the chemical process did not alter the crystalline structure of cellulose fibres. The cellulose type I can be altered to dissimilar polymorphs by an alkaline treatment (NaOH) known as mercerization and the cellulose type II chains have an antiparallel arrangement with the ability to produce improved structures. It is fundamental to know how the structure, the morphology and the crystallinity of the melon fibres are transformed after each treatment. The degree of crystallinity (DC) was determined for the untreated LMB, melon residues (RHCl, RCA and RTA) and their respective MCC (**Table 8.5**). The DC was calculated from the height ratio between intensity of crystalline peak and total intensity of non-crystalline peak using the equation reported by Segal et al. (1959) ($DC = (I_{200} - I_{am})/I_{200}$), where DC is crystallinity, I_{200} is the maximum intensity of the peak, and I_{am} the intensity of diffraction of the non-crystalline material. The DC increased after the hot-acid treatment, starting with 31.82% for the LMB to 42.35-47.75%

for melon residues. Also, the DC of MCC samples after one bleaching treatment increased (47.03-52.01%), but values were slightly lower when compared with the traditional process (54.80-55.07%). These results could be attributed to the higher concentration of NaOH used for traditional method (4.5%) than the thermo-alkaline one-bleaching step (2%), making more efficient the solubilization of the lignin and consequently given an increment on cellulose crystallinity (Wu et al., 2019; Haldar and Purkait, 2020). After the double bleaching step, a higher value of DC was obtained (51.51-61.94%), representing a higher percentage than the traditional process (54.80-55.07%). These results could be attributed to the extra removal of the non-cellulosic components that may still linked in the amorphous regions of the fibres. The DC of the bleached MCC from melon residues was in the range of previous reports for other vegetable materials e.g., 22.20-56.20% from rose stems (Ventura-Cruz and Tecante, 2019), 44.00% from sago seed shell (Naduparambath et al., 2018), 62.00% from palm seeds (Abu-Thabit et al., 2020), 62.50% from bamboo (Rasheed et al., 2020). Diverse researchers have described those drastic conditions of acid concentration and time, not only hydrolyse the amorphous regions of cellulose, but can deteriorate the crystalline regions, resulting in a less quality MCC (Liu et al., 2016; Naduparambath et al., 2018; Beroual et al., 2020). In this respect, the melon MCC samples obtained seemed to not be affected by the conditions implemented in this study and falls within the crystallinity range of the commercial MCC, which is in the range of 55–80%.

Table 8.5. Degree of crystallinity (%DC) of the melon samples treated with the different processes

Sample	Treatment (%DC)			
	Hot-acid process (Residues)	Thermo-alkaline (2% NaOH)	Thermo-alkaline (2% NaOH-DB)	Traditional (4.5% NaOH)
LMB	31.82 ± 1.53			
MCC-HCl	47.75 ± 0.34	52.01 ± 0.30	61.94 ± 0.59	54.80 ± 5.58
MCC-CA	42.35 ± 0.53	49.72 ± 1.44	51.51 ± 0.97	54.87 ± 1.08
MCC-TA	44.13 ± 0.24	47.03 ± 1.92	56.53 ± 0.60	55.07 ± 0.41

LMB: lignocellulosic melon by-products; MCC: microcrystalline cellulose from HCl: hydrochloric acid; CA: citric acid; DB: double-bleaching; MCC represent the final dried and milled samples.

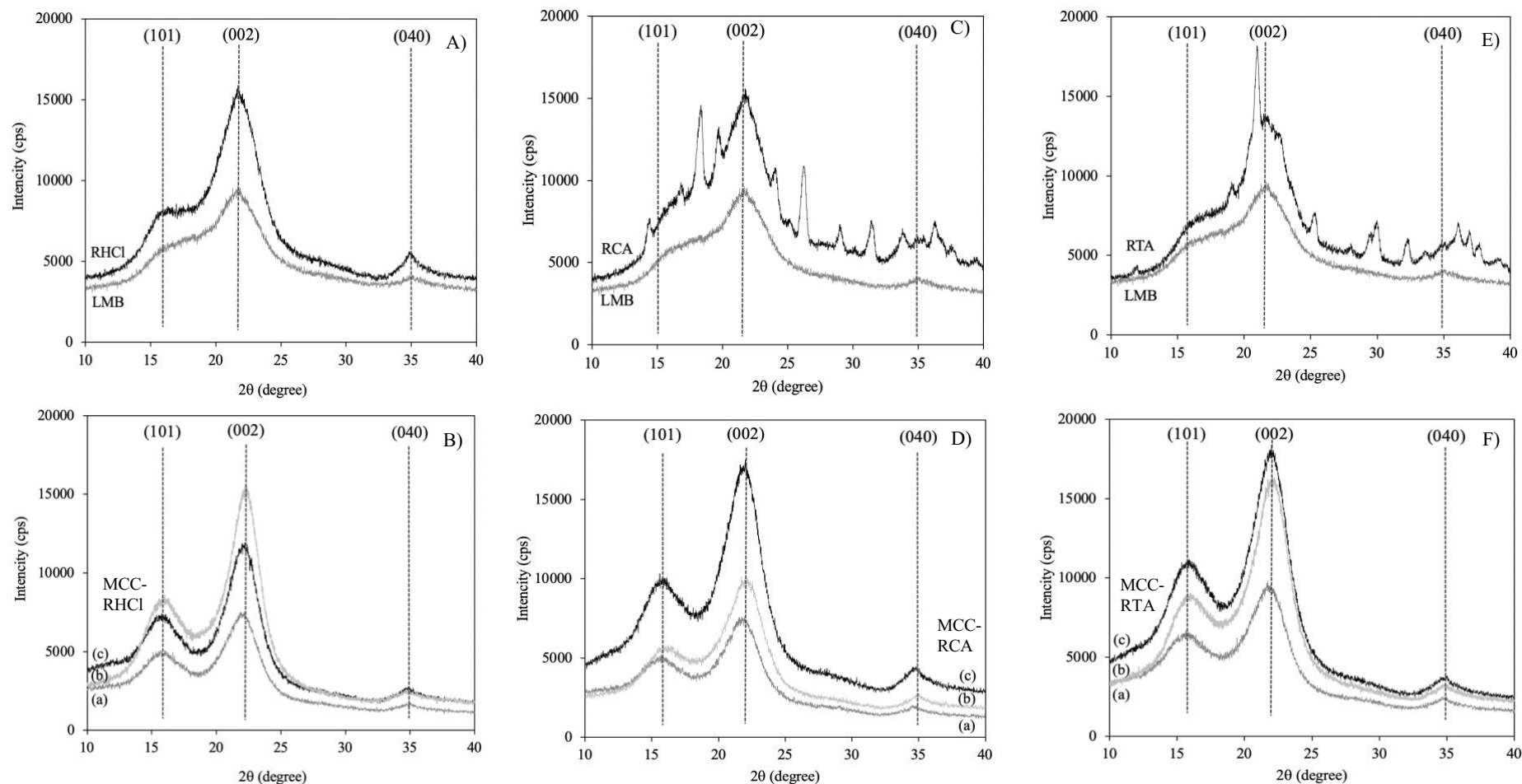


Figure 8.3. X-ray diffraction patterns of lignocellulosic melon by-products (LMB), melon residues after hot-acid treatment with A) hydrochloric acid (RHCl), C) citric acid (RCA) and E) tartaric acid (RTA) and their microcrystalline cellulose (MCC) B), D) and F), respectively, obtained through the (a) thermo-alkaline, (b) thermo-alkaline double-bleaching and (c) traditional treatments.

8.3.4. FTIR

The spectra of LMB, melon residues (RHCl, TCA and RTA) and MCC samples are shown in **Figure 8.4**. During the transition from macro- to micro- materials, the alterations are controlled by variations in the hydroxyl and carboxyl zones and those related to lignin structure (Moriana et al., 2016). In the FTIR spectrum of LMB, melon residues and MCC samples (**Figure 8.4A, B, C and D**), the peak positioned at 3333.2 cm^{-1} falls inside the range of $3335\text{-}3350\text{ cm}^{-1}$, which correspond to the stretching vibrations O-H in cellulose (Naduparambath and Purushothaman, 2016). The increase in the peak suggests an increase in cellulose composition and removal of lignin polymer after acid hydrolysis. Harini and Chandra Mohan, (2020) isolated micro- and nanocrystalline cellulose from different plant-based sources such as walnut shell, corncobs and sugarcane bagasse and also reaffirmed the same behaviors in the intensification of peaks between 3500 and 3200 cm^{-1} associated to the removal of the lignin and subsequently, giving rise highly crystalline cellulose fibres. Also, the increase of the intensity of this absorption band after acid hydrolysis could be attributed to the elimination of the amorphous components, increasing hydrogen bonding between cellulose chains. The peak between $2850\text{-}2900\text{ cm}^{-1}$, positioned at 2894.7 cm^{-1} in all the spectrum of melon samples corresponds to C-H stretching vibrations (Madureira et al., 2018). The band observed at 1730.1 cm^{-1} is originated from the acetyl and ester groups in hemicellulose, or carboxylic acid groups of the phenolic compounds linked to lignin, and the peaks at $1450\text{-}1600\text{ cm}^{-1}$ correspond to stretching structures of the aromatic groups of lignin (Liu et al., 2016; Madureira et al., 2018). Moreover, the small peaks ranging from 1100 and 1500 cm^{-1} were attributed to proteins (Zhao et al., 2018). The peak at 1730.1 cm^{-1} was present in the spectrum profile of the LMB, which was intensified in all the residues (RHCl, RCA and RTA) by the hot-acid treatment and after the one bleaching step the peak is still present, indicating the presence of hemicellulose in the MCC samples. However, in the spectrum of the MCC samples obtained after double bleaching and traditional process, the hemicellulose peak disappeared, showing the elimination of hemicellulose from melon MCC during chemical extraction. This peak observed at 1730.1 cm^{-1} is related to the C=O bonds of unconjugated ketones present in hemicellulose (Zhang et al., 2016; Zhao et al., 2018). This result could indicate that the thermo-alkaline treatment by autoclave 2% NaOH was more efficient to remove hemicellulose from melon fibres than the traditional process.

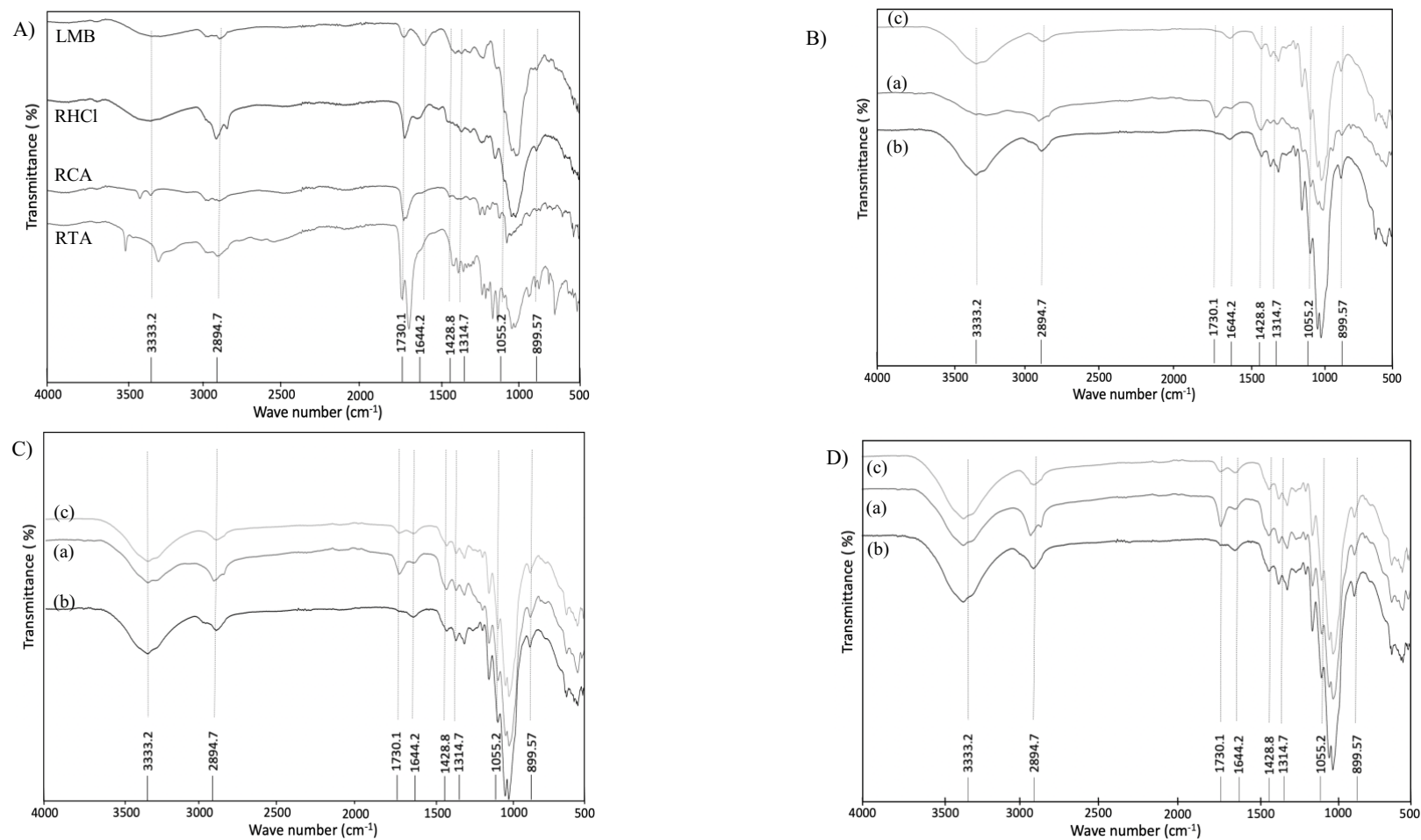


Figure 8.4. Spectrums of A) lignocellulosic melon by-products (LMB) and melon residues after hot-acid treatment and microcrystalline cellulose (MCC) from B) RHCl, C) RCA and D) RTA through the (a) thermo-alkaline, (b) thermo-alkaline double-bleaching and (c) traditional treatments.

The peak at 1600 cm^{-1} in the spectrum of MCC samples were attributed to the C=C bond extending from the aromatic ring of lignin and the peaks near to 1055.2 , 1314.7 and 1428.8 cm^{-1} were associated with C-O stretching, C-O-C asymmetric stretching and C-H oscillating vibrations of cellulose, respectively, appearing in all of the spectra and were increased during the extraction process (Ahmadi et al., 2015; Madureira et al., 2018; Vallejo et al., 2021). The peak at 899.57 cm^{-1} represents the glycosidic deformation -C₁-O-C₄, characteristic of the β -glycosidic bond of cellulose (Zhang et al., 2020). This peak showed the typical characteristics of cellulose structure and its existence was normally observed in the FTIR spectrum of microcrystalline cellulose obtained with chemical methods involving alkaline-bleaching-acid hydrolysis, from lemon seeds (Zhang et al., 2020), esparto grass (Beroual et al., 2020) and corn, grape, pomegranate, strawberry (Vallejo et al., 2021) as well as in the commercial MCC (**Figure 8.5**).

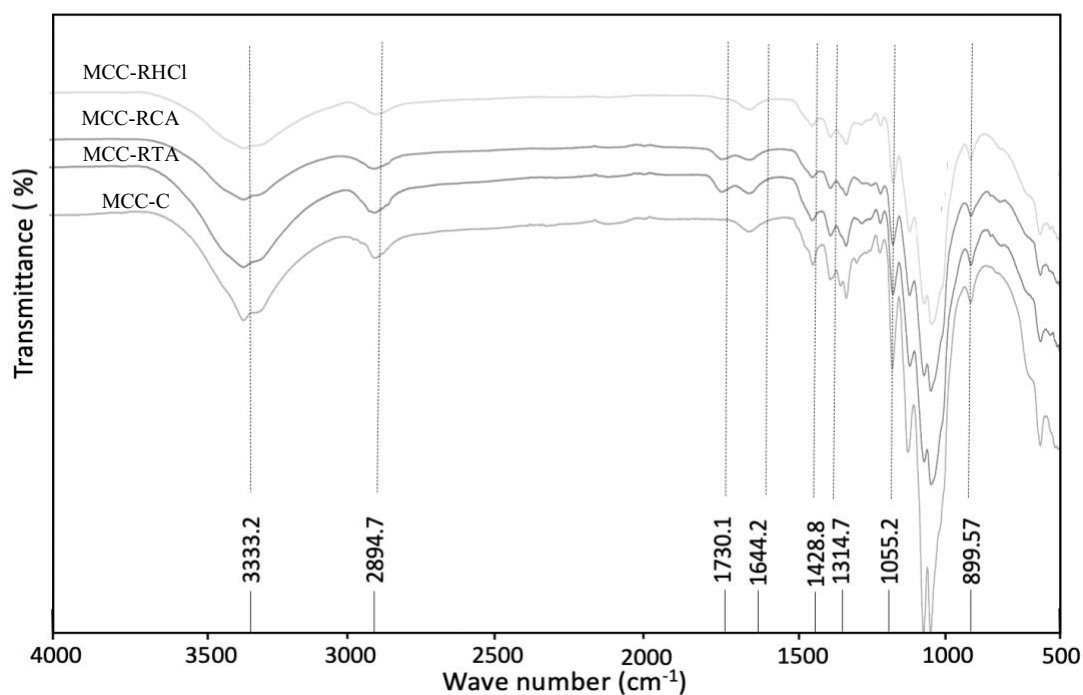


Figure 8.5. Spectrum of microcrystalline cellulose (MCC) obtained by thermo-alkaline double-bleaching process from melon residues compared to commercial microcrystalline cellulose (MCC-C).

8.3.5. SEM

The morphologies of LMB and MCC samples are shown in **Figure 8.6**. The structure of LMB (**Figure 8.6A**) presents a well-closed and agglomerated structure with a protective

layer covering the grooves of the fibre structure. Besides, untreated LMB sample had pectin, globular wax particles, and extractives, in addition to lignin and hemicellulose. Significant alterations in morphology were observed in the MCC samples obtained from RHCl, RCA and RTA (**Figure 8.6B, C and D**, respectively), in which the fibres became more exposed after two bleaching treatments, due to effective removal of the lignin matrix, and separated into individual fibres, showing microcrystals formation with numerous micropores, cylindrical shapes, and fissured and rough surfaces. This was probably produced by the penetration of H₂SO₄ acid solution into the amorphous regions of cellulose during the acid hydrolysis process and breakdown the β -1,4-glycosidic linkage between the cellulose repeating units and, subsequently, undergoing fragmentation to form smaller size of cellulose microcrystals (Kian et al., 2020). Microcrystalline cellulose are particles of hydrolysed cellulose, comprising a very large amount of cellulose micro-crystals together with amorphous areas. Micro- and nano-porosity is an outstanding characteristic with potential in pharmaceutical and biomedical applications for tissue engineering and biomaterials developments (Ahmadi et al., 2015; Sharma et al., 2018). Microcrystalline cellulose with high micro- and nano- porosity could be useful as potential active site for cell growth and blood vessel invasion as well as tablet filler, binder-disintegrant and drug carrier due to their large surface area and high moisture retaining property (Liu et al., 2016; Kargarzadeh et al., 2017). The possibility of using this porous material as a sustainable functional additive/ingredient is a current investigation trend for the development of hydrogels or pharmaceutical tablets for drug delivery. For efficient drug delivery, pharmaceutical tablets must disintegrate in a short period without delay so that the liberated active drug is available for dissolution and hence, immediate absorption (Chaerunisaa, et al., 2019). For example, Pachuau et al. (2019) extracted and used MCC from *Ensete glaucum* with 53.41% crystallinity and high porosity for tablets formulation, highlighting its ability to produce adequately hard, yet rapidly disintegrating tablets, which was attributed to the swelling of its particles and consequent decrease of the bonding forces holding them together. Therefore, melon peels could be applied as raw material with low cost for the obtention of MCC, which could be an emerging prototype of an engineered material with a great application because of the properties showed, associated with its potential biodegradability, biocompatibility, low toxicity and excellent mechanical properties.

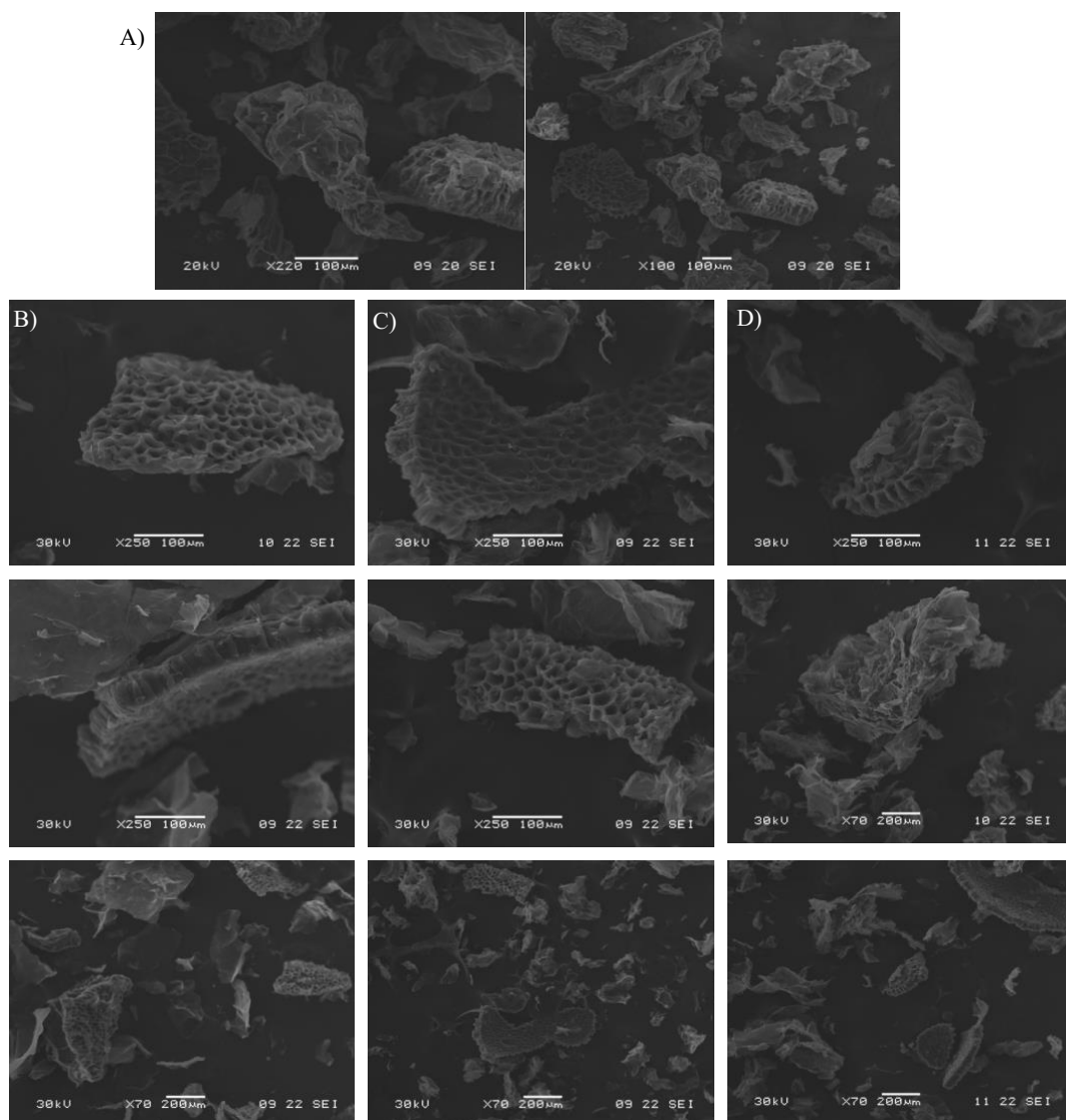


Figure 8.6. Micrographs of A) LMB and freeze-dried MCC from B) RHCl (left-row), C) RCA (middle-row) and D) RTA (right-row) through the thermo-alkaline double-bleaching treatment.

8.4. Conclusions

The results showed that melon residues can be used as bioresource to obtain partially microcrystalline cellulose. As expected, the traditional process allowed to eliminate more precisely the non-cellulosic constituents but using the thermo-alkaline process with double bleaching step allowed a better elimination of impurities, resulting in a purer MCC with higher degree of crystallinity (61.94%) than the traditional process (54.80%). Overall, both methods allowed the reduction of the lignocellulosic melon fibres to the microscale as observed in the SEM micrographs. The microstructure with high porosity and the degree of crystallinity of the final white powder could highlight its potential applications as an additive in the formulation of novel biocomposites.

RT IV – Green chemistry approach and application

CHAPTER 9 – Biological protein precipitation: a green process for the extraction of cucumisin from melon (*Cucumis melo* L. *inodorus*) by-products

Ricardo Gómez-García^{a,b}, Débora A. Campos^a, Cristóbal N. Aguilar^b, Ana R. Madureira^a and Manuela Pintado^{a*}

^a*Universidade Católica Portuguesa, CBQF – Centro de Biotecnologia e Química Fina – Laboratório Associado, Escola Superior de Biotecnologia, Rua Diogo Botelho 1327, 42169-005 Porto, Portugal*

^b*BBG-DIA. Bioprocesses and Bioproducts Group. Food Research Department, School of Chemistry, Autonomous University of Coahuila, Saltillo, Coahuila, Mexico.*

Published:

Journal of Food Hydrocolloids - ELSEVIER

Abstract

Cucumisin (CUC) from industrial melon by-products was separated for the first time through biological precipitation using carrageenan (CRG). This approach could represent a cost-effective and environmentally friendly process for the industries, avoiding the use of expensive equipment and toxic salts or solvents, such as butanol and ethanol. In this study, biological precipitation of proteins from melon by-products using CRG was studied and compared with conventional precipitation with ammonium sulphate. Different methods were applied for the identification and characterization of isolated proteins, including SDS-PAGE gel, FPLC and proteolytic activity assays. The isolated CUC confirmed a molecular weight of 68 kDa and showed highly stable proteolytic (PA) and milk-clotting (MCA) activities in a wide range of CaCl₂ (20 to 60 mM), pH (5 to 7) and temperatures (30 to 85 °C). Melon peel extract demonstrated to possess significant PA (4.24 U/mg protein) and MCA (191.50 MCU/mg protein), but such values were increased by ammonium sulphate precipitation (1.60 and 2.06-folds, respectively), and specially a noticeable increment was observed by biological precipitation with 2.11 and 17.65-folds, respectively, demonstrating the capability to be an effective strategy to isolate and purify CUC, allowing a yield of 0.17 g CUC/100 g of by-products and keeping its biological properties.

Keywords: Biological precipitation, cucumisin, melon by-products, milk-clotting and proteolytic enzyme, polyelectrolyte

9.1. Introduction

Globally, 1.3 billion tonnes of food by-products are generated mainly by the food producers and processing industries with an estimated economic loss of 990 billion dollars. In 2017, Europe generated 96 million metric tonnes of fruits and vegetables, corresponding to 8.5% of the global production and around 30% of such production has been rejected as by-products (Trigo et al., 2019; Campos et al 2020b). These by-products are poorly managed and discarded in landfills, causing environmental pollution and economic issues (Yousuf, Bonk, and Schmidt, 2016). In this context, melon fruit (*Cucumis melo* L.) is one of many examples related with fruit by-product generation, due to its high industrialization, producing great number of food products, such as juices, ready to eat salads, snacks, among other products. These industrial activities lead to an overproduction of melon by-products mainly seeds and peels, with around 8 to 20 million tonnes of melon by-products per year, which despite on their richness of nutritional and bio-functional compounds are still mismanaged or ignored (Rolim, Seabra, and de Macedo, 2019; Gómez-García et al., 2020).

Currently, food by-products management has been recognized by the circular economy as one of the principal keys to reduce environmental and economic problems. Based on this fact, during the last decade biotechnological efforts have increased, focusing on the valorisation of food by-products, since they have been well-reported to keep high concentration of value-added biomolecules, such as proteolytic enzymes. In this regard, cucumisin (CUC) is an extracellular serine protease with molecular weight of 67 kDa, already purified from different Cucurbitaceae plants and characterized as plant subtilisin (Murayama et al., 2012). Serine proteases are one of the largest groups of proteolytic enzymes involved in several biological processes. Moreover, CUC is well-recognized as milk-clotting enzyme. Such enzymes are used in cheese making for promotion and regulation of milk coagulation properties (Ben Amira, A., Besbes, S., Attia, H., and Blecker, 2017). Based on its biological properties, many studies tested different techniques to isolate and extract this enzyme from melon juice. Traditional methods include precipitation with ammonium sulphate, ultrafiltration or gel and affinity chromatography, however such techniques have some disadvantages related with toxicity, high implementation costs and difficult to scale up (Galanakis, 2012). Biological precipitation using natural polyelectrolytes is a well-documented extractive method, which represent a non-toxic, low cost and efficient green-technological process for protein extraction which release proteins conserving its structure and biological activity

(Woitovich, Brassesco and Picó, 2016). Polyelectrolytes interact with proteins in solution arising soluble or non-soluble complex by the modification of pH or ionic strength, forming a semisolid (gel) mixture between proteins and polyelectrolyte, which then is precipitated by centrifugation (Campos et al., 2017). Carrageenan (CRG) is a natural polyelectrolyte obtained from certain species of red seaweed and is considered non-toxic and a water-soluble compound. This compound is well accepted in cosmetic, pharmaceutical and food industries. Recently, researchers from our group, successfully used CRG as precipitant agent to isolate and extract bromelain enzyme from pineapple by-products (Campos et al., 2019). Hence, the present research work tested this polyelectrolyte with CUC, since there are no studies regarding the molecular mechanism of complex formation between both compounds, and it is a good opportunity to develop a green process for precipitation of this enzyme.

9.2. Materials and methods

9.2.1. Chemicals

Azocasein, iota (ι)-carrageenan and all the other reagents of analytical grade were purchase from Sigma–Aldrich (St. Louis, Missouri, USA). Bradford Bio-Rad assay from Biorad (Hercules, CA, USA). Skim milk was obtained from NILACTM (NIZO, Ede, The Netherlands).

9.2.2. Raw material - Melon peels

Melon fruits (*Cucumis melo* L. *inodorus*) were harvested (ripening stage was not controlled) from the Alentejo region in Portugal and processed by Nuvi Fruits S. A. Company Torres Vedras (Portugal), during the season of summer in August – September 2018. Fresh melon peels were generated as by-products and then transported to our facilities (Centro de Biotecnologia e Química Fina - CBQF) at -20 °C. The peels were kept at -20 °C until their processing and pre-treatment.

9.2.3. Melon peels juice (MPJ) preparation

Melon peels were processed as described previously by Gómez-García et al. (2021) and split in two fractions, fresh solid fraction (SF) and liquid fraction (LF), employing a commercial juice machine (HR1869/8, 900 W, Philips). The SF was manually pressed to recover the liquid excess, such liquid was mixed with the LF, which was subsequently

centrifuged (11469 g, 15 min, 4 °C), then the clarified supernatant was called as melon peels juice (MPJ). The MPJ was collected and kept at -20 °C until its analysis.

9.2.4. Protein precipitation with ammonium sulphate

Traditional salt precipitation with ammonium sulphate was applied to precipitate melon protein fraction from MPJ. The precipitation was carried out by saturation of 200 mL of MPJ with ammonium sulphate (60% w/v). MPJ was kept in constant stirring when the salt was added carefully, after total addition of salt, the mixture was kept in agitation during 1 h. Later, the mixture was subjected to centrifugation (11469 g, 15 min, 4 °C) and the pellet obtained was solubilized in sodium acetate buffer (0.1 M, pH 4.6) and dialyzed overnight against the same buffer (buffer was changed three times) using 14 kDa MWCO membrane. The clear mixture was freeze-dried and stored until its analysis. This fraction was called as MPJ-(NH₄) (melon peels juice precipitated with ammonium sulphate).

9.2.5. SDS-PAGE electrophoresis

Sodium dodecyl sulphate polyacrylamide gel electrophoresis (SDS-PAGE) was carried out using discontinuous gel, 12% (w/v) polyacrylamide for resolution gel and 6% (w/v) polyacrylamide for a stacking gel. Samples were analyzed employing a vertical system with running conditions for resolving gel established at 25 mA of intensity during 120 min. A standard mixture of proteins with a known molecular weight (precision plus protein dual color) obtained from Bio-Rad Laboratories (Hercules, CA, USA) was used for protein size estimation. Proteins were stained with Coomassie brilliant blue (0.25 %w/v). Protein patterns were then visualized after washing the gel with a destaining solution of 2.5:1 (v/v) acetic acid and methanol from Frilabo (Maia, Portugal), until protein bands became clearly visible in the colorless gel matrix.

9.2.6. Analysis by size exclusion chromatography (FPLC)

Protein profile was analyzed by gel filtration chromatography using the following conditions: the column was operated at a flow of 0.5 mL/min with phosphate buffer (0.025 M, pH 7) containing NaCl (0.15 M) and NaN₃ (0.02% w/v). Protein standards with known molecular weights (Thyroglobulin, 669 kDa; Ferritin, 440 kDa; Aldolase, 158 kDa; Conalbumin, 75 kDa; Ovalbumin, 43 kDa; Carbonic anhydrase, 29 kDa; Ribonuclease A, 13.7 kDa; Aprotinin, 6.5 kDa) were used to elaborate a calibration curve. AKTA pure 25 L system, from GE Healthcare Life Sciences (Freiburg, Germany), was

used with a configuration of two pumps with pressure control for column protection, a gel filtration column prepacked with Superdex® 200 10/300 GL connected in series with a column Superdex Peptide 10/300 GL (GE Healthcare Life Sciences, Freiburg, Germany) and an UV multiwavelength detection monitor U9-L, at a fixed wavelength of 280 nm. The software used to evaluate samples was UNICORN 7.0.

9.2.7. Turbidimetric titration curves vs pH

Turbidity of samples was measured at 420 nm. MPJ (10 mL) was mixture with phosphate buffer (8 mL, 0.1 M, pH 6) and CRG (at 0.001% (w/v) dissolved in ultrapure water). Medium pH modifications from 5.3 to 2 were performed by adding aliquots of HCl (0.1 M) and 5.3 to 12 with NaOH (0.1 M), leaving the system to equilibrate during 90 s before measuring the turbidity. These titration curves were made in order to estimate the pH range where the polyelectrolyte-protein complex was soluble or non-soluble (Valetti, Boeris, and Picó, 2013).

9.2.8. Turbidimetric titration curves with CRG

Formation of the CUC-CRG non-soluble complex was evaluated by the increment of turbidimetry in the solution. Briefly, 10 mL of MPJ were adjusted at pH 3 and titrated by adding successive aliquots (30 μ L) of CRG in solution (1 mg/mL) and the absorbance was recorded at 420 nm in a spectrophotometer (UV mini-1240, Shimadzu, Tokyo, Japan) at room temperature. To avoid changes in pH value during titration, both MPJ and CRG solutions were adjusted to pH 3, corresponding to the highest absorbance obtained by the complexation of CRG with proteins (section 2.5). The total CRG concentration on the mixture was plotted against the absorbance. The complex formation was followed in the absence and presence of different ionic strengths, adding NaCl to the medium.

9.2.9. Protein content determination

Total protein content (TPC) was determined by the Bradford, (1976) assay with a slight modification. Briefly, 0.05 mL of each sample was combined with 0.950 mL of Bradford's reagent at room temperature, the reaction was vortex mixed and then kept in darkness during 20 min. The absorbance was measured at 595 nm and the protein concentration was quantified with a calibration curve using bovine serum albumin (BSA) as standard. Results were expressed as mg BSA/mL. All the measurement was made in triplicated.

9.2.10. Proteolytic activity determination

Proteolytic activity (PA) was determined as described by Biondi, Maria, Paiva, Lúcia, and Vieira, (2003), using azocasein as substrate with slight modifications. Azocasein (1% w/v) was dissolved in Tris-HCl 0.2 M buffer in different ranges of pH (5, 6.5, 8, 9). In triplicate, the reaction was carried out with 0.1 mL of substrate mixed with 0.060 mL of sample at 37 °C in darkness during 1 h. Later, reaction was stopped by adding 0.480 mL of trichloroacetic acid (TCA) (10% w/v) and the precipitated protein was removed by centrifugation (16469 g, 5 min, 4 °C). A volume of 0.320 mL from the clear supernatant was mixed with 0.560 mL of sodium hydroxide (1 M) and the absorbance was measured at 440 nm. A blank was created by mixing TCA to the substrate prior to the sample addition. One unit (U) of enzyme activity was defined as the amount of enzyme able to hydrolyze azocasein, resulting in an increase of 0.001 units of absorbance per minute. The proteolytic recovery yield was defined according to equation 9.1:

$$Yield = \frac{PA_f}{PA_i} \quad (9.1)$$

Where PA_f is the proteolytic activity after the precipitation and PA_i is the initial proteolytic activity of MPJ. The purification factor (PF) was defined as equation 9.2:

$$PF = \frac{SPA_f}{SPA_i} \quad (9.2)$$

Where the SPA_f is the specific proteolytic activity after precipitation and the SPA_i is the specific proteolytic activity in the MPJ. The SPA was defined as equation 9.3.

$$SPA = \frac{PA}{TPC} \quad (9.3)$$

Where the TPC is the total protein content.

9.2.11. Milk-clotting activity

Milk-Clotting Activity (MCA) was determined by triplicated following the procedure described by Arima et al. (1970). Low-heat skim milk powder was reconstituted (10% w/v) in 10 mM aqueous CaCl₂ (pH 6.5). Enzyme extract was added a volume rate of 0.1 mL per mL of a pre-incubated milk (10 min, 37 °C). Test tubes containing the reaction were gently rotated by hand (at short time intervals) and time taken for solid clot formation was recorded. One Milk-Clotting Unit (MCU) was defined as the amount of protein that clots 10 mL of reconstituted milk at 37 °C within 40 min (2400 s). The following equation 9.4 was employed:

$$MCA = \frac{MCU}{mL} = \frac{(2400) * (V)}{(t) * (v)} \quad (9.4)$$

Where “V” is the volume of milk (mL), “v” the volume of enzyme (mL), “t” the clotting time taken in seconds. The MCA/PA is the ratio between specific milk-clotting activity (SMCA) and specific proteolytic activity (SPA). The effect of different concentrations of CaCl₂ on MCA was determined using a milk solution with varying concentration of CaCl₂ (0–60 mM). Additionally, MCA was tested by using different temperatures ranging from 30 to 85 °C and pH ranges from 5-7.

9.3. Results and discussions

9.3.1. SDS-PAGE analysis and FPLC profile

The protein profile by SDS-PAGE (**Figure 9.1a**) and FPLC (**Figure 9.1b**) of MPJ confirmed the presence of native proteins and homogeneity. SDS-PAGE shows 5 main bands of proteins. One protein is identified with an estimated molecular weight (MW) of 68 kDa, which was in agreement with the well-characterized cucumisin identified in *Cucumis melo* (Sotokawauchi et al., 2016). Also with the range of cucumisin-like serine proteases from different plant sources (60-80 kDa), including *Ficus religiosa* (Sharma, Kumari, and Jagannadham, 2012), *Cucumis rigonus* Roxburghi (Asif-Ullah, Kim, and Yu, 2006) and *Euphorbia supina* (Arima et al., 2000). Moreover, proteins with MW of 54 kDa protease and ca. 17 kDa polypeptide were identified in the MPJ. Both bands may be originated from the autolysis products of original cucumisin (Nakagawa et al., 2010). Also, two other bands were identified with 25 and 27 kDa of MW which have been

reported as proteins without relevant proteolytic activity and correspondent to fragments or contaminants of the native enzyme (Gagaoua et al., 2017). Additionally, through precipitation with ammonium sulphate was possible to concentrate and identify a protein with molecular size around 60 kDa (**Figure 9.1c**), indicating that melon peel by-products keep considerable amount of proteins with potential biological activity.

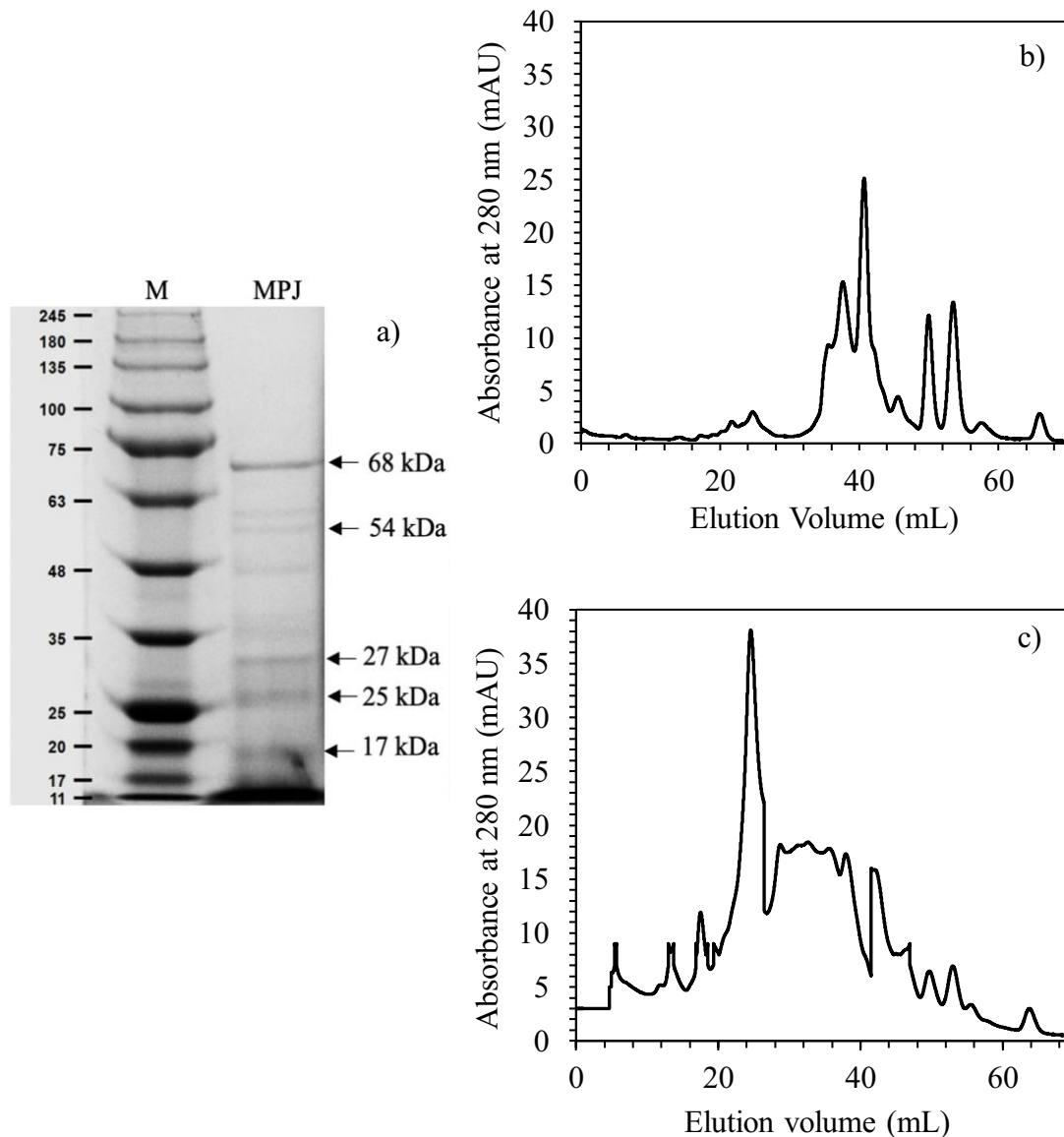


Figure 9.1. a) Electrophoresis gel by SDS-PAGE from *Cucumis melo* L. *inodorus* peels and protein molecular size profile by FPLC of b) melon peel juice (MPJ) and c) proteins precipitated with ammonium sulphate MPJ-(NH₄). M: molecular weight standards.

9.3.2. Solubility phase diagram of CRG and MPJ proteins

Proteins precipitation from melon by-products was investigated through complex formation with commercial CRG as function of pH and ionic strength. The complex

formation showed to be strongly influenced by the modification of pH medium. When the pH decreased below the initial pH 5.3 in the MPJ, the absorbance increased, showing a high turbidity at pH 3 (**Figure 9.2a**). This behavior could be attributed due to the presence of proteins, such as CUC with an isoelectric pH of 8.7, which is positively charged in acid pH (Gagaoua et al 2017). This protein interacts directly with the negative electric charges of CRG sulphonic groups, allowing the complex formation (CUC-CRG), which is a semisolid (gel) mixture. The turbidity decreased at higher values than pH 5.3 because the positive electric charge of CUC also decreased progressively, making difficult the interaction with CRG and therefore minor complex formation. **Figure 9.2b** presents the variation of the absorbance at 420 nm when MJP was present at pH 3 and tested against different ionic strength. The absorbance values increased until constant value (plateau) representing a higher extent of complex formation. It was possible to calculate the minimal amount of CRG to precipitate melon peel proteins, which corresponds to the case in which most proteins have been precipitated as an insoluble complex. The stoichiometric ratios of proteins/CRG were 3 and 1.65 mg of proteins/mg CRG, were two CRG concentrations were predicted by the maximum absorbances given. These values correspond to the minimal concentrations needed to precipitate CUC, 0.0033% (C1) and 0.006% (C2) (w/v) respectively, allowing the partial precipitation of CUC from melon by-products. On the other hand, the salt added to the medium helps to break the non-soluble complex, releasing the proteins from CRG by increasing the solubility of the complex through the electrostatic interaction between proteins and Na⁺ and Cl⁻. This helps to improve the repulsive electrostatic forces between proteins and CGR, resulting in a salting effect as observed in the reduction of turbidity, being almost null at 500 mM NaCl (**Figure 9.2b**). The interaction between CUC positively charged and CRG negatively charged appears to be natural coulombic attraction. These results obtained by this methodology showed that very low concentration of CRG was needed to precipitate proteins, compared with different reports employing time consuming processes or toxic salts, demonstrating great potentiality for its application as green extractive technology.

9.3.3. Effect of CRG on MPJ proteins

The MPJ was subjected to biological precipitation using the two predicted CRG concentrations (C1 and C2). The non-soluble complex (COM) was separated from the supernatant (SUP) by centrifugation and re-dissolved in 0.5 Tris-HCl buffer (adding, 0.5

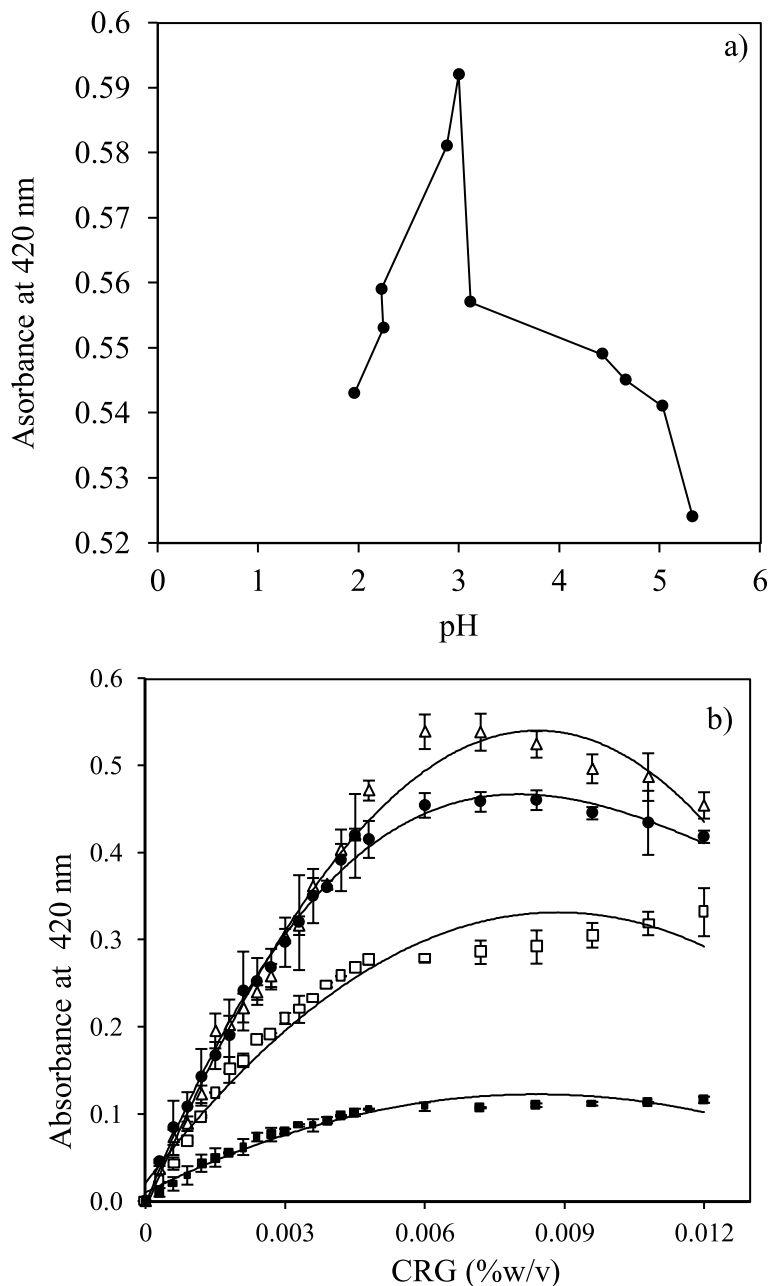


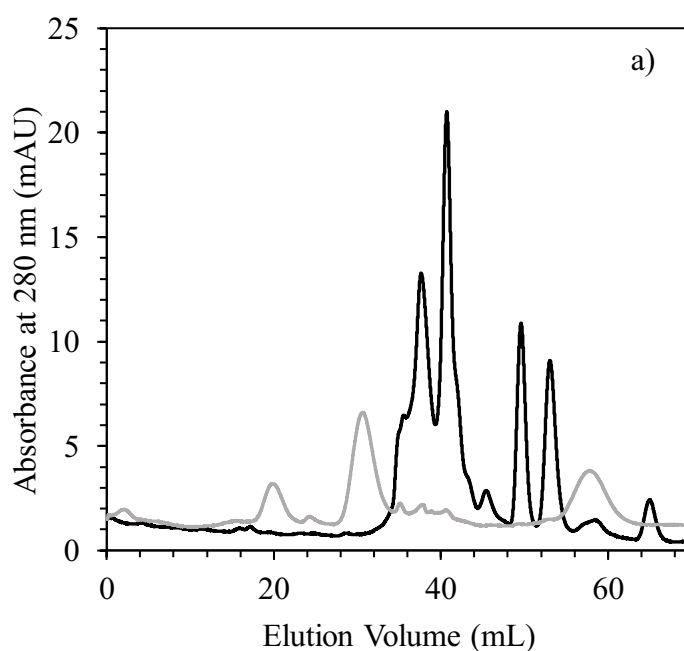
Figure 9.2. a) Turbidimetric evaluation of CUC-CRG non-soluble complex and b) Titration of CUC from melon peels juice with increasing concentration of CRG at different constant concentration of NaCl (Δ 0, \bullet 200, \square 400 and \blacksquare 500 mM). All determinations were carried out in triplicated and mean value \pm standard deviation.

M NaCl at pH 8.2), then the COM was again centrifuged to eliminate the excess of CRG. The COM and SUP both filtered through 0.45 μ m (Orange Scientific, Braine-l'Alleud, Belgium) were analysed by FPLC to observe the protein behaviour in contact with the CRG. **Figure 9.3a** presents the protein profile at 0.003% (w/v) and clearly shows that the CRG was able to precipitate proteins between 60 and 25 kDa (peaks at 22 and 32 mL).

This behaviour is probably due to the functional groups responsible for the anionic character of the polyelectrolyte, which consists of sulphated galactans, the sulfate moieties make it a strong anionic molecule that can attract positively charged proteins (Fabian, Huynh and Ju, 2010). Several studies reported the use of polyelectrolytes at low concentration as the best concentration to precipitate proteins instead using high concentration, since the increment of polyelectrolyte concentration in the medium could lead to an interaction between the same molecules, avoiding the non-soluble complex formation (Lombardi et al., 2013). Such effect can be observed at 0.006% (w/v) where most of the high MW proteins remain in SUP (peaks at 22 and 32 mL) and shows one peak in complex at 24 mL, corresponding to 60 kDa protein (**Figure 9.3b**). Previous reports have demonstrated that high concentration of polyelectrolyte influence and induce a modification of the secondary and tertiary protein structure, which could lead a loss of enzyme activity (Woitovich et al., 2012). Despite these effects, using low concentration of CRG (C1: 0.003% w/v) seems an appropriated concentration to be employed in protein extraction from melon by-products.

9.3.4. Complex formation phase diagrams of CRG and MPJ proteins

Proteins precipitation from MPJ was studied at pH 3 increasing the concentration of CRG. Non-soluble complex was handled as the same conditions described above. The TPC, PA and MCA were determined in complex (COM) and supernatant (SUP). **Figure 9.4a** shows that the



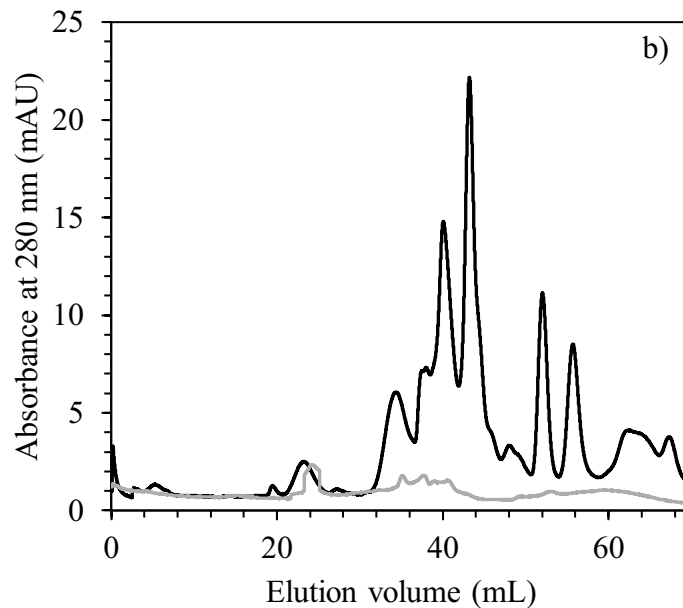


Figure 9.3. Size exclusion chromatograms from FPLC of MPJ precipitated with CRG at a) 0.003% and b) 0.006% (w/v). COM: complex (gray line); SUP: supernatant (black line).

concentration of non-precipitated protein in the supernatant decreased as the same time as the complex was formed, demonstrating the capacity of CRG to precipitate proteins from MPJ. Moreover, the PA reached a yield of 90% in the COM, while in the SUP was around 35% with total CRG concentration of 0.015% w/v (**Figure 9.4b**). On the other hand, COM presented stable clotting activity when low concentration of CRG (C1: 0.003% w/v) was used, while at higher concentrations than 0.004% (w/v) (data not shown) no clotting activity was detected. Therefore, CRG was removed by centrifugation and the recovery value of the MCA was around 60% in the COM, while for the SUP the enzymatic activity decreased until 12% at higher CRG concentrations (**Figure 9.4c**). This effect was similarly reported by different authors, describing a negative effect by excessive concentration of polyelectrolyte in the system, which could promote unwanted reactions or possible protein inactivation (Boeris, Spelzini, Farruggia, and Picó, 2009). Overall, the behaviors observed for TPC, PA and MCA confirmed that the equilibrium was displaced to a large extent to the insoluble complex formation. These effects could be attributed by the mechanism of complexation with proteins, which has been well-demonstrated that occurs in two steps: first, the formation of a primary link between protein-polyelectrolyte, which is soluble; and second the interaction of soluble complex molecules among them to form bigger and non-soluble composite (Valetti et al., 2013). Moreover, it is important to mention that this separation technique is highly

recommended to be firstly tested on pure/standard enzymes to understand the complexation behavior, since undesirable interactions may occur with other macromolecules with similar isoelectric charge as the target protein on the homogenous samples, thus, avoid such negative interactions are the main challenge to overcome in the recovery of the target enzymes in complex mixtures. However, pure CUC has presented several limitations associated with its availability on the market and its extraction, making difficult its obtainment. Therefore, the present work highlights a selective and efficient separation of proteins from melon peels through precipitation with CRG.

9.3.5. Enzymatic activities: PA and MCA

Based on the results obtained through the biological precipitation process in section 3.3 and 3.4, the lower concentration (C1) of CRG was selected to continue with the enzymatic evaluations, due to such C1 was able to preserve both enzymatic activities (PA and MCA). **Figure 9.5** shows the results of PA obtained from the evaluation using azocasein at different pH values. The specific activity was favored, preserved and increased progressively increasing pH. According to the previous reports of subtilisin/cucumisin serine proteases, they were more active in alkaline ranges of pH (8-9) than in acid ranges (Gagaoua et al., 2019). However, the best conditions (**Table 9.1**) were obtained from the complex at pH 6.5 with 74.86 U/mg protein of PA and 405 MCU/mg protein of MCA. These were 17.65 and 2.11-folds higher than the maximum initial PA (4.24 U/mg protein) and MAC (192.50 MCU/mg protein) of MPJ, respectively. Although, through traditional precipitation the results of PA (6.78 U/mg protein) and MCA (389.33 MCU/mg protein) were similar to those obtained in MPJ, biological precipitation showed better results regarding time saving, less volumes usage and the null use of toxic chemicals, as well as better purification factors. To the best of our knowledge, this was the first study related with the extraction of CUC from melon peel by-products applying polyelectrolytes. Hence, these results indicated that melon by-products still keep attractive concentration of proteins, which can be effectively extracted by green precipitation keeping their biological activity.

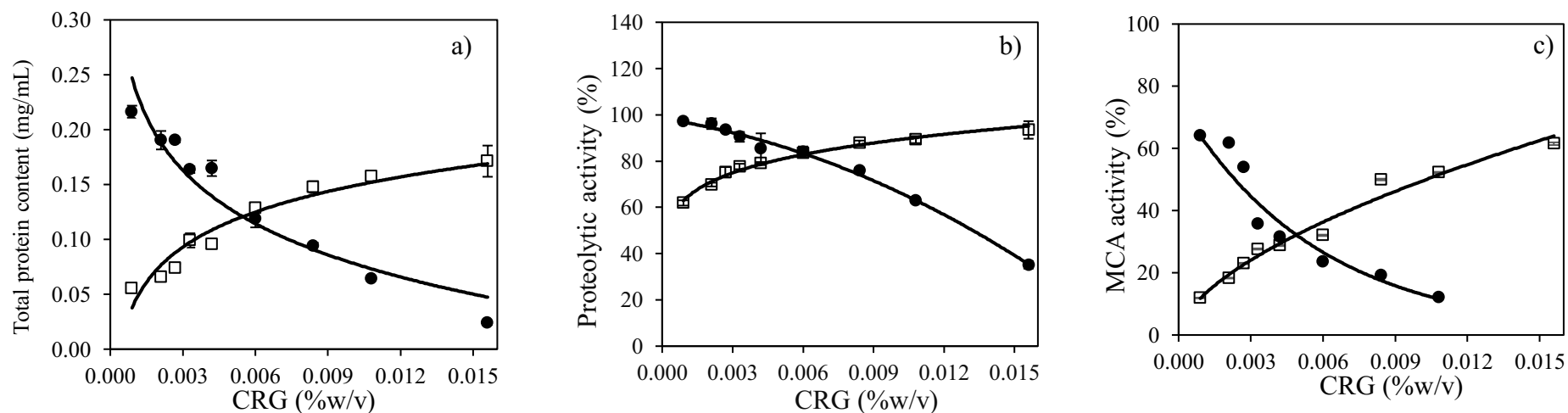


Figure 9.4. a) Total protein content, b) recovery of proteolytic activity and c) milk-clotting activity measured in the complex (• COM) and in the supernatant (• SUP) at different initial concentration of CRG. Proteolytic activity was measured using azocasein 1% w/v; MCA; milk-clotting activity was measured at constant temperature (37 °C) and pH (6.5). All determinations were carried out in triplicated and mean value \pm standard

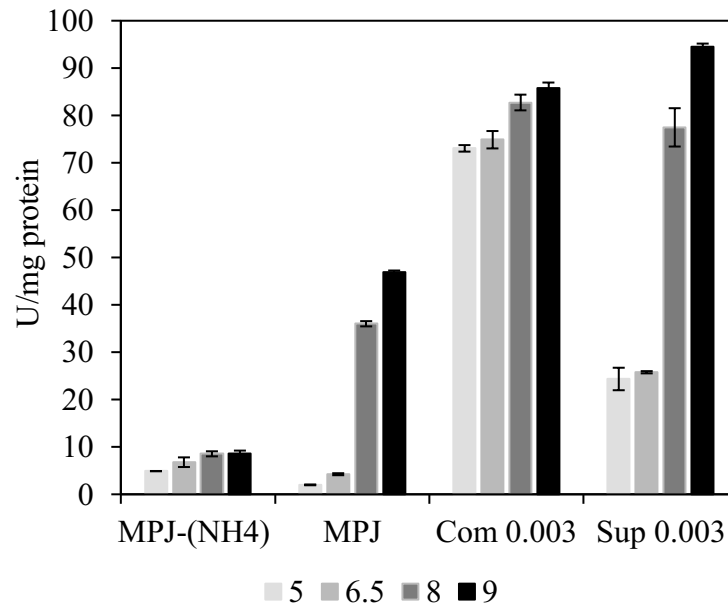


Figure 9.5. Specific proteolytic activity of melon samples at different range of pH using azocasein (1% w/v) as substrate. MPJ: melon peels juice; MPJ-(NH₄): melon peels juice precipitated with ammonium sulphate; COM 0.003: complex at 0.003% w/v of CRG. All determinations were carried out in triplicated and mean value \pm standard deviation.

Table 9.1. Protein purification from melon peels

	MPJ	MPJ-(NH ₄)	COM 0.003
Total protein content (mg/mL)	0.202 \pm 0.0	1.96 \pm 0.1	0.089 \pm 0.0
PA (U/mL)	0.87 \pm 0.0	13.30 \pm 0.4	6.66 \pm 0.4
Specific PA (U/mg protein)	4.24 \pm 0.2	6.78 \pm 1.0	74.86 \pm 1.8
Fold purification of PA		1.60 \pm 0.6	17.65 \pm 1.3
MCA (MCU/mL)	38.63 \pm 0.6	764.29 \pm 86.6	36.10 \pm 0.1
Specific MCA (MCU/mg protein)	191.50 \pm 1.0	389.33 \pm 33.7	405.28 \pm 3.3
Fold purification of MCA		2.03 \pm 0.9	2.11 \pm 0.3

MPJ: melon peels juice; MPJ-(NH₄): melon peels juice precipitated with ammonium sulphate; COM 0.003: complex at 0.003% w/v of CRG. PA: proteolytic activity; MCA: milk-clotting activity; MCU: milk-clotting units. The values are means of three independent measurements.

9.3.6. Effect of CaCl₂, temperature and pH on MCA

The effects of CaCl₂, pH and temperature on MCA were studied using the MPJ and COM at 0.003% (w/v). The results show that milk-clotting time is dependent on these parameters (**Figure 9.6**). Commonly, CaCl₂ is added to milk to improve the milk coagulation in cheese manufacture. Thus, the effect of CaCl₂ on milk-clotting time is given in **Figure 9.6a** where in both cases the clotting time decreased, which means that

clotting activity increased by increasing the concentration of salt, where COM presented the highest MCA (1300 MCU/ mg protein) at 60 mM (**Figure 9.6b**). As observed, clotting time of COM decreased by increasing CaCl_2 concentration until a plateau is reached between 30 to 60 mM of salt. Thus, the enzymatic activity was progressively increased, and this behavior could be attributed to the native structures of serine proteases, which are stabilized by calcium ions. According to Hedayati and Ani, 2015, the calcium ions do not interfere in the binding and catalytic sites of proteins, providing additional electrostatic binding with anionic bonds of the enzyme. On the other hand, by increasing pH values from 5 to 7 (**Figure 9.6c and d**), the clotting time increased because of the reduction of the enzymatic activity, in which MPJ had higher MCA (880 MCU/ mg protein) than COM (490 MCU/ mg protein) at pH 5 while under this value and above pH 7 were not showed coagulation activity. The effect at lower pH could be attributed by the disorganization of caseins micelles structural properties, since caseins are near to their isoelectric point (pH 4.6). This decreases the net charge, and therefore, decreases the electrostatic repulsion between charged groups, leading to milk clots agglomeration and enzymatic action (Ranadheera et al., 2019). Previous reports on MCA from plant proteases (*Wrightia tinctorial*, *Ficus carica*, *Colatropis procera*) also exhibited activity over a wide range of pH (Rajagopalan and Sukumaran, 2018). **Figure 9.6e** shows the progression of milk-clotting time between 30 to 85 °C. This parameter showed that the clotting time decreased as function of increased temperature. 1 mL of milk was coagulated with 0.1 mL of MPJ or COM within (5-55 min) with an acceptable coagulation time (less than 90 min). The ample range of temperatures showed the high thermal stability of both MPJ and COM, producing the best MCA values at 85 °C with titles of 6300 and 4200 MCU/mg protein, respectively. These results are in concordance with the reported for milk-clotting proteases from *Citrus aurantium* L., *Wrightia tinctoria* and *Morinda citrifolia* L. at temperatures of 35-80 °C (Mazorra-Manzano et al., 2013; Rajagopalan and Sukumaran, 2018; de Farias et al., 2020). To the best of our knowledge, these findings were obtained for the first time from melon by-products, suggesting that MPJ still maintained bioactive proteins with relevant enzymatic activity, which can be effectively extracted by the natural chemical interaction with CRG without any previous purification step, leading a reduction of process time and cost when compare with traditional extractive methods.

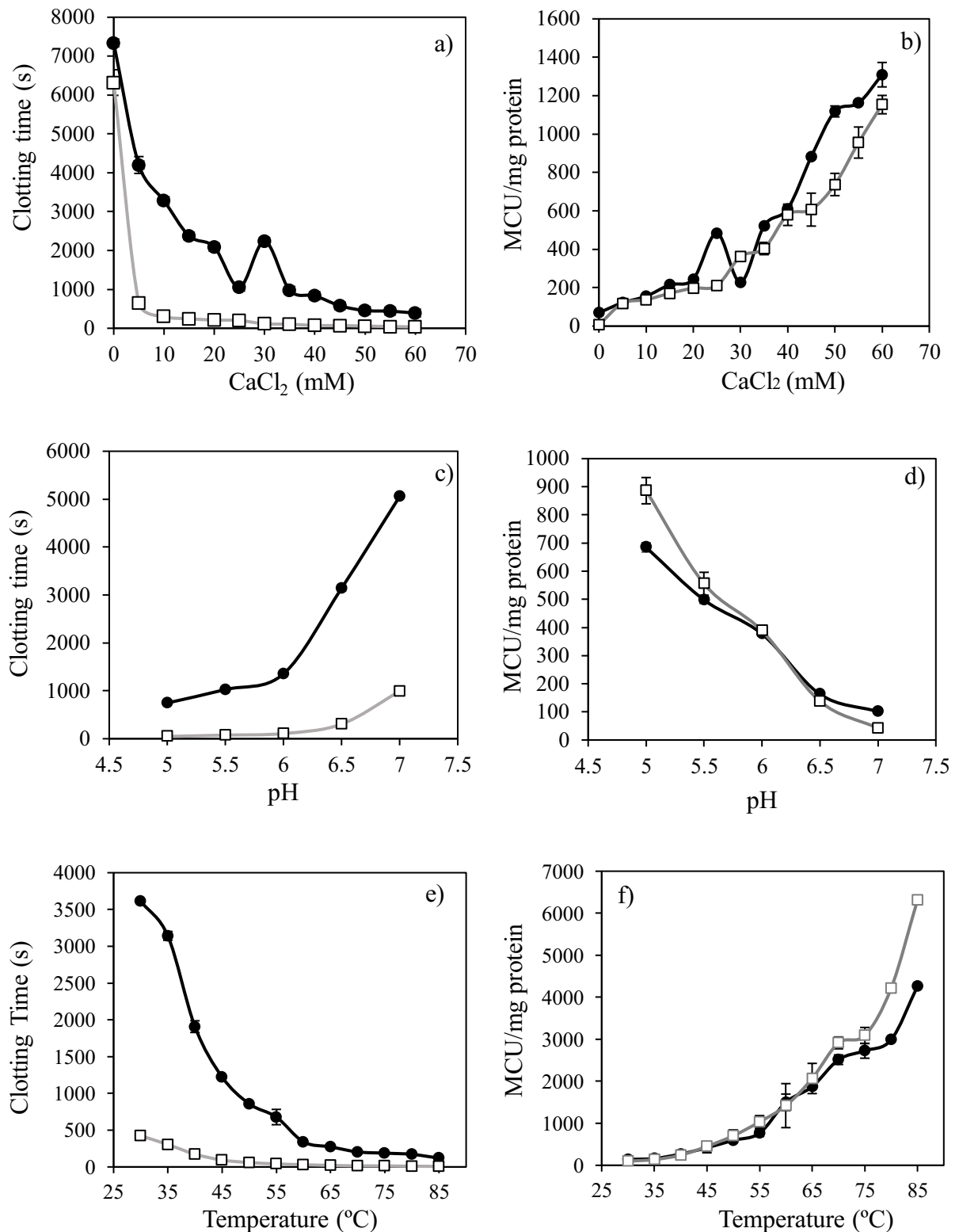


Figure 9.6. Effect of CaCl₂, pH and temperature on milk-clotting activity of the COM 0.003 (●) and MPJ (□). a) and b) Effect of CaCl₂ concentration, c) and d) pH and e) and f) temperature. Data are average of three independent experiments ± standard deviation of determined clotting activity.

9.3.7. Melon by-products as sources of proteolytic enzymes

The industrial enzymes market, especially those used in food industry, is expected to increase their global demand of over \$3.6 billion by 2024, and proteases are one of the most important groups of industrial enzymes, with approximately 60% of the enzyme market (Mangiagalli, Brocca, Orlando, and Lotti, 2020; Ibrahim et al., 2019). Hence, different practical strategies for future melon by-products applications could be developed as vegetable rennet for cheese production: this approach could be achieved taking into account the current increasing demand of alternatives against animal rennet, since different issues have been arrived related with its production, less consumers acceptance and high cost. In order to evaluate melon peels extracts as vegetable rennet, one important parameter that must be considered is the ratio of milk-clotting activity to proteolytic activity (MCA/PA). It is well-known that excessive proteolysis negatively affect coagulation force, as well as some, sensorial characteristics of the final products (Gomes et al., 2019). In turn, depending on the temperature MPJ showed an MCA/PA ratio of 995.34 ± 111.6 and 1485.84 ± 107.2 at temperatures of 80 and 85 °C, respectively. These values were similar to the commercial rennet such as CoelhoPar® rennet (1730.4), Halamix® rennet (1077.6) and some plant extracts from *Cryptostegia grandiflora* (1154.8) and *Morinda citrifolia* L. (1124.31) (Freitas et al., 2016; Farias et al., 2020), showing the possible application of MPJ as a vegetable rennet. Other possible application could be the production of bioactive peptides from whey protein or different protein sources by enzymatic hydrolysis. Bioactive peptides have a wide spectrum of bioactivities, such as, antioxidant, antimicrobial, anti-inflammatory activity and enzyme inhibition, which could be used in cosmetic and pharmacological industries (Aguilar-Toalá et al., 2019). Several researchers employed *Cynara cardunculus* and *Maclura pomifera* proteases to produce bioactive peptides from bovine whey, such peptides exhibited antioxidant and ACE-inhibitory activity (Tavares et al., 2011; Corrons, Bertucci, Liggieri, López, and Bruno, 2012). Therefore, melon by-products coupled with biological precipitation can deliver different proteolytic fractions to be tested for their ability to produce value-added molecules. These evaluations should be conducted in future research studies to improve the application of melon by-products as sources of bioactive proteins.

9.4. Conclusions

The use of melon by-products as new feedstock for proteins recovery by biological precipitation could decrease the environmental impact as well as minimize the costs associated to the traditional extractive processes. This research demonstrated that melon peels have proteolytic (4.24 U/mg protein) and milk-clotting (6300 MCU/mg protein) activities with an MCA/PA ratio of 1485 at 85 °C. Besides, biological precipitation with CRG allows to improve the biological activity of the proteins recovered from melon peels. A yield of 0.17 g of CUC/100 g of melon by-products can be obtained with the best conditions of precipitation at pH 3 with low concentration of CRG (0.003% w/v), improving 17.65 and 2.11-folds the PA (74.86 U/mg protein) and MCA (405 MCU/mg protein), respectively. Furthermore, these findings support the importance to valorise melon by-products to avoid economic and environmental issues through their reincorporation into the industrial chains as rich sources of value-added proteins.

CHAPTER 10 – Proteins-like antifreeze proteins identified and extracted from melon (*Cucumis melo* L. *inodorus* cultivar) peels by green precipitation using carrageenan: recrystallization inhibition and amino acid profile

Ricardo Gómez-García^{a,b}, Débora A. Campos^a, Cristóbal N. Aguilar^b, Ana R.

Madureira^a and Manuela Pintado^{a*}

^a*Universidade Católica Portuguesa, CBQF – Centro de Biotecnologia e Química Fina – Laboratório Associado, Escola Superior de Biotecnologia, Rua Diogo Botelho 1327, 42169-005 Porto, Portugal*

^b*BBG-DIA. Bioprocesses and Bioproducts Group. Food Research Department, School of Chemistry, Autonomous University of Coahuila, Saltillo, Coahuila, Mexico.*

Submitted

Journal of Food Hydrocolloids

Abstract

Antifreeze proteins (AFPs) modify ice crystal growth, an important biotechnological and industrial property. Hence, there is an increased interest in the identification of new sources of these value biomolecules, and their sustainable extraction. In this study, proteins with high amino acid content were extracted from melon peels with carrageenan (CRG) at very low concentration (0.003% w/v). Low and high molecular weight proteins with 3.5 to 60 kDa, were identified with an amino acid content, ranging from 4.79 to 13.41 g/100 g protein, where serine, aspartic and glycine were the most representative amino acids. The resulting melon protein rich extract exhibited recrystallization inhibition which was attributed to the great similitude and homology in the structure and amino acids profile described from melon peel proteins with respect to reported AFPs. Overall, the results from this study provide new insight into the potential of further exploring the potential of this melon peels as novel resources of proteins with antifreeze-like activity and their potential applications as cryoprotectants.

Keywords: Antifreeze proteins; melon peels; protein recovery; recrystallization inhibition; cryoprotectants.

10.1. Introduction

Within the last decades, various organisms in nature have been investigated due to their ability to produce certain functional biomolecules to survive in subzero temperatures and protect them from freezing, such biomolecules are called antifreeze proteins, which in turn are catalogued into two principal groups: i) antifreeze proteins (AFPs) and ii) antifreeze glycoproteins (AFGPs) (Hassas-Roudsari and Goff, 2012; Congdon, Notman, and Gibson, 2013). The AFGPs have been isolated from fish blood serum (Antarctic Notothenioids and Arctic Cod) and they range in molecular weight (MW) from 2.6 to 33.7 kDa (Tsuda et al., 2020). The AFPs can be either thermal hysteresis proteins (THPs) or ice structuring proteins (ISPs). The THPs depress the freezing temperature point of water in a non-colligative way by binding to different crystallographic ice planes, while having no effect on the melting point (Park et al., 2013). The ISPs present ice recrystallization inhibition (IRI), which in turn is the property to inhibit ice recrystallization/growth into a large ice crystals, controlling the size, shape and aggregation of ice crystals rather than to avoid water from freezing (**Figure 10.1**) (Chasnitsky and Braslavsky, 2019). Additionally, AFPs are divided into 4 types: type I with MW of 3.3 to 4.5 kDa (alanine rich); type II with MW of 11 to 24 kDa (cysteine-rich); type III with MW of 6.5 kDa (no cysteine residues); and type IV with MW of 12 kDa (glycine-rich) (Verreault et al., 2018; Vance, Bayer-Giraldi, Davies, and Mangiagalli, 2019). The THPs have been identified in fish (Ocean Pout), plants (Antarctic hairgrass), insects (*Tenebrio molitor*), fungi (*Typhula ishikariensis*) and bacteria (*Flavobacterium frigidis*), where ISPs also have been reported to be present in overwintering plants when they have been exposed to low temperatures (Provesi, Valentim Neto, Arisi, and Amante, 2019). For example, species of perennial have shown ISPs in their different parts, including seeds, stems, crowns, branches, buds, petioles, leaf, flowers, berries, roots and tubers. The thermal hysteresis (TH) activity in plant ISPs is reported to be 0.2 to 0.4 °C, however, they showed high IRI activity (Sharma and Deswal, 2014).

On the other hand, AFPs have gained relevant attention for biotechnological application in food and biomedical industries as cryoprotectants since they can be used for preserving the textural quality of frozen foods, improving storage of blood, organs and tissues, and protecting crops from freezing in a freeze-thaw cycle to minimize or prevent damage to cells and tissues (Mangiagalli, Brocca, Orlando, and Lotti, 2020). However, the limited

availability of these natural AFPs as well as the techniques used for their production or extraction have restricted their use in such applications (Tian, Zhu, and Sun, 2020). For these reasons, researchers have been looking for new sources (cheap, accessible and renewable) and novel eco-friendly-effective methods for extraction of these biomolecules, avoiding hazardous solvents, expensive and time-consuming process. In this regard, melon fruit and its by-products have been reported as rich sources of bioactive proteins especially cucumisin with proteolytic activity, and they present complexity on their MWs, starting from 3 to 68 kDa (Sotokawauchi et al., 2016; Gómez-García et al., 2021b). Furthermore, precipitation using natural polyelectrolytes like carrageenan (CRG) is a well-documented extractive method, representing a non-toxic, low cost and efficient green process for protein extraction, which release proteins conserving their structure and biological activity (Woitovich, Brassesco, and Picó, 2016). The CRG is obtained from certain species of red seaweed and is considered non-toxic water-soluble compound, it interact with proteins in solution, arising a soluble or non-soluble complex by the modification of pH medium or ionic strength (Campos et al., 2017). Hence, to the best of our knowledge, this research study is the first work reporting AFPs from melon fruit and no previous studies regarding their extraction by a polysaccharide have been reported. Thus, it is a good opportunity to identify novel sources of AFPs and develop a green process for their extraction. So, the main objectives of this study were to i) characterise melon proteins by their molecular weight and amino acid profile, and ii) evaluate their antifreeze properties after precipitation process by CRG.

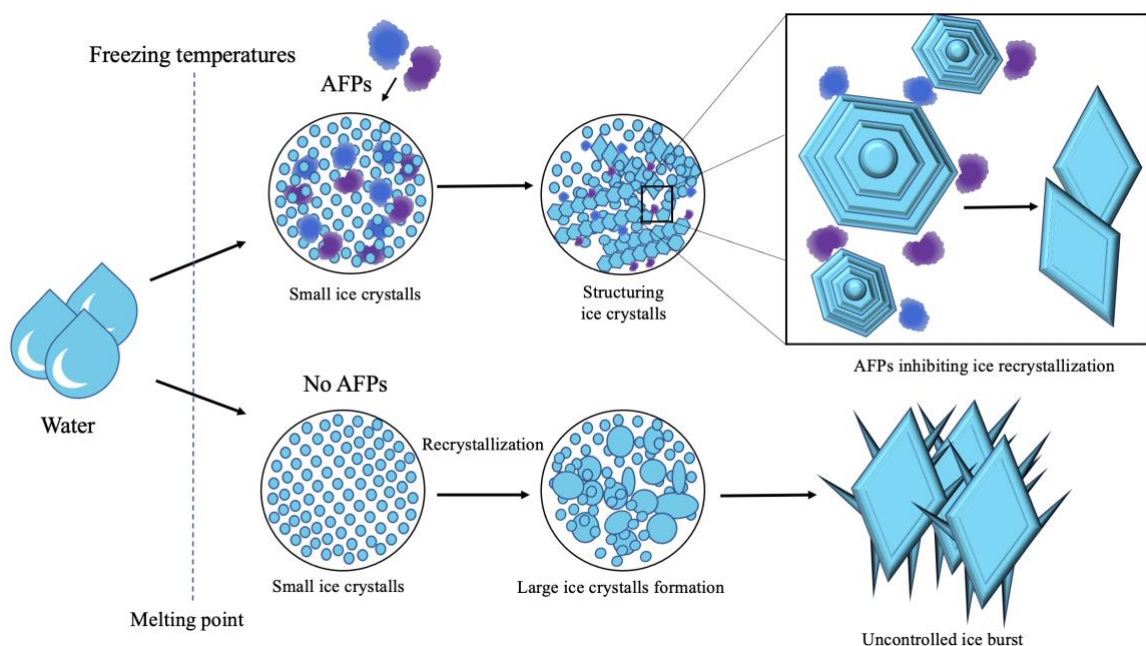


Figure 10.1. Ice recrystallization inhibition. In the absence of ISPs, large ice crystals grow at the expenses of smaller ones (ice recrystallization). The ISPs stabilize small ice crystals, inhibiting the recrystallization process. Ice crystal growth inhibition by AFPs formed a hexagonal plate with six prism planes visible. New disc additions on to the hexagonal plate with addition of AFPs, eventually forming an ice-crystal barrel that ultimately develops to a bipyramidal ice crystal. Adapted from and Mangiagalli et al. (2020).

10.2. Material and methods

10.2.1. Chemicals

Bovine serum albumin (BSA, $\geq 96\%$), hydrogen tetrachloroaurate (III) trihydrate ($\text{HAuCl}_4 \cdot 3\text{H}_2\text{O}$, 99.9%), iota (ι)-carrageenan, sodium citrate dihydrate (trisodium salt, $\text{C}_6\text{H}_5\text{Na}_3\text{O}_7 \cdot 2\text{H}_2\text{O}$) and mercaptosuccinic acid (MSA, $\geq 99.0\%$) were purchased from Sigma–Aldrich (St. Louis, Missouri, USA). Bradford Bio-Rad assay from Biorad (Hercules, CA, USA). All the chemicals were of analytical grade and were used as received.

10.2.2. Raw material - Melon peels

Melon fruits (*Cucumis melo* L. *inodorus*) were harvested (ripening stage was not controlled) from the Alentejo region in Portugal and processed by Nuvi Fruits S. A. Company Torres Vedras (Portugal), during the season of summer (August-September 2018). Fresh melon peels were generated as by-products and then transported to our facilities (Centro de Biotecnologia e Química Fina - CBQF) at $-20\text{ }^\circ\text{C}$. The peels were kept at $-20\text{ }^\circ\text{C}$ until their processing and pre-treatment.

10.2.3. Melon peels juice (MPJ) preparation

Melon peels were processed as described previously by Gómez-García et al. (2021b) and split in two fractions, fresh solid fraction (SF) and liquid fraction (LF), employing a commercial juice machine (HR1869/8, 900 W, Philips). The SF was manually pressed to recover the liquid excess, such liquid was mixed with the LF, which was subsequently centrifuged (11469 g, 15 min, $4\text{ }^\circ\text{C}$) and then the clarified supernatant was called as melon peels juice (MPJ). The MPJ was collected and kept at $-20\text{ }^\circ\text{C}$ until its analysis.

10.2.4. Extraction of melon peel proteins by precipitation with CRG

The extraction of melon proteins was conducted following the results reported in Chapter

9 (Gómez-García et al., 2021a). According to the turbidimetric titrations with CRG, melon proteins were precipitated as non-soluble complex at final polysaccharide concentration of 0.003% (w/v) in the system. The non-soluble complex (COM 0.003) was separated from the supernatant (SUP 0.003) by centrifugation and re-dissolved in 0.5 Tris-HCl buffer (adding, 0.5 M NaCl at pH 8.2), then the COM 0.003 was again centrifuged to eliminate the excess of CRG. The COM 0.003 and SUP 0.003 extracts were filtered through 0.45 µm (Orange Scientific, Braine-l'Alleud, Belgium) and stored at -20 °C until their analysis of protein profile by FPLC and content.

10.2.5. Analysis by size exclusion chromatography (FPLC)

Protein profile was analysed by gel filtration chromatography using the following conditions: the column was operated at a flow of 0.5 mL/min with phosphate buffer (0.025 M, pH 7) containing NaCl (0.15 M) and NaN₃ (0.02 %w/v). Protein standards with known molecular weights (Thyroglobulin, 669 kDa; Ferritin, 440 kDa; Aldolase, 158 kDa; Conalbumin, 75 kDa; Ovalbumin, 43 kDa; Carbonic anhydrase, 29 kDa; Ribonuclease A, 13.7 kDa; Aprotinin, 6.5 kDa) were used to elaborate a calibration curve. AKTA pure 25 L system, from GE Healthcare Life Sciences (Freiburg, Germany), was used with a configuration of two pumps with pressure control for column protection, a gel filtration column prepacked with Superdex® 200 10/300 GL and an-UV multiwavelength detection monitor U9-L, at a fixed wavelength of 280 nm. The software used to evaluate samples was UNICORN 7.0.

10.2.6. Protein content determination

Total protein content (TPC) was determined by the Bradford assay (Bradford, 1976) with slight modifications. Briefly, 50 µL of each sample was combined with 950 µL of Bradford's reagent at room temperature, the reaction was vortex mixed and then kept in darkness during 20 min. The absorbance was measured at 595 nm in a microplate reader (Synergy H1 Hybrid Multi-Mode - BioTek Instruments) and the protein concentration was quantified with a calibration curve using bovine serum albumin (BSA) as standard. Results were expressed as mg BSA/mL. All the measurement was made in triplicated.

10.2.7. Identification and quantification of amino acids by HPLC

Free amino acids content of each fraction was performed by pre-column derivatization

with orthophthalaldehyde (OPA) methodology. Isoindole-type fluorescent derivatives were formed in an alkaline solution (borate buffer pH 10.4) from OPA, 2-sulfanylethanol and the primary amine group of the amino acid. The derivatives were separated by RP-HPLC (Beckman coulter, California USA) coupled to a fluorescence detector (Waters, Milford, MA, USA) according to the procedure of Proestos et al. (2008). 100 μ L of each sample, at concentration 10 mg/mL, was derivatized according described method and injection volume of derivatives was 20 μ L. All analysis were made in triplicate and quantified using a calibration curve built with amino acids pure standards (SigmaAldrich, St. Louis, MO, USA) and expressed as g/100 g of sample DM.

10.2.8. Production of AuNPs

Citrate gold nanoparticles (Cit-AuNPs) were synthesized, as previously described by Grabar et al., (1995) and previously reported by Park et al., (2013) with some modifications. Briefly, in an Erlenmeyer flask, 20 mL of 1 mM HAuCl₄·3H₂O was mixed with 50 mL of distilled water to reach a final concentration of 300 nM. The mixture was heated until boiling under vigorous stirring, followed by the addition of 2 mL of 30 mM sodium citrate, resulting in a color change from pale-yellow to red brown. The red solution was kept boiling for an extra 20 min and was cooled to room temperature maintaining in stirring. A supplementary modification was performed by adding 2 mL of 30 mM MSA to the Cit-AuNPs solution, followed by vigorous stirring at RT for 1 h, this solution was called Cit-MSA-AuNPs.

10.2.9. Colorimetric assay of AFP activity

Antifreeze activity of melon protein extracts was assessed according to the method described by Park et al. (2013) with some modification. In a 96-microwell plate 25 μ L of COM 0.003 sample ten folds-diluted in ultrapure water was mixed with 100 μ L of nanoparticles solution (Cit-AuNPs and Cit-MSA-AuNPs), followed by the addition of 75 μ L of distilled water. Different dilutions folds were tested during this assay, but ten times dilution exhibited better results against self-assembly inhibition of AuNPs (data not shown). BSA was used as a negative control (0.1 mg/mL). The reaction was subjected to a cycle of freezing at -20 °C for 60 min and thawing at 37 °C for 15 min. Before and after the freezing/thawing cycle, the extinction spectrum was obtained by measuring absorbance in an UV/VIS microplate reader (Thermo Scientific Multiskan GO) from 400

to 800 nm.

10.2.10. Zeta potential and size of the AuNPS

A Zetasizer Nano ZSP (Malvern Instruments, Worcestershire, UK) using dynamic light scattering (DLS) was used to measure the particle size (PS) and ξ -potential (ZP) of the AuNPs synthesized with sodium citrate and MSA. Particle sizes (hydrodynamic radius) were measured by taking into account the first order result from a DLS experiment as an intensity distribution of PS. The intensity distribution was weighted according to the scattering intensity of each particle fraction or family. Data were validated only if the cumulant fit error was <0.005 . ξ -potential was measured using Laser Doppler Anemometry (LDA). All analyses were carried out three times and sample readings were done in triplicate with an angle of 90° at 25°C .

10.2.11. Recrystallization inhibition assay

10.2.11.1 Proposed method

The recrystallization inhibition activity was determined following the sucrose sandwich splat assay reported by Provesi et al. (2019) with modifications. An amount of $50\ \mu\text{L}$ of 30% (w/v) sucrose was put in a microscope glass slide and $10\ \mu\text{L}$ of the sample used in section 2.9 was added. Then another microscope glass slide was settled in order to compress the sample with the sucrose. The ‘sandwich’ was placed inside of a conventional freezer at -20°C during different periods of time - 5, 15 and 30 min. After each incubation, the growth of ice crystal was observed under an optical electronic microscope (Kozo, XJS900, China), with a 40x objective. A visual assessment was carried out to detect whether any recrystallization took place by comparing the size of the ice crystals of the test sample for each incubation time.

10.3. Results and discussion

10.3.1. Protein extraction from melon peels juice (MPJ)

The total protein contents of MPJ and proteins extracted by green precipitation using ι -carrageenan (CRG) are depicted in **Table 10.1**, and the protein profile of both samples in **Figure 10.2**. Concerning protein content of the extracts, extraction with CRG showed a precipitation protein effect ($74.30 \pm 4.50\ \mu\text{g/mL}$), exhibiting that almost 40% of the total

concentration was extracted with respect to the MPJ ($201.74 \pm 3.61 \mu\text{g/mL}$). Comparable values were obtained for AFPs extracted from *Drimys angustifolia* leaves with different buffers (105.38 to $194.52 \mu\text{g/mL}$) (Provesi et al., 2019). The protein profile of MPJ is shown in **Figure 10.2a**, which according to the calibration curve different molecular weight proteins (MWs) such as 60, 25, 6.2 and 3.5 kDa were presented in the sample. **Figure 10.2b** and **c** present the protein profile precipitated with CRG (COM 0.003) and clearly shows that the CRG was able to precipitate these proteins from the MPJ. This behaviour is probably due to the functional groups responsible for the anionic character of the polyelectrolyte, which consists of sulphated galactans. The sulphate moieties strengths the anionic side of the molecules, that can attract positively charged proteins present in the melon samples (Fabian, Huynh and Ju, 2010; Woitovich et al., 2012). These results showed that very low concentration of CRG is needed to precipitate proteins, compared with different reports employing time consuming processes or toxic salts, demonstrating great potentiality for its application as green extractive technology to obtain value-added molecules with interesting properties.

Table 10.1. Protein content of melon peel juice (MPJ) and proteins extracted by precipitation with ι -carrageenan (CRG).

Extract	protein content ($\mu\text{g/mL}$)
MPJ	201.74 ± 3.61
COM 0.003	74.30 ± 4.50
SUP 0.003	112.56 ± 10.12

COM 0.003: complex; SUP 0.003: Supernatant. Data are presented as means \pm standard deviation (SD) (n=3).

10.3.2. Effect of proteins precipitated with CRG on aggregation of AuNPs

According to Park et al. (2013), a solution with AFPs should be capable to protect AuNPs from self-aggregation, due to their preferential binding to ice crystals, resulting in a strong scattering peak at near 520 nm in the extinction spectrum. On the other hand, a AFPs-free solution cause AuNPs self-assembled during the freezing/thawing cycle, increasing their size, resulting in a colour change from red to blue (**Figure 10.3**). In this study, proteins from melon peels precipitated by CRG (COM 0.003) with a final protein concentration of $7.43 \mu\text{g/mL}$, were reacted with the solution of AuNPs at a cycle of 60 min freezing at $-20 \text{ }^\circ\text{C}$ and and 15 min-thawing at $37 \text{ }^\circ\text{C}$. Two different solutions of nanoparticles were used, Cit-AuNPs and modified Cit-MSA-AuNPs with estimated diameters of 24.01 and 35.61 nm, respectively (Zetasizer Nano ZSP). As a result of the freezing/thawing process,

Figure 10.2a shows the extinction coefficient profile of the samples tested on Cit-AuNPs with the COM 0.003, keeping the same profile as the Cit-AuNPs before freezing, maintaining a high scattering peak at 520 nm, thus they were not aggregated. However, nanoparticles with BSA over the given concentration (0.1 mg/mL) and the protein-free AuNPs solution were both aggregated as well as MPJ and SUP 0.003 (**Figure 10.4b**) losing the high scattering peak after the freezing/thawing cycle. Unlike to the results reported by Park et al. (2013), which mentioned that only Cit-MSA-AuNPs gives rise to a significant difference in the frozen assembly between BSA and AFPs, while the Cit-AuNPs (without MSA) did not differentiate the frozen assembly between BSA and AFPs, wherein BSA made Cit-AuNPs (without MSA) stable by surface binding via cysteine residues at its outmost, endowing the improved resistance to self-assembly of AuNPs during freezing process. However, an aggregation behaviour was observed using Cit-AuNPs and Cit-MSA-AuNPs with BSA with the samples tested (**Figure 10.4a** and **c**). On the other hand, the proteins identified in MPJ and COM 0.003 (**Figure 10.2c**), such as cucumisin (60 kDa), are classified as serine proteases with a C-terminal domain and cysteine poor protein in its structure (Murayama et al., 2012; Sotokawauchi et al., 2016). These characteristics could eliminate the possibility of Cit-AuNPs being stabilized by cysteine residues. Besides, proteins with 6.2 and 3.5 kDa are in agreement with the characteristics and MW already reported for Type III AFPs (C-terminal domain, few alanine and no cysteine residues) and Type I AFPs (alanine rich), respectively (Hassas-Roudsari and Goff, 2012). Although a completely mechanism of action explaining the relationship between proteins structure and ice-binding crystals on the surface of AuNPs is still remains unclear, the synergic combination of the proteins precipitated by CRG seems to attribute the stability of Cit-AuNPs. Thus, these results suggest that melon peel possess proteins with antifreeze activity.

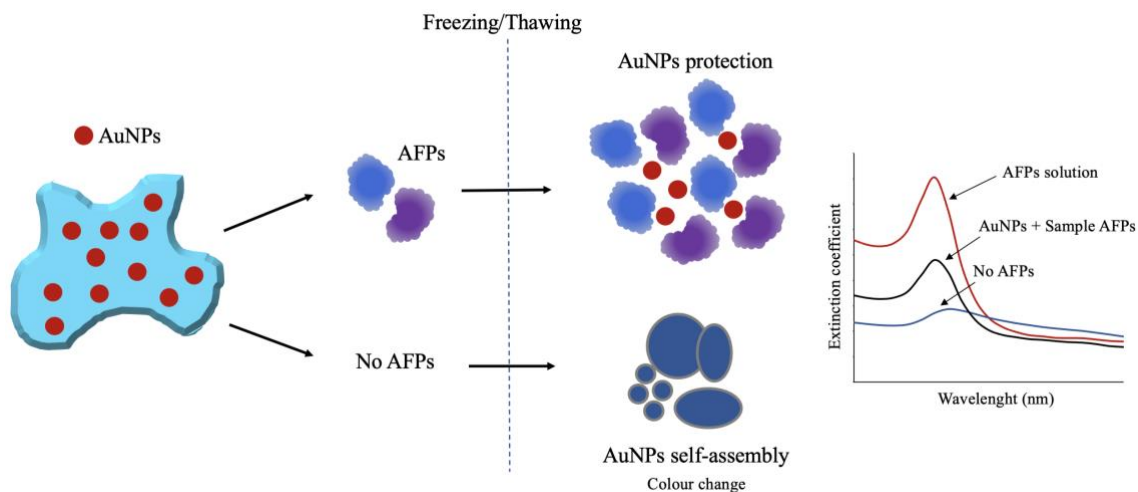


Figure 10.3. Graphic representation of AuNPs-based colorimetric assay of AFP activity. In the presence of AFP, the self-assembly (blue) of AuNPs (red) is strongly inhibited after a freezing/thawing cycle, and the freeze-induced assembly can be quantified by the extinction spectrum. Adapted from Park et al. (2013).

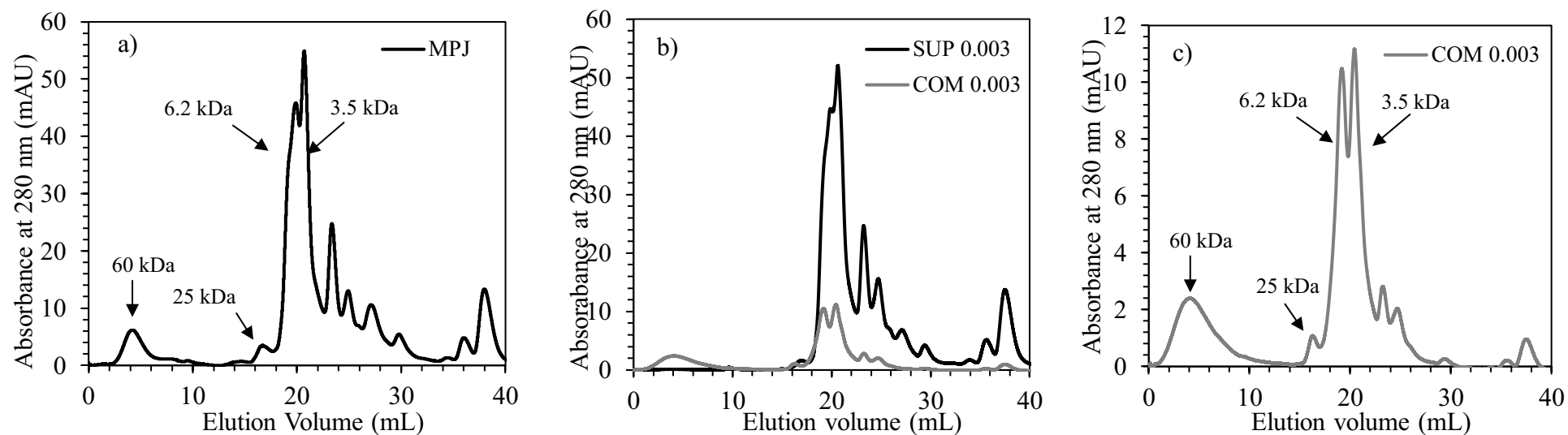


Figure 10.2. Protein chromatograms of (a) Melon Peel Juice (MPJ), (b) MPJ subjected to precipitation with carrageenan (CRG) and (c) proteins precipitated by CRG at 0.003% (w/v) and solubilized in buffer of 0.5 M Tris-HCl – 0.5 M NaCl pH 8.2. COM 0.003: complex; SUP: supernatant.

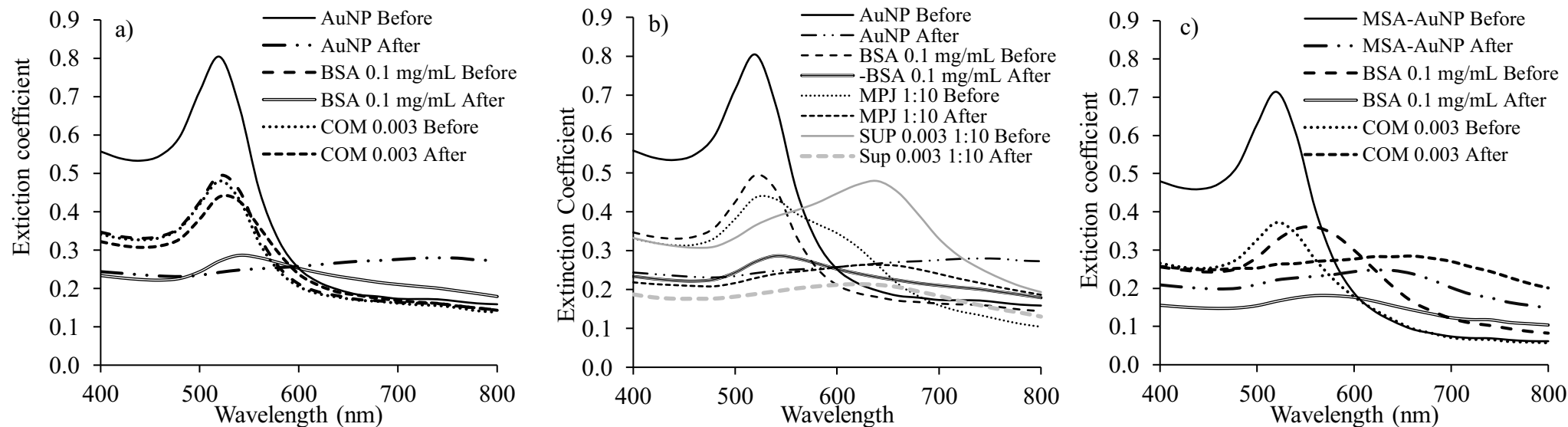


Figure 10.4. Extinction spectra of AuNPs before and after freezing/thawing process reacted with proteins precipitated by ι -carrageenan (CRG). a) and b) Solutions of citrate gold nanoparticles (Cit-AuNPs) and c) citrate gold nanoparticles modified with mercaptosuccinic acid (Cit-MSA-AuNPs). Before: before freezing; After: after thawing.

10.3.3. Recrystallization activity

Ice recrystallization is the process by which large ice crystals grow at the expense of smaller crystals in frozen materials and occurs by the spontaneous coalescence of small ice crystals into larger ones. Adsorption of ISPs onto small ice crystals results in their stabilization, and inhibition of the recrystallization (IRI) process (Mangiagalli et al., 2020). This ice growth occurs by the movement of water across ice grain boundaries and is accelerated as the melting temperature is approached. Recrystallization leads to a loss of quality in frozen foods and threatens freeze-tolerant organisms with tissue damage and dehydration. The IRI appears to be the primary function of ISPs found in plants, such as rye grass and carrot, as they have poor thermal hysteresis activity ($< 1\text{ }^{\circ}\text{C}$) but strong IRI activity (Graham, Agrawal, Oleschuk and Davies, 2018). To further explore possible IRI activity for melon peel proteins, an additional assay to directly detect IRI was used to observe the inhibitory effects on the formation of ice crystals in the presence of very low protein concentration (proposed method). Moreover, only the protein extract (COM 0.003) extracted by CRG in contrast to the MPJ and SUP 0.003 extracts (data not shown), showed recrystallization inhibition activity at the protein concentrations obtained (7.43 $\mu\text{g/mL}$). **Figure 10.5** shows that this phenomenon occurs by the maintenance of small crystals after the incubation time, which is better during 30 min at $-20\text{ }^{\circ}\text{C}$ (**Figure 10.5c**). Other authors have reported recrystallization inhibition activity for higher or lower concentrations of antifreeze proteins in extracts of different plant species. In this regard, ISPs already inhibit recrystallization at very low, micromolar concentrations which is equal to more than milligram range per mL (Park et al., 2013). In this study a very low protein concentration (7.43 $\mu\text{g/mL}$) present in COM 0.003 seems to be enough to positively inhibit the recrystallization effect of the water under freezing temperatures. Although the exact mechanism of action of all AFPs has not been fully explored, the most accepted mechanism using AFPs to decrease freezing point and inhibit ice formation is based on the adsorption-inhibition theory. Nevertheless, there exists a big lack in the deep details to fully understand ice recognition and binding, and crystallization inhibition (Tian et al., 2020).

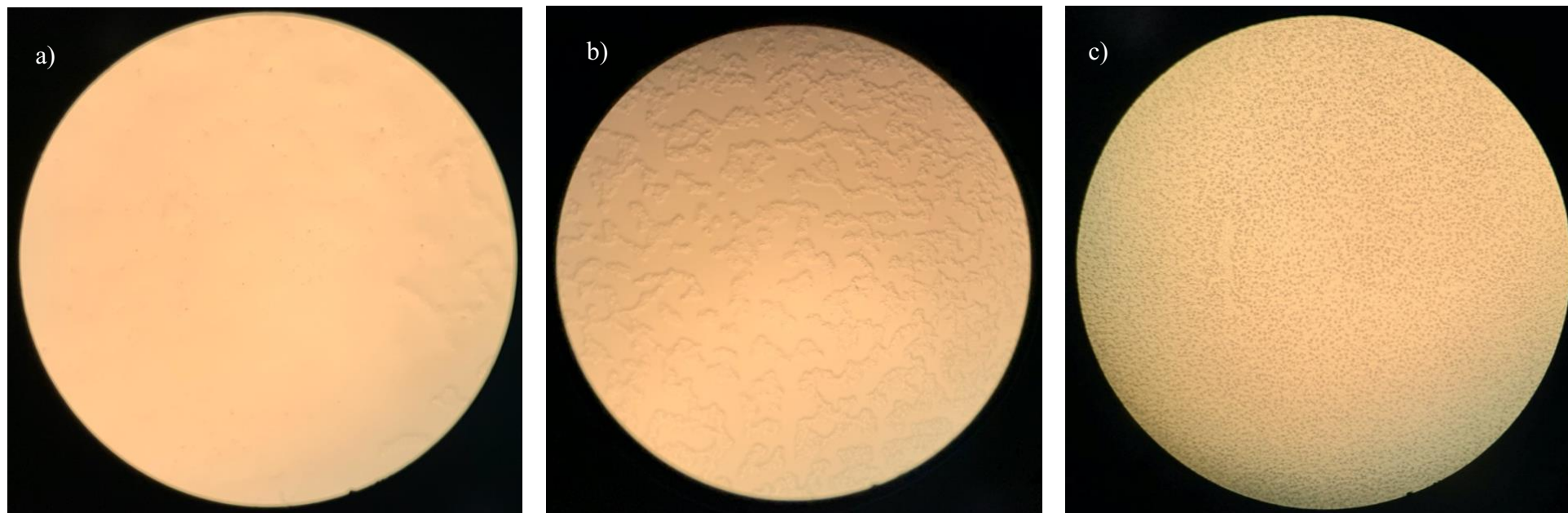


Figure 10.5. Inhibition of ice recrystallization by melon proteins after precipitation by ι -carrageenan (CRG) (COM 0.003) after a) 5, b) 15 and c) 30 min of incubation at $-20\text{ }^{\circ}\text{C}$. Proposed method.

10.3.4. Amino acid content of MPJ

The amino acid content of fruits is widely considered because these molecules contribute to their nutritional value, aroma, taste, and health-promoting effects, especially for essential amino acids, such as isoleucine, leucine, lysine, methionine, phenylalanine, threonine, and valine. In addition, several free amino acids may influence fruit taste. The best-known amino acids, including glutamic acid and aspartic acid, are responsible for freshness and taste. Lysine, glycine, threonine, serine, and alanine increases pulp sweetness, while arginine, isoleucine, phenylalanine, methionine, and histidine increase bitterness in fruits. In this study, 13 amino acids were found in *inodorus* melon peels as showed in **Table 10.2**. The total content of the amino acids profile ranged from 4.79 to 13.41 g/100 g protein, which is in concordance with the reported for Jingyu melon pulp (2.03 g/100 g protein) (Huang et al., 2017). Melon peels protein were rich in five essential amino acids, especially tryptophan (0.33 g/100 g protein), leucine (0.33 g/100 g protein), phenylalanine (0.21 g/100 g protein) and valine (0.32 g/100 g protein). These results were higher than the reported for leucine, phenylalanine and valine (0.011, 0.010 and 0.016 g/100 g protein, respectively) from *reticulatus* melon juice (Pei et al., 2020), but lower than the reported from Maazoun melon seeds for tryptophan, leucine, phenylalanine and valine (12.9, 9.64, 6.30 and 1.43 g/100 g protein, respectively) (Mallek-Ayadi, Bahloul and Kechaou, 2019). These differences in the amino acid content could be attributed to several factors such as variety, maturity, repining stage and post-harvest conditions as well as the protein content between each matrix, for example, melon pulp, peels, and seeds have been reported to possess 10-15%, 15-20% and 20-40% on a dry basis, respectively, (Rolim, Seabra, and de Macedo, 2020; Al-Sayed and Ahmed, 2013; Petkova and Antova, 2015). Furthermore, *inodorus* melon peels contained all the essential amino acids (excluding histidine) which demonstrates their attractiveness in terms of nutritional quality. These findings proves that melon by-products are suitable for the development of protein-rich food ingredients. On the other hand, the non-essential amino acids, especially serine, arginine, aspartic acid and glutamic acid were the compounds with the highest values, accounting for 3.93, 3.45, 1.98 and 1.45 g/100 g protein, respectively. According to Mallek-Ayadi, Bahloul and Kechaou, 2019, various melon parts, especially seeds, contained considerable amounts of glutamic acid (20.52 g/100 g protein), arginine (13.04 g/100 g protein) and aspartic acid (7.3 g/100 g protein). It is crucial to note that glutamic acid contributes to maintaining growth and health in both neonates and adults.

Dietary supplementation with glutamic acid improves intestinal and immune function, as well as energy production. Arginine holds a huge promise as a safe nutrient to reduce adiposity, increase muscle mass, and improve the metabolic profile. Aspartic acid is a precursor of such essential amino acids as asparagine, methionine, threonine, and lysine. However, to the best of our knowledge, this is the first study remarking the amino acid content from *inodorus* melon peels or from other melon variety (Das, Kim, Hong and Eun, 2019). Therefore, melon peel by-products were rich in value-added compounds, which could highlight them as potential raw materials for the formulations of novel food additives or ingredients with high amino acid content and thus enhanced nutritional quality.

Table 10.2. Amino acid profile by HPLC of melon peel juice (MPJ) and proteins extracted by precipitation with *i*-carrageenan (CRG) (COM 0.003).

Compound		g/100 g protein)	
Non-essential		MPJ	COM 0.003
Aspartic acid	Asp - Asn	1.98 ± 0.09	1.37 ± 0.02
Glutamic acid	Glu - Gln	1.45 ± 0.02	UD
Cystine	Cys	UD	ND
Serine	Ser	3.93 ± 0.06	2.11 ± 0.05
Glycine	Gly	0.54 ± 0.04	0.58 ± 0.01
Arginine	Arg	3.45 ± 0.08	0.01 ± 0.01
Alanine	Ala	0.75 ± 0.06	0.07 ± 1.96
Tyrosine	Tyr	0.24 ± 0.04	ND
Essential			
Threonine	Thr	0.01 ± 0.01	UD
Valine	Val	0.32 ± 0.02	UD
Phenylalanine	Phe	0.21 ± 0.03	0.32 ± 0.01
Isoleucine	Ile	0.19 ± 0.03	0.28 ± 0.01
Leucine	Leu	0.33 ± 0.03	0.04 ± 0.11
Total content		13.41 ± 0.37	4.79 ± 0.07

UD: under detection limit; ND: not detected. All determinations were carried out in triplicated and mean value ± standard deviation.

10.3.5. Amino acid profile after protein precipitation

As can be seen in **Table 10.2**, 11 amino acids were identified from the complexed proteins with carrageenan (COM 0.003) and at least 8 were quantified (3 essential and 5 non-essential amino acids) in which phenylalanine, isoleucine and leucine (0.32, 0.28 and 0.04 g/100 g protein) were the essential acids with the higher values, and serine (Ser), aspartic (Asn) acid and glycine (Gly) (2.11, 1.37 and 0.58 g/100 g protein, respectively) were the most representative non-essential acids. It is important to note that cysteine was identified in the MPJ, while was not detected in COM 0.003. The serine protease family possesses a catalytic triad that generally consists of serine, histidine, and aspartic/glutamic acid. These residues correspond to Ser525, His204, and Asp140 in cucumisin. Moreover,

among plant subtilase propeptides, most of their hydrophobic residues, including Val4, Leu80, Leu88, Val94, and Val97 located within N1 and N2 motifs of subtilisin E. It is assumed that these hydrophobic amino acids are important for the functions of the cucumisin propeptide. In this regard, the sequence of the first 13 amino acid residues from the NH₂ terminus of the native 67 kDa cucumisin and the first 7 amino acid residues from the 14 kDa polypeptide that is an autolytic product of native 67 kDa cumisin were determined by Edman degradation as Thr-Thr-Arg-Ser-Trp-Asp-Phe-Lys-Gly-Phe-Pro-Leu-Thr and Gly-Asp-Tyr-Ser-Ala-Cys-Thr, respectively (Nakagawa et al., 2010). On the other hand, several researchers have been reported the contribution of the similar amino acids profile and content on the antifreeze properties of AFPs, for example, Le Tri et al., (2019) compared the antifreeze properties of a novel AFPs - Fr10 - from wood frogs (*Rana sylvatica*), with respect of a well-known - LS-12 - type-IV AFP isolated from the longhorn sculpin (*Myoxocephalus octodecemspinosus*), due to their great structural homology in terms of size (72 and 108 amino acids, respectively), alanine content (9.7% and 11%, respectively), Glu/Gln content (22% and 26%, respectively), and their predicted structures (a four α -helical antiparallel bundle). Furthermore, the ice-binding sites of type I and III AFPs have been systematically altered to probe the relative importance of specific amino acids for ice-binding and activity. A delicate interplay of ISP/interactions seems likely, involving contributions of van der Waals interactions, hydrogen bonding, hydrophobic forces and water structuring (Voets, 2017). A previous model of Sea raven type II AFP suggests that the part of the primary peptide chain that is exposed to the aqueous environment is composed mainly of hydrophilic residues (Thr, Asn, Gln), which are capable of hydrogen bonding. The type III AFP consists of short, non-canonical β -strands, with a single turn of α -helix in the loop region. The predicted structure shows a relatively flat, amphipathic ice binding face where the residues important in ice binding such as Gln, Thr, Asn are exposed (Barrett, 2001). The THP from the Spruce budworm (*Choristoneura fumiferana*) appears to be totally unrelated to the other insect THPs. It has a high serine (Ser) and threonine (Thr) content (33 mol%) and an unusual β -helix structure. Interestingly these insect THPs all contain a predicted three-dimensional fold similar to trypsin inhibitor. One other insect THP has been partially characterised from the diapausing Milkweed bug (*Oncopeltus fasciatus*), these proteins have a high serine (Ser) content (30.5 mol%) as well and also a very high glycine (Gly) content (20 mol%) (Arima et al., 2000; Sharma and Deswal, 2014). Based on the amino acid profile and

contents of melon peel proteins and on the previous findings/reports mentioning amino acids characteristics and key roles for antifreeze activity, it could be stated that exist similar patterns and behaviors with respect to the other AFPs sources (fishes and insects) on the antifreeze activity exhibited by melon proteins after being precipitated by CRG. However, more studies to better understand the mechanism of action of how amino acids of melon peel proteins can interact with water ice crystals and subsequently, exert their antifreeze properties are needed.

10.4. Conclusions

In this study, the presence of proteins-like AFPs on melon peels was described for the first time. The extraction process with CRG allowed to extract at least 40% of the total protein content of the MPJ and four proteins with different MWs of 3.5, 6.2, 25 and 60 kDa were also extracted confirmed by the FPLC profile. The amino acid content of MPJ was obtained by HPLC-DAD were MPJ still had highest concentration than the COM 0.003 (4.79 and 13.41 g/100 g protein, respectively). The COM 0.003 at very low protein concentration (7.43 µg/mL) exhibited positive ice recrystallization inhibition by both methods employed e.g., 30% of sucrose assay (30 min of freezing cycle) and self-assembly inhibition of gold nanoparticles (after a freezing/thawing cycle), leading to no color change in the AuNP solution. The results reported herein could be validated and corroborated due to the fact of the great homology between structure and amino acid profile of the melon proteins and their related antifreeze activity compared to Type-I and III AFPs. However, more deep studies should be conducted to enhance and verify such property and explore their potential applications as cryoprotectants aimed to increase the quality of frozen products. It is important to highlight that this study is one of the few that involve industrial fruit by-products employed as resources of novel bioactive proteins - AFPs, which were extracted by a green precipitation technique, representing a lower cost method and with lesser environmental impact when compared to the traditional precipitation processes, while achieving good extraction yields and high protein purity.

PART V – Conclusions and Final Remarks

CHAPTER 11 - Conclusions

This PhD thesis presented interesting results from a research work that represent an important effort to find scientific insights and knowledge for the integral valorisation of melon (*Cucumis melo* L. *inodorus*) by-products, one of the most popular fruit crops producing food waste during its industrial processing. These melon by-products – namely peels, contain great quantity of value-added bioactive compounds with high industrial interest. With these outcomes, we expect to contribute towards a suitable valorisation/exploitation of melon by-products as an example to be fundamentally applied on a big scale (pilot/industrial) through flexible/tailored processes within the biorefinery and zero-waste approaches promoted by the new European directives currently launched that must be implemented during the next years (**Figure 11.1**).

In a more detail, in chapter 3, a low-cost fractionation approach was developed to explore the different fractions from melon by-products samples as resources of new value-added ingredients. The fractionation delivered three fractions (solid, liquid and pellet fractions), which were chemical characterized to understand their similarities and differences as well as to identify key target compounds for their subsequently extraction. The pellet fraction was rich in proteins (34.90% DM) and pigments – chlorophylls (174.84 mg/100 g FW) and carotenoids (98.59 mg/100 g DM). The solid fraction represented the richest portion of dietary fibre (44.42% DM), pectin (44.80% DM) and cellulose (27.68% DM). The liquid fraction was the richest portion in soluble dietary fibre (20.55% DM) and had better antioxidant activity on DPPH and ABTS assays, 7 and 2-folds higher than solid fraction, respectively, and almost 2-folds higher on both tests than pellet fraction correlated with the great phenolic content/profile (798.43 mg/100 g DM). These experimental results demonstrated that it would be valuable to exploit the pellet fraction as rich source of natural colourings and solid and liquid fraction for applications as a potential prebiotic agent with antioxidant phenolics. Overall, this first chapter used the fractionation approach in a zero-waste context, as a new, sustainable, and promising process for converting melon by-products into multiple value-added ingredients.

In the chapter 4 the combination of several separative techniques to obtain value compounds among pigments, chlorophylls and carotenoids was evaluated. Initially, the process involved cell disruption approach based on the use of bead milling method, achieving protein extraction yield of 8.34 g/100 g sample DW followed by a solid-phase adsorption by AmberLite™ HPR900 OH resin for carotenoids purification (2.6-4.6%) and later ([N_{1,1,1,12}]⁺Br⁻) ionic liquid was used for chlorophylls recovery (58.35%). Overall, the design of suitable processes to

exploit melon peel fractions that allow the extraction at the same time several value-added compounds with better recovery yields, less time-consuming and low usage of toxic solvents are under research to design pilot or industrial downstream platforms, therefore, these preliminary findings from this study could provide important markers for future solutions that fruit processing industries may need for the complete valorisation of their by-products as novel bioresources for obtention of these kind of valuable compounds.

After the exploration of the chemical and bioactives composition of the liquid and solid fractions from melon peels, the next step (chapter 5 and 6) was to evaluate their potential health-promoting properties as novel functional food ingredients labelled as melon peels juice (MPJ) powder and flour (MPF), respectively, especially, stability of their bioactives and antioxidant activity as well as prebiotic effects throughout *in vitro* gastrointestinal tract (GIT) and human faecal fermentation. In this regard, specifically, in chapter 5, the MPJ powder suffered a reduction on the recovery percentage of fructose (47.14%), phenolic content (TPC = 65.31%) and antioxidant activity (ABTS = 39.77%; DPPH = 45.91%), however, stable accessibility index (fructose = 90.56, TPC = 81.89%, ABTS = 76.55% and DPPH = 54.07% respectively) to exert their health-related benefits was exhibited after GIT digestion. Also, MPJ at 2% w/v exhibited a growth impact on *Bifidobacterium* and *Lactobacillus*, even after intestinal digestion, improving their growth and had low impact on Caco-2 intestinal cells, guaranteeing safeness after its intake. In chapter 6, the MPF was also subjected to the GIT digestion and fermented by human gut microbiota. Results demonstrated a release of individual phenolics (tyrosol, coumaric and caffeic acids), corroborated to total phenolic content (126.91%) and an increase in antioxidant activity at the gastric and intestinal digestion. After digestion, the MPF was used by human gut microbiota, assuring the maintenance of the beneficial bacteria such as *Lactobacillus* spp. and *Bifidobacterium* spp. Moreover, the growth and fermentation of beneficial bacteria functioned as a metabolism enhancer, since increased the production of healthier organic acids especially, acetate > propionate > butyrate – well-known as SCFA. Based on the achieved results for both melon fractions, it was possible to conclude that melon peels have the potential to be used as cheap resources for the development of functional ingredients (MPJ and MPF) with high content of prebiotic (dietary fibre and simple sugars) and antioxidant (phenolics) compounds, which can respond the consumer's demand and industrial needs of clean label food ingredients with low-cost and -caloric power for the partial replacement of traditional flours or refined sugars.

On the other hand, in chapter 7, a natural bioresource recovery approach on melon solid fraction valorisation as novel raw materials for pectin biopolymer extraction was implemented. The

yields of melon pectin were higher when extracted with citric acid (34%) followed by tartaric acid (31%) and hydrochloric acid (20%) with high protein content. The *D*-GalA content and DE ranged from 60 to 70% and 74 to 87%, respectively and were categorized as high-methoxyl pectins (HMP). Melon pectins had different molecular weights, ranging from 70 to 146 kDa. Also, pectins were capable to form very stable water-oil emulsions 34 to 42%, even higher than the commercial pectin (36%). Gels produced with 1% (w/v) of any melon pectins were stable at pH 3.5, Ca^{2+} 10 mM and 65% of sucrose, showing a higher elastic profile (G') than the viscous (G''), demonstrating their capabilities as thickening and gelling agent and a colloidal stabilizer. Following the sequence of research for natural biopolymers obtention, in chapter 9, a biorefinery approach was applied on melon peel residues after pectin extraction for the obtention of microcrystalline cellulose (MCC) through thermo-alkaline (2% NaOH, 1 h, 100 °C) method against the traditional (4.5% NaOH, 2 h, 80 °C) process. FTIR spectra of the final MCC showed typical characteristics of cellulose structure obtained with chemical methods involving alkaline-bleaching-acid hydrolysis. The degree of crystallinity of MCC ranged from 51.51-61.94% and 54.80-55.07% for thermo-alkaline and traditional process, respectively. SEM analysis revealed microcrystals with rough surfaces and great porosity, which could remark their high-water absorption capacity and drug carrier. Based on these findings, involving pectin and cellulose biopolymers from melon peels, it can be inferred that these by-products can be effectively employed as novel alternatives for industrial pectin and cellulose derivatives production, which could respond the increasing demand for gelling and emulsifying ingredients as well as potential applications as biodegradable materials specially, for the market needs of food, nutraceutical pharmacological industries.

In chapter 9 was described a green precipitation method for the extraction of a native proteolytic enzyme – known as Cucumisin (CUC) from MPJ. It was demonstrated for the first time that natural polysaccharide (carrageenan) was capable to chemically interact with CUC and be precipitated as non-soluble complex, which can be re-solubilized, keeping its biological activities namely, proteolytic (PA) and milk-clotting activities (MCA). The green precipitation process represents an environmentally friendly process for the enzyme industry against the toxic salts or solvents procedures (common industrial precipitation), allowing better purity and recovery yields. High recovery yield of active CUC was obtained (PA = 70 - 80%). The isolated CUC showed a molecular weight of 68 kDa and presented highly stable MCA in a wide range of CaCl_2 (20 to 60 mM), pH (5 to 7) and temperatures (30 to 85 °C). Raw MPJ demonstrated to possess significant PA (4.24 U/mg protein) and MCA (191.50 MCU/mg protein), but such values were increased by ammonium sulphate precipitation (1.60 and 2.06-folds, respectively),

and specially a noticeable increment was observed by green precipitation with 2.11 and 17.65-folds, respectively, demonstrating the capability to be an effective strategy to isolate and purify CUC, making possible to obtain ca. 0.17 g CUC/100 g of by-products and keeping its biological properties, representing a lower cost method and with lesser environmental impact when compared to the traditional precipitation processes, while achieving good extraction yields and high protein purity. Although green precipitation process confirmed the precipitation of CUC, further experimental test also confirmed the precipitation of lower molecular weight proteins from MPJ with interesting antifreeze-like properties. In chapter 10, proteins-like antifreeze proteins (AFPs) were described for the first time from melon peels, showing great similitude and homology in structure and amino acids profile when compared to the already reported Type-I and III AFPs. The FPLC profile confirm the extraction of 3.5, 6.2, 25 and 60 kDa proteins and the HPLC-DAD settle the amino acid content, ranging from 4.79 to 13.41 g/100 g protein, where serine, aspartic and glycine were the most representative acids. Moreover, the melon protein extract at approximately 7.43 $\mu\text{g/mL}$ of protein exhibited recrystallization inhibition on gold nanoparticles colorimetric method and sucrose assay. Therefore, the results from these studies using green precipitation provide new insight into the potential of further exploration of melon peels as novel resources of bioactive proteins with proteolytic/milk-clotting and antifreeze-like activities for their potential applications in the cheese making and cryoprotective agents.

Taking in consideration the general findings of this research, we can conclude that is feasible to use melon peels as a remarkable bioresource for the obtention of several value-added ingredients with multi-functional properties, including polyphenols, pigments, fibres (pectin and cellulose) and bioactive proteins with potential food, nutraceutical and pharmacological industrial application.

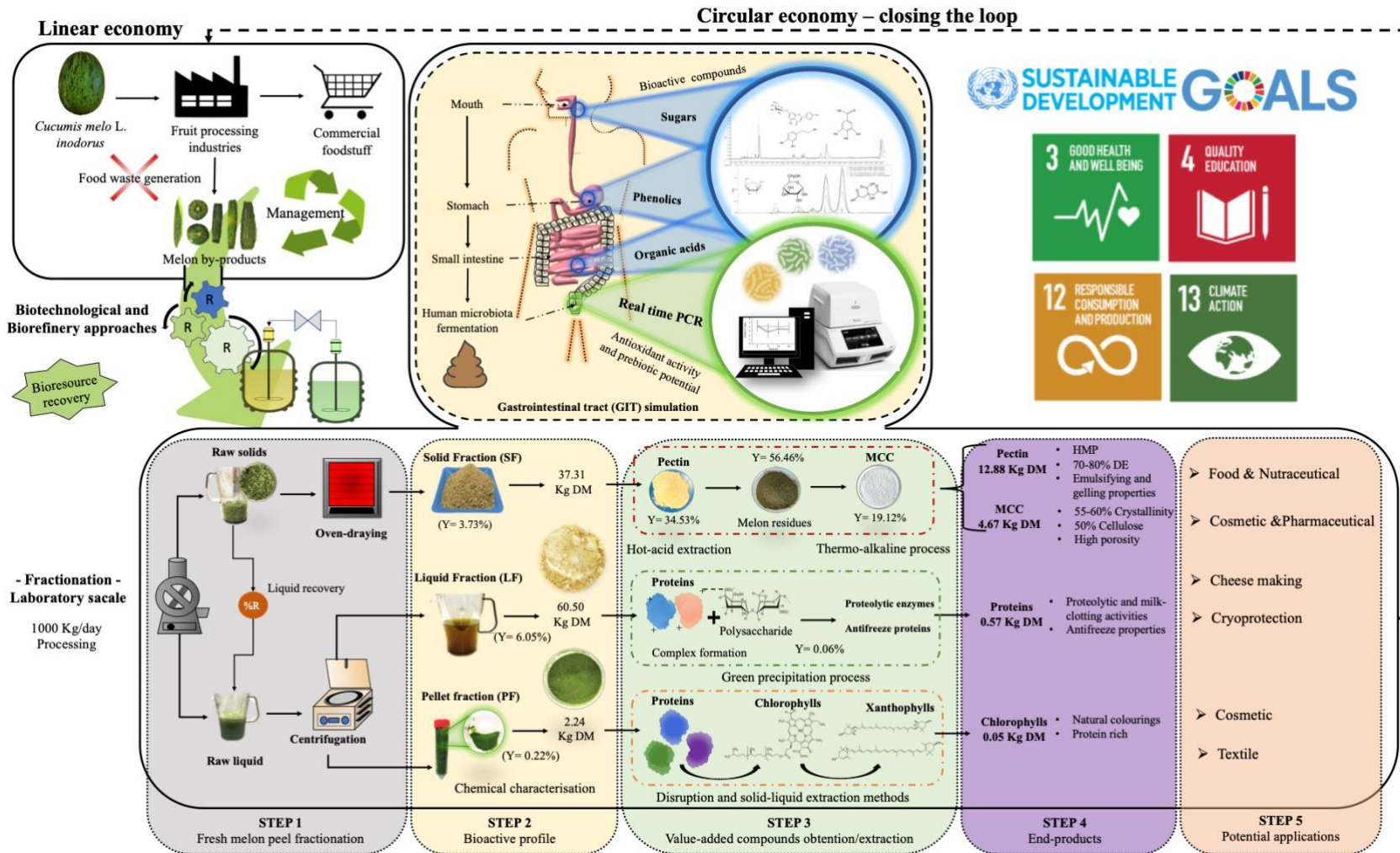


Figure 11.1. Proposed integrative process for melon peels valorisation into novel functional ingredients under biorefinery approach toward s a circular economy-based value chain to achieve the United Nations Sustainability Development Goals.

CHAPTER 12 – Future research and development

Although this research Ph D thesis delivered several interesting and promising outcomes under biorefinery and zero-waste approaches through a suitable fractionation of melon peel by-products for the identification and extraction of bioactive compounds namely pigments, pectins, cellulose and proteins with industrial potential, there are still several studies that should be carried out in order to improve these outputs and increase their industrial applicability. Thus, considering the conclusions obtained in this Ph D thesis, additional studies should be performed and, in this section, we propose some ideas that might be interesting and rewarding to be carried out in the future.

Regarding chapter 4, it could be interesting to explore the biological activities of each recovered fraction from the melon pellet fractions, including on one hand, antioxidant activities against DPPH, ABTS and ORAC (among others) for carotenoids and chlorophylls extracts, and on the other hand, proteolytic activities and protein profile for the protein extract. Also, the quantification and characterization of lignocellulosic (cellulose, hemicellulose and lignin) mass could be explored to achieve an integral valorisation of this melon fraction.

Concerning chapter 5 and 6, to improve melon LF and SF as potential plant-based food ingredients several bioactive evaluations should be explored such as antihypertensive activity through inhibition of ACE activity, analysis of anti-diabetic and anti-obesity properties. Also, the LF after GIT digestion should be evaluated on human microbiota to understand its prebiotic effect and the metabolic activity on the gut microbiota. Regarding, the SF a more detailed study on human microbiota fermentation as well as evaluations in cell lines, *in vivo* and clinical trials are needed to validate the outcomes resulting from the *in vitro* experiments described in this thesis.

In particular for chapter 7 and 8, the obtention of biopolymers with high industrial interest such as pectin and microcrystalline cellulose, respectively, could be enhanced by a statistical design to optimize the effect of temperature, time, pH and mass-to-solvent ratio on the yield as well as on physicochemical properties of melon peel pectin. Moreover, an evaluation of pectin bioactive/pharmacological properties, stability and cytotoxicity should be assessed to give a closer insight of a practical potential application of such pectin in food or pharmaceutical industry as a prototype of bio-functional hydrocolloid-gel or carrier of bioactive compounds. Together with this optimization process, it could be

needed a bigger lab-scale extraction, increasing the amount of melon peels (on dry or fresh basis) to at least 10 – 20 Kg. Also, microcrystalline cellulose (MCC) obtention after pectin extraction could be optimized and tested as a biomaterial/composite or carrier.

Besides, in chapter 9, cucumisin extraction by green precipitation process should be optimized using statistical tools to determine the best combination of variables (pH, protein extract and polyelectrolyte concentrations) to obtain the highest amounts of the protein precipitated by the polyelectrolyte without negative effect on its biological properties, namely proteolytic and milk-clotting activities. Once these parameters have been already optimized, the evaluation of the milk-clotting activity could be evaluated as vegetable rennet for cheese manufacture as an alternative of animal rennet. Furthermore, with the purpose to provide a realistic understanding of cucumisin extraction in an industrial environment for future food applications, a pilot scale of the precipitation process could be carried out by using 10 - 20 L of melon peel extract followed by a pilot scale cheese production, employing 5 – 10 L of raw milk. Finally, the pilot cheese production could be subjected to sensorial and cytotoxic studies as well as an evaluation of its physicochemical properties in order to guarantee a safe and high-quality food product.

Finally, from chapter 10, based on the preliminary and interesting results obtained regarding melon antifreeze proteins (AFPs), a complementary exploratory study on their extraction by green precipitation (after cucumisin extraction) and functionality should be conducted. Such exploration could be carried out by studying the behaviour of AFPs in different pH ranges and their interaction in contact with the polysaccharide followed by implementing different *in vitro* antifreeze activity assessments to increment their applicability as a natural cryoprotectant of cells and fruits.

All these aforementioned topics on pigments, pectin, microcrystalline cellulose, cucumisin and antifreeze proteins are important research trends in science and industrial areas, such as Biotechnology, Food and Nutrition and Pharmaceutical. Besides, these new studies are intended to generate more realistic and significative results for scientific and industrial interests, which allow an effective and correct management of melon peel by-products for their reincorporation into the food value chain as natural bioresources of bioactive compounds, allowing the implementation of circular economy and avoiding the environmental negative impact.

References

- Abboud, K. Y., Iacomini, M., Simas, F. F., Cordeiro, L. M. C., 2020. High methoxyl pectin from the soluble dietary fiber of passion fruit peel forms weak gel without the requirement of sugar addition. *Carbohydrate Polymers*, 246, 116616. <https://doi.org/10.1016/j.carbpol.2020.116616>
- Abenavoli, L., Scarpellini, E., Colica, C., Boccuto, L., Salehi, B., Sharifi-Rad, J., Aiello, V., Romano, B., De Lorenzo, A., Izzo, A. A., Capasso, R., 2019. Gut microbiota and obesity: A role for probiotics. *Nutrients*, 11(11), 2690. <https://doi.org/10.3390/nu11112690>.
- Abu-Thabit, N. Y., Judeh, A. A., Hakeem, A. S., Ul-Hamid, A., Umar, Y., Ahmad, A., 2020. Isolation and characterization of microcrystalline cellulose from date seeds (*Phoenix dactylifera* L.). *International journal of biological macromolecules*, 155, 730-739.
- Adiba, B.D., Nour-Eddine, B., Tamazouzt, C., Samia, K., Sonia, G., 2016. On the valorization of agro resource of Tizi Ouzou: Extraction for pectin from melon rinds and their application. *International Journal of Waste Resources*, 6(3Suppl), 73.
- Aggelis, A., Grierson, D., John, I., Karvouni, Z. 2000. Dna sequences from muskmelon (*Cucumis melo*) related to fruit ripening. U.S. Patent, Patent number 6,107,548.
- Aguilar-Toalá, J. E., Hernández-Mendoza, A., González-Córdova, A. F., Vallejo-Cordoba, B., Liceaga, A. M. 2019. Potential role of natural bioactive peptides for development of cosmeceutical skin products. *Peptides*. Elsevier Inc. <https://doi.org/10.1016/j.peptides.2019.170170>
- Ahmadi, F., Lee, Y.H., Lee, W.H., Oh, Y.K., Park, K.K., Kwak, W.S., 2018. Preservation of fruit and vegetable discards with sodium metabisulfite. *J. Environ. Manage.* 224, 113–121. <https://doi.org/10.1016/j.jenvman.2018.07.044>.
- Ahmadi, M., Madadlou, A., Sabouri, A.A., 2015. Isolation of micro- and nano-crystalline cellulose particles and fabrication of crystalline particles-loaded whey protein cold-set gel. *Food Chem.* 174, 97–103. <https://doi.org/10.1016/j.foodchem.2014.11.038>
- Al-Sayed, H.M.A., Ahmed, A.R., 2013. Utilization of watermelon rinds and sharlyn melon peels as a natural source of dietary fiber and antioxidants in cake. *Ann. Agric. Sci.* 58, 83–95. <https://doi.org/10.1016/j.aoas.2013.01.012>.
- Albert, C.G., 1930. Utilization of agricultural wastes. *Journal of Chemical Education*, 7(7), 1563. <https://doi.org/10.1021/ed007p1563>.
- Alexandra Silva, M., Gonçalves Albuquerque, T., Carneiro Alves, R., Oliveira, M.B.P.P., Costa, H.S. 2019. Melon seeds oil, fruit seeds oil and vegetable oils: a comparison study. *Annals of Medicine*, 51, 166–166.
- Amaro, A. L., Spadafora, N. D., Pereira, M. J., Dhorajiwala, R., Herbert, R. J., Müller, C. T., Pintado, M., 2018. Multitrait analysis of fresh-cut cantaloupe melon enables discrimination between storage times and temperatures and identifies potential markers for quality assessments. *Food Chemistry*, 241, 222–231. <https://doi.org/10.1016/j.foodchem.2017.08.050>
- Amaro, A.L., Almeida, D.P.F., Malcata, F.X., Beaulieu, J.C., Stein, R.E. 2010. Volatile composition and quality of fresh-cut *Cucumis melo* var. *Cantaloupensis* and *Inodorus* as affected by modified and controlled atmospheres. *Acta Horticulturae.* 877, 603–610.
- Amaro, A.L., Oliveira, A Almeida, D.P.F., 2015. Biologically Active Compounds in Melon: Modulation by Preharvest, Post-harvest, and Processing Factors. In: *Processing and Impact on Active Components in Food* (Preedy, V. Ed.). Amsterdam; Boston: Elsevier/Academic Press. pp. 165–171.
- Antosiewicz, J.M., Shugar, D., 2016. UV–Vis spectroscopy of tyrosine side-groups in studies of protein structure. Part 2: selected applications. *Biophys. Rev.* 8, 163–177.

- <https://doi.org/10.1007/s12551-016-0197-7>
- AOAC, 1997. Official methods of analyses (16th ed.). Washington, DC: Association of Official Analytical Chemists.
- AOAC, 1980. Official Methods of Analysis. Association of Official Analytical Chemists. Washington, D.C.
- AOAC, 1990. Official Methods of Analysis. (15th Edition)
- Aoe, S., Yamanaka, C., Fuwa, M., Tamiya, T., Nakayama, Y., Miyoshi, T., Kitazono, E., 2019. Effects of Barley max and high- β -glucan barley line on short-chain fatty acids production and microbiota from the cecum to the distal colon in rats. *PLoS One* 14, 1–14. <https://doi.org/10.1371/journal.pone.0218118>
- Arima, K., Uchikoba, T., Yonezawa, H., Kaneda, M., 2013. Cucumisin. In: Handbook of Proteolytic Enzymes (Rawlings, N.D., and Salvesen, G.S. Eds.). 3rd Ed. Amsterdam, the Netherlands, Elsevier Science BV. pp. 3254–3257.
- Arima, Kazunari, Uchikoba, T., Yonezawa, H., Shimada, M., Kaneda, M., 2000. Cucumisin-like protease from the latex of *Euphorbia supina*. *Phytochemistry*, 53(6), 639–644. [https://doi.org/10.1016/S0031-9422\(99\)00605-6](https://doi.org/10.1016/S0031-9422(99)00605-6)
- Arima, Kei, Yu, J., Iwasaki, S. 1970. Milk-clotting enzyme from *Mucor pusillus* var. Lindt. *Methods in Enzymology*, 19(C), 446–459. [https://doi.org/10.1016/0076-6879\(70\)19033-1](https://doi.org/10.1016/0076-6879(70)19033-1)
- Arnao, M., Cano, A., Acosta, M., 2001. The hydrophilic and lipophilic contribution to total antioxidant activity. *Food Chemistry*, 73(2), 239–244.
- Arscott, S. A., 2013. Food sources of carotenoids. In *Carotenoids and human health* (pp. 3–19). Humana Press, Totowa, NJ.
- Ascacio-Valdés, J.A., Buenrostro, J.J., De la Cruz, R., Sepúlveda, L., Aguilera, A.F., Prado, A., Contreras, J.C., Rodríguez, R., Aguilar, C.N., 2014. Fungal biodegradation of pomegranate ellagitannins. *Journal of basic microbiology*, 54(1), 28–34. <https://doi.org/10.1002/jobm.201200278>
- Asif-Ullah, M., Kim, K. S., Yu, Y. G., 2006. Purification and characterization of a serine protease from *Cucumis trigonus* Roxburghi. *Phytochemistry*, 67(9), 870–875. <https://doi.org/10.1016/j.phytochem.2006.02.020>
- Atef, A.M., Abou-Zaid, N., Ibrahim, I., Ramadan, M.T., Nadir, A. 2013. Quality evaluation of sheets, jam and juice from prickly pear and melon blends. *Life Science Journal*, 10, 200–208.
- Ayar, A., Siçramaz, H., Öztürk, S., Öztürk Yilmaz, S., 2018. Probiotic properties of ice creams produced with dietary fibres from by-products of the food industry. *International Journal of Dairy Technology*, 71(1), 174–182. <https://doi.org/10.1111/1471-0307.12387>
- Banerjee, J., Singh, R., Vijayaraghavan, R., MacFarlane, D., Patti, A. F., Arora, A. 2018. A hydrocolloid based biorefinery approach to the valorisation of mango peel waste. *Food Hydrocolloids*, 77, 142–151. <https://doi.org/10.1016/j.foodhyd.2017.09.029>
- Barrett, J. (2001). Thermal hysteresis proteins. *International Journal of Biochemistry and Cell Biology*, 33(2), 105–117. [https://doi.org/10.1016/S1357-2725\(00\)00083-2](https://doi.org/10.1016/S1357-2725(00)00083-2)
- Baumgarten, W., Bauernfeind, J.C., Boruff, C.S., 1944. Carotenoids in corn distillers' by-products. *Industrial and Engineering Chemistry*, 36(4), 344–347. <https://doi.org/10.1021/ie50412a015>.
- Ben Amira, A., Besbes, S., Attia, H., Blecker, C. 2017. Milk-clotting properties of plant rennets and their enzymatic, rheological, and sensory role in cheese making: A review. *International Journal of Food Properties*, 20, S76–S93. <https://doi.org/10.1080/10942912.2017.1289959>
- Ben-Gera, I., Kramer, A., 1969. The utilization of food Industries wastes. *Adv. Food Res.* 17, 77–152. [https://doi.org/10.1016/S0065-2628\(08\)60309-2](https://doi.org/10.1016/S0065-2628(08)60309-2).

- Bensaude-Vincent, B., Simon, J., 2008. Chemistry: The impure science. *Ann. Sci.* 67, 579–581. <https://doi.org/10.1080/00033790903395108>.
- Beroual, M., Boumaza, L., Mehelli, O., Trache, D., Tarchoun, A.F., Khimeche, K., 2021. Physicochemical properties and thermal stability of microcrystalline cellulose isolated from esparto grass using different delignification approaches. *J. Polym. Environ.* 29, 130–142. <https://doi.org/10.1007/s10924-020-01858-w>
- Bertha, C. T., Alberto, S. B. J., Tovar, J., Sáyago-Ayerdi, S. G., Zamora-Gasga, V. M., 2019. *In vitro* gastrointestinal digestion of mango by-product snacks: Potential absorption of polyphenols and antioxidant capacity. *International Journal of Food Science and Technology*, 54(11), 3091-3098.
- Biehler, E., Mayer, F., Hoffmann, L., Krause, E., Bo, T., 2010. Comparison of 3 Spectrophotometric Methods for Carotenoid Determination in Frequently Consumed Fruits and Vegetables. *J. Food Sci.* 75, C55–C61. <https://doi.org/10.1111/j.1750-3841.2009.01417.x>
- Bilal, M., Asgher, M., Iqbal, H.M.N., Hu, H., 2017. Biotransformation of lignocellulosic materials into value-added products — A review. *Int. J. Biol. Macromol.* 98, 447–458. <https://doi.org/10.1016/j.ijbiomac.2017.01.133>.
- Biondi, M. M., Maria, P., Paiva, G., Lúcia, V., Vieira, A., 2003. Proteases Alcalinas do Trato Digestório. *Braz. J. Food Technol.*, Vol. 6, 279–284.
- Blahuskova, V., Vlcek, J., Jancar, D., 2019. Study connective capabilities of solid residues from the waste incineration. *J. Environ. Manage.* 231, 1048–1055. <https://doi.org/10.1016/j.jenvman.2018.10.112>.
- Boeris, V., Spelzini, D., Farruggia, B., Picó, G., 2009. Aqueous two-phase extraction and polyelectrolyte precipitation combination: A simple and economically technologies for pepsin isolation from bovine abomasum homogenate. *Process Biochemistry*, 44(11), 1260–1264. <https://doi.org/10.1016/j.procbio.2009.07.001>
- Bonesi, M., Saab, A.M., Tenuta, M.C., Leporini, M., Saab, M.J., Loizzo, M.R., Tundis, R., 2019. Screening of traditional Lebanese medicinal plants as antioxidants and inhibitors of key enzymes linked to type 2 diabetes. *Plant Biosystems - An International Journal Dealing with all Aspects of Plant Biology*,
- Bradford, M. M., 1976. A rapid and sensitive method for the quantitation of microgram quantities of protein utilizing the principle of protein-dye binding. *Analytical Biochemistry*, 72(1–2), 248–254. [https://doi.org/10.1016/0003-2697\(76\)90527-3](https://doi.org/10.1016/0003-2697(76)90527-3)
- Brand-Williams, W., Cuvelier, M. E., Berset, C. L. W. T., 1995. Use of a free radical method to evaluate antioxidant activity. *LWT-Food science and Technology*, 28(1), 25-30.
- Buenrostro-Figueroa, J., Ascacio-Valdés, A., Sepúlveda, L., De la Cruz, R., Prado-Barragán, A., Aguilar-González, M., Rodríguez, R., Aguilar, C.N., 2013. Potential use of different agroindustrial by-products as supports for fungal ellagitannase production under solid-state fermentation. *Food Bioprod. Process.* 92, 376–382. <https://doi.org/10.1016/j.fbp.2013.08.010>.
- Campos, D.A., Coscueta, E.R., Valetti, N. W., Pastrana-Castro, L.M., Teixeira, J.A., Picó, G.A., Pintado, M.M., 2019. Optimization of bromelain isolation from pineapple byproducts by polysaccharide complex formation. *Food Hydrocolloids*, 87, 792-804 <https://doi.org/10.1016/j.foodhyd.2018.09.009>.
- Campos, D.A., Coscueta, E.R., Vilas-Boas, A.A., Silva, S., Teixeira, J.A., Pastrana, L.M., Pintado, M.M., 2020a. Impact of functional flours from pineapple by-products on human intestinal microbiota. *J. Funct. Foods* 67, 103830. <https://doi.org/10.1016/j.jff.2020.103830>.
- Campos, D.A., Gómez-García, R., Vilas-Boas, A.A., Madureira, A.R., Pintado, M.M., 2020b. Management of fruit industrial by-products—a case study on circular economy

- approach. *Molecules* 25. <https://doi.org/10.3390/molecules25020320>.
- Campos, D.A., Madureira, A.R., Sarmiento, B., Gomes, A.M., Pintado, M.M., 2015. Stability of bioactive solid lipid nanoparticles loaded with herbal extracts when exposed to simulated gastrointestinal tract conditions. *Food Res. Int.* 78, 131–140. <https://doi.org/10.1016/j.foodres.2015.10.025>
- Campos, D.A., Ribeiro, T.B., Teixeira, J.A., Pastrana, L., Pintado, M.M., 2020c. Integral valorization of pineapple (*Ananas comosus* L.) by-products through a green chemistry approach towards added value ingredients. *Foods*, 9(1), 60. <https://doi.org/10.3390/foods9010060>.
- Campos, D.A., Valetti, N.W., Oliveira, A., Pastrana-Castro, L. M., Teixeira, J.A., Pintado, M.M., Picó, G., 2017. Platform design for extraction and isolation of bromelain: complex formation and precipitation with carrageenan. *Process Biochem.* 54, 156–161. <https://doi.org/10.1016/j.procbio.2016.12.014>.
- Carmona-Cabello, M., García, I.L., Sáez-Bastante, J., Pinzi, S., Koutinas, A.A., Dorado, M.P., 2020. Food waste from restaurant sector – Characterization for biorefinery approach. *Bioresour. Technol.* 301, 122779. <https://doi.org/10.1016/j.biortech.2020.122779>.
- Catarino, M.D., Marçal, C., Bonifácio-Lopes, T., Campos, D., Mateus, N., Silva, A.M.S., Pintado, M.M., Cardoso, S.M., 2021. Impact of phlorotannin extracts from *fucus vesiculosus* on human gut microbiota. *Mar. Drugs* 19. <https://doi.org/10.3390/md19070375>
- Cervantes-Paz, B., Yahia, E.M., De Jesús Ornelas-Paz, J., Victoria-Campos, C.I., Ibarra-Junquera, V., Pérez-Martínez, J.D., Escalante-Minakata, P., 2014. Antioxidant activity and content of chlorophylls and carotenoids in raw and heat-processed Jalapeño peppers at intermediate stages of ripening. *Food Chem.* 146, 188–196. <https://doi.org/10.1016/j.foodchem.2013.09.060>
- Chaerunisaa, A. Y., Sriwidodo, S., Abdassah, M. 2019. Microcrystalline cellulose as pharmaceutical excipient. In *Pharmaceutical formulation design-recent practices*. IntechOpen. ISO 690
- Chan, K.T., Li, K., Liu, S.L., Chu, K.H., Toh, M., Xie, W.D., 2010. Cucurbitacin B inhibits STAT3 and the Raf/MEK/ERK pathway in leukemia cell line K562. *Cancer Letter.* 289, 46–52.
- Chasnitsky, M., Braslavsky, I., 2019. Ice-binding proteins and the applicability and limitations of the kinetic pinning model. *Philosophical Transactions of the Royal Society A: Mathematical, Physical and Engineering Sciences*, 377(2146). <https://doi.org/10.1098/rsta.2018.0391>
- Chedea, V.S., Kefalas, P., Socaciu, C., 2010. Patterns of carotenoid pigments extracted from two orange peel wastes (Valencia and Navel var.). *J. Food Biochem.* 34, 101–110. <https://doi.org/10.1111/j.1745-4514.2009.00267.x>.
- Chen, J., Cheng, H., Zhi, Z., Zhang, H., Linhardt, R. J., Zhang, F., Ye, X., 2021. Extraction temperature is a decisive factor for the properties of pectin. *Food Hydrocolloids*, 112, 106160. <https://doi.org/10.1016/j.foodhyd.2020.106160>
- Chen, M., Lahaye, M., 2021. Natural deep eutectic solvents pretreatment as an aid for pectin extraction from apple pomace. *Food Hydrocolloids*, 115, 106601. <https://doi.org/10.1016/j.foodhyd.2021.106601>
- Cheng, J.R., Liu, X.M., Zhang, W., Chen, Z.Y., Wang, X.P., 2018. Stability of phenolic compounds and antioxidant capacity of concentrated mulberry juice-enriched dried-minced pork slices during preparation and storage. *Food Control* 89, 187–195. <https://doi.org/10.1016/j.foodcont.2018.02.008>
- Chiappetta Jabbour, C.J., Seuring, S., Lopes de Sousa Jabbour, A.B., Jugend, D., De

- Camargo Fiorini, P., Latan, H., Izeppi, W.C., 2020. Stakeholders, innovative business models for the circular economy and sustainable performance of firms in an emerging economy facing institutional voids. *J. Environ. Manage.* 264, 110416. <https://doi.org/10.1016/j.jenvman.2020.110416>
- Cho, S., Song, N., Choi, J.Y., Shin, A., 2020. Effect of citric acid cycle genetic variants and their interactions with obesity, physical activity and energy intake on the risk of colorectal cancer: Results from a nested case-control study in the UK biobank. *Cancers (Basel)*. 12, 1–22. <https://doi.org/10.3390/cancers12102939>
- Chojnacka, K., Mikula, K., Izydorczyk, G., Skrzypczak, D., Witek-Krowiak, A., Gersz, A., Moustakas, K., Iwaniuk, J., Grzędzicki, M., Korczyński, M., 2021. Innovative high digestibility protein feed materials reducing environmental impact through improved nitrogen-use efficiency in sustainable agriculture. *J. Environ. Manage.* 291. <https://doi.org/10.1016/j.jenvman.2021.112693>.
- Chuyen, H.V., Nguyen, M.H., Roach, P.D., Golding, J.B., Parks, S.E., 2015. Gac fruit (*Momordica cochinchinensis* Spreng.): a rich source of bioactive compounds and its potential health benefits. *International Journal of Food Science and Technology*, 50(3), 567-577. <https://doi.org/10.1111/ijfs.12721>.
- Cláudio, A.F. M., Ferreira, A. M., Freire, C. S. R., Silvestre, A. J. D., Freire, M. G., Coutinho, J. A. P., 2012. Optimization of the gallic acid extraction using ionic-liquid-based aqueous two-phase systems. *Sep. Purif. Technol.* 97, 142–149. <https://doi.org/10.1016/j.seppur.2012.02.036>.
- Coelho, M., Pereira, R., Rodrigues, A. S., Teixeira, J. A., Pintado, M. E., 2019. Extraction of tomato by-products' bioactive compounds using ohmic technology. *Food and Bioproducts Processing*, 117, 329-339. <https://doi.org/10.1016/j.fbp.2019.08.005>.
- Coelho, M.C., Ribeiro, T.B., Oliveira, C., Batista, P., Castro, P., Monforte, A.R., Rodrigues, A.S., Teixeira, J., Pintado, M., 2021. *In vitro* gastrointestinal digestion impact on the bioaccessibility and antioxidant capacity of bioactive compounds from tomato flours obtained after conventional and ohmic heating extraction. *Foods* 10. <https://doi.org/10.3390/foods10030554>
- Condurso, C., Verzera, A., Dima, G., Tripodi, G., Crinò, P., Paratore, A., Romano, D., 2012. Effects of different rootstocks on aroma volatile compounds and carotenoid content of melon fruits. *Scientia Horticulturae*. 148, 9–16.
- Congdon, T., Notman, R., Gibson, M. I., 2013. Antifreeze (Glyco)protein mimetic behavior of poly(vinyl alcohol): Detailed structure ice recrystallization inhibition activity study. *Biomacromolecules*, 14(5), 1578–1586. <https://doi.org/10.1021/bm400217j>
- Connolly, M. L., Lovegrove, J. A., Tuohy, K. M., 2010. Konjac glucomannan hydrolysate beneficially modulates bacterial composition and activity within the faecal microbiota. *J. Funct. Foods* 2, 219–224. <https://doi.org/10.1016/j.jff.2010.05.001>
- Corrons, M. A., Bertucci, J. I., Liggieri, C. S., López, L. M. I., Bruno, M. A., 2012. Milk clotting activity and production of bioactive peptides from whey using *Maclura pomifera* proteases. *LWT - Food Science and Technology*, 47(1), 103–109. <https://doi.org/10.1016/j.lwt.2011.12.028>
- Costa, J. R., Amorim, M., Vilas-Boas, A., Tonon, R. V., Cabral, L. M., Pastrana, L., Pintado, M., 2019. Impact of *in vitro* gastrointestinal digestion on the chemical composition, bioactive properties, and cytotoxicity of *Vitis vinifera* L. cv. *Syrah* grape pomace extract. *Food and function*, 10(4), 1856-1869. <https://doi.org/10.1039/C8FO02534G>
- D'Amato, G., Cecchi, L., D'amato, M., Liccardi, G., 2010. Urban air pollution and climate change as environmental risk factors of respiratory allergy: an update. *Journal of Investigational Allergology and Clinical Immunology*, 20(2), 95-102.
- Da Silva, A.C., Jorge, N. 2014. Bioactive compounds of the lipid fractions of agro-industrial

- waste. *Food Research International*, 66, 493–500.
- da Silva, A.C., Jorge, N., 2017. Bioactive compounds of oils extracted from fruits seeds obtained from agroindustrial waste. *Eur. J. Lipid Sci. Technol.* 119, 1–5. <https://doi.org/10.1002/ejlt.201600024>.
- Da Silva, Larissa Morais Ribeiro, De Figueiredo, E. A. T., Ricardo, N. M. P. S., Vieira, I. G. P., De Figueiredo, R. W., Brasil, I. M., Gomes, C. L., 2014. Quantification of bioactive compounds in pulps and by-products of tropical fruits from Brazil. *Food Chem.* 143, 398–404. <https://doi.org/10.1016/j.foodchem.2013.08.00>.
- Dahiya, S., Kumar, A.N., Shanthi Sraavan, J., Chatterjee, S., Sarkar, O., Mohan, S.V., 2018. Food waste biorefinery: Sustainable strategy for circular bioeconomy. *Bioresour. Technol.* 248, 2–12. <https://doi.org/10.1016/j.biortech.2017.07.176>
- Das, P. R., Kim, Y., Hong, S. J., Eun, J. B., 2019. Profiling of volatile and non-phenolic metabolites—Amino acids, organic acids, and sugars of green tea extracts obtained by different extraction techniques. *Food Chem.* 296, 69–77. <https://doi.org/10.1016/j.foodchem.2019.05.194>.
- Dávalos, A., Gómez-Cordovés, C., Bartolomé, B., 2004. Extending applicability of the oxygen radical absorbance capacity (ORAC– fluorescein) assay. *Journal of agricultural and food chemistry*, 52(1), 48–54
- Day, D. T., 1914. Petroleum and its derivatives. *Journal of the Franklin Institute*. Volume 177, Issue 3, Pages 271–28. [https://doi.org/10.1016/S0016-0032\(14\)90930-9](https://doi.org/10.1016/S0016-0032(14)90930-9).
- De Andrade, R. M. S., Silva, S., Costa, C. M. D. S. F., Veiga, M., Costa, E., Ferreira, M. S. L., Pintado, M. E., 2020. Potential prebiotic effect of fruit and vegetable byproducts flour using *in vitro* gastrointestinal digestion. *Food Research International*, 137, 109354.
- de Carvalho Silva, J., de França, P.R.L., Porto, T.S., 2018. Optimized extraction of polygalacturonase from *Aspergillus aculeatus* URM4953 by aqueous two-phase systems PEG/Citrate. *Journal of Molecular Liquids*, 263, 81–88. <https://doi.org/10.1016/j.molliq.2018.04.112>.
- De Carvalho, N. M., Madureira, A. R., Pintado, M. E., 2019. The potential of insects as food sources—a review. *Crit. Rev. Food Sci. Nutr.* 0, 1–11. <https://doi.org/10.1080/10408398.2019.1703170>
- De Carvalho, N. M., Teixeira, F., Silva, S., Madureira, A. R., Pintado, M. E., 2019. Potential prebiotic activity of *Tenebrio molitor* insect flour using an optimized *in vitro* gut microbiota model. *Food Funct.* 10, 3909–3922. <https://doi.org/10.1039/c8fo01536h>
- de Farias, V. A., da Rocha Lima, A. D., Santos Costa, A., de Freitas, C. D. T., da Silva Araújo, I. M., dos Santos Garruti, D., de Oliveira, H. D., 2020. Noni (*Morinda citrifolia* L.) fruit as a new source of milk-clotting cysteine proteases. *Food Research International*, 127(April 2019), 108689. <https://doi.org/10.1016/j.foodres.2019.108689>
- De La Cruz, R., Ascacio, J. A., Buenrostro, J., Sepulveda, L., Rodriguez, R., Prado-Barragan, A., Contreras, J. C., Aguilera, A., Aguilar, C. N., 2015. Optimization of ellagitannase production by *Aspergillus niger* GH1 by solid-state sermentation. *Prep. Biochem. Biotechnol.* 45, 617–631. <https://doi.org/10.1080/10826068.2014.940965>.
- Deng, Q., Penner, M. H., Zhao, Y., 2011. Chemical composition of dietary fiber and polyphenols of five different varieties of wine grape pomace skins. *Food Research International*, 44(9), 2712–2720. <https://doi.org/10.1016/j.foodres.2011.05.026>
- Desbois, A.P., Smith, V.J., 2010. Antibacterial free fatty acids: Activities, mechanisms of action and biotechnological potential. *Applied Microbiology and Biotechnology*, 85, 1629–1642.
- Dey, T.B., Chakraborty, S., Jain, K.K., Sharma, A., Kuhad, R.C., 2016. Antioxidant phenolics and their microbial production by submerged and solid-state fermentation process: A review. *Trends Food Sci. Technol.* 53, 60–74.

- <https://doi.org/10.1016/j.tifs.2016.04.007>
- Dhillon, G.S., Oberoi, H.S., Kaur, S., Bansal, S., Brar, S.K., 2011. Value-addition of agricultural wastes for augmented cellulase and xylanase production through solid-state tray fermentation employing mixed-culture of fungi. *Ind. Crops Prod.* 34, 1160–1167. <https://doi.org/10.1016/j.indcrop.2011.04.001>
- Di Rienzi, S. C., Britton, R. A., 2020. Adaptation of the gut microbiota to modern dietary sugars and sweeteners. *Adv. Nutr.* 11, 616–629. <https://doi.org/10.1093/advances/nmz118>
- Díaz-Gómez, J., Moreno, J.A., Angulo, E., Sandmann, G., Zhu, C., Capell, T., Nogareda, C., 2017. Provitamin A carotenoids from an engineered high-carotenoid maize are bioavailable and zeaxanthin does not compromise β -carotene absorption in poultry. *Transgenic Res.* 26, 591–601. <https://doi.org/10.1007/s11248-017-0029-y>
- Diergaard, P. J., Van Enckevort, L. J. G., Posthuma, K. I., Prins, M. W. 2014. Powdery mildew resistance providing genes in *Cucumis melo*. US Patent, Patent Number: US 2014/0189908 A1.
- Dinan, T. G., Cryan, J. F., 2013. Melancholic microbes: A link between gut microbiota and depression? *Neurogastroenterol. Motil.* 25, 713–719. <https://doi.org/10.1111/nmo.12198>
- Dombrowski, U., Wagner, T., 2014. Mental strain as field of action in the 4th industrial revolution. *Procedia CIRP* 17, 100–105. <https://doi.org/10.1016/j.procir.2014.01.077>
- Dorni, C., Sharma, P., Saikia, G., Longvah, T., 2018. Fatty acid profile of edible oils and fats consumed in India. *Food Chemistry*, 238, 9–15.
- Dreyer, A., Ginoux, J.-P., Philippe Roch, D.L., Yard, C., 2006. *Cucumis melo* extract coated and/or microencapsulated in a fat-soluble agent based on a fatty substance. US Patent, Patent Number: 7132118
- Duarte, A. W. F., Lopes, A. M., Molino, J. V. D., Pessoa, A., Sette, L. D., 2015. Liquid-liquid extraction of lipase produced by psychrotrophic yeast *Leucosporidium scottii* L117 using aqueous two-phase systems. *Sep. Purif. Technol.* 156, 215–225. <https://doi.org/10.1016/j.seppur.2015.10.001>.
- Dubois, M., Gilles, K., Hamilton, J., Rebers, P., Smith, F., 1956. Colorimetric method for determination of sugars and related substances. *Analytical Chemistry*, 28(3), 350–356. <https://doi.org/10.1021/ac60111a017>
- Ducoli, S., Zacco, A., Bontempi, E., 2021. Incineration of sewage sludge and recovery of residue ash as building material: A valuable option as a consequence of the COVID-19 pandemic. *Journal of Environmental Management*, 282, 111966. <https://doi.org/10.1016/j.jenvman.2021.111966>
- Elia, V., Gnoni, M.G., Tornese, F., 2017. Measuring circular economy strategies through index methods: A critical analysis. *J. Clean. Prod.* 142, 2741–2751. <https://doi.org/10.1016/j.jclepro.2016.10.196>.
- Encalada, A. M. I., Pérez, C. D., Flores, S. K., Rossetti, L., Fissore, E. N., Rojas, A. M., 2019. Antioxidant pectin enriched fractions obtained from discarded carrots (*Daucus carota* L.) by ultrasound-enzyme assisted extraction. *Food Chemistry*, 289, 453–460. <https://doi.org/10.1016/j.foodchem.2019.03.078>
- Esparza, I., Jiménez-Moreno, N., Bimbela, F., Ancín-Azpilicueta, C., Gandía, L.M., 2020. Fruit and vegetable waste management: Conventional and emerging approaches. *J. Environ. Manage.* 265. <https://doi.org/10.1016/j.jenvman.2020.110510>.
- Estevez-Pintado, M.M., 2017. Method for extraction and/or isolation of bromelain from pineapple 1, 1–22. Patent No. EP 3 252 156 A1.
- Fabian, C. B., Huynh, L. H., Ju, Y. H., 2010. Precipitation of rice bran protein using carrageenan and alginate. *LWT - Food Science and Technology*, 43(2), 375–379. <https://doi.org/10.1016/j.lwt.2009.08.005>

- Fagbohunge, M.O., Herbert, B.M.J., Hurst, L., Ibeto, C.N., Li, H., Usmani, S.Q., Semple, K.T., 2017. The challenges of anaerobic digestion and the role of biochar in optimizing anaerobic digestion. *Waste Manag.* 61, 236–249. <https://doi.org/10.1016/j.wasman.2016.11.028>.
- Falah, M.A.F., Nadine, M.D., Suryandono, A., 2015. Effects of storage conditions on quality and shelf-life of fresh-cut melon (*Cucumis Melo* L.) and papaya (*Carica papaya* L.). *Procedia Food Science*, 3, 313–322.
- FAO., 2019. The State of Food and Agriculture 2019. Moving forward on food loss and waste reduction. Rome. Licence: CC BY-NC-SA 3.0 IGO. Retrived from <http://www.fao.org/3/ca6030en/ca6030en.pdf>
- FAOSTAT, 2018. Food and Agriculture Organization of the United Nations. FOA. Retrieved from <http://www.fao.org/faostat/en/#data/QC>
- Felton, G.E., 1949. Use of Ion Exchangers in by-product recovery from pineapple waste. *Food Technology*, 3(2), 40-42.
- Fernández-Veledo, S., Ceperuelo-Mallafre, V., Vendrell, J., 2021. Rethinking succinate: an unexpected hormone-like metabolite in energy homeostasis. *Trends in Endocrinology and Metabolism*. <https://doi.org/10.1016/j.tem.2021.06.003>
- Ferreira, F. V., Mariano, M., Rabelo, S.C., Gouveia, R.F., Lona, L.M.F., 2018. Isolation and surface modification of cellulose nanocrystals from sugarcane bagasse waste: From a micro- to a nano-scale view. *Appl. Surf. Sci.* 436, 1113–1122. <https://doi.org/10.1016/j.apsusc.2017.12.137>
- Figlarz, M., 1994. Soft chemistry: Thermodynamic and structural aspects. In *Materials Science Forum*. Trans Tech Publ, pp. 55–68.
- Fissore, E. N., Rojas, A. M., Gerschenson, L. N., 2012. Rheological performance of pectin-enriched products isolated from red beet (*Beta vulgaris* L. var. *conditiva*) through alkaline and enzymatic treatments. *Food Hydrocolloids*, 26(1), 249–260. <https://doi.org/10.1016/j.foodhyd.2011.06.004>
- Fleshman, M.K., Lester, G.E., Riedl, K.M., Kopec, R.E., Narayanasamy, S., Curley, R.W., Schwartz, S.J. Harrison, E.H., 2011. Carotene and novel apocarotenoid concentrations in orange-fleshed *Cucumis melo* melons: Determinations of β -carotene bioaccessibility and bioavailability. *Journal of Agricultural and Food Chemistry*, 59,
- Food and Agricultural Organisation - FAO., 2013. Food wastage footprint: Impacts on natural resources. Retrived from <http://www.fao.org/3/i3347e/i3347e.pdf>
- Forbes, H., Quested, T., O'Connor, C., 2021. Food Waste Index Report 2021. United Nations Environment Programme: Nairobi, Kenya.
- Freitas, C. D. T., Leite, H. B., Oliveira, J. P. B., Amaral, J. L., Egito, A. S., Vairo-Cavalli, S., Ramos, M. V., 2016. Insights into milk-clotting activity of latex peptidases from *Calotropis procera* and *Cryptostegia grandiflora*. *Food Research International*, 87, 50–59. <https://doi.org/10.1016/j.foodres.2016.06.020>
- Freitas, C. M. P., Sousa, R. C. S., Dias, M. M. S., Coimbra, J. S. R., 2020. Extraction of pectin from passion fruit peel. *Food Engineering Reviews*, 12(4), 460–472. <https://doi.org/10.1007/s12393-020-09254-9>
- Fu, X., Liu, Z., Zhu, C., Mou, H., Kong, Q., 2019. Nondigestible carbohydrates, butyrate, and butyrate-producing bacteria. *Crit. Rev. Food Sci. Nutr.* 59, S130–S152. <https://doi.org/10.1080/10408398.2018.1542587>
- Fundo, J. F., Amaro, A. L., Madureira, A. R., Carvalho, A., Feio, G., Silva, C. L. M., Quintas, M. A. C., 2015. Fresh-cut melon quality during storage: An NMR study of water transverse relaxation time. *Journal of Food Engineering*, 167, 71–76. <https://doi.org/10.1016/j.jfoodeng.2015.03.028>
- Fundo, J.F., Miller, F.A., Garcia, E., Santos, J.R., Silva, C.L.M., Brandão, T.R.S., 2017.

- Physicochemical characteristics, bioactive compounds and antioxidant activity in juice, pulp, peel and seeds of Cantaloupe melon. *J. Food Meas. Charact.* 0, 0. <https://doi.org/10.1007/s11694-017-9640-0>.
- Gagaoua, M., Ziane, F., Rabah, S. N., Boucherba, N., El, A.A.K.E.H., Bouanane-Darenfed, A., Hafid, K., 2017. Three phase partitioning, a scalable method for the purification and recovery of cucumisin, a milk-clotting enzyme, from the juice of *Cucumis melo* var. *reticulatus*. *Int. J. Biol. Macromol.* 102, 515–525. <https://doi.org/10.1016/j.ijbiomac.2017.04.060>.
- Galanakis, C. M. (2012). Recovery of high added-value components from food wastes: Conventional, emerging technologies and commercialized applications. *Trends in Food Science and Technology*, 26(2), 68–87. <https://doi.org/10.1016/j.tifs.2012.03.003>
- Ganji, S.M., Singh, H., Friedman, M., 2019. Phenolic Content and Antioxidant Activity of Extracts of 12 Melon (*Cucumis melo*) peel powders prepared from commercial melons. *Journal of Food Science*, 84, 1943–1948.
- Gao, M., Li, S., Zou, H., Wen, F., Cai, A., Zhu, R., Tian, W., Shi, D., Chai, H., Gu, L., 2021. Aged landfill leachate enhances anaerobic digestion of waste activated sludge. *J. Environ. Manage.* 293, 112853. <https://doi.org/10.1016/j.jenvman.2021.112853>.
- Garcia-Andres, S., Bachlava, E., Chan, E.K.-F., Joobeur, T., King, J.J., Kraakman, P.J., Krishnamurthy, S., Mills, J. M., de Vries, J., 2016. Melon plants with improved disease Tolerance. European Patent, Patent Number: 15189209.8
- Garzón, C.G., Hours, R.A., 1992. Citrus waste: An alternative substrate for pectinase production in solid-state culture. *Bioresour. Technol.* 39, 93–95. [https://doi.org/10.1016/0960-8524\(92\)90061-2](https://doi.org/10.1016/0960-8524(92)90061-2).
- Geier, G.J., 2014. Melon Cutting Boards. US Patent, Patent Number: US 8,857,802 B1.
- Gergely Forgacs, Mohammad Pourbafrani, Claes Niklasson, M.J.T. and I.S.H., 2011. Methane production from citrus wastes: process development and cost estimation 250–255. <https://doi.org/10.1002/jctb.2707>.
- Ghisellini, P., Cialani, C., Ulgiati, S., 2016. A review on circular economy: The expected transition to a balanced interplay of environmental and economic systems. *J. Clean. Prod.* 114, 11–32. <https://doi.org/10.1016/j.jclepro.2015.09.007>.
- Giacometti, J., Bursać Kovačević, D., Putnik, P., Gabrić, D., Bilušić, T., Krešić, G., Stulić, V., Barba, F.J., Chemat, F., Barbosa-Cánovas, G., Režek Jambrak, A., 2018. Extraction of bioactive compounds and essential oils from mediterranean herbs by conventional and green innovative techniques: A review. *Food Research International*, 113, 245–262.
- Gibson, G. R., Hutkins, R., Sanders, M. E., Prescott, S. L., Reimer, R. A., Salminen, S. J., Reid, G., 2017. Expert consensus document: The International Scientific Association for Probiotics and Prebiotics (ISAPP) consensus statement on the definition and scope of prebiotics. *Nature reviews Gastroenterology and hepatology*, 14(8), 491–502.
- Giuliani, C., Marzorati, M., Daghio, M., Franzetti, A., Innocenti, M., de Wiele, T. Van, Mulinacci, N., 2019. Effects of olive and pomegranate by-products on human microbiota: A study using the SHIME® *in vitro* simulator. *Molecules* 24. <https://doi.org/10.3390/molecules24203791>
- Golbargi, F., Mohammad, S., Gharibzahedi, T., Zoghi, A., Mohammadi, M., Hashemifesharaki, R., 2021. Microwave-assisted extraction of arabinan-rich pectic polysaccharides from melon peels: Optimization, purification, and bioactivity. *Carbohydrate Polymers*, 256, 117522. <https://doi.org/10.1016/j.carbpol.2020.117522>
- Gomes, S., Belo, A. T., Alvarenga, N., Dias, J., Lage, P., Pinheiro, C., Martins, A. P. L., 2019. Characterization of *Cynara cardunculus* L. flower from Alentejo as a coagulant agent for cheesemaking. *International Dairy Journal*, 91, 178–184. <https://doi.org/10.1016/j.idairyj.2018.09.010>

- Gómez-García, R., Campos, D.A., Aguilar, C.N., Madureira, A.R., Pintado, M., 2020. Valorization of melon fruit (*Cucumis melo* L.) by-products: Phytochemical and biofunctional properties with emphasis on recent trends and advances. *Trends Food Sci. Technol.* 99, 507–519. <https://doi.org/10.1016/j.tifs.2020.03.033>.
- Gómez-García, R., Campos, D.A., Aguilar, C.N., Madureira, A.R., Pintado, M., 2021a. Biological protein precipitation: a green process for the extraction of cucumisin from melon (*Cucumis melo* L. *inodorus*) by-products. *Food Hydrocoll.* 116, 106650. <https://doi.org/10.1016/j.foodhyd.2021.106650>.
- Gómez-García, R., Campos, D. A., Oliveira, A., Aguilar, C. N., Madureira, A. R., Pintado, M., 2021b. A chemical valorisation of melon peels towards functional food ingredients: Bioactives profile and antioxidant properties. *Food Chem.* 335, 127579. <https://doi.org/10.1016/j.foodchem.2020.127579>.
- Gómez-García, R., Débora A. Campos, Cristóbal N. Aguilar, Ana R. Madureira, Manuela Pintado, 2021c. Valorisation of food agro-industrial by-products: From the past to the present and perspectives. <https://doi.org/10.1016/j.jenvman.2021.113571>
- Gómez-García, R., Martínez-Ávila, G.C.G., Aguilar, C.N., 2012. Enzyme-assisted extraction of antioxidative phenolics from grape (*Vitis vinifera* L.) residues. *3 Biotech* 2, 297–300. <https://doi.org/10.1007/s13205-012-0055-7>.
- Gómez, M., Martínez, M.M., 2018. Fruit and vegetable by-products as novel ingredients to improve the nutritional quality of baked goods. *Crit. Rev. Food Sci. Nutr.* 58, 2119–2135. <https://doi.org/10.1080/10408398.2017.1305946>
- Górnaś, P., Rudzińska, M., 2016. Seeds recovered from industry by-products of nine fruit species with a high potential utility as a source of unconventional oil for biodiesel and cosmetic and pharmaceutical sectors. *Industrial Crops and Products*, 83, 329–338.
- Górnaś, P., Pugajeva, I., Segliņa, D., 2014b. Seeds recovered from by-products of selected fruit processing as a rich source of tocochromanols: RP-HPLC/FLD and RP-UPLC-ESI/MSⁿ study. *European Food Research and Technology*, 239, 519–524.
- Górnaś, P., Soliven, A., Segliņa, D. 2014. Seed oils recovered from industrial fruit by-products are a rich source of tocopherols and tocotrienols: Rapid separation of $\alpha/\beta/\gamma/\delta$ homologues by RP-HPLC/FLD. *European journal of lipid science and technology*, 117(6), 773-777.
- Goulas, V., Manganaris, G.A., 2012. Exploring the phytochemical content and the antioxidant potential of Citrus fruits grown in Cyprus. *Food Chemistry*. 131, 39–47.
- Govea Salas, M., Rivas Estilla, A.M., Rodríguez Herrera, R., Lozano Sepúlveda, S.A., Aguilar Gonzalez, C.N., Zugasti Cruz, A., Zugasti-Cruz, A., Salas-Villalobos, T.B., Morlett Chávez, J.A., 2016. Gallic acid decreases hepatitis C virus expression through its antioxidant capacity. *Experimental and therapeutic medicine*, 11(2), 619-624. <https://doi.org/10.3892/etm.2015.2923>.
- Govea Salas, M., Zugasti Cruz, A., Silva Belmares, S., Valdivia Urdiales, B., Rodríguez Herrera, R., 2013. Anticancer Activity of Gallic Acid in Biological Models *in vitro*. *Scientific Magazine of the Autonomous University of Coahuila*, 5 (9), 5–11.
- Graham, L. A., Agrawal, P., Oleschuk, R. D., Davies, P. L., 2018. High-capacity ice-recrystallization endpoint assay employing superhydrophobic coatings that is equivalent to the ‘splat’ assay. *Cryobiology*, 81, 138–144. <https://doi.org/10.1016/j.cryobiol.2018.01.011>
- Grassino, A. N., Barba, F. J., Brnčić, M., Lorenzo, J. M., Lucini, L., Brnčić, S. R., 2018. Analytical tools used for the identification and quantification of pectin extracted from plant food matrices, wastes and by-products: A review. *Food Chemistry*, 266, 47–55. <https://doi.org/10.1016/j.foodchem.2018.05.105>
- Gullón, B., Gullón, P., Tavaría, F., Pintado, M., Gomes, A. M., Alonso, J. L., Parajó, J.C.,

2014. Structural features and assessment of prebiotic activity of refined arabinoxylooligosaccharides from wheat bran. *J. Funct. Foods* 6, 438–449. <https://doi.org/10.1016/j.jff.2013.11.010>
- Gullon, B., Pintado, M.E., Barber, X., Fernández-lópez, J., Pérez-álvarez, J.A., Viudamartos, M., 2015a. Bioaccessibility, changes in the antioxidant potential and colonic fermentation of date pits and apple bagasse flours obtained from co-products during simulated *in vitro* gastrointestinal digestion. *FRIN* 78, 169–176. <https://doi.org/10.1016/j.foodres.2015.10.021>
- Gullon, B., Pintado, M.E., Fernández-lópez, J., 2015b. *In vitro* gastrointestinal digestion of pomegranate peel (*Punica granatum*) flour obtained from co-products: Changes in the antioxidant potential and bioactive compounds 19, 617–628. <https://doi.org/10.1016/j.jff.2015.09.056>
- Guo, C., Yang, J., Wei, J., Li, Y., Xu, J., Jiang, Y., 2003. Antioxidant activities of peel, pulp and seed fractions of common fruits as determined by FRAP assay. *Nutrition Research*, 23 (12), 1719–1726.
- Gutiérrez-Sarmiento, W., Sáyago-Ayerdi, S. G., Goñi, I., Gutiérrez-Miceli, F. A., Abud-Archila, M., Rejón-Orantes, J. D. C., Ruíz-Valdiviezo, V. M., 2020. Changes in intestinal microbiota and predicted metabolic pathways during colonic fermentation of mango (*Mangifera indica* L.)—Based bar indigestible fraction. *Nutrients*, 12(3), 683. <https://doi.org/10.3390/nu12030683>
- Güzel, M., Akpınar, Ö., 2019. Valorisation of fruit by-products: Production characterization of pectins from fruit peels. *Food and Bioproducts Processing*, 115, 126–133.
- Haldar, D., Purkait, M.K., 2020. Micro and nanocrystalline cellulose derivatives of lignocellulosic biomass: A review on synthesis, applications and advancements. *Carbohydr. Polym.* 250, 116937. <https://doi.org/10.1016/j.carbpol.2020.116937>
- Han, W., Meng, Y., Hu, C., Dong, G., Qu, Y., Deng, H., Guo, Y., 2017. Mathematical model of Ca²⁺ concentration, pH, pectin concentration and soluble solids (sucrose) on the gelation of low methoxyl pectin. *Food Hydrocolloids*, 66, 37–48. <https://doi.org/10.1016/j.foodhyd.2016.12.011>
- Harini, K., Chandra Mohan, C., 2020. Isolation and characterization of micro and nanocrystalline cellulose fibers from the walnut shell, corncob and sugarcane bagasse. *Int. J. Biol. Macromol.* 163, 1375–1383. <https://doi.org/10.1016/j.ijbiomac.2020.07.239>
- Hashemi, Z., Ebrahimzadeh, M.A., Khalili, M., 2019. Sun protection factor, total phenol, flavonoid contents and antioxidant activity of medicinal plants from Iran. *Tropical Journal of Pharmaceutical Research*, 18, 1443–1448.
- Hassas-Roudsari, M., Goff, H. D., 2012. Ice structuring proteins from plants: Mechanism of action and food application. *Food Research International*, 46(1), 425–436. <https://doi.org/10.1016/j.foodres.2011.12.018>
- Henan, I., Tlili, I., Him, T.R., Ali, A.B.E.N., Jebari, H., 2016. Carotenoid content and antioxidant activity of local varieties of muskmelon (*Cucumis melo* L.) grown in Tunisia. *Journal of New Sciences, Agriculture and Biotechnology*, 29 (4), 1672–1675.
- Ho, K.K.H.Y., Ferruzzi, M.G., Liceaga, A.M., San Martín-González, M.F., 2015. Microwave-assisted extraction of lycopene in tomato peels: Effect of extraction conditions on all-trans and cis-isomer yields. *LWT - Food Sci. Technol.* 62, 160–168. <https://doi.org/10.1016/j.lwt.2014.12.061>
- Holscher, H. D., 2020. Diet affects the gastrointestinal microbiota and health. *Journal of the Academy of Nutrition and Dietetics*, 120(4), 495–499. <https://doi.org/10.1016/j.jand.2019.12.016>
- Horax, R., Hettiarachchy, N., Chen, P. 2010. Extraction, quantification, and antioxidant activities of phenolics from pericarp and seeds of bitter melons (*Momordica charantia*)

- harvested at three maturity stages (Immature, Mature, and Ripe). *Journal of Agricultural and Food Chemistry*, 58(7), 4428–4433. <https://doi.org/10.1021/jf9029578>
- Hosseini, S. S., Khodaiyan, F., Kazemi, M., Najari, Z., 2019. Optimization and characterization of pectin extracted from sour orange peel by ultrasound assisted method. *International Journal of Biological Macromolecules*, 125, 621–629. <https://doi.org/10.1016/j.ijbiomac.2018.12.096>
- Huang, Y., Li, W., Zhao, L., Shen, T., Sun, J., Chen, H., Kong, Q., Nawaz, M.A., Bie, Z., 2017. Melon fruit sugar and amino acid contents are affected by fruit setting method under protected cultivation. *Sci. Hortic. (Amsterdam)*. 214, 288–294. <https://doi.org/10.1016/j.scienta.2016.11.055>
- Hurtado-Romero, A., Del Toro-Barbosa, M., Gradilla-Hernández, M.S., Garcia-Amezquita, L.E., García-Cayuela, T., 2021. Probiotic properties, prebiotic fermentability, and GABA-producing capacity of microorganisms isolated from Mexican milk kefir grains: A clustering evaluation for functional dairy food applications. *Foods* 10, 2275. <https://doi.org/10.3390/foods10102275>
- Huynh, N.T., Van Camp, J., Smagghe, G., Raes, K., 2014. Improved release and metabolism of flavonoids by steered fermentation processes: a review. *International Journal of Molecular Sciences*, 15, 19369–19388.
- Ibarruri, J., Cebrián, M., Hernández, I., 2021. Valorisation of fruit and vegetable discards by fungal submerged and solid-state fermentation for alternative feed ingredients production. *J. Environ. Manage.* 281. <https://doi.org/10.1016/j.jenvman.2020.111901>.
- Ibrahim, A. S. S., Elbadawi, Y. B., El-Tayeb, M. A., Al-maary, K. S., Maany, D. A. F., Ibrahim, S. S. S., Elagib, A. A., 2019. Alkaline serine protease from the new halotolerant alkaliphilic *Salipaludibacillus agaradhaerens* strain AK-R: purification and properties. *3 Biotech*, 9(11), 1–11. <https://doi.org/10.1007/s13205-019-1928-9>
- Ibrahim, S., Al, R., Mohamed, G., Elkhayat, E., Moustafa, M., 2016. Cucumol A: a cytotoxic triterpenoid from *Cucumis melo* seeds. *Brazilian Journal of Pharmacognosy*, 26, 701–704.
- Ibrahim, S.R.M., Mohamed, G.A., 2015. Cucumin S, a new phenylethyl chromone from *Cucumis melo* var. *Reticulatus* seeds. *Brazilian Journal of Pharmacognosy*, 25, 462–464.
- Ikeyama, N., Murakami, T., Toyoda, A., Mori, H., Ino, T., Ohkuma, M., Sakamoto, M., 2020. Microbial interaction between the succinate-utilizing bacterium *Phascolarctobacterium faecium* and the gut commensal *Bacteroides thetaiotaomicron*. *Microbiologyopen*, 9(10), e1111. <https://doi.org/10.1002/mbo3.1111>
- Imbert, E., 2017. Food waste valorization options: Opportunities from the bioeconomy. *Open Agric.* 2, 195–204. <https://doi.org/10.1515/opag-2017-0020>.
- Ismail, H.I., Chan, K.W., Mariod, A.A., Ismail, M., 2010. Phenolic content and antioxidant activity of cantaloupe (*cucumis melo*) methanolic extracts. *Food Chem.* 119, 643–647. <https://doi.org/10.1016/j.foodchem.2009.07.023>.
- Ismail, M., 2010. Fatty acid composition and antioxidant activity of oils from two cultivars of Cantaloupe extracted by supercritical fluid extraction. *Fats and Oils*, 61 (1), 37–44.
- Jiang, W. xin, Qi, J. R., Huang, Y. xing, Zhang, Y., Yang, X. Q., 2020. Emulsifying properties of high methoxyl pectins in binary systems of water-ethanol. *Carbohydrate Polymers*, 229, 115420. <https://doi.org/10.1016/j.carbpol.2019.115420>
- Jin, E., Guo, J., Yang, F., Zhu, Y., Song, J., Jin, Y., Rojas, O.J., 2016. On the polymorphic and morphological changes of cellulose nanocrystals (CNC-I) upon mercerization and conversion to CNC-II. *Carbohydr. Polym.* 143, 327–335. <https://doi.org/10.1016/j.carbpol.2016.01.048>
- John, I., Muthukumar, K., Arunagiri, A., John, I., 2017. A review on the potential of citrus waste for D- Limonene, pectin, and bioethanol production production. *International*

- Journal of Green Energy, 00(00), 1–14. <https://doi.org/10.1080/15435075.2017.1307753>
- John, I., Muthukumar, K., Arunagiri, A., 2017. A review on the potential of citrus waste for *D*-Limonene, pectin, and bioethanol production. *International Journal of Green Energy*, 14(7), 599–612. <https://doi.org/10.1080/15435075.2017.1307753>.
- John, I., Yaragarla, P., Muthaiah, P., Ponnusamy, K., Appusamy, A., 2017. Statistical optimization of acid catalyzed steam pretreatment of citrus peel waste for bioethanol production 0, 1–5. <https://doi.org/10.1016/j.reffit.2017.04.001>
- Kalapathy, U., Proctor, A., 2001. Effect of acid extraction and alcohol precipitation conditions on the yield and purity of soy hull pectin. *Food Chemistry*, 73(4), 393–396. [https://doi.org/10.1016/S0308-8146\(00\)00307-1](https://doi.org/10.1016/S0308-8146(00)00307-1)
- Kalmykova, Y., Sadagopan, M., Rosado, L., 2018. Circular economy – From review of theories and practices to development of implementation tools. *Resour. Conserv. Recycl.* 135, 190–201. <https://doi.org/10.1016/j.resconrec.2017.10.034>.
- Kareem, S., Rahman, R., 2011. Utilization of banana peels for citric acid production by *Aspergillus niger*. *Agric. Biol. J. North Am.* 4, 384–387. <https://doi.org/10.5251/abjna.2013.4.4.384.387>.
- Kargarzadeh, H., Mariano, M., Huang, J., Lin, N., Ahmad, I., Dufresne, A., Thomas, S., 2017. Recent developments on nanocellulose reinforced polymer nanocomposites: A review. *Polymer* 132, 368–393.
- Karlsson, F., Tremaroli, V., Nielsen, J., Bäckhed, F., 2013. Assessing the human gut microbiota in metabolic diseases. *Diabetes* 62, 3341–3349. <https://doi.org/10.2337/db13-0844>
- Kassies, W., Ponsoda, T.M.M., Faber, N.M., Mazereeuw, J.P., Barrera, A.B.Z. 2015. Cvyv-resistant plants of the species *Cucumis melo*. US Patent, Patent Number: 8,962931 B2
- Kawabata, K., Yoshioka, Y., Terao, J., 2019. Role of intestinal microbiota in the bioavailability and physiological functions of dietary polyphenols. *Molecules* 24. <https://doi.org/10.3390/molecules24020370>.
- Kazemi, M., Khodaiyan, F., Labbafi, M., Hosseini, S. S., 2020. Ultrasonic and heating extraction of pistachio by-product pectin: physicochemical, structural characterization and functional measurement. *Journal of Food Measurement and Characterization*, 14(2), 679–693. <https://doi.org/10.1007/s11694-019-00315-0>
- Kazemi, M., Samani, A., Ezzati, S., Khodaiyan, F., 2021. High-quality pectin from cantaloupe waste: eco-friendly extraction process, optimization, characterization and bioactivity measurements. <https://doi.org/10.1002/jsfa.11327>
- Kharismi, R.R.A.Y., Sutriyo, Suryadi, H., 2018. Preparation and characterization of microcrystalline cellulose produced from betung bamboo (*Dendrocalamus asper*) through acid hydrolysis. *J. Young Pharm.* 10, s79–s83. <https://doi.org/10.5530/jyp.2018.2s.15>
- Khatkar, A., Nanda, A., Kumar, P., Narasimhan, B., 2015. Synthesis and antimicrobial evaluation of ferulic acid derivatives. *Res. Chem. Intermed.* 41, 299–309. <https://doi.org/10.1016/j.ejmech.2014.01.026>.
- Kian, L. K., Saba, N., Jawaid, M., Fouad, H., 2020. Characterization of microcrystalline cellulose extracted from olive fiber. *International journal of biological macromolecules*, 156, 347–353.
- Kim, J. S., Choi, G. G., 2018. Pyrolysis of lignocellulosic biomass for biochemical production. In *Waste Biorefinery* (pp. 323–348). Elsevier.
- Kolayli, S., Kara, M., Tezcan, F., Erim, F.B., Sahin, H., Ulusoy, E., Aliyazicioglu, R., 2010. Comparative study of chemical and biochemical properties of different melon cultivars: Standard, hybrid, and grafted melons. *Journal of Agricultural and Food Chemistry*, 58, 9764–9769.

- Kostik, V., Memeti, S., Bauer, B., 2013. Fatty acid composition of edible oils and fats. *Journal of Hygienic Engineering and Design*, 112–116.
- Kowlgi, N. G., Chhabra, L., 2015. D-lactic acidosis: An underrecognized complication of short bowel syndrome, 2015 *Gastroenterology Research and Practice*, 1–8. <https://doi.org/10.1155/2015/476215>.
- Kuhad, R.C., Gupta, R., Singh, A., 2011. Microbial Cellulases and Their Industrial Applications. *Enzyme Research*, 2011, 1-10.
- Laforge, F.B., Mains, G.H., 1923. Furfural from corncobs. *Industrial and Engineering Chemistry*, 15(8), 823-829. <https://doi.org/10.1021/ie50164a022>.
- Lai, C.S., Wu, J.C., Pan, M.H., 2015. Molecular mechanism on functional food bioactives for anti-obesity. *Curr. Opin. Food Sci.* 2, 9–13. <https://doi.org/10.1016/j.cofs.2014.11.008>.
- Lane, A.G., 1983. Anaerobic digestion of citrus peel press liquors. *Environmental Technology*, 4(8-9), 349-352. 10.1080/09593338309384217.
- Larios-Cruz, R., Buenrostro-Figueroa, J., Prado-Barragán, A., Rodríguez-Jasso, R.M., Rodríguez-Herrera, R., Montañez, J.C., Aguilar, C.N., 2019. Valorization of grapefruit by-products as solid support for solid-state fermentation to produce antioxidant bioactive extracts. *Waste and Biomass Valorization*, 10(4), 763-769. <https://doi.org/10.1007/s12649-017-0156-y>.
- Larsen, E., Christensen, L.P., 2005. Simple saponification method for the quantitative determination of carotenoids in green vegetables. *J. Agric. Food Chem.* 53, 6598–6602. <https://doi.org/10.1021/jf050622>+
- Laur, L.M., Tian, L., 2011. Provitamin A and vitamin C contents in selected California-grown cantaloupe and honeydew melons and imported melons. *Journal of Food Composition and Analysis*, 24, 194–201.
- Lavefve, L., Howard, L.R., Carbonero, F., 2019. Berry polyphenols metabolism and impact on human gut microbiota and health. *Food Funct.* 11, 45–65. <https://doi.org/10.1039/c9fo01634a>
- Le Tri, D., Childers, C. L., Adam, M. K., Ben, R. N., Storey, K. B., Biggar, K. K., 2019. Characterization of ice recrystallization inhibition activity in the novel freeze-responsive protein Fr10 from freeze-tolerant wood frogs, *Rana sylvatica*. *Journal of Thermal Biology*, 84, 426–430. <https://doi.org/10.1016/j.jtherbio.2019.07.030>
- Lee, K.M., Kalyani, D., Tiwari, M.K., Kim, T.S., Dhiman, S.S., Lee, J.K., Kim, I.W., 2012. Enhanced enzymatic hydrolysis of rice straw by removal of phenolic compounds using a novel laccase from yeast *Yarrowia lipolytica*. *Bioresour. Technol.* 123, 636–645. <https://doi.org/10.1016/j.biortech.2012.07.066>.
- Lee, S. C., Prosky, L. DeVries, J. W., 1992. Determination of total, soluble, and insoluble, dietary fiber in foods - enzymatic gravimetric method, MES-TRIS buffer: Collaborative study. *J. Assoc. Off. Anal. Chem.*, 75, 395-416
- Lester, G. E., 2008. Antioxidant, sugar, mineral, and phytonutrient concentrations across edible fruit tissues of orange-fleshed honeydew melon (*Cucumis melo* L.). *Journal of Agricultural and Food Chemistry*, 56(10), 3694–3698. <https://doi.org/10.1021/jf8001735>
- Leung, C.C.J., Cheung, A.S.Y., Zhang, A.Y.Z., Lam, K.F., Lin, C.S.K. 2012., Utilisation of waste bread for fermentative succinic acid production. *Biochemical engineering journal*, 65, 10-15.
- Levine, M., Nelson, G.H., Anderson, D.Q., Jacobs, P.B., 1935. Utilization of agricultural wastes I. Lignin and microbial decomposition. *Industrial and Engineering Chemistry*, 27(2), 195-200. <https://doi.org/10.1021/ie50302a020>.
- Li, N., Feng, Z., Niu, Y., Yu, L. L., 2018. Structural, rheological and functional properties of modified soluble dietary fiber from tomato peels. *Food Hydrocolloids*, 77, 557–565.

- <https://doi.org/10.1016/j.foodhyd.2017.10.034>
- Lichtenthaler, H. K., 1987. Chlorophylls and Carotenoids: Pigments of Photosynthetic Biomembranes. *Methods in Enzymology*, 148(C), 350–382. [https://doi.org/10.1016/0076-6879\(87\)48036-1](https://doi.org/10.1016/0076-6879(87)48036-1)
- Lieschova, M.A., Bilan, M. V., Bohomaz, A.A., Tishkina, N.M., Brygadyrenko, V. V., 2020. Effect of succinic acid on the organism of mice and their intestinal microbiota against the background of excessive fat consumption. *Regul. Mech. Biosyst.* 11, 153–161. <https://doi.org/10.15421/022023>
- Liguori, R., Faraco, V., 2016. Biological processes for advancing lignocellulosic waste biorefinery by advocating circular economy. *Bioresour. Technol.* 215, 13–20. <https://doi.org/10.1016/j.biortech.2016.04.054>
- Lima, B. N. B., Lima, F. F., Tavares, M. I. B., Costa, A. M. M., Pierucci, A. P. T. R., 2014. Determination of the centesimal composition and characterization of flours from fruit seeds. *Food chemistry*, 151, 293-299.
- Liu, C., Li, B., Du, H., Lv, D., Zhang, Y., Yu, G., Peng, H., 2016. Properties of nanocellulose isolated from corncob residue using sulfuric acid, formic acid, oxidative and mechanical methods. *Carbohydrate polymers*, 151, 716-724. <https://doi.org/10.1016/j.carbpol.2016.06.025>
- Liu, G., Ying, D., Guo, B., Cheng, L. J., May, B., Bird, T., Augustin, M., 2019. Extrusion of apple pomace increases antioxidant activity upon *in vitro* digestion. *Food and function*, 10(2), 951-963.
- Liu, Y., Nguyen, A., Allen, A., Zoldan, J., Huang, Y., Chen, J.Y., 2017. Regenerated cellulose micro-nano fiber matrices for transdermal drug release. *Mater. Sci. Eng. C* 74, 485–492. <https://doi.org/10.1016/j.msec.2016.12.048>
- Lo, H.Y., Li, C.C., Chen, F.Y., Chen, J.C., Hsiang, C.Y., Ho, T.Y., 2017. Gastro-resistant insulin receptor-binding peptide from momordica charantia improved the glucose tolerance in streptozotocin-induced diabetic mice via insulin receptor signaling pathway. *Journal of Agricultural and Food Chemistry*, 65(42), 9266-9274. <https://doi.org/10.1021/acs.jafc.7b0358>.
- Löfgren, C., Guillotin, S., Evenbratt, H., Schols, H., Hermansson, A. M., 2005. Effects of calcium, pH, and blockiness on kinetic rheological behavior and microstructure of HM pectin gels. *Biomacromolecules*, 6(2), 646–652. <https://doi.org/10.1021/bm049619>
- Lombardi, J., Valetti, N.W., Picó, G., Boeris, V., 2013. Obtainment of a highly concentrated pancreatic serine proteases extract from bovine pancreas by precipitation with polyacrylate. *Sep. Purif. Technol.* 116, 170–174. <https://doi.org/10.1016/j.seppur.2013.05.047>.
- Long, S.K., Patrick, R., 1965. Production of 2, 3-butylene glycol from citrus wastes. II. The *Bacillus polymyxa* fermentation. *Applied microbiology*, 13(6), 973-976.
- Lonsane, B.K., Ghildyal, N.P., Budiartman, S., Ramakrishna, S.V., 1985. Engineering aspects of solid-state fermentation. *Enzyme Microb. Technol.* 7, 258–265. [https://doi.org/10.1016/0141-0229\(85\)90083-3](https://doi.org/10.1016/0141-0229(85)90083-3).
- López-Salas, L., Borrás-Linares, I., Quintin, D., García-Gomez, P., Giménez-Martínez, R., Segura-Carretero, A., Lozano-Sánchez, J., 2021. Artichoke by-products as natural source of phenolic food ingredient. *Appl. Sci.* 11. <https://doi.org/10.3390/app11093788>
- Lopresto, C.G., Petrillo, F., Casazza, A.A., Aliakbarian, B., Perego, P., Calabrò, V., 2014. A non-conventional method to extract *D*-limonene from waste lemon peels and comparison with traditional Soxhlet extraction. *Separation and Purification Technology*, 137, 13-20. <https://doi.org/10.1016/j.seppur.2014.09.015>.
- Lourenço, S.C., Campos, D.A., Gómez-García, R., Pintado, M., Oliveira, M.C., Santos, D. I., Moldão-Martins, M., Corrêa-Filho, L.C., Alves, V.D., 2021. Optimization of natural

- antioxidants extraction from pineapple peel and their stabilization by spray drying. *Foods*, 10(6), 1255. <https://doi.org/10.3390/foods10061255>.
- Lucas-gonzalez, R., Navarro-coves, S., Pérez-álvarez, J.A., Viuda-martos, M., Fernández-lópez, J., Mu, L.A., 2016. Assessment of polyphenolic profile stability and changes in the antioxidant potential of maqui berry (*Aristotelia chilensis* (Molina) Stuntz) during *in vitro* gastrointestinal digestion. *Ind. Crops Prod.* 94, 774–782.
- Lucas-González, R., Viuda-Martos, M., Álvarez, J. A. P., Fernández-López, J., 2018. Changes in bioaccessibility, polyphenol profile and antioxidant potential of flours obtained from persimmon fruit (*Diospyros kaki*) co-products during *in vitro* gastrointestinal digestion. *Food chemistry*, 256, 252-258. <https://doi.org/10.1016/j.foodchem.2018.02.128>
- Lucas-Torres, C., Lorente, A., Cabañas, B., Moreno, A., 2016. Microwave heating for the catalytic conversion of melon rind waste into biofuel precursors. *Journal of Cleaner Production.* 138, 59–69.
- Ma, Y., Yang, Y., Gao, J., Feng, J., Shang, Y., Wei, Z. 2020. Phenolics and antioxidant activity of bamboo leaves soup as affected by *in vitro* digestion. *Food and Chemical Toxicology*, 135, 110941.
- Madureira, A.R., Amorim, M., Gomes, A.M., Pintado, M.E., Malcata, F.X., 2011. Protective effect of whey cheese matrix on probiotic strains exposed to simulated gastrointestinal conditions. *Food Res. Int.* 44, 465–470. <https://doi.org/10.1016/j.foodres.2010.09.010>
- Madureira, A.R., Atatoprak, T., Çabuk, D., Sousa, F., Pullar, R.C., Pintado, M., 2018. Extraction and characterisation of cellulose nanocrystals from pineapple peel. *Int. J. Food Stud.* 7, 24–33. <https://doi.org/10.7455/ijfs/7.1.2018.a3>
- Madureira, A.R., Campos, D., Gullon, B., Marques, C., Rodríguez-Alcalá, L.M., Calhau, C., Alonso, J.L., Sarmiento, B., Gomes, A.M., Pintado, M., 2016. Fermentation of bioactive solid lipid nanoparticles by human gut microflora. *Food Funct.* 7, 516–529.
- Madureira, A.R., Campos, D.A., Oliveira, A., Sarmiento, B., Pintado, M.M., Gomes, A.M., 2016. Insights into the protective role of solid lipid nanoparticles on rosmarinic acid bioactivity during exposure to simulated gastrointestinal conditions. *Colloids Surfaces B Biointerfaces* 139, 277–284. <https://doi.org/10.1016/j.colsurfb.2015.11.039>
- Mallek-Ayadi, S., Bahloul, N., Kechaou, N., 2019. Phytochemical profile, nutraceutical potential and functional properties of *Cucumis melo* L. seeds. *Journal of the Science of Food and Agriculture*, 99(3), 1294–1301. <https://doi.org/10.1002/jsfa.9304>
- Mallek-Ayadi, S., Bahloul, N., Kechaou, N., 2017. Characterization, phenolic compounds and functional properties of *Cucumis melo* L. peels. *Food Chem.* 221, 1691–1697. <https://doi.org/10.1016/j.foodchem.2016.10.117>.
- Mallek-Ayadi, S., Bahloul, N., Kechaou, N., 2018. Chemical composition and bioactive compounds of *Cucumis melo* L. seeds: Potential source for new trends of plant oils. *Process Saf. Environ. Prot.* <https://doi.org/10.1016/j.psep.2017.09.016>.
- Malone, J. J., Hulton, A. T., MacLaren, D. P. 2021. Exogenous carbohydrate and regulation of muscle carbohydrate utilisation during exercise. *European Journal of Applied Physiology*, 1-15.
- Mancini, E., Raggi, A., 2021. A review of circularity and sustainability in anaerobic digestion processes. *J. Environ. Manage.* 291, 112695. <https://doi.org/10.1016/j.jenvman.2021.112695>.
- Mangiagalli, M., Brocca, S., Orlando, M., Lotti, M., 2020. The “cold revolution”. Present and future applications of cold-active enzymes and ice-binding proteins. *New Biotechnology*, 55, 5–11. <https://doi.org/10.1016/j.nbt.2019.09.003>
- Markowiak-Kopec, P., Ślizewska, K., 2020. The effect of probiotics on the production of short-chain fatty acids by human intestinal microbiome. *Nutrients*, 12(4), 1107.

- <https://doi.org/10.3390/nu12041107>
- Martin-Rios, C., Hofmann, A., Mackenzie, N., 2021. Sustainability-oriented innovations in food waste management technology. *Sustain.* 13, 1–12. <https://doi.org/10.3390/su13010210>.
- Martínez-Ávila, G.C., Aguilera-Carbó, A.F., Rodríguez-Herrera, R., Aguilar, C.N., 2012. Fungal enhancement of the antioxidant properties of grape waste. *Annals of microbiology*, 62(3), 923-930. <https://doi.org/10.1007/s13213-011-0329-z>.
- Martins, M., Fernandes, A.P.M., Torres-Acosta, M.A., Collén, P.N., Abreu, M.H., Ventura, S.P.M., 2021a. Extraction of chlorophyll from wild and farmed *Ulva* spp. using aqueous solutions of ionic liquids. *Sep. Purif. Technol.* 254, 117589. <https://doi.org/10.1016/j.seppur.2020.117589>
- Martins, M., Soares, B.P., Santos, J.H.P.M., Bharmoria, P., Torres Acosta, M.A., Dias, A.C.R.V., Coutinho, J.A.P., Ventura, S.P.M., 2021b. Sustainable strategy based on induced precipitation for the purification of phycobiliproteins. *ACS Sustain. Chem. Eng.* 9, 3942–3954. <https://doi.org/10.1021/acssuschemeng.0c09218>
- Martins, S., Mussatto, S.I., Martínez-Avila, G., Montañez-Saenz, J., Aguilar, C.N., Teixeira, J.A., 2011. Bioactive phenolic compounds: Production and extraction by solid-state fermentation. A review. *Biotechnol. Adv.* 29, 365–373. <https://doi.org/10.1016/j.biotechadv.2011.01.008>.
- Masci, A., Carradori, S., Casadei, M. A., Petralito, S., Ragno, R., Cesa, S., La, R., 2018. *Lycium barbarum* polysaccharides: extraction, purification, structural characterisation and evidence about hypoglycaemic and hypolipidaemic effects. A review. *Food Chemistry*. <https://doi.org/10.1016/j.foodchem.2018.01.176>
- Matharu, A.S., Melo, E.M. De, Houghton, J.A., 2016. Opportunity for high value-added chemicals from food supply chain wastes. *Bioresour. Technol.* 215, 123–130. <https://doi.org/10.1016/j.biortech.2016.03.039>.
- Mazorra-Manzano, M. A., Moreno-Hernández, J. M., Ramírez-Suarez, J. C., Torres-Llanez, M. de J., González-Córdova, A. F., Vallejo-Córdova, B., 2013. Sour orange *Citrus aurantium* L. flowers: A new vegetable source of milk-clotting proteases. *LWT - Food Science and Technology*, 54(2), 325–330. <https://doi.org/10.1016/j.lwt.2013.07.009>
- McElhinney, T.R., Becker, B.M., Jacobs, P.B., 1938. Destructive distillation of corncobs effect of temperature on yields of products. *Industrial and Engineering Chemistry*, 30(6), 697-703. <https://doi.org/10.1021/ie50342a018>.
- Medeiros, A. K. de O. C., Gomes, C. de C., Amaral, M. L. Q. de A., Medeiros, L. D. G. de, Medeiros, I., Porto, D. L., Passos, T. S., 2019. Nanoencapsulation improved water solubility and color stability of carotenoids extracted from Cantaloupe melon (*Cucumis melo* L.). *Food Chemistry*, 270, 562–572. <https://doi.org/10.1016/j.foodchem.2018.07.099>
- Medina-Morales, M., Martínez-Hernández, J.L., De La Garza, H., Aguilar, C.N., 2011. Cellulolytic enzymes production by solid state culture using pecan nutshell as substrate and support. *AJABS*, 6(2), 196-200. <https://doi.org/10.3844/ajabssp.2011.196.200>.
- Medina, J. M., Fernández-López, R., Crespo, J., Cruz, F. D. L., 2021. Propionate fermentative genes of the gut microbiome decrease in inflammatory bowel disease. *Journal of clinical medicine*, 10(10), 2176. <https://doi.org/10.3390/jcm10102176>
- Mellinas, C., Ramos, M., Jiménez, A., Garrigós, M. C., 2020. Recent trends in the use of pectin from agro-waste residues as a natural-based biopolymer for food packaging applications. *Materials*, 13(3). <https://doi.org/10.3390/ma13030673>
- Mhamdi, B., Abbassi, F., Abdelly, C., 2015. Chemical composition, antioxidant and antimicrobial activities of the edible medicinal *Ononis natrix* growing wild in Tunisia. *Natural Product Research*, 29, 1157–1160.

- Michiel De Both, B., Sophia Ben Tahar, C.-F., Marianne Noel, C.-F., Joel Perret, O.R., 1995. Transgenic plants belonging to the species *Cucumis melo*. US Patent, Patent Number: US 5,422,259 A.
- Mills, J. M., 2017. U.S. Patent No. 9,622,432. Washington, DC: U.S. Patent and Trademark Office.
- Moco, S., Martin, F.P.J., Rezzi, S., 2012. Metabolomics view on gut microbiome modulation by polyphenol-rich foods. *J. Proteome Res.* 11, 4781–4790. <https://doi.org/10.1021/pr300581s>
- Monforte, Ana Rita, Martins, Sara I.F.S., Silva Ferreira, Antonio C., 2018. Strecker aldehyde formation in wine: new insights into the role of gallic acid, glucose, and metals in phenylacetaldehyde formation. *Journal of Agricultural and Food Chemistry*, 66(10), 2459–2466. <https://doi.org/10.1021/acs.jafc.7b00264>
- Morais, D.R., Rotta, E.M., Sargi, S.C., Schmidt, E.M., Bonafe, E.G., Eberlin, M.N., Sawaya, A.C.H.F, Visentainer, J.V., 2015. Antioxidant activity, phenolics and UPLC-ESI(-)-MS of extracts from different tropical fruits parts and processed peels. *Food Res. Int.* 77, 392–399. <https://doi.org/10.1016/j.foodres.2015.08.036>.
- Mota de Carvalho, N., Costa, E. M., Silva, S., Pimentel, L., Fernandes, T. H., Pintado, M. E., 2018. Fermented foods and beverages in human diet and their influence on gut microbiota and health. *Fermentation* 4, 1–13. <https://doi.org/10.3390/fermentation4040090>
- Murayama, K., Kato-Murayama, M., Hosaka, T., Sotokawauchi, A., Yokoyama, S., Arima, K., Shirouzu, M., 2012. Crystal structure of cucumisin, a subtilisin-like endoprotease from *cucumis melo* L. *Journal of Molecular Biology*, 423(3), 386–396. <https://doi.org/10.1016/j.jmb.2012.07.013>
- Muthukumar, C., Banupriya, L., Harinee, S., Sivaranjani, S., Sharmila, G., Rajasekar, V., Kumar, N. M., 2017. Pectin from muskmelon (*Cucumis melo* var. *reticulatus*) peels: extraction optimization and physicochemical properties. *3 Biotech*, 7(1), 1–10. <https://doi.org/10.1007/s13205-017-0655-3>
- Nadar, S.S., Pawar, R.G., Rathod, V.K., 2017. Recent advances in enzyme extraction strategies: A comprehensive review. *Int. J. Biol. Macromol.* 101, 931–957. <https://doi.org/10.1016/j.ijbiomac.2017.03.055>.
- Naduparambath, S., Purushothaman, E., 2016. Sago seed shell: determination of the composition and isolation of microcrystalline cellulose (MCC). *Cellulose* 23, 1803–1812. <https://doi.org/10.1007/s10570-016-0904-3>
- Naduparambath, S., T.V., J., Shaniba, V., M.P., S., Balan, A.K., Purushothaman, E., 2018. Isolation and characterisation of cellulose nanocrystals from sago seed shells. *Carbohydr. Polym.* 180, 13–20. <https://doi.org/10.1016/j.carbpol.2017.09.088>
- Nakagawa, M., Ueyama, M., Tsuruta, H., Uno, T., Kanamaru, K., Mikami, B., Yamagata, H., 2010. Functional analysis of the cucumisin propeptide as a potent inhibitor of its mature enzyme. *Journal of Biological Chemistry*, 285(39), 29797–29807. <https://doi.org/10.1074/jbc.M109.083162>
- Nakagawa, M., Ueyama, M., Tsuruta, H., Uno, T., Kanamaru, K., Mikami, B., Yamagata, H., 2010. Functional analysis of the cucumisin propeptide as a potent inhibitor of its mature enzyme. *Journal of Biological Chemistry*, 285(39), 29797–29807. <https://doi.org/10.1074/jbc.M109.083162>
- Namitha, K.K., Negi, P.S., 2010. Chemistry and Biotechnology of Carotenoids. *Critical Reviews in Food Science and Nutrition*, 50 (8), 728-760.
- Neubert, A.M., Graham, D.W., Henry, J.L., Brekke, J.E., Beardsley, C.L., 1954. Sugar recovery: Recovery of pугars from pear-canning waste. *J. Agric. Food Chem.* 2, 30–36. <https://doi.org/10.1021/jf60021a006>.

- Nomi-Golzar, S., Mahboob, S., Tavakkoli, S., Asghari Jafarabadi, M., Rezazadeh, K., Vaghef-Mehrabany, E., Ebrahimi-Mameghani, M., 2021. Effects of hydroxy citric acid on body weight and serum hepcidin level in women with non-alcoholic fatty liver disease a randomized clinical trial. *Adv. Integr. Med.* 8, 122–128. <https://doi.org/10.1016/j.aimed.2020.07.013>
- Nunes, M.A., Costa, A.S., Bessada, S., Santos, J., Puga, H., Alves, R.C., Freitas, V., Oliveira, M. B. P., 2018. Olive pomace as a valuable source of bioactive compounds: A study regarding its lipid-and water-soluble components. *Science of the total environment*, 644, 229-236. <https://doi.org/10.1016/j.scitotenv.2018.06.350>.
- Obando-Ulloa, J.M., Eduardo, I., Monforte, A.J., Fernández-Trujillo, J.P., 2009. Identification of QTLs related to sugar and organic acid composition in melon using near-isogenic lines. *Sci. Hort.* (Amsterdam). 121, 425–433. <https://doi.org/10.1016/j.scienta.2009.02.023>
- Ok, S., Yilmaz, E., 2019. The Pretreatment of the Seeds Affects the Quality and Physicochemical Characteristics of Watermelon Oil and Its By-Products. *Journal of the American Oil Chemists' Society*, 96, 453–466.
- Oldfield, T.L., White, E., Holden, N.M., 2016. An environmental analysis of options for utilising wasted food and food residue. *J. Environ. Manage.* 183, 826–835. <https://doi.org/10.1016/j.jenvman.2016.09.035>.
- Oliveira, A. L., Gondim, S., Gómez-García, R., Ribeiro, T., Pintado, M. 2021., Olive leaf phenolic extract from two Portuguese cultivars–bioactivities for potential food and cosmetic application. *Journal of Environmental Chemical Engineering*, 106175. <https://doi.org/10.1016/j.jece.2021.106175>
- Oliveira, A., Coelho, M., Alexandre, E. M. C., Gomes, M. H., Almeida, D. P. F., Pintado, M., 2015. Effect of modified atmosphere on phytochemical profile of pasteurized peach purées. *LWT - Food Science and Technology*, 64(2), 520–527. <https://doi.org/10.1016/j.lwt.2015.06.023>
- Oliveira, A., Pintado, M., Almeida, D. P. F., 2012. Phytochemical composition and antioxidant activity of peach as affected by pasteurization and storage duration. *LWT - Food Science and Technology*, 49(2), 202–207. <https://doi.org/10.1016/j.lwt.2012.07.008>
- Olubunmi, I.P., Olajumoke, A.A., Bamidele, J.A., Omolara, O.F., 2019. Phytochemical Composition and *in vitro* Antioxidant Activity of Golden Melon (*Cucumis melo* L.) Seeds for Functional Food Application. *International Journal of Biochemistry Research*, 25, 1–13.
- Pachau, L., Dutta, R. S., Hauzel, L., Devi, T. B., Deka, D., 2019. Evaluation of novel microcrystalline cellulose from *Ensete glaucum* (Roxb.) Cheesman biomass as sustainable drug delivery biomaterial. *Carbohydrate polymers*, 206, 336-343. <https://doi.org/10.1016/j.carbpol.2018.11.013>
- Palacios, S., Ruiz, H.A., Ramos-Gonzalez, R., Martínez, J., Segura, E., Aguilar, M., Aguilera, A., Michelena, G., Aguilar C., Ilyina, A., 2017. Comparison of physicochemical pretreatments of banana peels for bioethanol production. *Food science and biotechnology*, 26(4), 993-1001. <https://doi.org/doi.10.1007/s10068-017-0128-9>.
- Panchal, R., Singh, A., Diwan, H., 2021. Does circular economy performance lead to sustainable development? – A systematic literature review. *J. Environ. Manage.* 293, 112811. <https://doi.org/10.1016/j.jenvman.2021.112811>
- Panda, S.K., Mishra, S.S., Kayitesi, E., Ray, R.C., 2016. Microbial processing of fruit and vegetable wastes for production of vital enzymes and organic acids: Biotechnology and scopes. *Environ. Res.* 146, 161–172. <https://doi.org/10.1016/j.envres.2015.12.035>.
- Park, J. I., Lee, J. H., Gwak, Y., Kim, H. J., Jin, E. S., Kim, Y. P., 2013. Frozen assembly of gold nanoparticles for rapid analysis of antifreeze protein activity. *Biosensors and*

- Bioelectronics, 41(1), 752–757. <https://doi.org/10.1016/j.bios.2012.09.052>
- Parle, M., Singh, K., 2011. Musk melon is Eat-Must melon. *International Research Journal of Pharmacy* 2, 52–57.
- Patel, A., Hružová, K., Rova, U., Christakopoulos, P., Matsakas, L., 2019. Sustainable biorefinery concept for biofuel production through holistic valorization of food waste. *Bioresour. Technol.* 294. <https://doi.org/10.1016/j.biortech.2019.122247>
- Pei, L., Li, J., Xu, Z., Chen, N., Wu, X., Chen, J., 2020. Effect of high hydrostatic pressure on aroma components, amino acids, and fatty acids of Hami melon (*Cucumis melo* L. var. *reticulatus* naud.) juice. *Food Science and Nutrition*, 8(3), 1394–1405. <https://doi.org/10.1002/fsn3.1406>
- Peña-Lucio, E.M., Londoño-Hernández, L., Ascacio-Valdes, J.A., Chavéz-González, M.L., Bankole, O.E., Aguilar, C.N., 2020. Use of coffee pulp and sorghum mixtures in the production of n-demethylases by solid-state fermentation. *Bioresource technology*, 305, 123112. <https://doi.org/10.1016/j.biortech.2020.123112>.
- Pereira, A.P., Ferreira, I.C.F.R., Marcelino, F., Valentão, P., Andrade, P.B., Seabra, R., Estevinho, L., Bento, A., Pereira, J.A., 2007. Phenolic compounds and antimicrobial activity of olive (*Olea europaea* L. Cv. *Cobrançosa*) leaves. *Molecules* 12, 1153–1162. <https://doi.org/10.3390/12051153>.
- Petkova, Z., Antova, G., 2015. Proximate composition of seeds and seed oils from melon (*Cucumis melo* L.) cultivated in Bulgaria. *Cogent Food and Agriculture*, 1(1), 1018779. <https://doi.org/10.1080/23311932.2015.1018779>
- Poiroux-Gonord, F., Bidel, L.P.R., Fanciullino, A.L., Gautier, H., Lauri-Lopez, F., Urban, L., 2010. Health benefits of vitamins and secondary metabolites of fruits and vegetables and prospects to increase their concentrations by agronomic approaches. *J. Agric. Food Chem.* 58, 12065–12082. <https://doi.org/10.1021/jf1037745>.
- Pokusaeva, K., Fitzgerald, G.F., Van Sinderen, D., 2011. Carbohydrate metabolism in *Bifidobacteria*. *Genes Nutr.* 6, 285–306. <https://doi.org/10.1007/s12263-010-0206-6>
- Poli, A., Strazzullo, G., De Giulio, A., Tommonaro, G., De Prisco, R., Nicolaus, B., Malinconico, M., 2006. New Bioproducts from Solid Waste of Tomato Processing Industry. In X International Symposium on the Processing Tomato 758 (pp. 37-42). <https://doi.org/10.17660/ActaHortic.2007.758.2>.
- Postma, P.R., Suarez-garcia, E., Safi, C., Yonathan, K., Olivieri, G., Barbosa, M.J., Wijffels, R.H., Eppink, M.H.M., 2017. Energy efficient bead milling of microalgae: Effect of bead size on disintegration and release of proteins and carbohydrates. *Bioresour. Technol.* 224, 670–679. <https://doi.org/10.1016/j.biortech.2016.11.071>
- Pourbafrani, M., Forgács, G., Horváth, I. S., Niklasson, C., Taherzadeh, M. J., 2010. Production of biofuels, limonene and pectin from citrus wastes. *Bioresource technology*, 101(11), 4246-4250. <https://doi.org/10.1016/j.biortech.2010.01.077>
- Provesi, J. G., Valentim Neto, P. A., Arisi, A. C. M., Amante, E. R., 2019. Extraction of antifreeze proteins from cold acclimated leaves of *Drimys angustifolia* and their application to star fruit (*Averrhoa carambola*) freezing. *Food Chemistry*, 289(March), 65–73. <https://doi.org/10.1016/j.foodchem.2019.03.055>
- Quirós-Sauceda, A. E., Palafox, H., Robles-Sánchez, R. M., González-Aguilar, G. A., 2011. Phenolic compounds and dietary fiber interaction: antioxidant capacity and bioavailability. *BIOTecnia*, 13.
- Rabelo, S.C., Carrere, H., Maciel Filho, R., Costa, A.C., 2011. Production of bioethanol, methane and heat from sugarcane bagasse in a biorefinery concept. *Bioresour. Technol.* 102, 7887–7895. <https://doi.org/10.1016/j.biortech.2011.05.081>.
- Raji, Z., Khodaiyan, F., Rezaei, K., Kiani, H., Hosseini, S. S., 2017. Extraction optimization and physicochemical properties of pectin from melon peel. *International Journal of*

- Biological Macromolecules, 98, 709–716.
<https://doi.org/10.1016/j.ijbiomac.2017.01.146>
- Ranadheera, C. S., Liyanarachchi, W. S., Dissanayake, M., Chandrapala, J., Huppertz, T., Vasiljevic, T., 2019. Impact of shear and pH on properties of casein micelles in milk protein concentrate. *Lwt*, 108, 370–376. <https://doi.org/10.1016/j.lwt.2019.03.090>
- Rao, J., Chen, B., McClements, D.J., 2019. Improving the Efficacy of Essential Oils as Antimicrobials in Foods: Mechanisms of Action. *Annual Review of Food Science and Technology*, 10, 365–387.
- Rao, L.V., Goli, J.K., Gentela, J., Koti, S., 2016. Bioconversion of lignocellulosic biomass to xylitol: an overview. *Bioresource Technology*, 213, 299–310. <https://doi.org/10.1016/j.biortech.2016.04.092>.
- Rasheed, M., Jawaid, M., Karim, Z., 2020. Morphological, physiochemical and thermal properties of microcrystalline cellulose (MCC) extracted from bamboo fiber. *Molecules* 25. <https://doi.org/doi:10.3390/molecules25122824>
- Rashid, U., Rehman, H.A., Hussain, I., Ibrahim, M., Haider, M.S., 2011. Muskmelon (*Cucumis melo*) seed oil: A potential non-food oil source for biodiesel production. *Energy*, 36, 5632–5639.
- Ravindran, R., Jaiswal, A.K., 2016. Exploitation of food industry waste for high-value products. *Trends in Biotechnology*, 34(1), 58–69. <http://dx.doi.org/10.1016/j.tibtech.2015.10.008>.
- Rezig, L., Chouaibi, M., Meddeb, W., Msaada, K., Hamdi, S., 2019. Chemical composition and bioactive compounds of Cucurbitaceae seeds: Potential sources for new trends of plant oils. *Process Safety and Environmental Protection*, 127, 73–81.
- Ribeiro, T.B., Costa, C.M., Bonifácio-Lopes, T., Silva, S., Veiga, M., Monforte, A.R., Nunes, J., Vicente, A.A., Pintado, M., 2021. Prebiotic effects of olive pomace powders in the gut: *In vitro* evaluation of the inhibition of adhesion of pathogens, prebiotic and antioxidant effects. *Food Hydrocoll.* 112. <https://doi.org/10.1016/j.foodhyd.2020.106312>.
- Ribeiro, T.B., Oliveira, A., Campos, D., Nunes, J., Vicente, A.A., Pintado, M., 2020. Simulated digestion of an olive pomace water-soluble ingredient: relationship between the bioaccessibility of compounds and their potential health benefits. *Food Funct.* 11, 2238–2254. <https://doi.org/10.1039/c9fo03000j>
- Ríos-Covián, D., Ruas-Madiedo, P., Margolles, A., Gueimonde, M., De Los Reyes-gavilán, C. G., Salazar, N., 2016. Intestinal short chain fatty acids and their link with diet and human health. *Frontiers in microbiology*, 7, 185. <https://doi.org/10.3389/fmicb.2016.00185>
- Roadjanakamolson, M., Suntornsuk, W., 2010. Production of β -carotene-enriched rice bran using solid-state fermentation of *Rhodotorula glutinis*. *Journal of Microbiology and Biotechnology*, 20, 525–531.
- Rodríguez-Luna, D., Ruiz, H. A., González-Morales, S., Sandoval-Rangel, A., de la Fuente, M. C., Charles-Rodríguez, A. V., Robledo-Olivo, A., 2020. Recovery of melon residues (*Cucumis melo*) to produce lignocellulolytic enzymes. *Biomass Conversion and Biorefinery*, 1–8. <https://doi.org/10.1007/s13399-020-01055-8>
- Rodríguez-Pérez, C., Quirantes-Piné, R., Fernández-Gutiérrez, A., Segura-Carretero, A., 2013. Comparative characterization of phenolic and other polar compounds in Spanish melon cultivars by using high-performance liquid chromatography coupled to electrospray ionization quadrupole-time of flight mass spectrometry. *Food Research International*, 54(2), 1519–1527. <https://doi.org/10.1016/j.foodres.2013.09.011>.
- Rojas, R., Alvarez-Pérez, O.B., Contreras-Esquivel, J.C., Vicente, A., Flores, A., Sandoval, J., Aguilar, C.N., 2018. Valorisation of mango peels: Extraction of pectin and antioxidant

- and antifungal polyphenols. *Waste and Biomass Valorization*, 11(1), 89-98. <https://doi.org/10.1007/s12649-018-0433-4>.
- Rolim, P.M., Seabra, L.M.J., de Macedo, G.R., 2019. Melon By-Products: Biopotential in Human Health and Food Processing. *Food Reviews International*, 0, 1–24.
- Roman, L., Guo, M., Terekhov, A., Grossutti, M., Vidal, N. P., Reuhs, B. L., Martinez, M. M., 2021. Extraction and isolation of pectin rich in homogalacturonan domains from two cultivars of hawthorn berry (*Crataegus pinnatifida*). *Food Hydrocolloids*, 113, 106476. <https://doi.org/10.1016/j.foodhyd.2020.106476>
- Ronny, H., Navam, H., Ken, O., Pengyin, C., Edward, G., 2010. Extraction, fractionation and characterization of bitter melon seed proteins. *Journal of Agricultural and Food Chemistry*, 58(3), 1892–1897. <https://doi.org/10.1021/jf902903s>
- Rosset, R., Egli, L., Lecoultre, V., 2017. Glucose–fructose ingestion and exercise performance: The gastrointestinal tract and beyond. *Eur. J. Sport Sci.* 17, 874–884. <https://doi.org/10.1080/17461391.2017.1317035>
- Rtibi, K., Hammami, I., Selmi, S., Grami, D., Sebai, H., Amri, M., Marzouki, L., 2017. Phytochemical properties and pharmacological effects of *Quercus ilex* L. aqueous extract on gastrointestinal physiological parameters *in vitro* and *in vivo*. *Biomedicine and Pharmacotherapy*, 94, 787-793. <https://doi.org/10.1016/j.biopha.2017.08.008>
- Saffouri, G.B., Shields-Cutler, R.R., Chen, J., Yang, Y., Lekatz, H.R., Hale, V.L., Cho, J.M., Battaglioli, E.J., Bhattarai, Y., Thompson, K.J., Kalari, K.K., Behera, G., Berry, J.C., Peters, S.A., Patel, R., Schuetz, A.N., Faith, J.J., Camilleri, M., Sonnenburg, J.L., Farrugia, G., Swann, J.R., Grover, M., Knights, D., Kashyap, P.C., 2019. Small intestinal microbial dysbiosis underlies symptoms associated with functional gastrointestinal disorders. *Nat. Commun.* 10, 1–11. <https://doi.org/10.1038/s41467-019-09964-7>
- Saini, R.K., Nile, S.H., Park, S.W., 2015. Carotenoids from fruits and vegetables: Chemistry, analysis, occurrence, bioavailability and biological activities. *Food Res. Int.* 76, 735–750. <https://doi.org/10.1016/j.foodres.2015.07.047>.
- Saltveit, M.E., 2011. Melon (*Cucumis melo* L.). In: *Postharvest Biology and Technology of Tropical and Subtropical Fruits*. Woodhead Publishing Limited. pp. 483-501.
- Samanta, A.K., Senani, S., Kolte, A.P., Sridhar, M., Sampath, K.T., Jayapal, N., Devi, A., 2012. Production and *in vitro* evaluation of xylooligosaccharides generated from corn cobs. *Food Bioprod. Process.* 90, 466–474. <https://doi.org/10.1016/j.fbp.2011.11.001>
- Sánchez-Trasviña, C., González-Valdez, J., Mayolo-Deloisa, K., Rito-Palomares, M., 2015. Impact of aqueous two-phase system design parameters upon the *in-situ* refolding and recovery of invertase. *J. Chem. Technol. Biotechnol.* 90, 1765–1772. <https://doi.org/10.1002/jctb.4758>.
- Santos, E. S. D., Rolim, P. M., Oliveira Júnior, S. D. D., Oliveira, A. C. D. S. M. D., Macedo, G. R. D., 2018. Nutritional value, cellulase activity and prebiotic effect of melon residues (*Cucumis melo* L. *reticulatus* group) as a fermentative substrate. <https://repositorio.ufrn.br/handle/123456789/32672>
- Sarungallo, Z.L., Hariyadi, P., Andarwulan, N., Purnomo, E.H., Wada, M., 2015. Analysis of α -Cryptoxanthin, β -Cryptoxanthin, α -Carotene, and β -Carotene of Pandanus Conoideus Oil by High-performance Liquid Chromatography (HPLC). *Procedia Food Science*, 3, 231–243.
- Savatović, S.M., Četković, G.S., Čanadanović-Brunet, J.M., Đilas, S.M., 2010. Utilization of tomato waste as a source of polyphenolic antioxidants. *Acta periodica technologica*, (41), 187-194. <https://doi.org/10.2298/APT1041187S>.
- Scientific, T., 2007. BCA TM Protein Assay Kit. BCA Protein Assay Kit 0747, 6–7.
- Segal, L. G. J. M. A., Creely, J. J., Martin Jr, A. E., Conrad, C. M., 1959. An empirical method for estimating the degree of crystallinity of native cellulose using the X-ray

- diffractometer. *Textile research journal*, 29(10), 786-794. <https://doi.org/10.1177/004051755902901003>
- Sepúlveda, L., Aguilera-Carbó, A., Ascacio-Valdés, J.A., Rodríguez-Herrera, R., Martínez-Hernández, J.L., Aguilar, C.N., 2012. Optimization of ellagic acid accumulation by *Aspergillus niger* GH1 in solid state culture using pomegranate shell powder as a support. *Process Biochem.* 47, 2199–2203. <https://doi.org/10.1016/j.procbio.2012.08.013>.
- Serna, L.D., Toro, J.S., Loaiza, S.S., Perez, Y.C., Alzate, C.C., 2016. Agricultural waste management through energy producing biorefineries: The Colombian case. *Waste and biomass valorization*, 7(4), 789-798. <https://doi.org/10.1007/s12649-016-9576-3>.
- Sharma, A., Kumari, M., Jagannadham, M.V., 2012. Religiosin C, a cucumisin-like serine protease from *Ficus religiosa*. *Process Biochem.* 47, 914–921. <https://doi.org/10.1016/j.procbio.2012.02.015>.
- Sharma, B., Deswal, R., 2014. Antifreeze proteins in plants: an overview with an insight into the detection techniques including nanobiotechnology. *Journal of Proteins and Proteomics*, 5, 89–107.
- Sharma, S., Gupta, A., Kumar, A., Kee, C.G., Kamyab, H., Saufi, S.M., 2018. An efficient conversion of waste feather keratin into ecofriendly bioplastic film. *Clean Technol. Environ. Policy.* <https://doi.org/10.1007/s10098-018-1498-2>
- Shi, K., Song, D., Chen, G., Pistolozzi, M., Wu, Z., Quan, L., 2015. Controlling composition and color characteristics of *Monascus* pigments by pH and nitrogen sources in submerged fermentation. *J. Biosci. Bioeng.* 120, 145–154. <https://doi.org/10.1016/j.jbiosc.2015.01.001>.
- Shofian, N.M., Hamid, A.A., Osman, A., Saari, N., Anwar, F., Dek, M.S.P., Hairuddin, M.R., 2011. Effect of freeze-drying on the antioxidant compounds and antioxidant activity of selected tropical fruits. *International Journal of Molecular Sciences*, 12, 4678–4692.
- Silva, M.A., Albuquerque, T.G., Alves, R.C., Oliveira, M.B.P.P., Costa, H.S., 2018. Melon (*Cucumis melo* L.) by-products: potential food ingredients for novel functional foods? *Trends Food Sci. Technol.* 0–1. <https://doi.org/10.1016/j.tifs.2018.07.005>.
- Sindhu, R., Gnansounou, E., Rebello, S., Binod, P., Varjani, S., Thakur, I.S., Nair, R.B., Pandey, A., 2019. Conversion of food and kitchen waste to value-added products. *J. Environ. Manage.* 241, 619–630. <https://doi.org/10.1016/j.jenvman.2019.02.053>.
- Singleton, V. L., Rossi, J. A., 1965. Colorimetry of total phenolics with phosphomolybdic-phosphotungstic acid reagents. *American Journal of Enology and Viticulture*, 16, 144–158.
- Sluiter, A., Hames, B., Ruiz, R., Scarlata, C., Sluiter, J., Crocker, D., Templeton, D., 2008. Determination of structural carbohydrates and lignin in biomass. *Laboratory Analytical Procedure (LAP)*, Version 08, 17. <http://www.nrel.gov/docs/gen/fy13/42618.pdf>
- Socol, C.R., Scopel, E., Alberto, L., Letti, J., Karp, S.G., Woiciechowski, A.L., Porto, L., Vandenberghe, D.S., 2017. Recent developments and innovations in solid state fermentation. *Biotechnology Research and Innovation*, 1 (1), 52-71.
- Sosiati, H., Wijayanti, D.A., Triyana, K., Kamiel, B., 2017. Morphology and crystallinity of sisal nanocellulose after sonication. *AIP Conf. Proc.* 1877. <https://doi.org/10.1063/1.4999859>
- Sotokawauchi, A., Kato-Murayama, M., Murayama, K., Hosaka, T., Maeda, I., Onjo, M., Shirouzu, M., 2016. Structural basis of cucumisin protease activity regulation by its propeptide. *Journal of Biochemistry*, 161(1), 45–53. <https://doi.org/10.1093/jb/mvw053>
- Sotokawauchi, A., Kato-Murayama, M., Murayama, K., Hosaka, T., Maeda, I., Onjo, M., Shirouzu, M., 2016. Structural basis of cucumisin protease activity regulation by its propeptide. *Journal of Biochemistry*, 161(1), 45–53. <https://doi.org/10.1093/jb/mvw053>

- Stocks, S.M., 2013. Industrial enzyme production for the food and beverage industries: process scale up and scale down. In *Microbial Production of Food Ingredients, Enzymes and Nutraceuticals*. (pp. 144-172). Woodhead Publishing Limited. <https://doi.org/10.1533/9780857093547.1.144>.
- Ström, A., Schuster, E., Goh, S. M., 2014. Rheological characterization of acid pectin samples in the absence and presence of monovalent ions. *Carbohydrate Polymers*, 113, 336–343. <https://doi.org/10.1016/j.carbpol.2014.06.090>
- Sulaiman, S.F., Ooi, K.L., 2014. Antioxidant and α -glucosidase inhibitory activities of 40 tropical juices from Malaysia and identification of phenolics from the bioactive fruit juices of *Barringtonia racemosa* and *Phyllanthus acidus*. *Journal of agricultural and food chemistry*, 62(39), 9576-9585. <https://doi.org/10.1021/jf502912t>.
- Tadmor, Y., Burger, J., Yaakov, I., Feder, A., Libhaber, S.E., Portnoy, V., Meir, A., Tzuri, G., Sa'Ar, U., Rogachev, I., Aharoni, A., Abeliovich, H., Schaffer, A.A., Lewinsohn, E., Katzir, N., 2010. Genetics of flavonoid, carotenoid, and chlorophyll pigments in melon fruit rinds. *Journal of Agricultural and Food Chemistry*, 58, 10722–10728.
- Tan, S., Zhang, Z., Sun, J., Wang, Q., 2013. Recent progress of catalytic pyrolysis of biomass by HZSM-5. *Chinese Journal of Catalysis*, 34(4), 641-650.
- Tang, M., Bie, Z. long, Wu, M. zhu, Yi, H. ping, Feng, J. xin, 2010. Changes in organic acids and acid metabolism enzymes in melon fruit during development. *Sci. Hortic. (Amsterdam)*. 123, 360–365. <https://doi.org/10.1016/j.scienta.2009.11.001>
- Tavares, T. G., Contreras, M. M., Amorim, M., Martín-Álvarez, P. J., Pintado, M. E., Recio, I., Malcata, F. X., 2011. Optimisation, by response surface methodology, of degree of hydrolysis and antioxidant and ACE-inhibitory activities of whey protein hydrolysates obtained with cardoon extract. *International Dairy Journal*, 21(12), 926–933. <https://doi.org/10.1016/j.idairyj.2011.05.013>
- Teigiserova, D.A., Tiruta-Barna, L., Ahmadi, A., Hamelin, L., Thomsen, M., 2021. A step closer to circular bioeconomy for citrus peel waste: A review of yields and technologies for sustainable management of essential oils. *J. Environ. Manage.* 280, 111832. <https://doi.org/10.1016/j.jenvman.2020.111832>.
- Teresa Pacheco, M., Villamiel, M., Moreno, R., Moreno, F. J., 2019. Structural and rheological properties of pectins extracted from industrial sugar beet by-products. *Molecules*, 24(3), 1–17. <https://doi.org/10.3390/molecules24030392>
- Thaipong, K., Boonprakob, U., Crosby, K., Cisneros-zevallos, L., Hawkins, D., 2006. Comparison of ABTS, DPPH, FRAP, and ORAC assays for estimating antioxidant activity from guava fruit extracts, 19, 669–675. <https://doi.org/10.1016/j.jfca.2006.01.003>
- Thielmann, J., Kohnen, S., Hauser, C., 2017. Antimicrobial activity of *Olea europaea* Linné extracts and their applicability as natural food preservative agents. *International Journal of Food Microbiology*, 251, 48-66. <https://doi.org/10.1016/j.ijfoodmicro.2017.03.019>
- Thu Dao, T. A., Webb, H. K., Malherbe, F., 2021. Optimization of pectin extraction from fruit peels by response surface method: Conventional versus microwave-assisted heating. *Food Hydrocolloids*, 113, 106475. <https://doi.org/10.1016/j.foodhyd.2020.106475>
- Tian, Y., Zhu, Z., Sun, D. W., 2020. Naturally sourced biosubstances for regulating freezing points in food researches: Fundamentals, current applications and future trends. *Trends in Food Science and Technology*, 95(November 2019), 131–140. <https://doi.org/10.1016/j.tifs.2019.11.009>
- Tinline-Goodfellow, C. T., West, D. W., Malowany, J. M., Gillen, J. B., Moore, D. R., 2020. An acute reduction in habitual protein intake attenuates post exercise anabolism and may bias oxidation-derived protein requirements in resistance trained men. *Frontiers in nutrition*, 7, 55.

- Torres-León, C., Ramírez-Guzman, N., Londoño-Hernandez, L., Martinez-Medina, G.A., Díaz-Herrera, R., Navarro-Macias, V., Alvarez-Perez., O.B., Picazo, B., Villarreal, M., Ascacio, J., Aguilar, C.N., 2018. Food waste and byproducts: An opportunity to minimize malnutrition and hunger in developing countries. *Frontiers in Sustainable Food Systems*, 2, 52. <https://doi.org/10.3389/FSUFS.2018.00052>.
- Tóth, J., 1979. Utilization of tropical agricultural wastes. *Conserv. Recycl.* 2, 277–281. [https://doi.org/10.1016/0361-3658\(78\)90020-6](https://doi.org/10.1016/0361-3658(78)90020-6).
- Tran, C.T., Mitchell, D.A., 1995. Pineapple waste—a novel substrate for citric acid production by solid-state fermentation. *Biotechnology letters*, 17(10), 1107-1110. <https://doi.org/10.1007/BF00143111>
- Trigo, J. P., Alexandre, E. M., Saraiva, J. A., Pintado, M. E., 2019. High value-added compounds from fruit and vegetable by-products—Characterization, bioactivities, and application in the development of novel food products. *Critical reviews in food science and nutrition*, 60(8), 1388-1416.
- Tsuda, S., Yamauchi, A., Uddin Khan, N. M. M., Arai, T., Mahatabuddin, S., Miura, A., Kondo, H., 2020. Fish-derived antifreeze proteins and antifreeze glycoprotein exhibit a different ice-binding property with increasing concentration. *Biomolecules*, 10(3). <https://doi.org/10.3390/biom10030423>
- Turhal, S., Turanbaev, M., Argun, H., 2018. Hydrogen production from melon and watermelon mixture by dark fermentation. *International Journal of Hydrogen Energy*, 44 (34), 18811–18817.
- Ullah, N., Zahoor, M., Ali, F., Khan, S. K., 2014. A review on general introduction to medicinal plants, its phytochemicals and role of heavy metal and inorganic constituents. *Life Science Journal* 11, 520–527.
- Ullah, N., Zahoor, M., Farhat, A., 2014. A review on general introduction to medicinal plants, its phytochemicals and role of heavy metal and inorganic constituents. *Life Science Journal*, 11(7s), 520-527.
- United Nations Department of Economic and Social Affairs., 2017. World population prospects: the 2017 revision, key findings and advance tables. 1–46. <https://doi.org/10.1017/CBO9781107415324.004>.
- Urbanovich, E.A., Afonnikov, D.A., Nikolaev, S. V., 2021. Determination of the quantitative content of chlorophylls in leaves by reflection spectra using the random forest algorithm. *Vavilovskii Zhurnal Genet. Seleksii* 25, 64–70. <https://doi.org/10.18699/VJ21.008>
- Valetti, N. W., Boeris, V., Picó, G., 2013. Characterization of chymotrypsin carrageenan complex in aqueous solution: A solubility and thermodynamical stability study. *International Journal of Biological Macromolecules*, 52, 45–51. <https://doi.org/10.1016/j.ijbiomac.2012.10.014>
- Vallejo, M., Cordeiro, R., Dias, P.A.N., Moura, C., Henriques, M., Seabra, I.J., Malça, C.M., Morouço, P., 2021. Recovery and evaluation of cellulose from agroindustrial residues of corn, grape, pomegranate, strawberry-tree fruit and fava. *Bioresour. Bioprocess.* 8. <https://doi.org/10.1186/s40643-021-00377-3>
- Van Soest, P. J., Robertson, J. B., Lewis, B. A., 1991. Methods for dietary fiber, neutral detergent fiber, and nonstarch polysaccharides in relation to animal nutrition. *Journal of Dairy Science*, 74(10), 3583–3597. [https://doi.org/10.3168/jds.S0022-0302\(91\)78551-2](https://doi.org/10.3168/jds.S0022-0302(91)78551-2)
- Vance, T. D. R., Bayer-Giraldi, M., Davies, P. L., Mangiagalli, M., 2019. Ice-binding proteins and the ‘domain of unknown function’ 3494 family. *FEBS Journal*, 286(5), 855–873. <https://doi.org/10.1111/febs.14764>
- Vaz, B.M.C., Martins, M., de Souza Mesquita, L.M., Fernandes, A.P.M., Pinto, D.C.G.A., Neves, M.G.P.M.S., Neves, M.C., Coutinho, J.A.P., Ventura, S.P.M., 2022. Using

- aqueous solutions of ionic liquids as chlorophyll eluents in solid-phase extraction processes. *Chem. Eng. J.* 428, 131073. <https://doi.org/10.1016/j.cej.2021.131073>
- Veiga, M., Costa, E.M., Silva, S., Pintado, M., 2018. Impact of plant extracts upon human health: A review. *Critical reviews in food science and nutrition*, 60(5), 873-886. <https://doi.org/10.1080/10408398.2018.1540969>.
- Veiga, M., Costa, E.M., Silva, S., Pintado, M., Veiga, M., Costa, E.M., Silva, S., Pintado, M., Costa, E.M., Silva, S., 2018. Impact of plant extracts upon human health: A review. *Critical Reviews in Food Science and Nutrition*, 1–14.
- Velan, M., Krishnan, M.R.V., Lakshmanan, C.M., 1995. Conversion of mango kernel starch to glucose syrups by enzymatic hydrolysis. *Bioprocess Engineering*, 12(6), 323-326. <https://doi.org/10.1007/BF00369509>.
- Vella, F.M., Cautela, D., Laratta, B., 2019. Characterization of polyphenolic compounds in cantaloupe melon by-products. *Foods*, 8, 2–11.
- Ventura-Cruz, S., Flores-Alamo, N., Tecante, A., 2020. Preparation of microcrystalline cellulose from residual Rose stems (*Rosa* spp.) by successive delignification with alkaline hydrogen peroxide. *Int. J. Biol. Macromol.* 155, 324–329. <https://doi.org/10.1016/j.ijbiomac.2020.03.222>
- Ventura-Cruz, S., Tecante, A., 2019. Extraction and characterization of cellulose nanofibers from Rose stems (*Rosa* spp.). *Carbohydr. Polym.* 220, 53–59. <https://doi.org/10.1016/j.carbpol.2019.05.053>
- Verreault, D., Alamdari, S., Roeters, S. J., Pandey, R., Pfaendtner, J., Weidner, T., 2018. Ice-binding site of surface-bound type III antifreeze protein partially decoupled from water. *Physical Chemistry Chemical Physics*, 20(42), 26926–26933. <https://doi.org/10.1039/c8cp03382j>
- Vicente, F.A., Lario, L.D., Pessoa, A., Ventura, S.P.M., 2016. Recovery of bromelain from pineapple stem residues using aqueous micellar two-phase systems with ionic liquids as co-surfactants. *Process Biochem.* 51, 528–534. <https://doi.org/10.1016/j.procbio.2016.01.004>.
- Vilas-Boas, A. A., Oliveira, A., Jesus, D., Rodrigues, C., Figueira, C., Gomes, A., Pintado, M., 2020. Chlorogenic acids composition and the impact of *in vitro* gastrointestinal digestion on espresso coffee from single-dose capsule. *Food Research International*, 134, 109223. <https://doi.org/10.1016/j.foodres.2020.109223>
- Vilas-Boas, A.A., Oliveira, A., Ribeiro, T.B., Ribeiro, S., Nunes, C., Gómez-García, R., Nunes, J., Pintado, M., 2021. Impact of extraction process in non-compliant ‘Bravo de Esmolfe’ apples towards the development of natural antioxidant extracts. *Applied Sciences*, 11(13), 5916. <https://doi.org/10.3390/app11135916>.
- Viniegra-González, G., Favela-Torres, E., Aguilar, C.N., Romero-Gomez, S.J., Díaz-Godínez, G., Augur, C., 2003. Advantages of fungal enzyme production in solid state over liquid fermentation systems. *Biochem. Eng. J.* 13, 157–167. [https://doi.org/10.1016/S1369-703X\(02\)00128-6](https://doi.org/10.1016/S1369-703X(02)00128-6).
- Vishwakarma, V.K., Gupta, J.K., Upadhyay, P.K., 2017. Pharmacological importance of *Cucumis melo* L.: An overview. *Asian Journal of Pharmaceutical and Clinical Research*, 10, 8–12.
- Vlachokostas, C., Achillas, C., Diamantis, V., Michailidou, A. V., Baginetas, K., Aidonis, D., 2021. Supporting decision making to achieve circularity via a biodegradable waste-to-bioenergy and compost facility. *J. Environ. Manage.* 285, 112215. <https://doi.org/10.1016/j.jenvman.2021.112215>.
- Voets, I. K., 2017. From ice-binding proteins to bio-inspired antifreeze materials. *Soft Matter*, 13(28), 4808–4823. <https://doi.org/10.1039/c6sm02867e>
- Wadhwa, M., Bakshi, M. P. S., 2013. Utilization of fruit and vegetable wastes as livestock

- feed and as substrates for generation of other value-added products. *Rap Publication*, 4, 1-67.
- Wan, M. L. Y., Co, V. A., El-Nezami, H. 2021. Dietary polyphenol impact on gut health and microbiota. *Critical reviews in food science and nutrition*, 61(4), 690-711. <https://doi.org/10.1080/10408398.2020.1744512>
- Wang, A., Zhang, F., Huang, L., Yin, X., Li, H., Wang, Q., Zeng, Z., Xie, T., 2010. New progress in biocatalysis and biotransformation of flavonoids. *Journal of Medicinal Plants Research*, 4, 847–856.
- Wang, C., Qiu, W. Y., Chen, T. T., Yan, J. K., 2021. Effects of structural and conformational characteristics of citrus pectin on its functional properties. *Food Chemistry*, 339, 128064. <https://doi.org/10.1016/j.foodchem.2020.128064>
- Wikandari, R., Gudipudi, S., Pandiyan, I., Millati, R., Taherzadeh, M.J., 2013. Inhibitory effects of fruit flavors on methane production during anaerobic digestion. *Bioresour. Technol.* 145, 188–192. <https://doi.org/10.1016/j.biortech.2013.01.041>.
- Wikandari, R., Nguyen, H., Millati, R., Niklasson, C., Taherzadeh, M.J., 2015. Improvement of biogas production from orange peel waste by leaching of limonene. *BioMed Research International*. <https://doi.org/10.1155/2015/494182>.
- Winans, K., Kendall, A., Deng, H., 2017. The history and current applications of the circular economy concept. *Renewable and Sustainable Energy Reviews*, 68, 825-833. <https://doi.org/10.1016/j.rser.2016.09.123>.
- Woitovich Valetti, N., Brassesco, M.E., Picó, G.A., 2016. Polyelectrolytes–protein complexes: A viable platform in the downstream processes of industrial enzymes at scaling up level. *Journal of Chemical Technology and Biotechnology*, 91(12), 2921-2928. <https://doi.org/10.1002/jctb.5050>.
- Woitovich Valetti, N., Lombardi, J., Boeris, V., Picó, G., 2012. Precipitation of chymotrypsin from fresh bovine pancreas using ι -carrageenan. *Process Biochemistry*, 47(12), 2570–2574. <https://doi.org/10.1016/j.procbio.2012.09.021>
- Wojtunik-Kulesza, K., Oniszczuk, A., Oniszczuk, T., Combrzyński, M., Nowakowska, D., Matwijczuk, A., 2020. Influence of *in vitro* digestion on composition, bioaccessibility and antioxidant activity of food polyphenols—a non-systematic review. *Nutrients* 12. <https://doi.org/10.3390/nu12051401>
- Wu, Y., Wu, J., Yang, F., Tang, C., Huang, Q., 2019. Effect of H₂O₂ bleaching treatment on the properties of finished transparent wood. *Polymers (Basel)*. 11, 1–13. <https://doi.org/10.3390/polym11050776>
- Xie, L., Zhao, J., Wu, J., Gao, M., Zhao, Z., Lei, X., Zhao, Y., Yang, W., Gao, X., Ma, C., Liu, H., Wu, F., Wang, X., Zhang, F., Guo, P., Dai, G., 2015. Efficient hydrolysis of corncob residue through cellulolytic enzymes from *Trichoderma strain* G26 and L-lactic acid preparation with the hydrolysate. *Bioresour. Technol.* 193, 331–336. <https://doi.org/10.1016/j.biortech.2015.06.101>.
- Xie, Pu jun, Huang, Li xin, Zhang, Cai hong, Zhang, Y. lei. (2015). Phenolic compositions, and antioxidant performance of olive leaf and fruit (*Olea europaea* L.) extracts and their structure-activity relationships. *Journal of Functional Foods*, 16(16), 460–471. <https://doi.org/10.1016/j.jff.2015.05.005>
- Yan, L.Y., Teng, L.T., Jhi, T.J., 2006. Antioxidant properties of guava fruit: comparison with some local fruits. *Sunway Academic Journal*, 3, 9–20.
- Yang, S. S., 1988. Protein enrichment of sweet potato residue with amylolytic yeasts by solid-state fermentation. *Biotechnol. Bioeng.* 32, 886–890. <https://doi.org/10.1002/bit.260320706>.
- Yano, M., Kato, M., Ikoma, Y., Kawasaki, A., Fukazawa, Y., Sugiura, M., Matsumoto, H., Oohara, Y., Nagao, A., Ogawa, K., 2005. Quantitation of Carotenoids in Raw and

- Processed Fruits in Japan. *Food Science and Technology Research*, 11, 13–18.
- Yousuf, A., Bonk, F., Schmidt, J. E., 2016. Recovery of carboxylic acids produced during dark fermentation of food waste by adsorption on Amberlite IRA-67 and activated carbon. *Bioresource Technology*, 217, 137–140. <https://doi.org/10.1016/j.biortech.2016.02.035>
- Yusuf, M., 2017. Agro-industrial waste materials and their recycled value-added applications: Review. *Handbook of Ecomaterials*, 1-11. https://doi.org/10.1007/978-3-319-48281-1_48-1.
- Zahed, M.A., Movahed, E., Khodayari, A., Zanganeh, S., Badamaki, M., 2021. Biotechnology for carbon capture and fixation: Critical review and future directions. *J. Environ. Manage.* 293, 112830. <https://doi.org/10.1016/j.jenvman.2021.112830>
- Zareba, D., Ziarno, M., Obiedzinski, M., 2012. Volatile profile of non-fermented milk and milk fermented by *bifidobacterium animalissub* sp. lactis. *Int. J. Food Prop.* 15, 1010–1021. <https://doi.org/10.1080/10942912.2010.513024>
- Zhang, C., Su, H., Baeyens, J., Tan, T., 2014. Reviewing the anaerobic digestion of food waste for biogas production. *Renewable and Sustainable Energy Reviews*, 38, 383–392.
- Zhang, H., Chen, Y., Wang, S., Ma, L., Yu, Y., Dai, H., Zhang, Y., 2020. Extraction and comparison of cellulose nanocrystals from lemon (*Citrus limon*) seeds using sulfuric acid hydrolysis and oxidation methods. *Carbohydr. Polym.* 238, 116180. <https://doi.org/10.1016/j.carbpol.2020.116180>
- Zhang, M.F., Qin, Y.H., Ma, J.Y., Yang, L., Wu, Z.K., Wang, T.L., Wang, W.G., Wang, C.W., 2016. Depolymerization of microcrystalline cellulose by the combination of ultrasound and Fenton reagent. *Ultrason. Sonochem.* 31, 404–408. <https://doi.org/10.1016/j.ultsonch.2016.01.027>
- Zhang, T., Guo, X., Meng, H., Tang, X., Ai, C., Chen, H., Yu, S., 2020. Effects of bovine serum albumin on the ethanol precipitation of sugar beet pulp pectins. *Food Hydrocolloids*, 105, 105813. <https://doi.org/10.1016/j.foodhyd.2020.105813>
- Zhao, T., Chen, Z., Lin, X., Ren, Z., Li, B., Zhang, Y., 2018. Preparation and characterization of microcrystalline cellulose (MCC) from tea waste. *Carbohydrate Polymers*, 184, 164–170.
- Zheng, J., Chen, J., Zhang, H., Wu, D., Ye, X., Linardt, R. J., Chen, S., 2020. Gelling mechanism of RG-I enriched citrus pectin: Role of arabinose side-chains in cation- and acid-induced gelation. *Food Hydrocolloids*, 101. <https://doi.org/10.1016/j.foodhyd.2019.105536>